Studies on the Synthesis and Reactivity of Diradical Generating Molecules

Thesis submitted to the

Indian Institute of Technology Kharagpur

For award of the degree of

Doctor of Philosophy

by

Joyee Das

Under the supervision of

Prof. Amit Basak

Department of Chemistry

Indian Institute of Technology Kharagpur

June 2017

Dedicated to My Parents

APPROVAL OF THE VIVA-VOCE BOARD

Certified that the thesis entitled “Studies on the Synthesis and Reactivity of Diradical Generating Molecules” submitted by JOYEE DAS to the Indian Institute of Technology Kharagpur, for the award of the degree of Doctor of Philosophy has been accepted by the external examiners and that the student has successfully defended the thesis in the viva-voce examination held today.

Prof. S. Nanda	Prof. A. K. Das	Prof. M. Bhattacharjee
(Member of the DSC)	(Member of the DSC)	(Member of the DSC)

Prof. A. Chaudhuri	Prof. A. Basak	Prof. M. Bhattacharjee
(External Examiner)	(Supervisor)	(Chairman)

==========

Dr. Amit Basak, FNA, FASc, FNASc
FWAST, J.C. Bose National Fellow
Ph.D (Calcutta), D. Phil. (Oxford)
Professor, Department of Chemistry
Indian Institute of Technology Kharagpur
Kharagpur-721302, INDIA

Fax: 91-03222-255303

Ph: (03222)283300 (O)
Cell: 09434013294
Email: absk@chem.iitkgp.ernet.in

==========

Certificate

This is to certify that the thesis entitled **"Studies on the Synthesis and Reactivity of Diradical Generating Molecules"** submitted by **Joyee Das** to the Indian Institute of Technology Kharagpur, for the award of Doctor of Philosophy, is a record of bona fide research work carried out by her under my supervision and guidance and I consider it worthy of consideration for the award of the degree of Doctor of Philosophy of the Institute.

Date:
IIT Kharagpur

Prof. Amit Basak
(Supervisor)

DECLARATION

I certify that

a) The work contained in the thesis is original and has been done by myself under the guidance of my supervisor.

b) The work has not been submitted to any other Institute for any degree or diploma.

c) I have followed the guidelines provided by the Institute in preparing the thesis.

d) I have conformed to the norms and guidelines given in the Ethical Code of Conduct of the Institute.

e) Whenever I have used materials (data, theoretical analysis, and text) from other sources, I have given due credit to them by citing them in the text of the thesis and giving their details in the references. Further, I have taken permission from copyright owners of the sources, whenever necessary.

_____ _____

Date Joyee Das

IIT Kharagpur

As it's rightly said,"If you want to go fast, go alone. But if you want to go far, go together." A lot more valuable results can be achieved if proper teamwork comes into place. After four and half years of long swashbuckling roller coaster ride of gruelling research work, I have been able to present my thesis for which many people has supported and provided valuable inputs. Now the time has come to express my gratitude to all of them.

It gives me an immense pleasure to showcase my gratitude to my mentor & guide Prof. Amit Basak for his sheer inspirational guidance throughout these rigorous years. The journey started from my M.Sc days in IIT Kharagpur after I got the opportunity to pursue my last one year research project under his guidance. I have considered myself to be extremely lucky to be a part of his mentoring which has resulted this research work into an astounding success venture through tireless hard work. He has shared tons of experience to us when it mattered most, which has helped us to be enriched by unforgettable learning experience. An enormous debt of knowledge to Prof. Basak who has shown us ways of overcoming difficult phases of these years and we are happy to be indebted. I wish to express my deep gratitude to Prof. Amit Basak to introduce me to this intriguing field of organic chemistry.

I am also grateful to Council of Scientific and Industrial Research (CSIR), India for the monetary assistance throughout this phase. Also different instrumental facilities provided by IIT Kharagpur, IISC Bangalore are also deeply appreciated.

I wish to express my thanks to Prof. M. Bhattacharjee, Head, Department of Chemistry, Ex-HOD Prof. T. Pathak, Prof. D. Mal for providing me all the departmental facilities for the research work.

It is unforgettable for me to acknowledge the invaluable suggestions provided by my DSC members, Prof. Samik Nanda, Prof. A. K. Das (Dept. of Biotechnology) and Prof. M. Bhattacharjee. I am also thankful to Prof. A. Ayyappan for helping me to perform computational studies, Dr. Subhendu Sekhar Bag (IIT Guwahati) for performing EPR studies and Dr. Sayantani Roy (School of Bioscience, IIT Kharagpur) for purifying proteins.

A special reference is to be made for all the teachers in my life especially Dr. Chandan Saha (Calcutta School of Tropical Medicine), Prof. Nilmoni Sarkar and Prof. Gour Gopal Roy (Dept. of Metallurgical and Materials Engineering, IIT Khargpur) for their advices and constant encouragement that boosted my confidence and inspired me to reach my ultimate goal.

It gives me a great joy to thank all my colleagues Dr. Tapobrata Mitra, Dr. Raja Mukherjee, Dr. Manasi Maji, Dr. Partha Sarathi Addy, Dr. Debranjan Banerjee, Dr. Ishita Hatial, Dr. Debaki Ghosh, Dr. Arpita

Panja, Dr. Prabuddha Bhattacharya, Arundhoti Mandal, Eshani Das, Monisha Singha, Rajesh and Dhruba da for creating a friendly atmosphere in lab during the course of work.

Madam (Mrs. Nupur Basak), Babai and Riya also deserve special appreciation for their exceptional hospitality and homely attitude.

I thank Mukulika di, Arup da, and Chandrakanta da for their instrumental (NMR, X-ray crystallography) help in recording the data.

Last but not the least my parents have always supported me and showed me the right path to choose. The credit of whatever I have achieved till now all goes to them.

I also express my gratitude to all individuals who directly or indirectly helped me. Any missing in this brief acknowledgement does not mean lack of gratitude.

Date

Indian Institute of Technology Kharagpur (Joyee Das)

Joyee Das
Department of Chemistry
Indian Institute of Technology Kharagpur, India 721302
Voice: +91-9434474597
e-mail: joyeeds@gmail.com; joyee@chem.iitkgp.ernet.in

Personal Date of Birth: 03.04.1990
Sex: Female
Nationality: Indian

Education 2012 M.Sc in Chemistry from IIT Kharagpur (95.8%) **1st Class 2nd**
(Awarded best project work)
2010 B.Sc in Chemistry from University of Calcutta (67%) **1st Class**

Award 2011 (Dec) Qualified for CSIR fellowship in National EligibilityTest (NET)
(All India rank 30)
2012 Qualified for the Graduate Aptitude Test in Engineering (GATE)
(All India rank 119)
Recipient of National Merit Scholarship by Government of India for securing a rank of 44 in Secondary Examination

Research Experience

Specialization: Organic Synthesis/Bio-organic Chemistry

Brief research Activities (2012-present)

- Design, synthesis and reactivity studies of various unsymmetrical deuterated bis-propargyl sulfones and ethers, application of various experimental techniques to solve the diradical-cycloaddition puzzle in Garratt-Braverman cyclization reaction.
- Use of Enediyne moiety acting as a photoaffinity label in design of capture compounds for Human Carbonic Anhydrase II: Support for ionic mechanism in Bergman cyclization.
- Shifting the Reactivity of Bis-Propargyl Ethers from Aryl Naphthalenes to 3,4-Disubstituted Furans via 1,5-H shift Pathway.
- Mechanistic Studies on the Base Induced Cyclization of Propargyl Alkenyl Sulfones.
- A One-Pot Garratt-Braverman and Scholl oxidation Reaction: Application in the Synthesis of Polyaromatic Compounds with Low Lying LUMO.
- Guided three M. Sc. students and one Indian Academy of Science fellow in their projects and had three years' experience in taking tutorial and organic laboratory classes of Bachelors and Masters students during Ph.D.

List of publications

- Mitra, T.; **Das, J.**; Maji, M.; Das, R.; Das, U. K.; Chattaraj, P. K.; Basak, A. A One-pot Garratt-Braverman Cyclization and Scholl Oxidation Route to Acene-Helicene Hybrids. *RSC Adv*. **2013**, *3*, 19844-19848.
- **Das, J.**; Mukherjee, R.; Basak, A. Selectivity in Garratt-Braverman Cyclization of Aryl/Heteroaryl Substituted Unsymmetrical Bispropargyl Systems: Formal Synthesis of 7'-Desmethylkealiiquinone. *J. Org. Chem*. **2014**, *79*, 3789-3798.
- Hatial, I.*; **Das, J.***; Ghosh, A.; Basak, A. Base Induced Cyclization of Propargyl Alkenyl Sulfones: A High Yielding Synthesis of 4,5-Disubstituted 2H-Thiopyran 1,1-dioxides. *Eur. J. Org. Chem*. **2015**, *27*, 6017-6024. (* = Equal Contribution)
- **Das, J.**; Das, E.; Jana, S.; Addy, P. S.; Anoop, A.; Basak, A. Shifting the Reactivity of Bis-propargyl Ethers from Garratt-Braverman Cyclization Mode to 1,5-H Shift Pathway To Yield 3,4-Disubstituted Furans: A Combined Experimental and Computational Study. *J. Org. Chem*. **2016**, *81*, 450-457.

- **Das, J.**; Bag, S. S.; Basak, A. Mechanistic Studies on Garratt-Braverman Cyclization: Solving the Diradical-Cycloaddition Puzzle. *J. Org. Chem*. **2016**, *81*, 4623-4632.
- **Das, J.**; Halnor, S.; Roy, S.; Basak, A. Enediyne Based Protein Capture Agents: Demonstration of An Enediyne Moiety Acting as Photoaffinity Label. *Org. Biomol. Chem*. **2017**, *15*, 1122-1129.
- **Das, J.**; Ghosh, P.; Mukhopadhyay, K. S.; Banerjee, P.; Basak, A. Explosive and Pollutant TNP Detection by LANS: DFT Study, In Vitro Detection and Test Strip Preparation. *Sensors and Actuators B* **2017**, *251*, 985-992.

Symposium and conference attended

- Participated in the International Symposium entitled "Diamond Jubilee Symposium on Recent Trends in Chemistry" (DJSRTC) held at Indian Institute of Technology Kharagpur during October 21-23, 2011.
- Participated in 3rd Research Scholars' Day organized by Department of chemistry, Indian Institute of Technology Kharagpur on April 4, 2012.
- Participated in 4th Research Scholars' Day organized by Department of chemistry, Indian Institute of Technology Kharagpur on April 1, 2013.
- Poster presentation in one day Symposium 'ACS on Campus Kharagpur Episode' held at Indian Institute of Technology Kharagpur on November 25, 2013.
- Poster presentation in 10th mid-year CRSI symposium in Chemistry held at NIT Trichy on 23-25th July, 2015.
- Participated in 22nd Conference of NMR Society of India organized by Department of Chemistry, Indian Institute of Technology Kharagpur on February 18, 2016.
- Poster presentation in symposium 'Organic Molecules: Synthesis and Applications' held at Indian Institute of Technology Kharagpur on February 17-18, 2017.

Abstract

Studies on the Synthesis and Reactivity of Diradical Generating Molecules

This thesis is a compilation of mechanistic studies and synthetic potential of diradical generating cycloaromatization reactions, in particular, the Garratt-Braverman cyclization (GBC) and the Bergman cyclization (BC). The first chapter contains a brief review on sequential developments on the mechanistic aspects of BC and GBC. The second chapter deals with the mechanistic investigation on GBC. By using various experimental techniques like ^{2}H NMR, LA-LDI and from the fate of deuterium labeled substrates we have been able to propose a diradical pathway for bis-propargyl sulfones and an anionic intramolecular Diels Alder (IMDAR) pathway for bis-propargyl ethers (**Scheme 1**). The third chapter comprises the validation of enediyne moiety to act as a photoaffinity label in protein capture. The probable mechanism of capture *via* a photo-Bergman cyclization of enediynes has also been described (**Scheme 2**). The fourth chapter contains differential reactivity of bis-propargyl ethers appended with aliphatic substituents. These systems may undergo either GBC to aryl (dihydro) naphthalenes or follow a 1,5-H shift pathway to yield 3,4-disubstituted furans. Strategies have been developed to shift the preference from GBC to 1,5-H shift process to yield 3,4-disubstituted furans that are otherwise difficult to obtain and also constitute an important skeleton in medicinal chemistry (**Scheme 3**). Unlike the ethers which follow a GBC pathway under base treatment, the corresponding propargyl alkenyl sulfones follow a base-mediated 6π-electrocyclizaton reaction to substituted thiopyran dioxides. The mechanistic investigations (briefly represented in **Scheme 4**) of this 6π-electrocyclization process have been discussed in the fifth chapter. In the sixth chapter, the synthetic potential of GBC was further exploited by carrying out a one pot GBC and Scholl oxidation reaction to polyaromatic compounds having low lying E_{LUMO} level without sacrificing the band gap and the aerial stability of the compounds (**Scheme 5**).

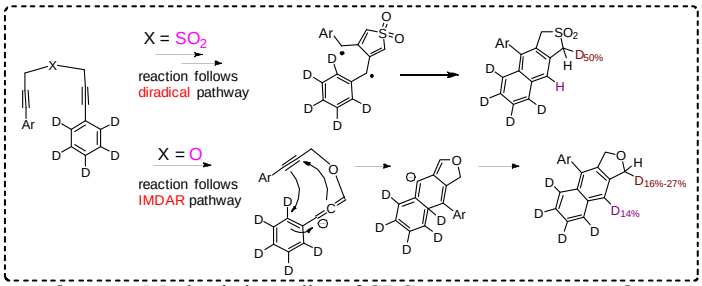

Scheme 1: Mechanistic studies of GBC

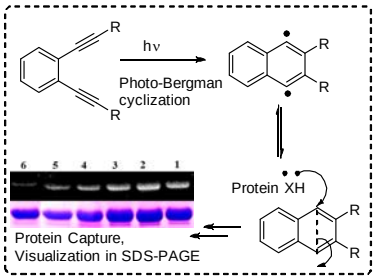

Scheme 2: Protein capture using photo-Bergman cyclization

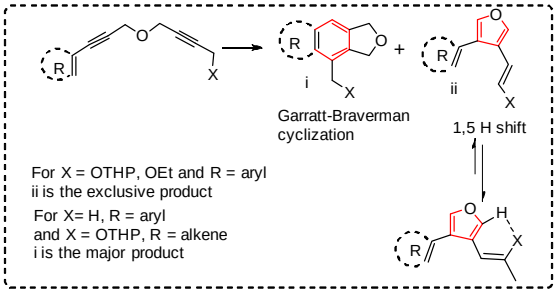

Scheme 3: Base mediated rearrangement of bis-propargyl ethers

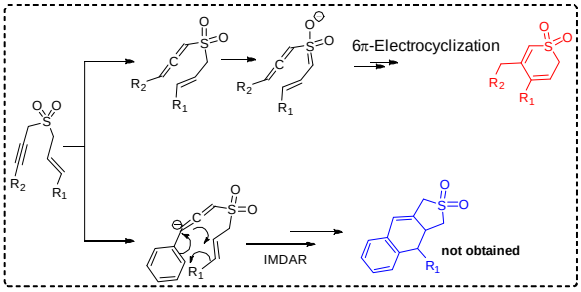

Scheme 4: Base mediated rearrangement of propargyl alkenyl sulfones

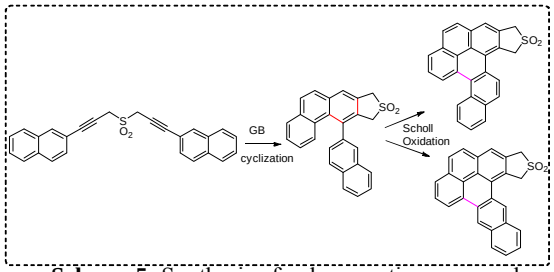

Scheme 5: Synthesis of polyaromatic compounds

Keywords: Radical, ionic, Garratt-Braverman cyclization, Bergman cyclization, mechanism, furans, thiopyran dioxides, protein capture.

Ac	Acetyl
ACTH (18-39)	Adrenocorticotropic hormone fragment 18-39
Anh.	Anhydrous
Ar	Aryl
BC	Bergmann Cyclization
BSA	Bovine Serum Albumin
Bn	Benzyl
Calcd	Calculated
Cat.	Catalytic
CH_3CN	Acetonitrile
CLIP	Corticotropin-like intermediate [lobe] peptide
cm	Centimeter
Conc	Concentrated
COSY	Correlation Spectroscopy
1,4-CHD	1,4-Cyclohexadiene
Da	Dalton
DBU	1,8-diazabicyclo[5.4.0]undec-7-ene
DEPT	Distortionless Enhancement by Polarization Transfer
DHP	Dihydropyran
DMP	Dess-Martin Periodinane
DMPO	5,5-dimethyl-1-pyrrolidine *N*-oxide
DNA	Deoxyribonucleic Acid
DCM	Dichloromethane
DIPEA	N,N-Diisopropyl ethyl amine
DMAP	N, N-Dimethylamino pyridine
DMF	N, N-Dimethylformamide
DMSO	Dimethylsulfoxide
EA/EtOAc	Ethyl Acetate
e.g	For example
EPR	Electron Paramagnetic resonance
eq./ equiv.	Equivalent
ESI	Electro Spray Ionization
ESR	Electron Spin resonance
Et	Ethyl
et al.	And others
etc.	et cetera
Et_3N/TEA	Triethylamine
FTIR	Fourier transform infrared spectroscopy
GB	Garratt-Braverman
GBC	Garratt-Braverman cyclization
h	Hour
HCA	Human Carbonic Anhydrase

HCCA	α- cyano-4-hydroxycinnamic acid
HCL	Hydrochloric acid
HEPES	4-(2-hydroxyethyl)-1-piperazineethanesulfonic acid
HOMO	Highest Energy Occupied Molecular Orbital
HPLC	High Performance Liquid Chromatography
HRMS	High Resolution Mass Spectroscopy
IBX	2-Iodoxybenzoic acid
IC_{50}	Half Maximal Inhibitory Concentration
i.e	That is
IMDAR	Intramolecular anionic Diels Alder reaction
IPA	Isopropyl alcohol
IR	Infrared Spectroscopy
K	Potassium
Kcal	Kilo calories
K_2CO_3	Potassium Carbonate
LA-LDI	label Assisted Laser Desorption/Ionization
LUMO	Lowest Energy Unoccupied Molecular Orbital
M	Molar
MALDI-TOF	Matrix Assisted Laser Desorption/Ionization-Time of Flight
MO	Molecular orbital
mCPBA	*meta*-Chloroperoxybenzoic acid
MeOH	Methanol
mins	minutes
mL	milliliter
mmol	millimoles
mM	milimolar
mol	Mole
MNP	2-methyl-2-nitrosopropane
Ms	Methanesulfonyl
MS	Mass Spectroscopy
m.p.	Melting point
MW	Microwave
Na	Sodium
$NaHCO_3$	Sodium bicarbonate
Na_2SO_4	Sodium Sulfate
ng	nanogram
NH_4Cl	Ammonium Chloride

NMR	Nuclear Magnetic Resonance
N_2	Nitrogen
NOESY	Nuclear Overhauser Effect Spectroscopy
Ns	*p*-nitrobenzenesulfonyl
ORTEP	Oak Ridge Thermal Ellipsoid Plot
PAGE	Polyacrylamide Gel Electrophoresis
PCC	Pyridinium Chlorochromate
Pd	Palladium
PE	Petroleum Ether
Ph	Phenyl
ppm	Parts per million
PPTS	Pyridinium *p*-toluenesulfonate
rds	Rate Determining Step
rt	Room temperature
SDS	Sodium dodecyl sulfate
Si	Silica
t	tertiary
TBAB	Tetrabutylammonium bromide
TBS	*tert*-Butyldimethylsilyl
Tris	tris(hydroxymethyl)aminomethane
KO^tBu	Potassium tertiary butoxide
TFA	Trifluoro acetic acid
THF	Tetrahydrofuran
THP	Tetrahydropyran
TIPS	Triisopropylsilyl
TLC	Thin Layer Chromatography
Ts	*p*-toluensulfonyl
UV	Ultraviolet
vs	Versus
V	Volume
Wt	Weight

Symbols

°C	Degree celsius
Δ	Heat
hυ	Light (Irradiation)
Å	Angstrom (10^{-6})
α	Alpha
β	Beta
γ	Gamma

λ	wavelength
π	Pi
g	Gram
K	Kelvin
k	Rate constant
m	Meta
o	Ortho
p	Para
T	Temperature
µL	Microlitre
µM	Micromolar
NMR data	
ABq	AB quartet
app	apparent
s	singlet
bs	broad singlet
d	doublet
dd	doublet of doublet
t	Triplet
td	Triplet of doublet
q	quartet
m	multiplet
δ	chemical shift in ppm
J	coupling constant in Hz
Hz	Hertz
MHz	Mega hertz

Table of Contents

Chapter 1

Developments on the Mechanistic Aspects of Bergman and Garratt-Braverman Cyclization Reaction: the Diradical-Ionic Controversy

1.1 Introduction

Cycloaromatization[1] reaction involves the generation of radicals from non radical starting materials like enyne allene or enediynes (**Figure 1.01**). The reaction is endothermic but the aromatic stabilization gained after cyclization can partially make it favourable towards cyclization.

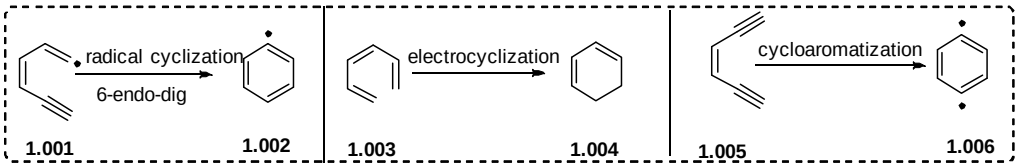

Figure 1.01: Different types of cyclization reactions

The diradicals generated during cycloaromatization reactions may either undergo self-quenching to form a new C-C bond or may abstract hydrogen from external hydrogen atom donor. Among various cycloaromatization reactions, Bergman cyclization deals with enediyne cyclization to give rise diradical that needs external sources for quenching whereas Garratt-Braverman cyclization involves the cyclization of bis-propargyl precursors to diradicals that undergo intramolecular quenching. Both the reactions are C-C bond forming reactions and are useful in synthesizing polyaromatic compounds, natural products and their mimics.

1.2 Bergman cyclization

Bergman cyclization[2], a typical example of cycloaromatization reaction is the rearrangement of cis 1,5-hexa-diyn-3-ene (**1.007**) to produce 1,4-didehydrobenzene (**1.008**) that can either revert back to starting material or can give rise to the rearranged product (**1.009**). In presence of an external hydrogen donor the reaction ends up with the formation of benzene (**1.010**) after radical quenching (**Scheme1.01**).

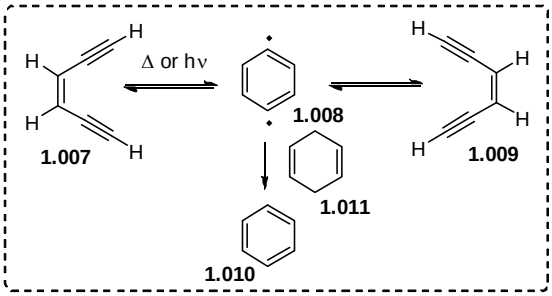

Scheme 1.01: Schematic representation of Bergman cyclization

The reaction provides low yield of products due to competing polymerization reactions. However, its unique H· abstraction ability from double stranded DNA as

well as proteins and subsequent apoptosis makes it a suitable candidate for designing therapeutic agents.[3] Such examples includes naturally occurring enediynes like Calicheamicin and Dynemicin (**Figure 1.02**) where the enediyne moiety is locked for safe delivery of the drugs to the target and the cyclization is triggered either *via* change of hybridization or by opening of an epoxide ring.

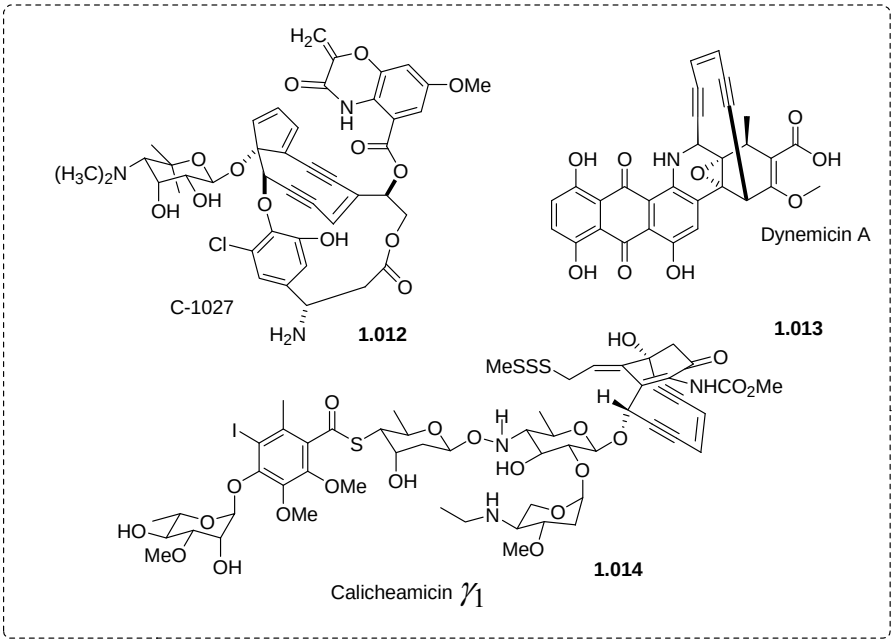

Figure 1.02: Naturally occurring enediynes

1.3 Garratt-Braverman cyclization

Heteroatom substituted bis-allenes give rise to a different variant of cycloaromatization reaction namely Garratt-Braverman cyclization[4]. The substrate includes bis-alleneic sulfide, sulfoxide, sulfone, ether and protected amine that are generated upon base treatment from their corresponding bis-propargyl counterparts (**Scheme 1.02**).

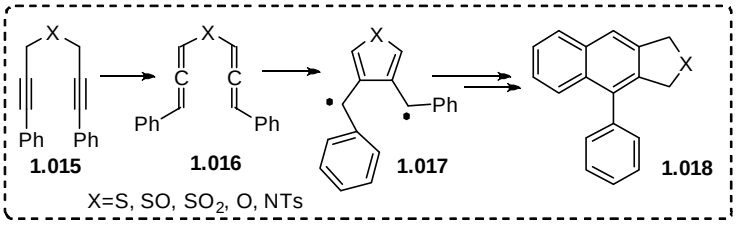

Scheme 1.02: Schematic representation of Garratt Braverman cyclization

As GBC is a self-quenching process involving the diradical, DNA damage by H· abstraction was ruled out and an alternate mechanism *via* nucleophilic addition of

DNA bases on bis-allene followed by DNA cleavage was proposed by Nicolaou *et al*. (**Figure 1.03**).[5]

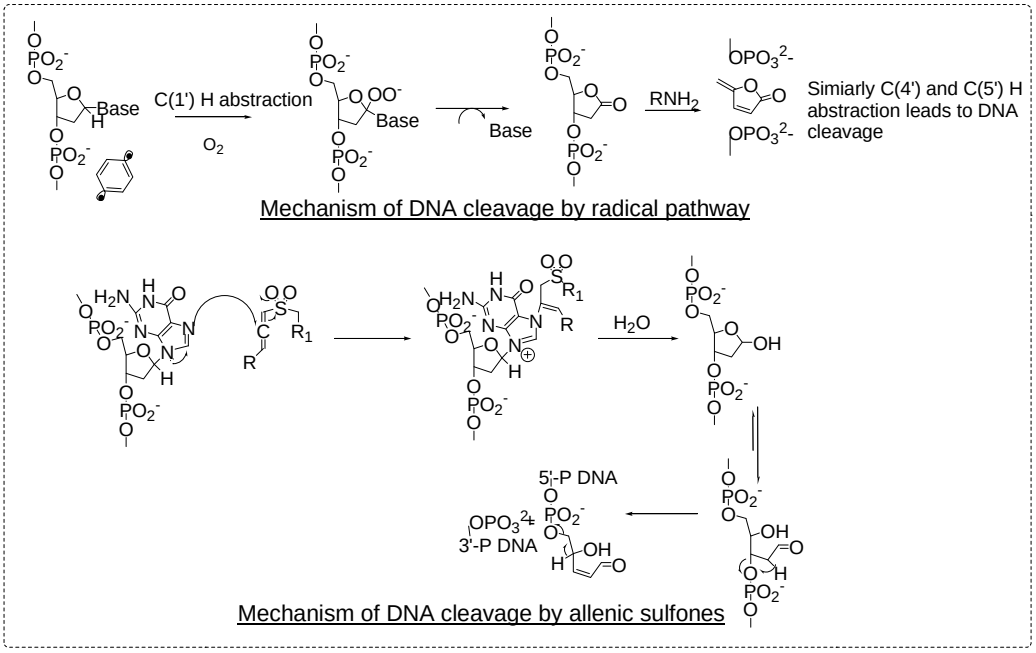

Figure 1.03: Mechanism of DNA cleavage by diradical and bis-allene

Thus, judging from the importance of development of new drugs associated with antitumor properties, it is important to be acquainted with mechanistic aspects of cyclization chemistry of enediyne and bis-propargyl systems.

In this review, we would like to discuss about the developments on the mechanistic aspects of Bergman and Garratt-Braverman cyclization reaction. The most accepted mechanism for both of these cycloaromatization reactions is *via* a radical pathway but there are reports of involvement of an ionic mechanism as well.

1.2.1 Sequential developments on the mechanistic aspects of Bergman cyclization

In 1972 Bergman and Jones reported[2a,2b] that cis 1,5-hexadiyn-3-ene **1.019** on pyrolysis at 300 °C undergo thermal rearrangement to **1.022** where deuterium was completely scrambled in acetylenic and vinylic position of **1.019** without contamination of compound **1.020** and **1.021** (**Scheme 1.03**).

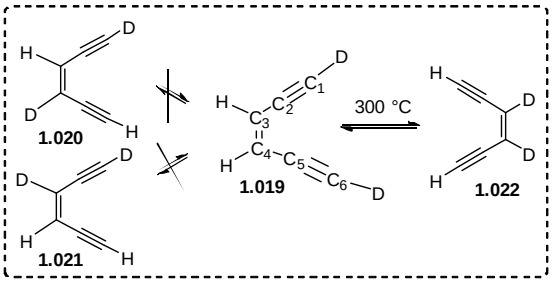

Scheme 1.03: Isotope labeling study with enediynes

The reaction was believed to proceed *via* a C_2 symmetric intermediate or transition state that rendered C-1, C-3 and C-4, C-6 chemically equivalent. The structures of intermediate or transition state were best represented as follows where each of them possesses a C_2 axis (**Figure 1.04**).

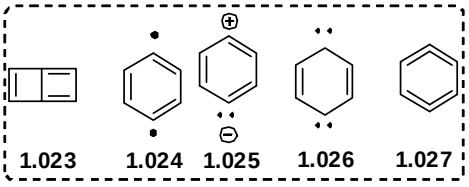

Figure 1.04: Probable structure of C_2 symmetric intermediate

The intermediate rather than transition state was proposed as 1,4-benzene diradical **1.024** based on the trapping of the radical by carrying out the pyrolysis of **1.007** in solution in presence of 0.01M 2,6,10,14-tetramethylpentadecane that yielded benzene. The fact was further supported by the isolation of *p*-dichlorobenzene when the reaction was performed in CCl_4. Besides when the reaction was carried out in MeOH, where MeOH can either act as a nucleophile or H atom donor, it ended up with the formation of benzene and benzyl alcohol as minor product rather than anisole (**Scheme 1.04**).

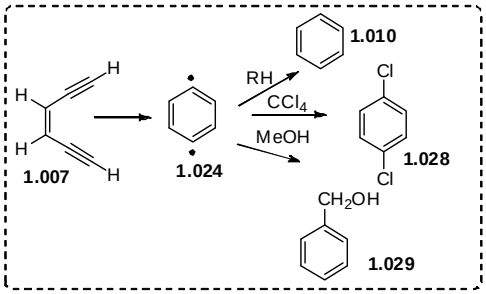

Scheme 1.04: Radical trapping with polar and non polar reagents

All the above observations were in conformity with the intermediacy of 1,4-benzene diradical during Bergman cyclization. The heat of formation and the activation energy of the diradical were calculated to be +140 Kcal/mol and 32 Kcal/mol respectively.

Parrallely, Masamune's group in 1973 reported[2f] that compound **1.030** and **1.035** on treatment with sodium methoxide afforded **1.033** and **1.038** that was best explained to be formed *via* the diradical intermediate **1.032** and **1.037** as shown in **Scheme 1.05**.

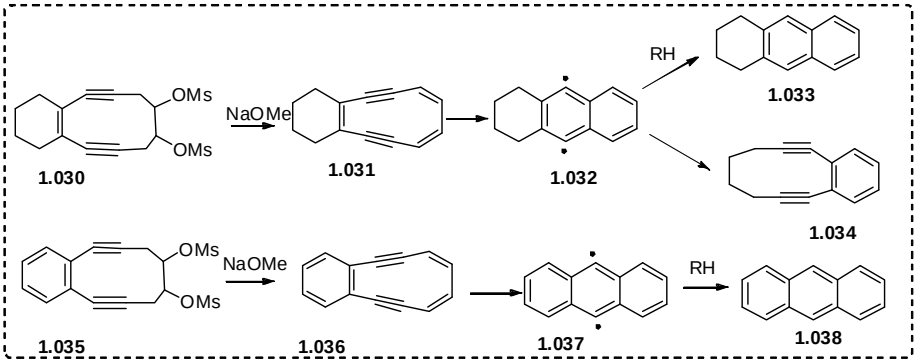

Scheme 1.05: Schematic representation of Masamune Bergman cyclization

Consecutively, Hoffmann, Imamura and Hehre by using Hückel molecular orbital theory predicted that conversion of **1.007** to diradical **1.024** is a symmetry allowed process and a coupling interaction existed between the two radicals but considering the repulsion between C-1 and C-4 it was inferred that no true σ bond existed between them thus, discarding butalene structure **1.023**. Indeed the energy gained from formation of the σ bond could not compensate the strain energy of the cyclobutene ring introduced after bond formation which is also antiaromatic in nature. Later Hoffmann and Gheorgiu by using more advanced method comprehended the ground state of the 1,4-diradical as triplet state although no spectroscopic evidences could be provided.[2b]

Due to the inconveniences associated with handling of cis 1,5-hexadiyn-3-ene **1.007** towards air sensitivity and polymerization even at 30 °C, later Bergman *et al*. in 1981 introduced *n*-Pr and Et substitution at C-3 and C-4 position of **1.007** for mechanistic studies[2c] associated with 1,4-benzene diradical formation. Both gas and solution phase reactivity was checked for them. For gas phase thermal rearrangement, **1.039** produced unimolecular products along with the isomeric enediyne **1.040**. In case of solution phase reactivity **1.039** was heated at 196 °C in presence of diethyl

ether, chlorobenzene or benzene that gave rise to the formation of **1.040**, **1.041**, **and 1.042** in reasonable yields (**Scheme 1.06**).

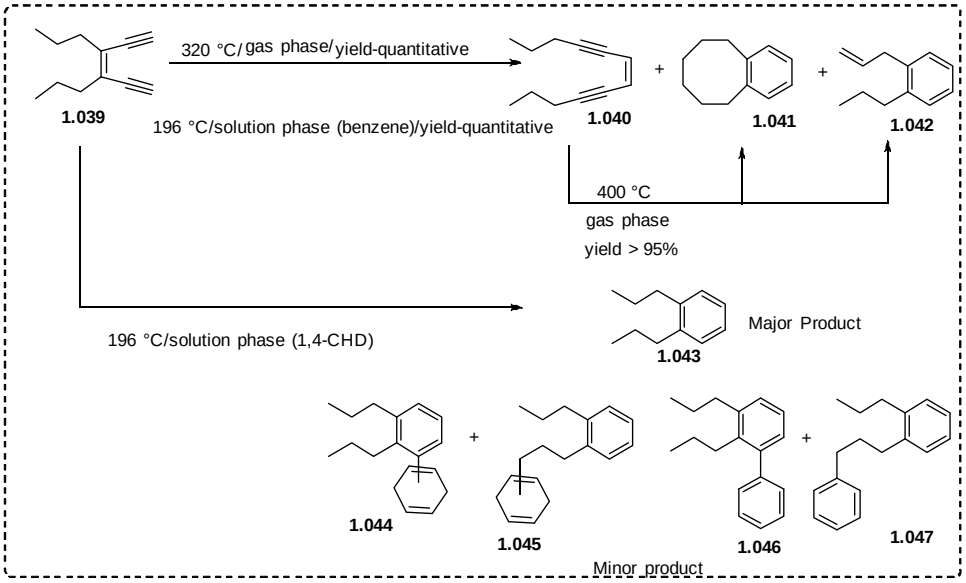

Scheme 1.06: Differences in gas and solution phase reactivity of n-propyl substituted enediyne

In presence of trapping agents 1,4-CHD and 9,10-dihydoanthracene which are good hydrogen donors, a new product **1.043** formed in high yield along with some high molecular weight products **1.044-1.047**. Subsequently, reaction performed with 1,4-CHD-d_4 yielded **1.048-1.050** (**Scheme 1.07**).

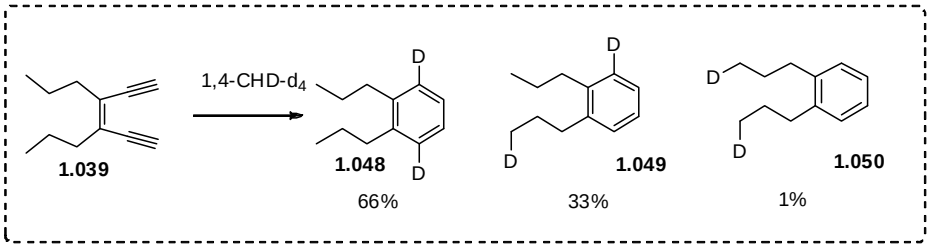

Scheme 1.07: Deuterium scrambling experiment

The most acceptable mechanism[2c] that can explain all these observations were depicted as follows (**Scheme 1.08**) *via* the intermediate formation of *p*-benzyne **1.051** that further rearranged to **1.052** and **1.053** by 1,5-H shift to produce more stable radical **1.053** *via* a favourable six membered transition state.

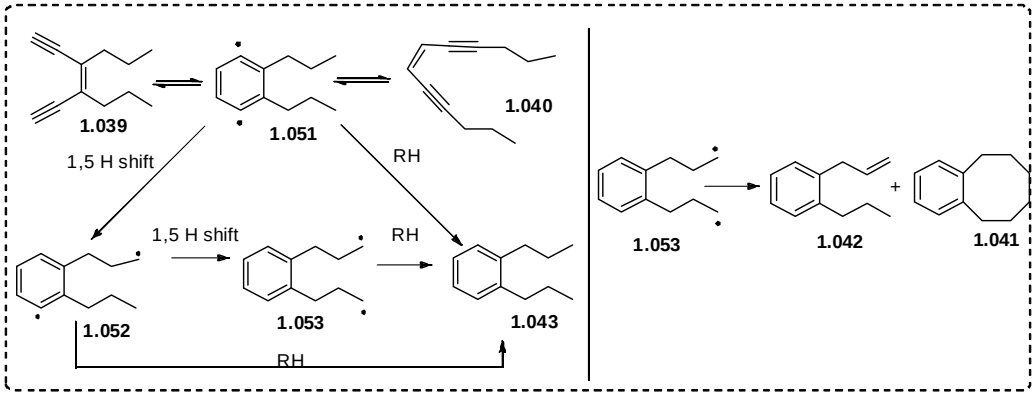

Scheme 1.08: Mechanism of alkyl diradical formation from aryl diradical

The existence of the intermediate diradical **1.053** was further proved by CIDNP by heating **1.039** at 160 °C in the probe of an NMR spectrometer. Several emissive signals were observed corresponding to the vinyl protons of **1.042** that was formed from **1.053**.

In 1993, Grissom *et al.* synthesized[6] a variety of enediynes **1.054-1.060** and trapped the intermediate 1,4 diradical, intramolecularly by a radical trapping alkene functionality attached to the molecule itself to give 2,3-dihydrobenz[*e*]indene **1.061-1.067** or tetrahydrophenanthrene derivative **1.069** (**Scheme 1.09**) .

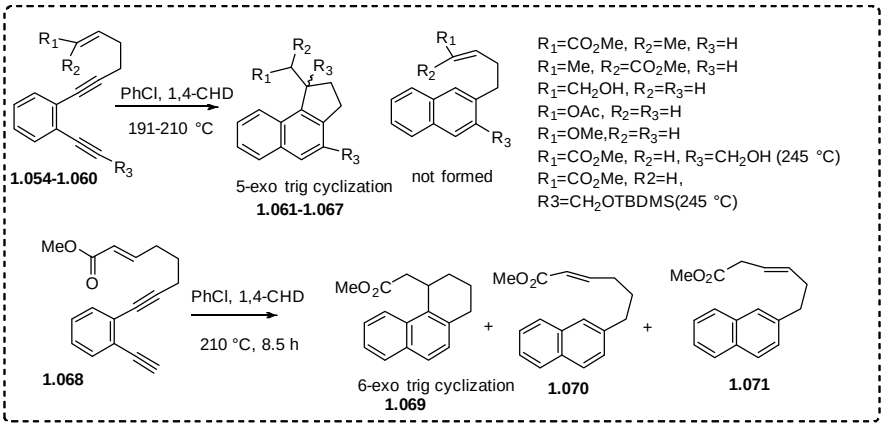

Scheme 1.09: Intramolecular radical trapping with an alkene appended to enediyne

It appeared that 5-exo cyclization was much faster than 6-exo cyclization and the intermediate **1.072** could not be trapped by increasing concentration of external radical quencher 1,4-CHD. Three different reaction mechanisms as depicted below (**Scheme 1.10**) were proposed that were suitable with all these observations.

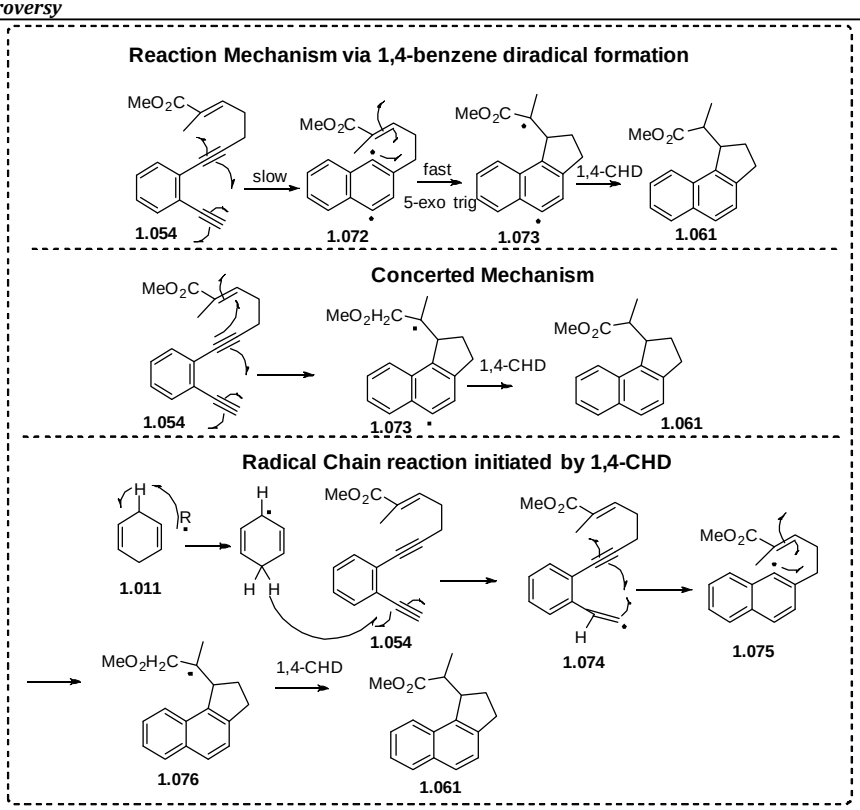

Scheme 1.10: Mechanism of cyclization

If the reaction followed radical chain mechanism then increased concentration of 1,4-CHD would increase the reaction rate as it would come into *rds* and also changing the electronic nature of alkene functionality would make an impact on rate if the reaction proceeded in a concerted manner. Both these two phenomena discarded radical chain reaction and concerted mechanism for cyclization and revealed 1,4-benzene diradical formation to be the *rds* of the reaction which was also supported from the formation of *β*,*γ* unsaturated ester **1.071** produced by abstraction of allylic H to more stable allylic radical than phenyl radical.

Subsequently, in 1994 Grissom *et al.* reported[7] that substitution at the acetylenic end of the enediynes had an effect on increasing the activation energy barrier of Bergman cyclization. The reaction followed first order kinetics with formation of 1,4-benzene diradical as *rds* of the reaction. The activation energies calculated for different systems are summarized as follows (**Figure 1.05)**

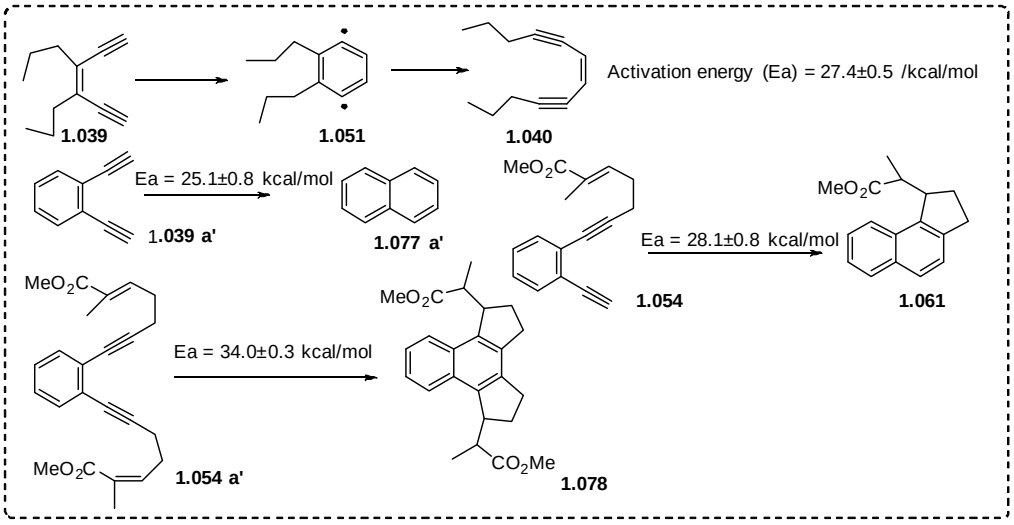

Figure 1.05: Activation energy of enediynes

Due to higher energy requirement in thermal rearrangement of enediynes, researchers then turned attention to cyclization through photochemical triggering. Taking into account of the fact Sankararaman *et al*. in 1996 synthesized[8] a series of compounds **1.079-1.080** and subjected them to photo irradiation condition that gave rise to 1,5-cyclized product **1.081-1.082**. All these products were predicted to be formed *via* symmetry allowed process in spite of 1,6 mode of Bergman cyclization. Similar results were obtained from chemical and electrochemical oxidation of enediyne **1.079, 1.080** that pointed out the involvement of radical cation species **1.083** during cyclization (**Scheme 1.11**).

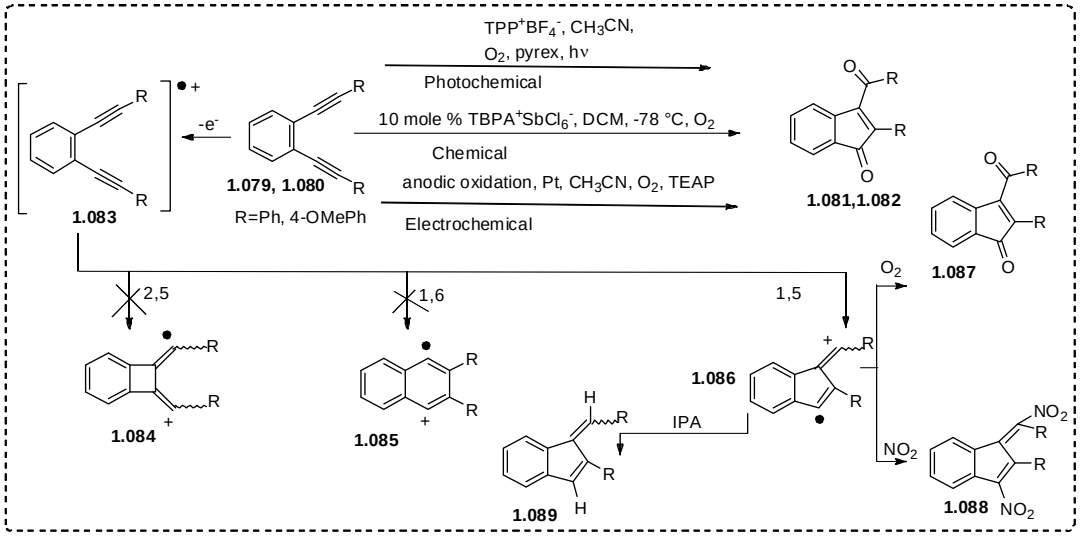

Scheme 1.11: Photochemical oxidation of enediynes to indene derivative

The intermediate radical cation was trapped by IPA (isopropyl alcohol) as well as by ESR in presence of N-*tert*-butyl-α-phenylnitrone during photolysis of **1.079** in CH_3CN at room temperature.

In 1997 Kerwin[9] *et al*. synthesized C, N-dialkynyl imines **1.090-1.091** and studied their outcome under thermal reaction condition (**Scheme 1.12**). Though they named it as Aza-Bergman cyclization considering the similarities regarding unchanged reaction rate with solvent polarity and first order with respect to substrate concentration, the reaction had a lot of dissimilarities including the reaction condition as well as the nature of products *i.e*. the exclusive formation of nitriles **1.093, 1.094** *via* retro Bergman ring opening reaction. It was assumed that the intermediate could possess other structures **1.097**, **1.098** rather than discrete 1,4-diradical **1.092**.

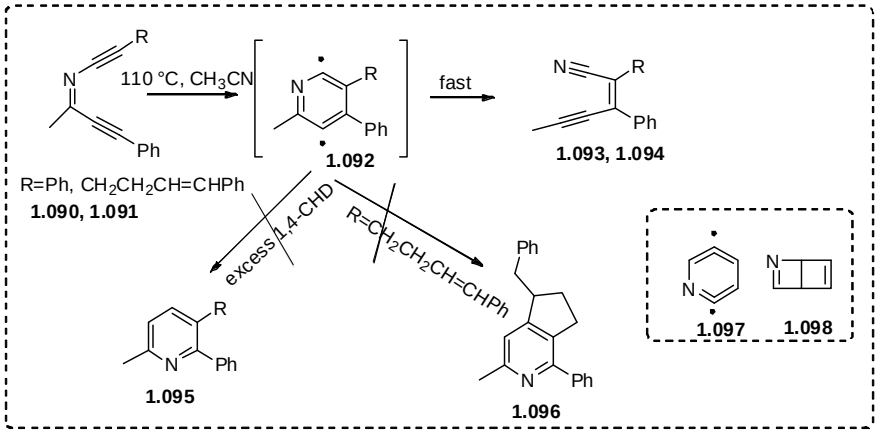

Scheme 1.12: Bergman cyclization of aza enediynes to enyne nitriles

In 1998 as an extension of the previous work Chen and his co-workers[10] trapped the intermediate 2,5-didehydropyridine diradical intermediate **1.101** but in presence of an acid (**Scheme 1.13**). It was shown by theoretical calculations that for the aza-enediynes the singlet-triplet energy gap increased than *p*-benzyne which further decreased the probability of hydrogen abstraction as well as decreased the activation energy barrier for retro Aza-Bergman ring opening. This observation had a large impact on anti-tumour drug designing at low pH based upon resistance of aza enediynes to abstract H· after cyclization.

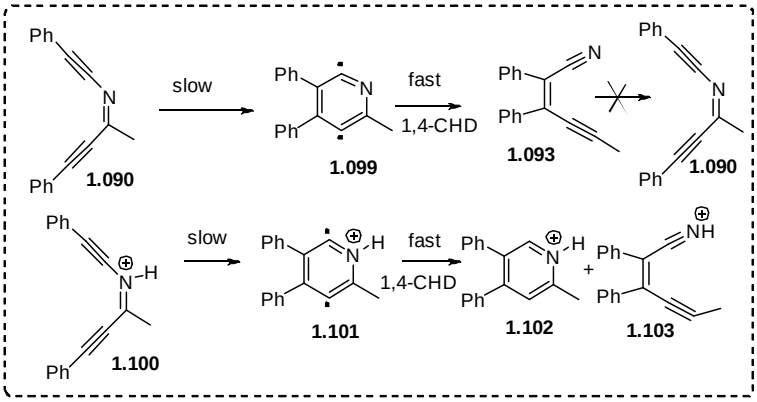

Scheme 1.13: Bergman cyclization of protonated aza enediynes

In view of photodynamic therapy to develop anticancer drugs researchers then shifted their attention to attain photoinduced Bergman cyclization. In 1998 Turo *et al.* reported[11] cyclization of two differentially substituted enediynes **1.104**, **1.105** by photo irradiation in presence of *i*-PrOH that produced reduced products **1.107, 1.108** along with expected Bergman cyclized product **1.106**, **1.109** (**Scheme 1.14**).

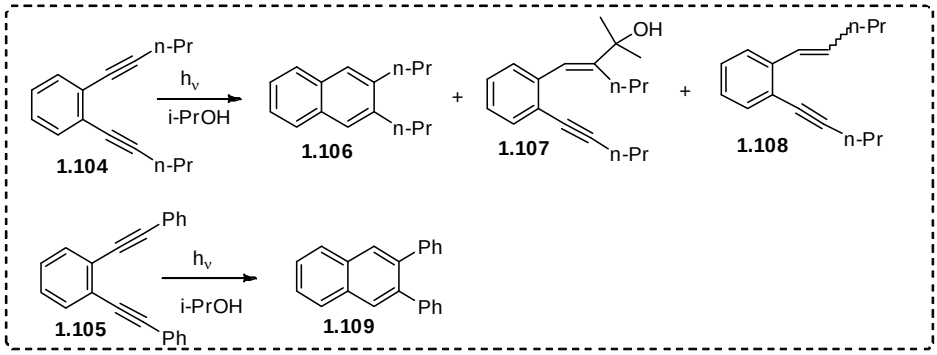

Scheme 1.14: Photoreduction and Bergman cyclization of enediynes

The rationale behind such observation was proposed as **1.105** underwent cyclization from singlet state *via* the formation of 1,4-diradical intermediate whereas for **1.104**, the cyclized product was obtained from the singlet state and the reduced products were formed from triplet state by an intersystem crossing from singlet state. The fact was further supported from the observation of increased acetylenic reduced product **1.107**, **1.108** in presence of triplet sensitizer xanthone whereas enediyne **1.105** failed to react under that condition. The presence of bulky Ph substituents at the acetylenic end interfered the singlet to triplet intersystem crossing for **1.105** that was also reflected from the higher fluorescence quantum yield of the substrate.

The ring closure of enediynes to 1,4-diradical formation was considered to be the rate determining step (*rds*) of the reaction. In 1999 Koseki *et al.*reported[12] that benzannelation changed the *rds* of Bergman cyclization from cyclization step to H· abstraction (**Scheme 1.15**).

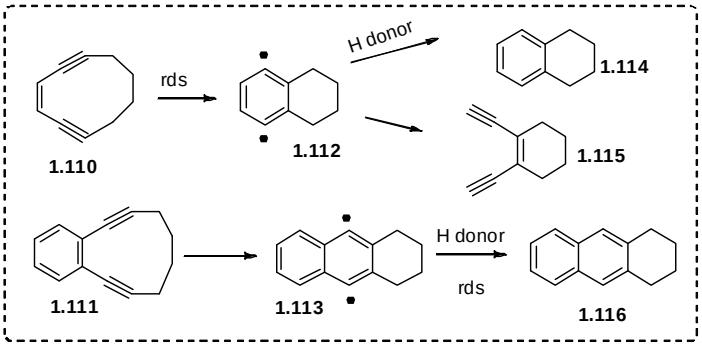

Scheme 1.15: Benzannelation effect on reaction mechanism

The reason behind the fact was first considered to be the singlet-triplet energy gap. Later it was confirmed from theoretical calculations not to be the actual scenario but the differences of activation energy barrier of retro Bergman cyclization and H· abstraction pathway for the two different systems.

In 2001 Jones and Warner[13] performed Bergman cyclization in aqueous buffer, a catalytic antibody, O_2 and ended up with a substituted *p*-benzoquinone product **1.120**-**1.122** *via* trapping the intermediate 1,4-diradical. The rate of the reaction increased with increasing concentration of O_2 indicating 1,4 diradical quenching with O_2 to be the *rds* of the reaction. Two different mechanisms were proposed i) 1,4 diradical formation and subsequent quenching with oxygen or ii) the enediyne itself reacted with oxygen followed by cyclization (**Scheme 1.16**). The later process was discarded due to higher energy requirement.

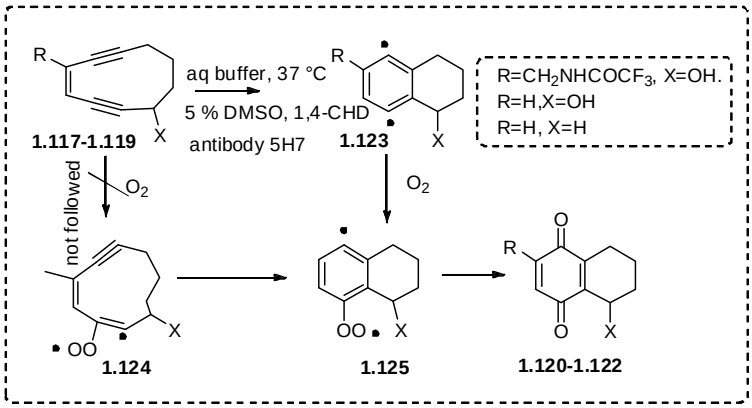

Scheme 1.16: 1,4-diradical trapping with triplet oxygen

In 2002 Alabugin *et al.* studied[14] the outcome of tetrafluoropyridinyl enediynes **1.126-1.129** under photochemical reaction condition. In contrast to the C1-C6 mode to six membered ring formation, the reaction yielded indenes **1.134-1.137** *via* C1-C5 mode of cyclization through a fulvene intermediate (**Scheme 1.17**).

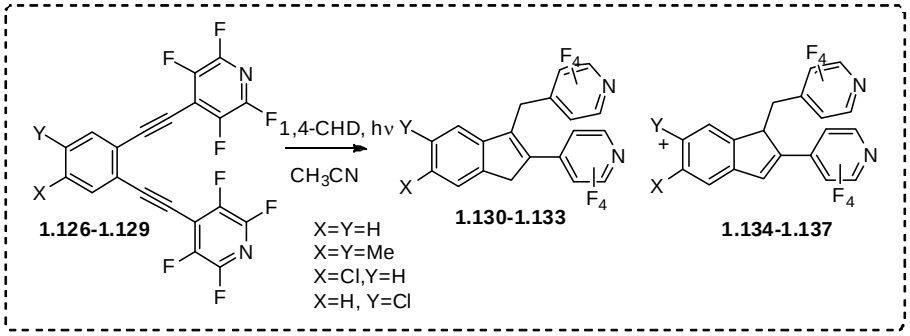

Scheme 1.17: C1-C5 mode of cyclization of tetrafluoropyridinyl enediynes

The rate of ring closure for tetrafluoropyridinyl enediynes were observed to be higher than corresponding phenyl rings and also the photochemical reaction failed to occur in presence of good hydrogen donor solvents like *i*-PrOH. The mechanism proposed with all these observations was *via* the involvement of a radical anion **1.138** (stabilized by tetrafluoropyridinyl moiety) to a stabilized cyclopentadienyl anion **1.140** and subsequent proton quenching by 1,4-CHD (**Scheme 1.18**).

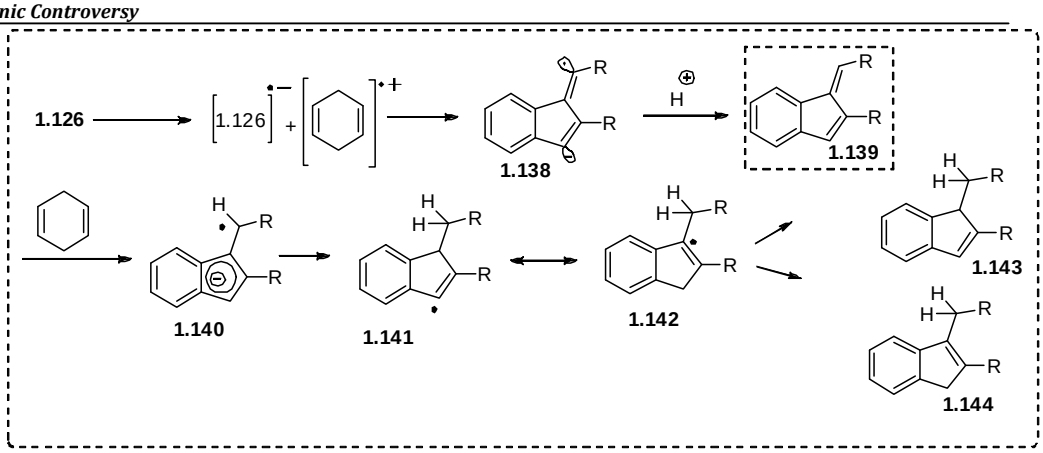

Scheme 1.18: Reaction mechanism *via* radical anion pathway

It was a challenge for the researchers to force acyclic enediynes to undergo Bergman cyclization under ambient condition. In 2002, O'Connor *et al.* reported Ruthenium mediated cyclization of acyclic enediynes **1.145** and **1.146** which were otherwise difficult to cyclize. The reaction mechanism involved complexation followed by Bergman cyclization (**Scheme 1.19**).[15]

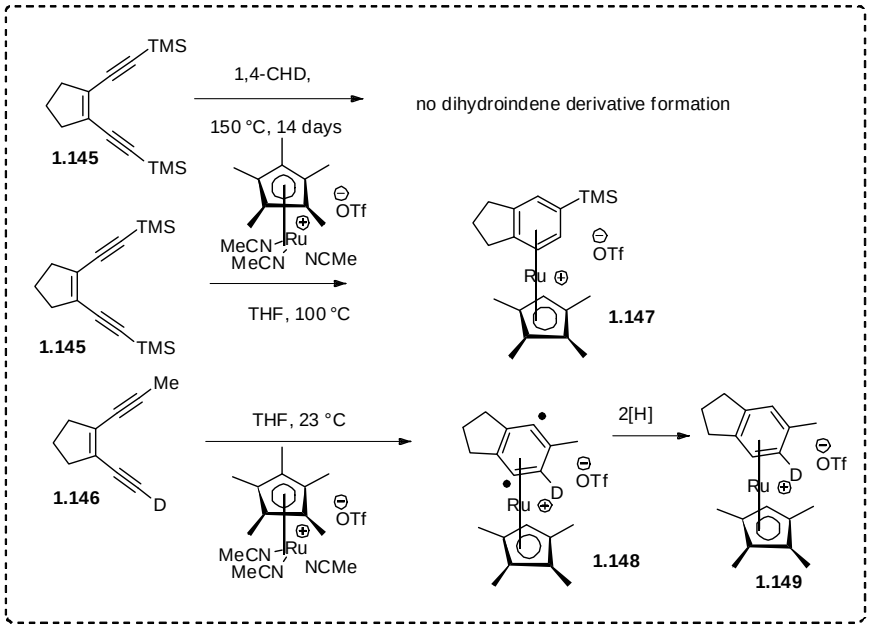

Scheme 1.19: Ruthenium mediated Bergman cyclization

Subsequently, in 2002, Alabugin *et al.* showed[16] the increased rate of Bergman cyclization of benzannelated enediynes by suitable electron donating substituents at *ortho* position. Like for –OMe, the intermediate diradical was stabilized by abstraction of H atom intramolecularly. Thus, the radical got stabilized and prevented the ring opening reaction to make the cyclization irreversible.

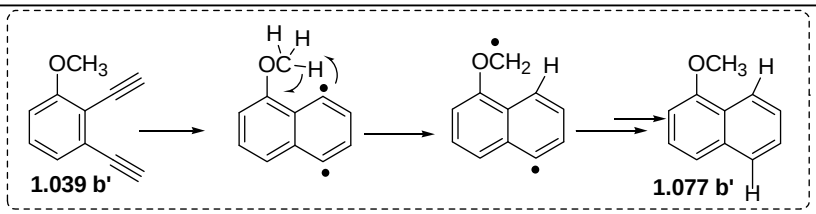

Scheme 1.20: Effect of substituents on benzannelated enediyne ring closure

In 2003, Kerwin[17] *et al.* attempted to trap 2,5-didehydropyridinium intermediate from Bergman rearrangement of 3-aza enediynes **1.150** with TfOH in presence of 1,4-CHD. They ended up with the formation of *β*-alkynylacryonitrile (**1.153**) products along with a formation of cyclopropane derivative of 1,4-CHD **1.154** from 5-oxazolylcarbene (**Scheme 1.21**).

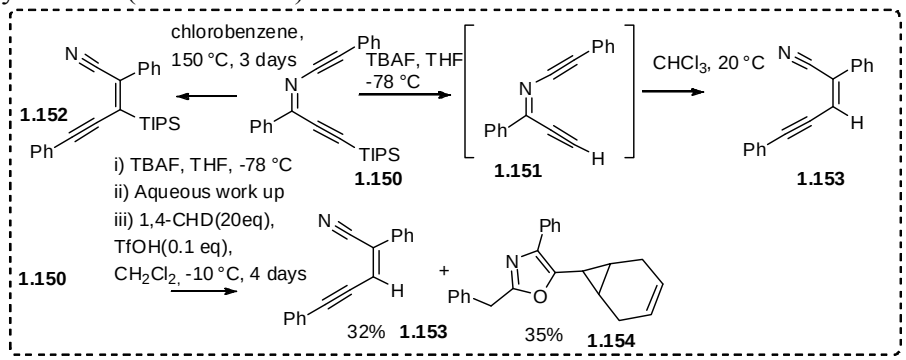

Scheme 1.21: Ring opening of aza enediynes and carbene formation

The reaction was believed to proceed *via* intermediate carbene **1.156** formation that added to 1,4-CHD (**Scheme 1.22**).

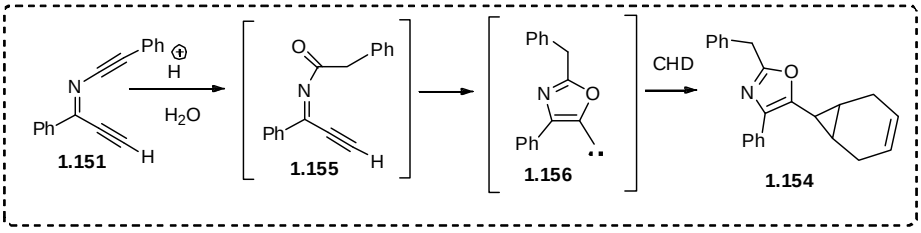

Scheme 1.22: Mechanism of carbene formation

In 2004 Smith, Jr. and Echegoyen *et al.* first time accomplished[18] EPR spectra of 1,4 diradical **1.162** during enediyne cyclization of bis-*ortho*-diynyl-arene (BODA) monomers **1.157-1.161** (**Scheme 1.23**). They reported that the rate of cycliation of enediynes was faster for pyridine and thiofene substituted enediynes probably because of decreased repulsion of incoming π-orbital in the cyclic transition state.

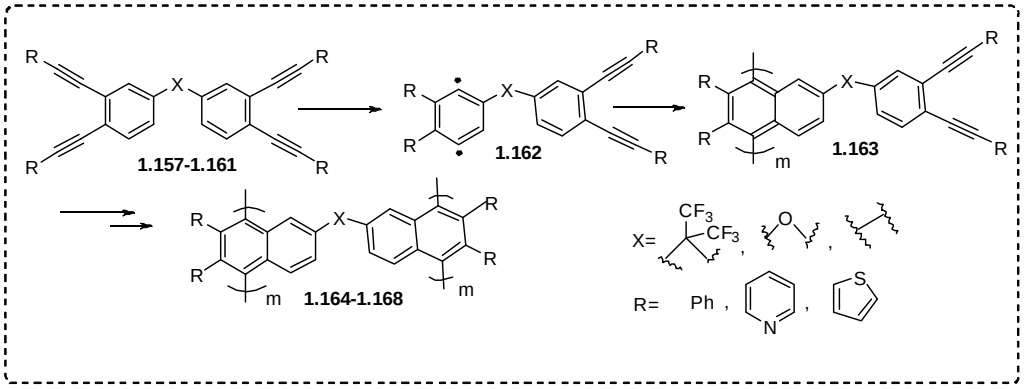

Scheme 1.23: EPR recognition of 1,4-carbon diradical

In 2004 Lear, Hirama, Akiyama *et al*. reported[19] ^{13}C labeled spin trapping of *p*-benzyne intermediates **1.169a**-**1.169c** generated during Bergman cyclization of cyclic enediynes (**Scheme 1.24**). The transient ^{13}C labeled diradical was reacted with 2-methyl-2-nitrosopropane (MNP) and 5,5-dimethyl-1-pyrrolidine *N*-oxide (DMPO) and the mono adducts **1.171**, **1.173** were detected by MALDI-TOF MS and EPR spectra where the signal for radicals coupled with ^{13}C nucleus were observed.

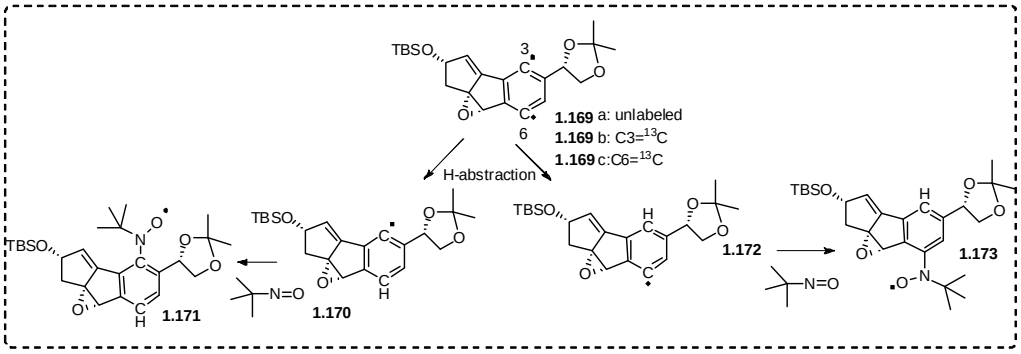

Scheme 1.24: EPR recognition of ^{13}C labeled monoadduct with MNP and DMPO

In 2005 Matzger *et al*. reported[20] the Bergman cyclization of sterically demanding enediyne **1.174** and observed a regular product **1.176** along with rearranged products **1.177**, **1.178**. The initially formed 1,4-diradical **1.175** underwent radical shift to *ortho* and *para* diradcals that were assumed to be more stable as well as to avoid the steric repulsion between two Ph groups (**Scheme 1.25**).

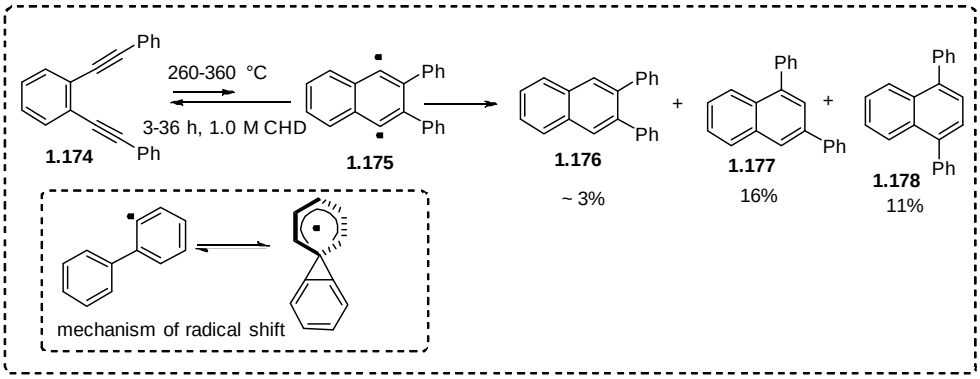

Scheme 1.25: Rearrangement of phenyl diradical

In 2006 Usuki and Ellestad *et al.*studied[21] the spin trapping of naturally occurring enediyne Calicheamicin γ_1^I and reported the EPR spectra of mono adduct **1.180**, **1.181** with *t*-butyl nitrone (**Scheme 1.26**). It was observed that phenyl *tert*-butyl nitrone (PBN) trapped C-3 radical more easily than C-6 radical.

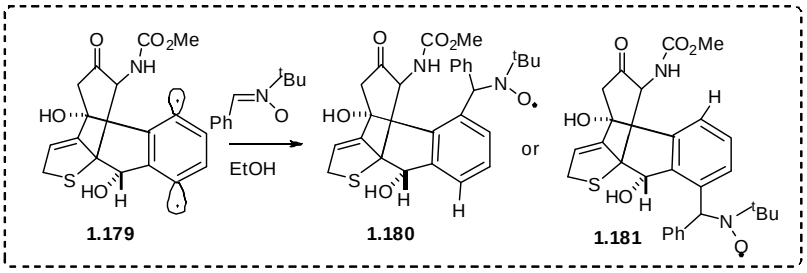

Scheme 1.26: EPR recognition of mono adduct with PBN

Although the most accepted mechanism of Bergman cyclization was by the involvement of radical intermediate, O'Connor and Perrin *et al*. in 2007 reported[22] ionic mechanism of Bergman cyclization *via* halide addition to enediyne **1.182** in presence of lithium halide and a weak acid. They proposed a mechanism based on singlet diradical **1.183** formation and subsequent mono halide incorporation. There interpretation was based on the kinetic studies that showed the rate of the reaction to be first order with respect to the concentration of enediyne and also independent of the concentration of acid and halides. A second mechanism was proposed involving an ionic intermediate **1.186**.

The fact of contribution from ionic intermediate may be further reinforced by the observation based on fast retro Bergman cyclization of aza enediynes as reported by Kerwin and his co-workers (**Scheme 1.27**). The diradical intermediate **1.189** might have stabilized by the interaction with nitrogen lone pair and that increased the

resonance contribution of the zwitterionic form of the singlet wave function.[1a,23] As a result, singlet-triplet energy gap increased that decreased the feasibility of H· abstraction.

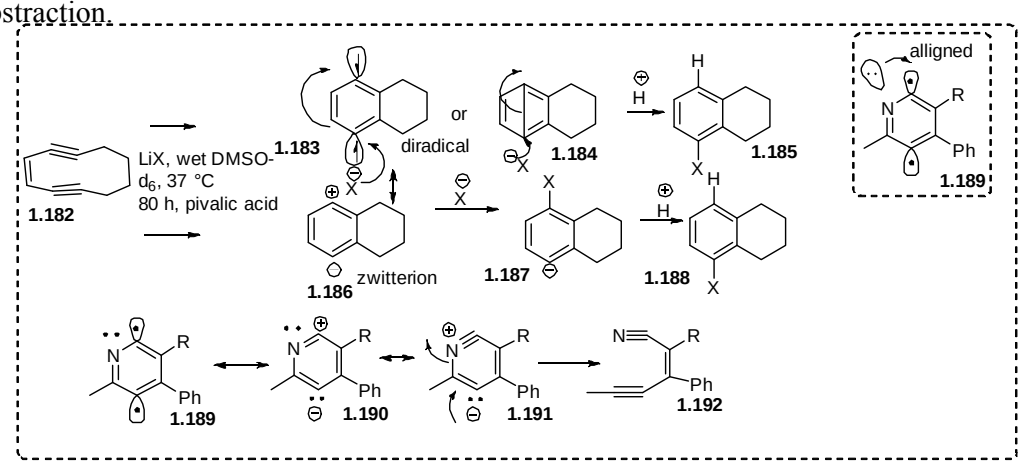

Scheme 1.27: Radical and Ionic dichotomy of Bergman cyclization

In 2010 Alabugin *et al.* showed[24] the mechanism of fragmentation of carbohydrate moiety of Esperamicin A_1 upon Bergman cyclization that ultimately led to the resistance of the enediyne. They showed the mechanism with a model compound **1.193** having THP molecule attached beside *p*-benzyne. Upon cyclization it underwent 1,4-diradical **1.194** formation that further abstracted H· intramolecularly from the anomeric position of THP moiety and subsequent fragmentation (**Scheme 1.28**). The method indirectly proved the involvement of 1,4-benezene diradical formation during Bergman cyclization.

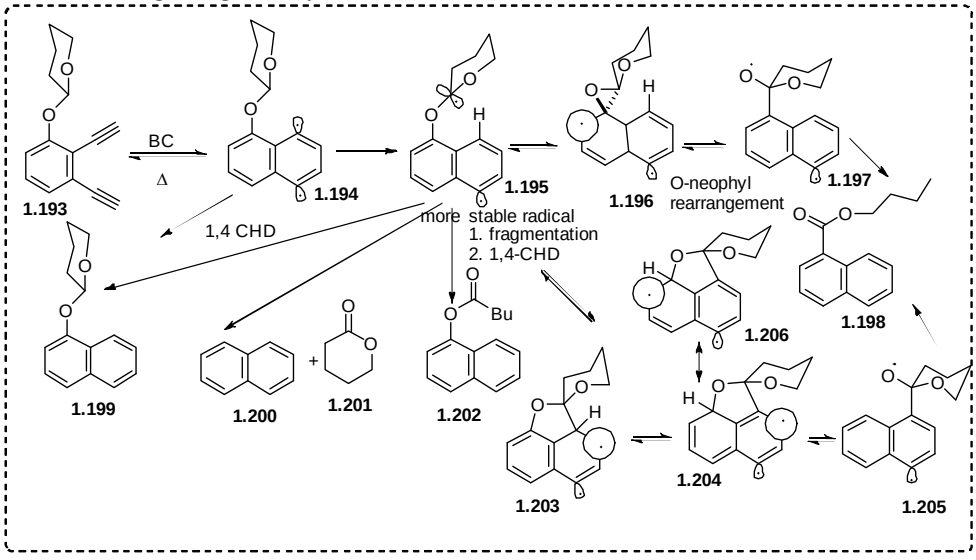

Scheme 1.28: Fragmentation of sugar pendant by anomeric H· abstraction

Enediynes attached with a peptide (**1.207-1.211**) undergo Bergman cyclization to give an eliminated product 2,3-dihydrobenzo-[*f*]isoindoles (**1.213-1.217)** as reported by Jerić *et al.*in 2010 (**Scheme 1.29**).[25] The importance of this discovery was in the fact that enediyne peptide conjugate cannot be taken for any model study of Bergman cyclization.

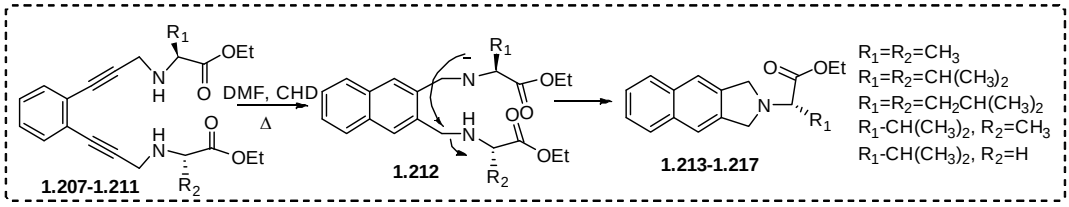

Scheme 1.29: Elimination of peptide enediynes to isoindoles

Substitution of one of the carbon by nitrogen in cyclic enediyne **1.218** changed the outcome of Bergman cyclization depending on ring size as was reported[26] by Popik *et al*. in 2010. In spite of conventional product *via* Bergman cyclization, the reaction followed an ionic mechanism to cycloaromatization along with addition of nucleophilic solvent to the triple bond (**Scheme 1.30**).

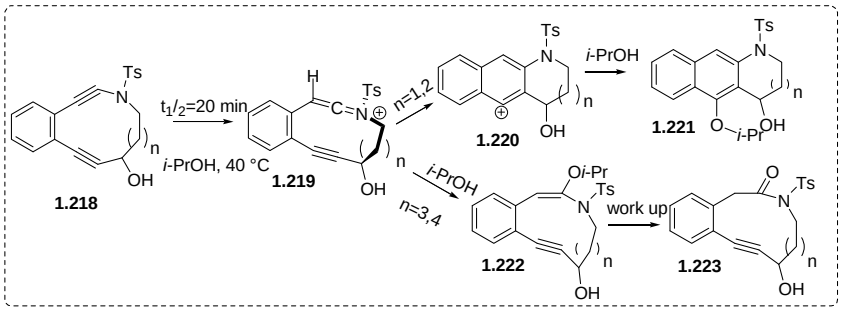

Scheme 1.30: Intermolecular ionic addition of *i*-PrOH

In 2011 Basak *et al*. reported[27] tandem radical cyclization of aryl alkeny N-substituted enediyne **1.224-1.228** to *ortho*fused polyaromatic [4] helicenes **1.233-1.237** (**Scheme 1.31**). The reaction was important in view of synthesis of polyaromatic compounds as well as indirect proof of radical intermediate that was trapped intramoleculary by an alkene. The initially formed 1,4 diradical **1.229** could not be quenched externally probably because of shielding by the molecular framework.

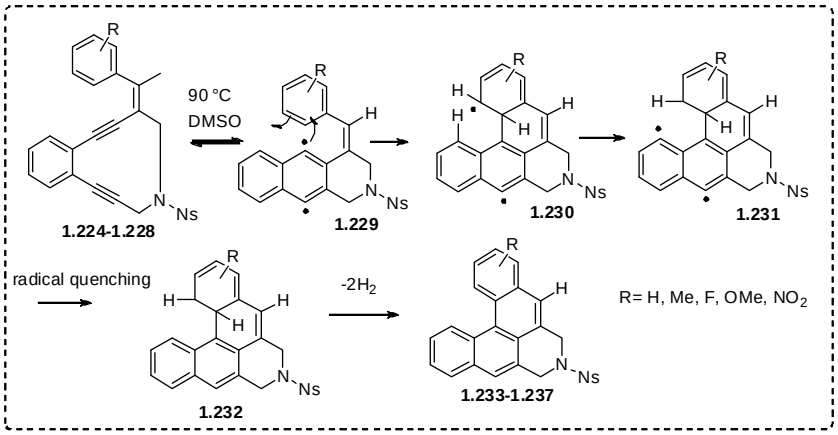

Scheme 1.31: Tandem Radical cyclization of enediynes

Kundig *et al*. in 2012 reported[28] the EPR trapping of triplet ground state of *p*-benzyne radical from Chromium tricarbonyl mediated Bergman cyclization of enediyne **1.239** that proved the intermediacy of 1,4-diradical during metal mediated Bergman cyclization (**Scheme 1.32**).

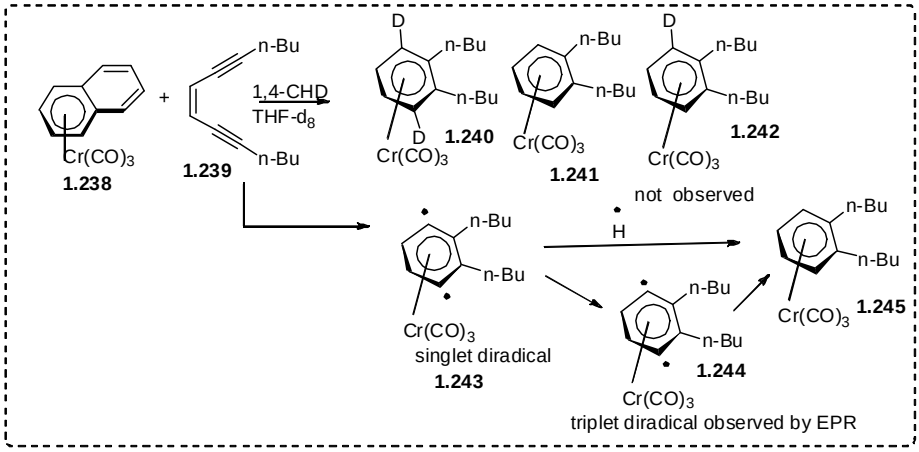

Scheme 1.32: Chromium mediated Bergman cyclization of enediynes

Recently, in 2014 Greer *et al*. reported[29] intramolecular scavenging of 1,4 diradical **1.246** from Bergman cyclization of butylated hydroxyl toluene (BHT) enediyne to form quinone methide intermediate **1.249** (**Scheme 1.33**). The reaction was believed to proceed stepwise *via* first abstraction of tolyl methyl H by C-5 radical centre to **1.248** followed by O-H abstraction by C-8 radical centre. The basis behind such proposed mechanistic pathway was greater bond energy of homolytic cleavage of O-H compared to C-H.

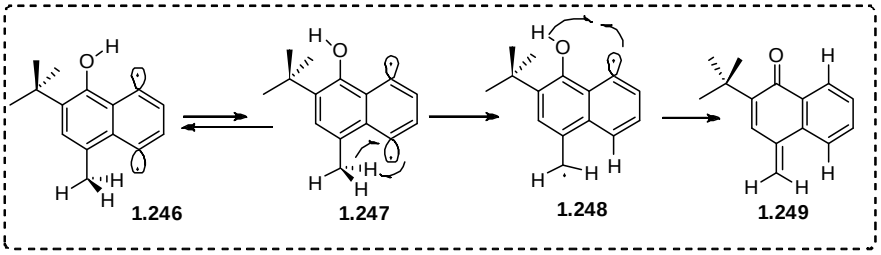

Scheme 1.33: Diradical trapping by BHT

1.3.1 Sequential Developments on the mechanistic aspects of Garratt-Braverman cyclization

In 1964 Iwai and Ide first proposed[30] rearrangement of various heteroatom substituted 1,7-diphenyl 1,6-heptadiynes **1.250** to aryl naphthalene derivative **1.256** under base catalyzed condition. The mechanism they proposed involved the formation of mono-allene **1.253** and subsequent [4+2] cycloaddition and protropic rearrangement to naphthalene derivative **1.256** (**Scheme 1.34**).

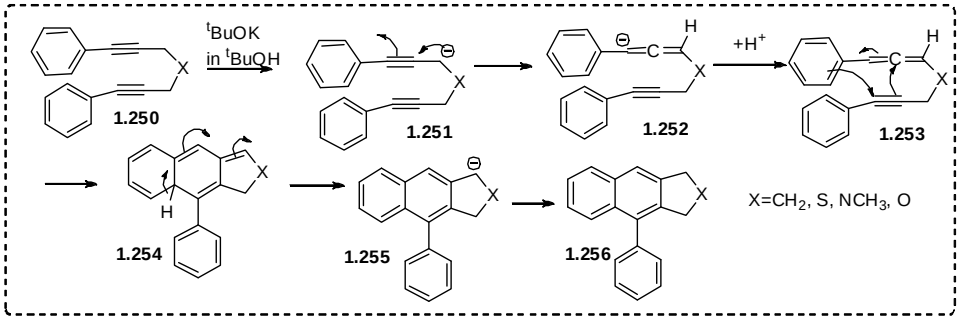

Scheme 1.34: Mechanism proposed by Iwai and Ide

In 1974 Braverman *et al*. reported[31] the thermal rearrangement of Bis-*γ*,*γ*-dimethyl allenyl sulfone **1.260** prepared from [2,3] sigmatropic shift of propargylic sulfoxylates **1.258** to 3-Isopropenyl-4-isopropylthiofene 1,l-dioxide **1.261**(**Scheme 1.35**).

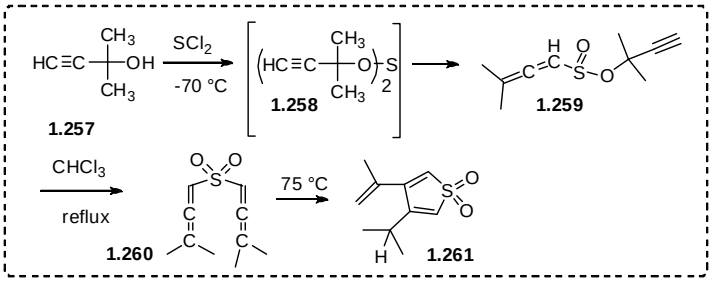

Scheme 1.35: Thermal rearrangement of bis-allenic sulfones

The rate of the reaction was insensitive towards the change of polarity of solvents. Based on this observation two different mechanisms were proposed for the reaction either i) a two step mechanism with formation of a diradical as the *rds* and subsequent hydrogen transfer to form a double bond or ii) an intramolecular ene reaction (**Scheme 1.36**). But at this stage it was not concluded about the actual mechanism involved.

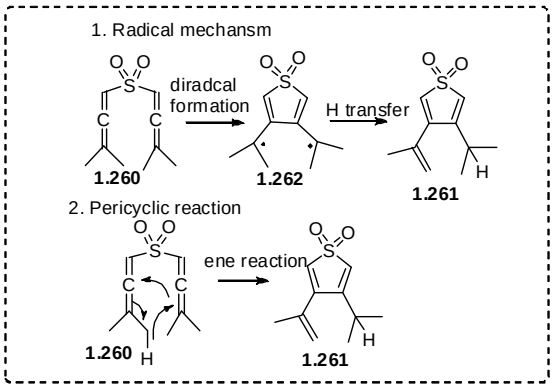

Scheme 1.36: Mechanism proposed by Braverman for thermal rearrangement of bis-allenes

With change of reaction condition and bases used for proton abstraction along with substitution pattern at acetylene termini the outcome of the reaction changed. In 1975 Garratt *et al*. reported[32] the base catalyzed rearrangement of bis-propargyl sulfides, ethers and amines represented by general structure **1.263**, **1.269** and proposed a reaction mechanism based on the formation of bis-allene **1.264/1.270**, diradical **1.265/1.271** formation and subsequent ring closure to the product (**Scheme 1.37**). Treatment of **1.263** with 14% KO^{t}Bu in *t*-BuOH gave rise to the formation of **1.268** whereas treatment with KO^{t}Bu in THF at 20 °C led to the formation of intermediate **1.267** followed by **1.268**. The formation of intermediate **1.267** confirmed the mechanism involving bis-allenes. For alkyl substituted acetylene termini **1.269** either the dimer of general structure **1.272** or the fused cyclobutane ring derivative **1.273** was the final product from the intermediate diradical **1.271** depending upon the reaction condition and substitution pattern that proved the diradical formation as an intermediate.

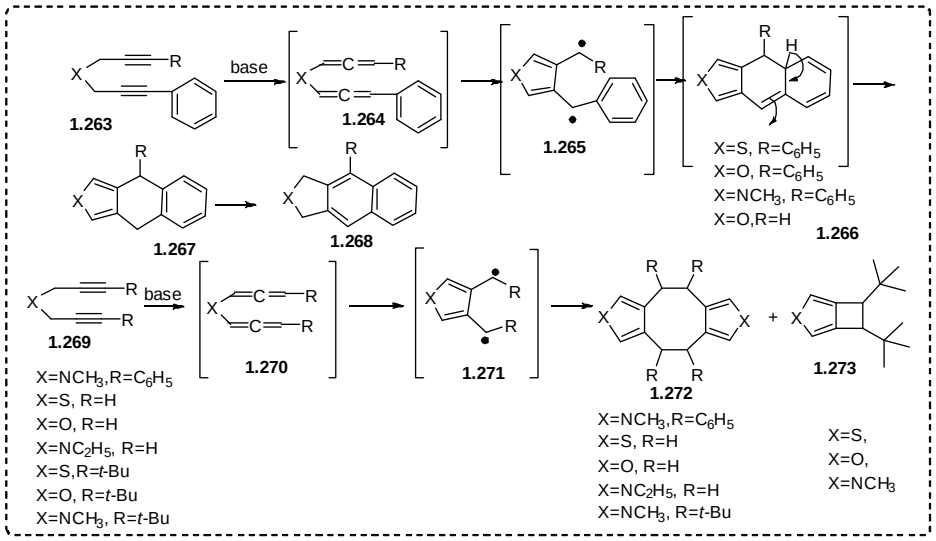

Scheme 1.37: Mechanism proposed by Garratt for heteroatom substituted base mediated cyclization of bis-propargyl systems

The bis-allene and diradical intermediate for the cyclization of bis-propargyl sulfides were further proved chemically by Garratt *et al*. in 1978. The dimer **1.282** formed upon heating of bis-propargyl sulfides with unsubstituted acetylenic termini and adduct **1.280** formation with $^3O_2$ and **1.283** with maleic anhydride confirmed the formation of bis-allene and diradical.[33] The mono-allenes prepared separately were unable to undergo any dimerization or reaction with $^3O_2$. The entire reaction outcome is schematically represented as follows (**Scheme 1.38**).

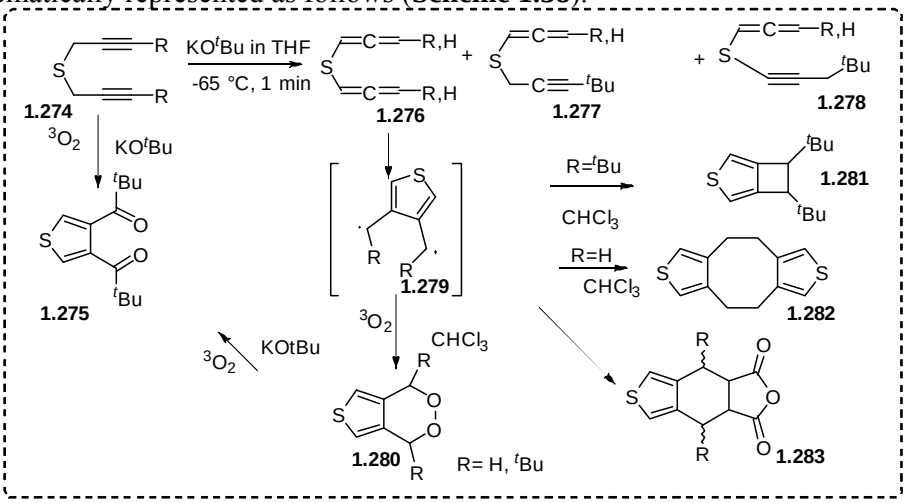

Scheme 1.38: Chemical trapping of intermediate diradical

Subsequently, Garratt *et al*. reported[4a] the isolation of 4,9-dihydronaphtho thiofene and furan intermediates that proved the diradical intermediacy during cyclization with

–Ph substituent at acetylene termini. The thiofene intermediate was further oxidised with mCPBA to the sulfone **1.284** that was thermally unstable though direct formation of sulfone intermediate **1.284** was not observed for cyclization with bis-propargyl sulfones (**Figure 1.06**).

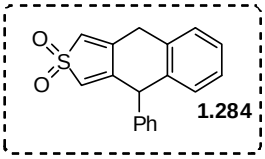

Figure 1.06: 4,9-dihydronaphtho thiofene dioxide

In 1990 Braverman *et al*. reported[34] the thermal rearrangement of heteroatom and alkyl (except *t*-Bu) substituted bis-allenes **1.290**, **1.292**, **1.294** and **1.296**. As they proposed, lack of kinetic isotope effect and unaffected rate of reaction with change of solvent polarity confirmed a two step pathway of ring closure in a slow rate determining step followed by a fast intramolecular 1,5-H transfer. The structure of the intermediate was not confirmed though they assumed to be structure **1.303**. Previously, diradical intermediates from cycloaromatization of S and *γ*- *t*-Bu substituted bis-allenes were trapped with $^3O_2$ (**1.280**) and maleic anhydride (**1.283**). But the authors failed to trap any such intermediates here for the rearrangement of **1.302** (**Scheme 1.39**).

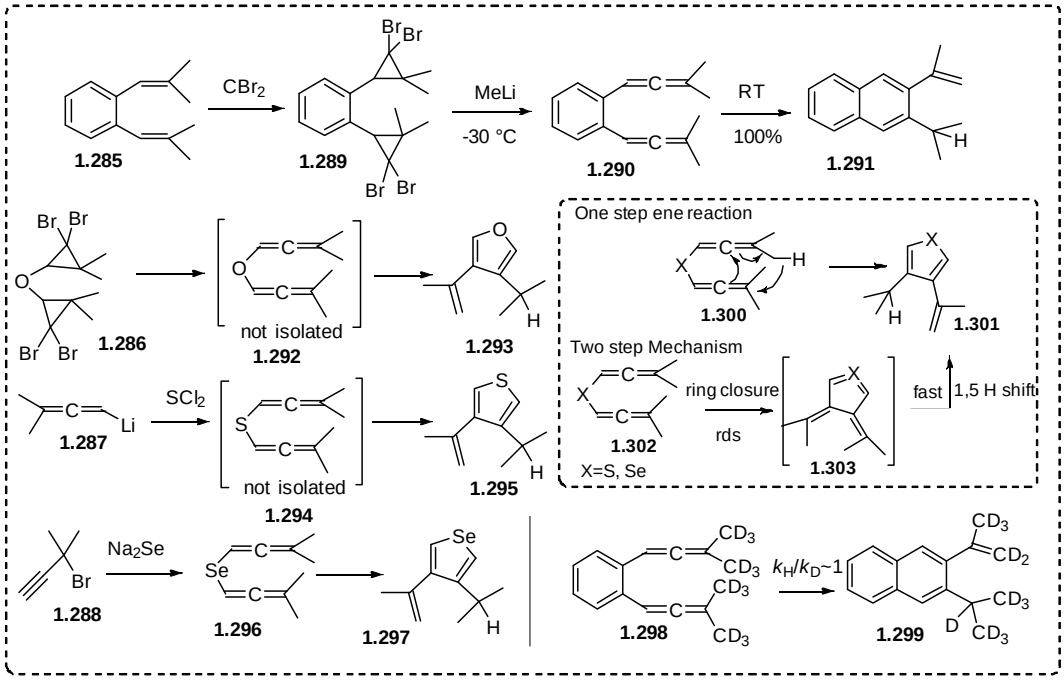

Scheme 1.39: Thermal cyclization of various heteroatom substituted bis-allenes

In 2000 Braverman *et al*. reported[35] the base mediated cyclization of bis-γ-phenylpropargyl sulfone, sulfoxide and sulfide **1.304** (**Scheme 1.40**). The rate of the reaction was found to be highest for sulfone than sulfoxide and sulfide and also the reaction proceeded faster in DMSO than $CDCl_3$.The author proposed an initial formation of a mono-allene **1.305** followed by a bis-allene **1.306**. The conclusion was based upon the fact that both the two rate constants k_1 and k_2 showed the same dependence on base concentration and the maximal concentration of the mono-allene remained unchanged with base concentration. The fact also discarded the IMDA reaction from mono-allene as previously proposed by Iwai and Ide as the change of base concentration would then have an impact on first step only. The formation of mono-allene was three times slower than the formation of bis-allene and the *rds* of the reaction involved the abstraction of α-H atom from bis-propargyl counterparts. Thus, the observed reactivity of sulfones, sulfoxides and sulfides could be explained based upon α-H acidity. If diradical formation was the *rds*, being nonaromatic, sulfoxide and sulfone diradical formation would be unfavourable and the rate of the reaction would show an inverse relationship.

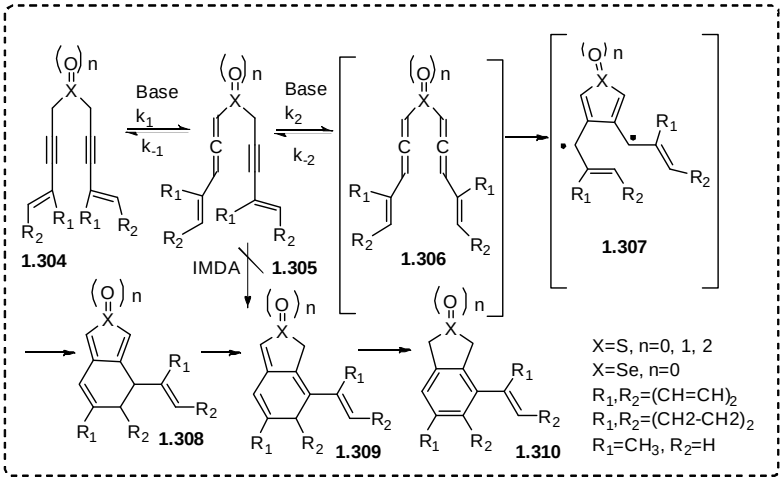

Scheme 1.40: Base mediated cyclization of bis-propargyl systems *via* mono-allene and diradical pathway

In 2003 Braverman *et al*. reported[36] an anionic cycloaromatization along with diradical cyclization of bridged di and tetrapropargylic sulfides and selenides **1.311**. In presence of weaker base like DBU the reaction followed diradical cyclization to **1.317** whereas anionic cycloaromatization resulted with stronger bases like KO^{t}Bu to 2-vinylthiofenes and selenophenes **1.312-1.313** (**Scheme 1.41, 1.42**).

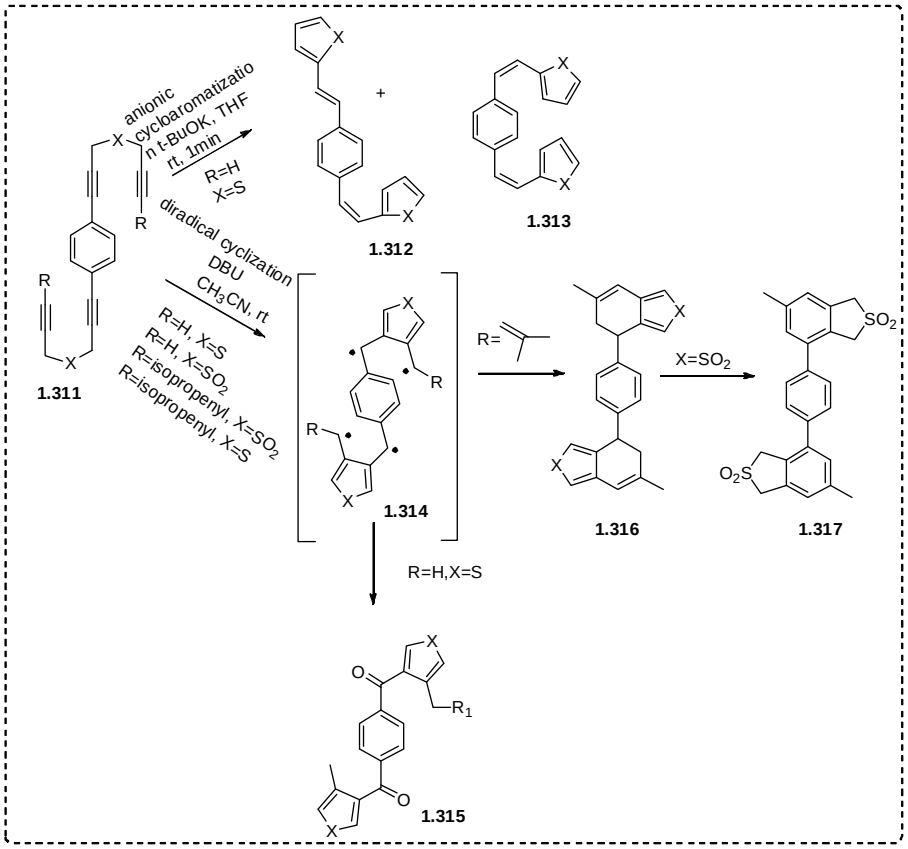

Scheme 1.41: Base mediated cyclization of tetrapropargylic systems *via* diradical and anionic pathway

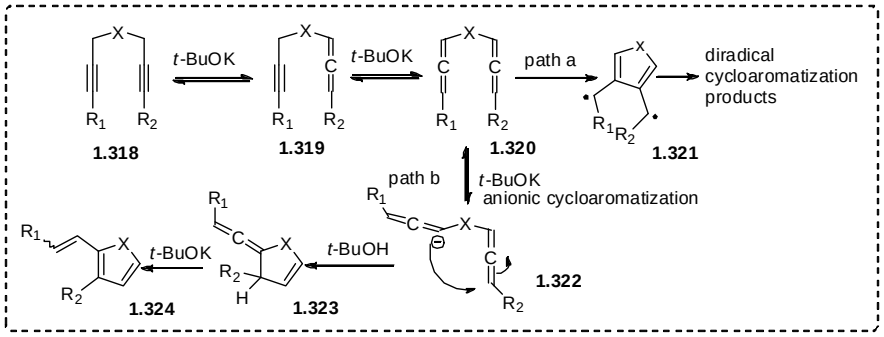

Scheme 1.42: Mechanism of diradical and anionic cyclization

In 2005 Braverman *et al*. reported[37] the tandem cyclization of bis (π-conjugated propargyl) sulfones **1.325**. It was observed that the fate of the reaction product as well as mechanism was dependent upon *γ*-substitution. The author depicted the first isolation and characterization of thiofene dioxide intermediates, mono-allene and bis-allene intermediate by NMR. Three different mechanisms were assumed as i) Mono-allene formation followed by intramolecular Diels Alder reaction ii) Bis-allene formation and then IMDA iii) Bis-allene formation and subsequent cyclization to

diradical followed by intramolecular radical quenching. In contrast to *γ*- methyl and cyclohexyl substitution, the reaction for *γ*-phenyl substituted propargyl sulfone proceeded by formation of diradical as the corresponding benzylic radical was more stable and led to the ds-DNA cleavage. For the former bis-propargyl sulfones the reaction followed the IMDA pathway *via* formation of bis-allene. The thiofene dioxide intermediate **1.331** was only isolable for methyl and cyclohexyl substitution only as for –Ph substitution the H-transfer process was fast considering the acidity of benzylic H (**Scheme 1.43**).

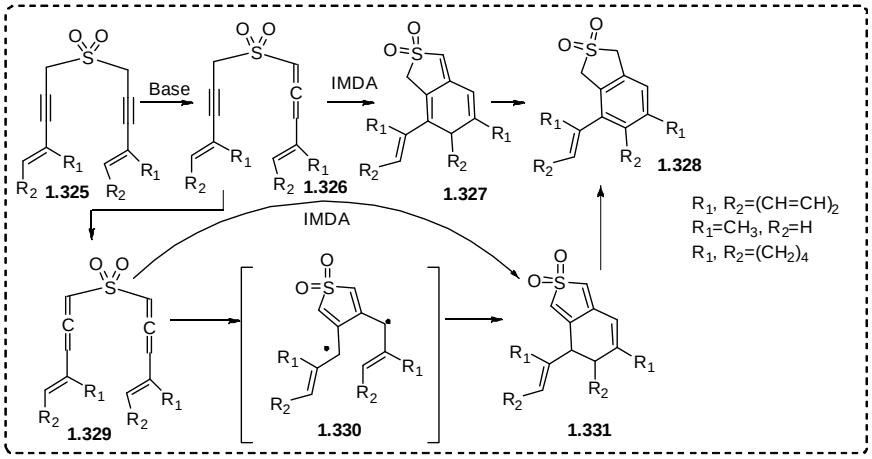

Scheme 1.43: Distinct mechanistic possibilities of base mediated cyclization of bis-propargyl systems

In 2007 Kudoh *et al*. proposed[38] an anionic [4+2] Diels Alder mechanism for base mediated cyclization of 4-Oxahepta-1,6-diynes **1.332** with different substituents attached at acetylenic end. There proposal was based on the fact that in presence of bases in DMSO there existed a rapid equilibrium between the allenide ion **1.334** formed and methylsulfinylmethide ($CH_3SOCH_2^-$) due to their similar p*K*a value. As a consequence the energy value of diene HOMO-1 level increased (DFT calculations) and made the anionic Diels Alder reaction feasible even at room temperature. The mechanism was further confirmed by carrying out the reaction in d_6-DMSO where deuterium incorporation was detected at C-3(40%) and C-9(38%) position by NMR (^{13}C-D triplets). According to their proposed mechanism the reaction involved a mono-allene anion which underwent intramolecular [4+2] cycloaddition and subsequent proton transfer to aryl naphthalenes (**Scheme 1.44**).

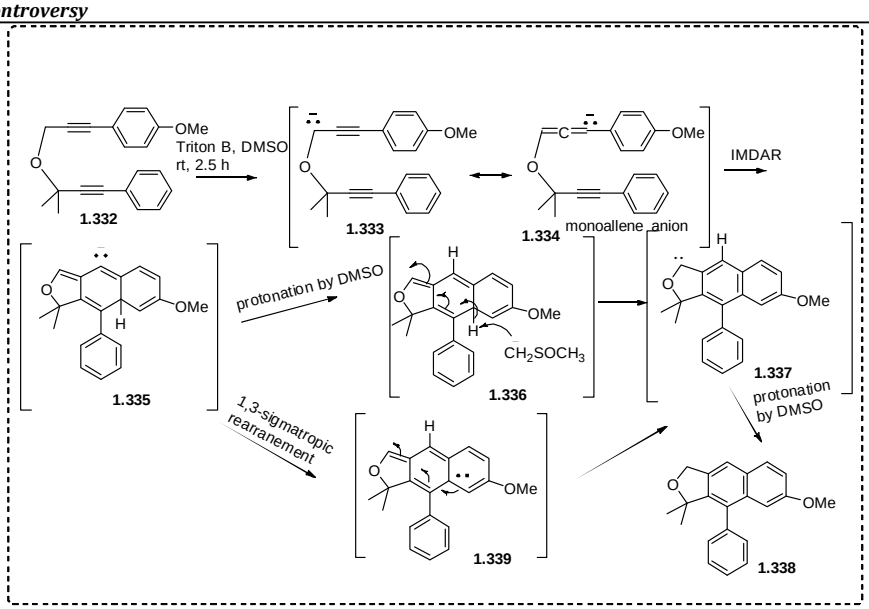

Scheme 1.44: Anionic [4+2] Diels Alder reaction mechanism for cyclization of bis-propargyl ethers

In 2011 Basak *et al*. reported[39] the base catalyzed cyclization of bis-propargyl sulfones **1.340** having Ph substituent of dissimilar nature attached to it. By the suitable use of electron donating and electron withdrawing groups on Ph ring it was observed that the major product formed *via* the participation of more electron donor Ph ring (**Scheme 1.45**).

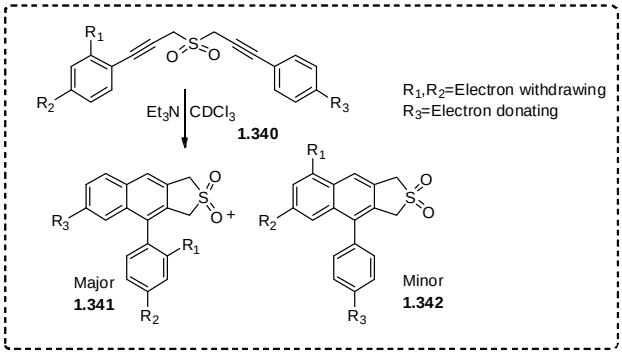

Scheme 1.45: Base mediated cyclization of unsymmetrical bis-propargyl sulfones

This observation then led to conclusion that the reaction followed a radical pathway instead of an ionic pathway as the radical attached to an electron donor Ph ring will be captodatively more stabilized (**Figure 1.07**) as well as more nucleophilic and the corresponding Ph ring will participate in cyclization (**Scheme 1.46**). The fact was also supported by DFT based calculations.

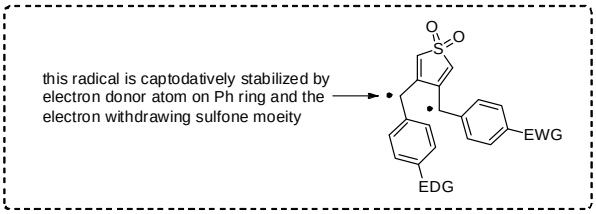

Figure 1.07: Captodatively stabilized radical

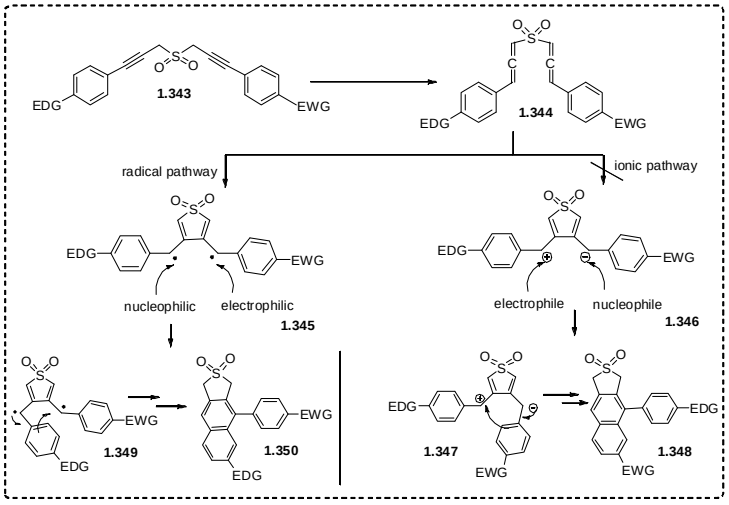

Scheme 1.46: Ionic and radical pathway of GB cyclization

1.4 Conclusion

- The sequential developments on mechanistic aspects of Bergman and Garratt-Braverman cyclization reaction are discussed.
- They are important in organic chemistry as well as in biology, specifically to damage the target DNA.
- In case of Bergman cyclization, the reaction may either follow a diradical pathway that undergo intermolecular quenching or an ionic pathway to the final products.
- For Garratt-Braverman cyclization, the reaction may follow either a diradical pathway that undergo intramolecular quenching or an anionic intramolecular Diels-Alder pathway.
- Still, mechanistic aspects of each of these reactions are needed to be explored thoroughly along with modifications.

Chapter 2

Solving the Diradical-Cycloaddition Puzzle in Garratt-Braverman Cyclization: Reactivity of Bis-Propargyl Precursors and Application of Various experimental Techniques

2.1 Introduction

The renewal of interest in cycloaromatization[1] reaction of bis-propargyl systems has drawn attention due to their biological implications[40c,41] and relevance in organic synthesis[40,42]. Among them Garratt-Braverman cyclization[32,43] involves the rearrangement of bis-allenic sulfone, sulfoxide, sulfide, ether and sulfonamide **2.001** to the polycyclic aromatic product **2.002** (**Scheme 2.01**).

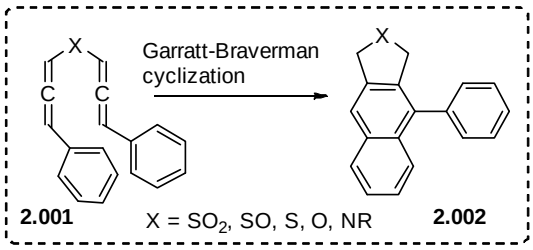

Scheme 2.01: Garratt-Braverman cyclization of bis-allenic systems

The generally accepted mechanism for the reaction is *via* the formation of bis-allene from bis-propargyl system under basic condition followed by diradical that undergo cyclization to aryl naphthalene products.[33,4a] The radical mechanism was supported by successful trapping of diradical with $^3O_2$ to form endoperoxides in case of sulfides[33,44], insensitivity of the rate of reaction with solvent polarity[34] and isolation of intermediates[4a] during reaction pathway. It was reported earlier by our group that GB cyclization of unsymmetrical sulfones followed a diradical mechanism instead of an ionic pathway where the aryl ring having greater electron donating character preferentially participated. The observed results were further supported by computational studies.[39]

In spite of all these progresses, ambiguities associated with the actual mechanism of the reaction still exist, especially the involvement of bis-allene. In experiments where bis-allenes are directly synthesized and subjected to cyclization[31], ambiguity regarding involvement of bis-allene does not arise. However, if mono-allene to bis-allene formation is slow, reactions that start from bis-propargyls may involve mono-allenes followed by an intramolecular [4+2] Diels Alder reaction to give the same product which can also be obtained *via* bis-allenes followed by a diradical. Such a mechanism was previously proposed by Iwai and Ide[30a,30b] and later reinforced by Kudoh *et al*.[38] for rearrangement of bis-propargyl ethers. They had performed labeling

experiments with deuterated solvents and theoretical calculations to support an anionic intramolecular Diels Alder reaction (IMDAR) of bis-propargyl ethers. It is to be noted that the system used by Kudoh *et al.* for labeling studies can isomerize to mono-allene only as in the other arm the propargylic carbon was disubstituted thus questioning the generality of such a mechanism, especially in systems capable of iomerization to bis-allenes.

In this chapter we have discussed the use of several experimental techniques to sort out the controversies associated with the mechanism of Garratt-Braverman cyclization mainly in two systems bis-propargyl ethers and sulfones.

2.2 Previous Studies

In 1964 Iwai and Ide investigated the rearrangement of bis (3-phenyl-2-propargyl) sulfide, ether and methylamine **2.003 A-C** in presence of 14% KO^{t}Bu in *t*-butyl alcohol to naphthalene derivatives **2.006**. They proposed a mechanism based on isomerization of one alkyne arm to allene followed by cycloaddition and proton transfer to give the final product (**Scheme 2.02**).[30a,30b]

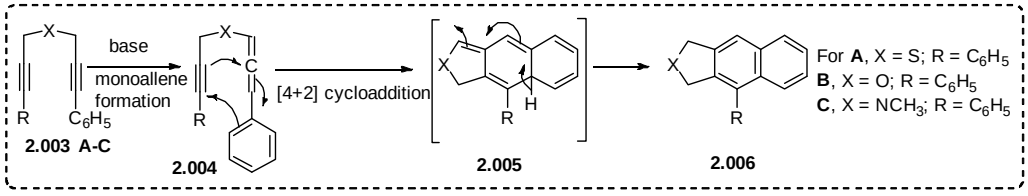

Scheme 2.02: [4+2] cycloaddition mechanism proposed by Iwai and Ide

In 1974 Braverman *et al.* reported[31] rearrangement of bis-γ,γ-dimethylallenyl sulfone **2.007** to 3-isopropenyl-4-isopropylthiofene 1,l-dioxide **2.009** upon heating at 75 °C in quantitative yield (**Scheme 2.03**). They also performed the reaction in various solvents and noticed that the rate of the reaction was not dependent upon the polarity of the solvent. Based on this observation they discarded the formation of any charged species *via* an ionic mechanism for the reaction and proposed two plausible mechanisms: i) either involving a diradical **2.008** formation in a slow rate determining step followed by intramolecular H transfer, ii) a one step intramolecular ene reaction.

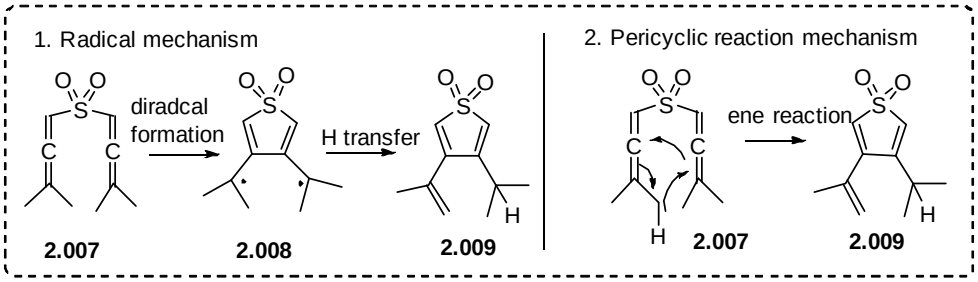

Scheme 2.03: Mechanism proposed by Braverman for thermal rearrangement of bis-allenic sulfones

In 1978 Garratt and his co-workers reported[33] the formation of a bis-allene **2.011** along with mono-allene **2.012**/**2.013** in case of base catalyzed rearrangement of bis-propargyl sulfides **2.010** (**Scheme 2.04**). The allenes were stable enough to be characterized and treatment of a $CHCl_3$ solution of a mixture of mono and bis-allenes with $^3O_2$ resulted formation of cyclic peroxides **2.018** and the mono-allenes were recovered unchanged. The studies proved the bis-allene and diradical intermediacy during base mediated cyclization of bis-propargyl sulfides.

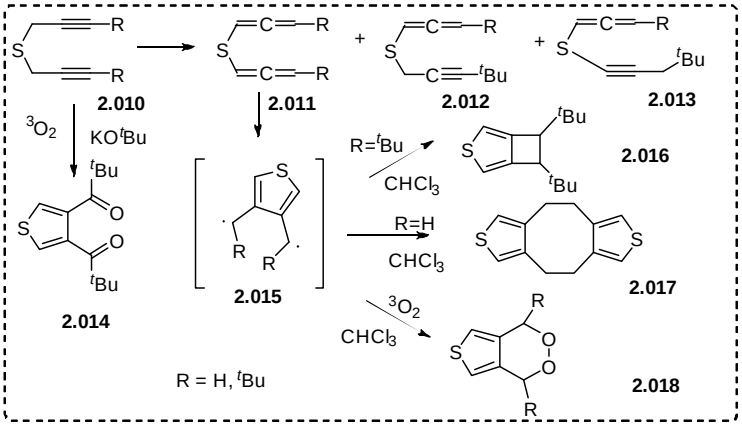

Scheme 2.04: Chemical trapping of intermediate diradical

In a subsequent paper Garratt *et al*. reported[4a] the isolation of 4,9-dihydronaphtho thiofene **2.019** and furan **2.021** intermediates (**Scheme 2.05**) during base catalyzed rearrangement of 1,7-diphenyl-4-thiahepta-1,6-diyne **2.003 A** and 1,7-diphenyl-4-oxahepta-1,6-diyne **2.003 B**. The isolation of these products supported the radical pathway for the GB cyclization. The thiofene intermediate was oxidised to the corresponding sulfone **2.020** in 30% yield that was thermally unstable and decomposed at 80 °C and its unstable nature can be explained by the non-aromatic character of the thiofene dioxide moiety. However, no direct isolation of thiofene dioxide intermediates from rearrangement of bis-propargyl sulfones was reported.

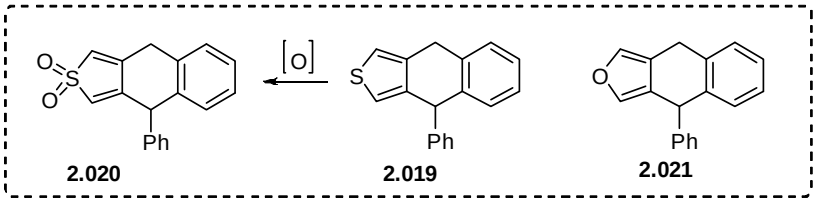

Scheme 2.05: Intermediates isolated during GB cyclization

In 2000 Braverman *et al*. reported[35] reactivity of π-conjugated bis-propargyl sulfides, sulfoxides and sulfones **2.003 A**, **2.022**, **2.023 (Scheme 2.06)**. Though they could not trap the diradical **2.026** and the bis-allene **2.025** but kinetic measurements by monitoring the change of maximal concentration of **2.024** with increased base concentration supported the formation of bis-allene and discarded intramolecular [4+2] cycloaddition pathway to the product.

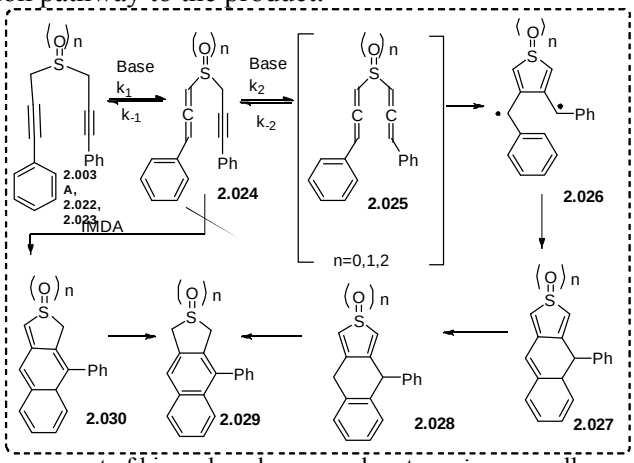

Scheme 2.06: Rearrangement of bis-*γ*-phenyl propargyl system *via* mono-allene and diradical pathway

The results of GB cyclization of unsymmetrical bis-propargyl sulfone **2.031** as reported by Basak *et al*.[39] supported the diradical mechanism. It was observed that for sulfones the major product was formed *via* the involvement of more electron donating aryl ring (**Scheme 2.07**) which could be explained nicely using the relative reactivity of the two radicals in the diradical intermediate. The observed results were also supported by DFT based calculations.

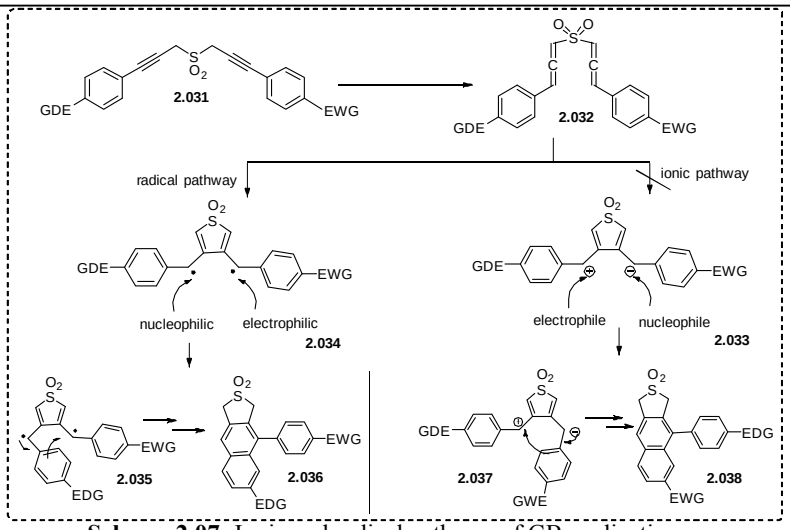

Scheme 2.07: Ionic and radical pathway of GB cyclization

In spite of mechanistic studies supporting the radical mechanism for GB cyclization there are also examples where [4+2] cycloaddition mechanism involving a diene and alkyne have been proposed.

In 2007 Kudoh *et al.* reported[38] an anionic intramolecular Diels Alder reaction at room temperature for base mediated cyclization of bis-propargyl ethers **2.039** to the same products **2.045** as was obtained *via* GB cyclization. They proposed a mono-allenide anion **2.041** formation (**Scheme 2.08 A**) that cyclized *via* [4+2] cycloaddition pathway. The authors also performed deuterium transfer experiment (**Scheme 2.08 B**) that showed deuterium incorporation which further supported the proposed mechanistic pathway.

A)

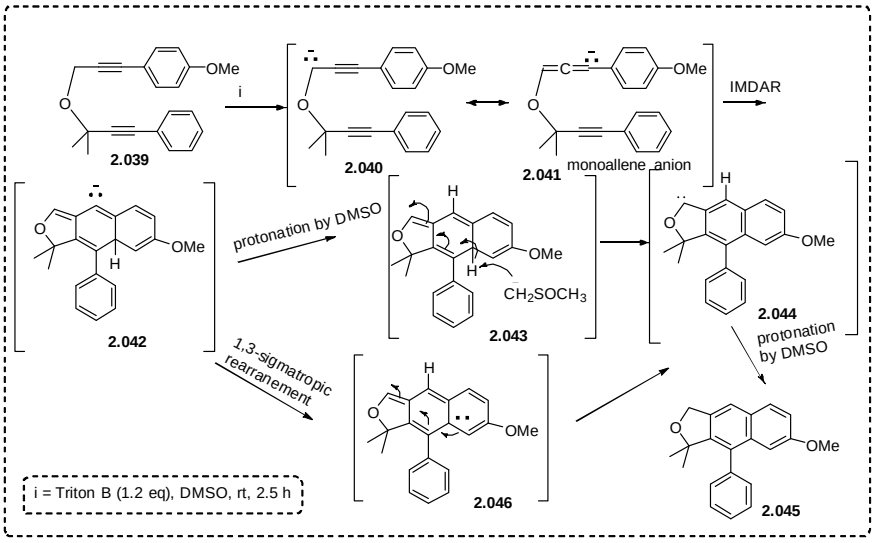

B)

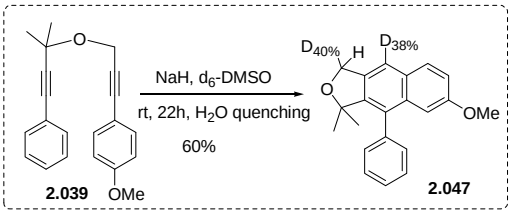

Scheme 2.08: A) Anionic [4+2] Diels Alder reaction mechanism for cyclization of bis-propargyl ethers as proposed by Kudoh *et al.* **B)** Deuterium transfer experiment performed by Kudoh *et al.*

Recently, Balci *et al*. in 2015 proposed[45] an intramolecular [4+2] cycloaddition pathway involving an alkyne and azadiene intermediate generated *in situ* during formation of chromenopyridines **2.051** (**Scheme 2.09**).

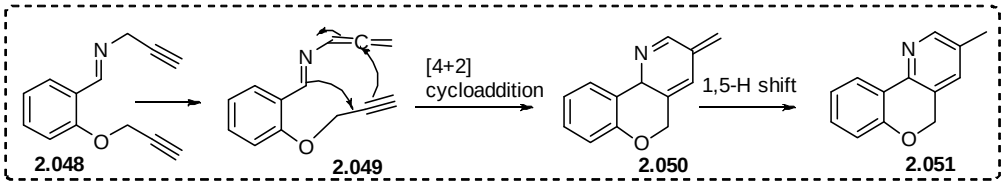

Scheme 2.09: [4+2] Cycloaddition mechanism proposed by Balci *et al.*

2.3 Objective

Based on the mechanistic studies on rearrangement of bis-propargyl systems as discussed, we apprehended that the bis-propargyl systems with differentially substituted heteroatoms (S, SO_2, O, NTs) may follow different mechanisms depending on the reaction conditions employed during GB cyclization. Thus we decided to undertake a thorough study that will shed light on the actual reaction pathway of the process. Our specific objectives were as follows:

- Synthesize various unsymmetrical diaryl bis-propargyl sulfones, ethers and sulfonamides.

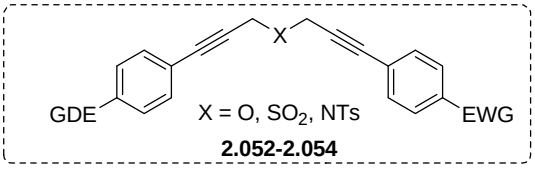

- Study their reactivity towards GB cyclization, mainly addressing the chemoselectivity.

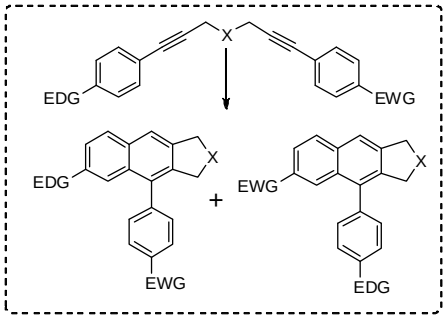

- Influence of the existing hetero functionality (sulfone, ether and sulfonamide) on the chemoselectivity and on the overall mechanism of the reaction.

- Synthesize bis-propargyl sulfones and ethers having deuterated aryl rings attached to one of the two acetylene termini and perform GB reaction to discriminate between mono-allene and bis-allene mechanism.

- Finally, perform EPR studies to find the involvement of radical.

2.4 Results and Discussion

2.4 A. Chemoselectivity during Garratt-Braverman Cyclization

2.4 A. 1 Synthesis of Unsymmetrical bis-propargyl systems

To address the selectivity issue, various bis-propargyl ethers **2.052 A-D**, sulfones **2.053 A-D** and sulfonamides **2.054 A-D** were synthesized. The key steps for the synthesis are mentioned here. The bis-propargyl ethers were prepared by NaH mediated O-alkylation of the alcohols **2.055 A-D** with the corresponding 3-phenylpropargyl bromide. The N-propargylation of sulfonamides was achieved by reacting N-tosyl protected 3-phenylpropargyl amine with respective bromides **2.056 A-D**. The bromides were prepared by bromination of the corresponding alcohols *via* mesylation and displacement with LiBr. The alcohols **2.055 A-D** were prepared by Sonogashira reaction between the corresponding iodo/bromo derivatives and propargyl alcohol. The unsymmetrical sulfides were prepared by alkylation of *in situ* generated thiol with the corresponding bromides **2.056 A-D** (**Scheme 2.10**) in presence of K_2CO_3. The thiol was obtained from hydrolysis of thioacetate **2.057**. For symmetrical sulfides, the 3-substituted propargyl bromides were treated with Na_2S in THF-water in presence of a phase transfer catalyst and the crude sulfides were converted to the sulfones by oxidation with oxone.

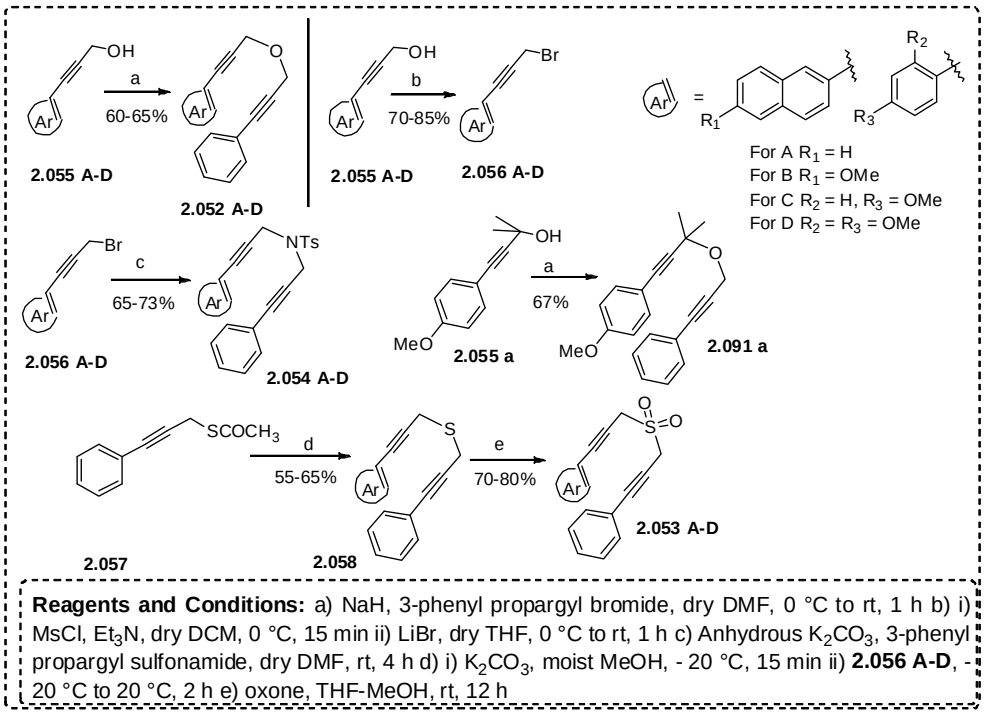

Scheme 2.10: Synthesis of unsymmetrical bis-propargyl systems

2.4 A. 2 Reactivity of bis-propargyl systems under basic condition

The synthesized unsymmetrical bis-propargyl ethers, sulfones and sulfonamides were then treated with suitable bases (KO^tBu/DMSO/rt for ethers, $Et_3N/CHCl_3$/rt for sulfones and DBU/toluene/reflux for sulfonamides) depending on the nature of heteroatom substitution to follow the outcome of GB cyclization. The structure of the products was determined by ^1H, ^{13}C, DEPT-135 NMR and correlation spectroscopy in some cases. The ratio of the two isomers formed during GB cyclization was interpreted by comparing the integration values of characteristic signals of the two structures in ^1H NMR of crude reaction mixtures. It was observed that the bis-propargyl ethers followed an opposite trend to that for the sulfones and the sulfonamides followed an intermediate trend. The results are shown in **Table 2.01**.

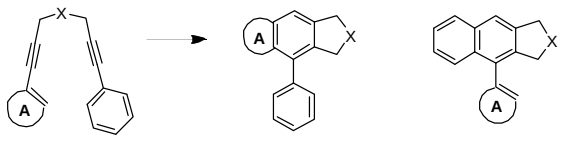

2.052 A-D	**2.059 A-D**	**2.060 A-D**
2.053 A-D	**2.061 A-D**	**2.062 A-D**
2.054 A-D	**2.063 A-D**	**2.064 A-D**

SM	X	A	Reaction conditions	Yield (%)	Product ratio
2.052 A	O	2-naphthyl	rt, 1 h, KO^{t}Bu,Dry DMSO	97	**2.059 A:2.060 A** (2:1)
2.052 B	O	6-Methoxynaphthyl	rt, 1 h, KO^{t}Bu, Dry DMSO	94	**2.059 B:2.060 B** (1:2)
2.052 C	O	4-Methoxyphenyl	rt, 1 h, KO^{t}Bu,Dry DMSO	95	**2.059 C:2.060 C** (1:8)
2.052 D	O	2,4-Dimethoxy phenyl	rt, 1 h, KO^{t}Bu,Dry DMSO	94	**2.059 D:2.060 D** (1:10)
2.053 A	SO_2	2-naphthyl	rt, 30 min, Et_3N, Dry $CHCl_3$	90	**2.061 A:2.062 A** (3.16:1)
2.053 B	SO_2	6-Methoxynaphthyl	rt, 30 min, Et_3N, Dry $CHCl_3$	90	**2.061 B:2.062 B** (5.16:1)
2.053 C	SO_2	4-Methoxyphenyl	rt, 30 min, Et_3N, Dry $CHCl_3$	85	**2.061 C:2.062 C** (2:1)
2.053 D	SO_2	2,4-Dimethoxy phenyl	rt, 30 min, Et_3N, Dry $CHCl_3$	93	**2.061 D:2.062 D** (5.16:1)
2.054 A	NTs	2-naphthyl	120 °C, 12 h, DBU, toluene	80	**2.063 A:2.064 A** (1.9:1)
2.054 B	NTs	6-Methoxynaphthyl	120 °C, 12 h, DBU, toluene	75	**2.063 B:2.064 B** (2.4:1)
2.054 C	NTs	4-Methoxyphenyl	120 °C , 12 h, DBU toluene,	73	**2.063 C:2.064 C** (1:4.9)
2.054 D	NTs	2,4-Dimethoxy phenyl	120 °C, 12 h, DBU, toluene	76	**2.063 D:2.064 D** (1:4)

Table 2.01: Results of GB cyclization

In case of sulfones **2.053 A-D** major products were obtained *via* the participation of more electron rich aryl ring while for the ethers **2.052 A-D** the less electron rich aryl ring preferentially participated in GB cyclization. To avoid further complications associated with change of reaction conditions, we have limited our discussion to base mediated rearrangement of bis-propargyl ethers and sulfones that underwent GB cyclization at room temperature. For sulfonamides, a temperature of 120 °C had to be maintained. The opposite trend of selectivity clearly indicated the involvement of two different reaction mechanisms for ethers and sulfones. The results can be well explained by anionic IMDAR for bis-propargyl ethers and diradical mechanism in

case of sulfones. For ethers, the base abstracts more acidic hydrogen from the propargyl hand attached with a less electron donating substituent and that serves as an anionic diene functionality followed by facile intramolecular cycloaddition with alkyne dienophile. In case of sulfones, the benzylic radical associated with more electron donating group being captodatively stabilized[39,46] (**Figure 2.01 A**) becomes more nucleophilic. It may be mentioned here that the involvement of a diradical intermediate in case of ether can also explain the experimental results keeping in mind the different electronic nature of sulfones (-I, -R effect) and ethers (-I, +R effect).[47] Unlike the sulfones the benzylic radical attached to the electron withdrawing group will be more stabilized in case of ethers (**Figure 2.01 B**).

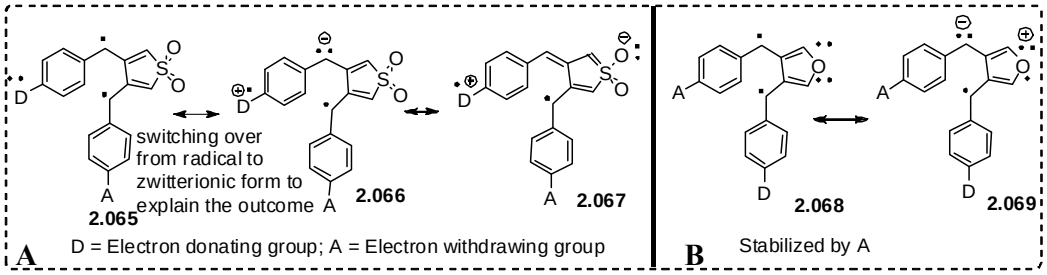

Figure 2.01: Captodative stabilization of nucleophilic radical

2.4 B. Role of Solvents; Deuterium Scrambling Experiment

We next set out to carry out the reactions in deuterated solvents in order to gain insight into the mechanism of the reaction. Since there is always a possibility of H/D exchange at C-1 and C-3 under basic conditions, we wanted to settle that issue before we carry out reaction with deuterated substrates. Thus, one of the protiated dihydroisofuran derivatives **2.060 D** was subjected to GB reaction condition at room temperature in d_6-DMSO/KO^{t}Bu and the dihydrothiofene dioxide derivative **2.075** in $CDCl_3$/Et_3N. The percentage of deuterium incorporation was determined by ^{1}H NMR spectrum analysis. In case of ethers, deuterium was incorporated at C-1 and C-3 position and the percentage of D incorporation changed with base concentration (**Scheme 2.11**). Thus, any mechanistic studies based on D incorporation at methylene positions may not be reliable. In case of dihydrothiofene dioxide derivative **2.075**, no such incorporation of deuterium was detected. We then performed GB cyclization of a bis-propargyl sulfone **2.074** in $CDCl_3$ and Et_3N. We could not detect any deuterium incorporation. This observation ruled out the involvement of anionic [4+2] Diels

Alder reaction pathway of bis-propargyl sulfones that was further confirmed by studies with deuterated substrates.

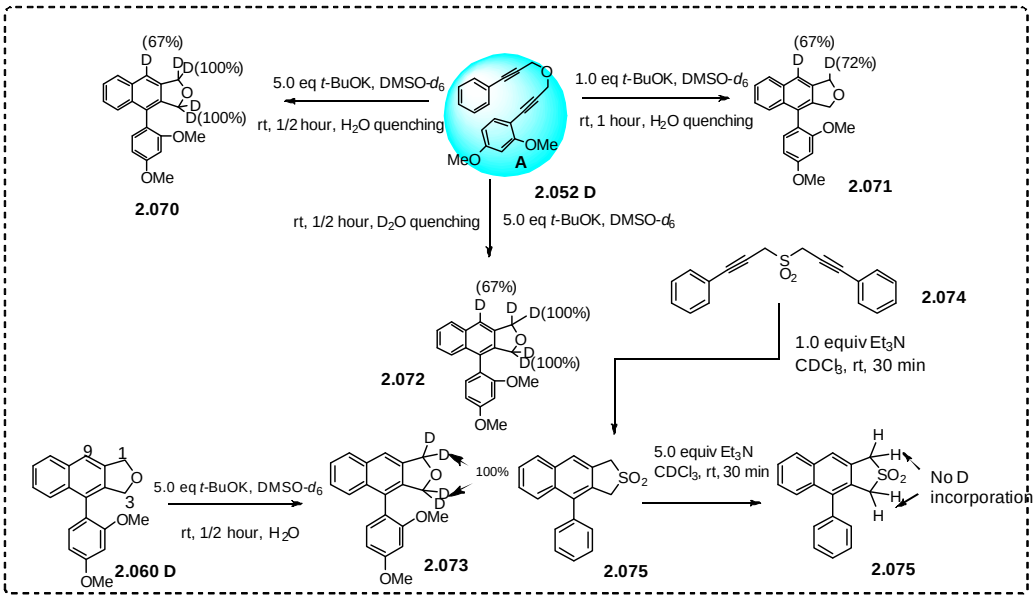

Scheme 2.11: Allenide generation and deuterium transfer experiment

2.4 C. Possible fate of deuterated substrates during GB reaction

The possible outcomes (retention, loss or migration to other positions) during GB reaction with labeled substrates having deuterium at both the *ortho* positions are shown in **Scheme 2.12**. In case of sulfones, if the reaction follows a diradical pathway, the intermediate diradical **2.078** will be formed with all the deuterium intact. The radical then undergoes cyclization to **2.079** and 1,3-H migration from C-4 to C-3 along with 1,5-D shift from C-11 to C-1 will give rise to the formation of final product **2.080**. Here the possibility of 1,3-D shift from C-11 to C-9 is discarded as that would give rise to the formation of nonaromatic 3,4-disubstituted thiofene dioxide derivatives **2.086**. The stability of the anion α to the sulfone moiety may also help the facile 1,5-D transfer. If the process of 1,5-D shift is concerted in nature, the deuterium is expected upto 50% at C-1 of the final product **2.080**. If this process is non-concerted, lower level of deuterium may be possible at C-1. It may be noted that the transoid geometry of diene framework may prohibit concerted pathway of D transfer. Feldman *et al*. in 2010 reported[40a] an attempt to trap thiofene dioxide derivatives from base mediated cyclization of bis-propargyl sulfone **2.087** with a pendant alkyne (**Scheme 2.13**) *via* an intramolecular Diels Alder reaction (IMDAR). Unfortunately, the reaction ended up with the formation of tetrahydrothiofene dioxide

derivative **2.088**. This observation was in conformity of 1,5-H shift process from C-11 to C-1 instead of C-11 to C-9 to give rise dihydrothiofene dioxide derivatives.

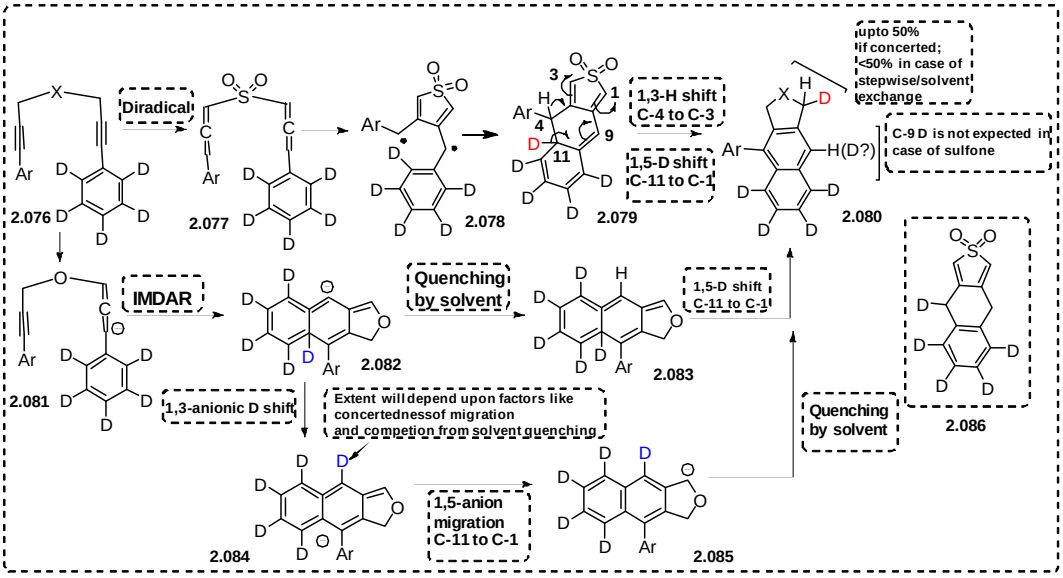

Scheme 2.12: Possible fate of deuterated substrates *via* radical and [4+2] cycloaddition pathway

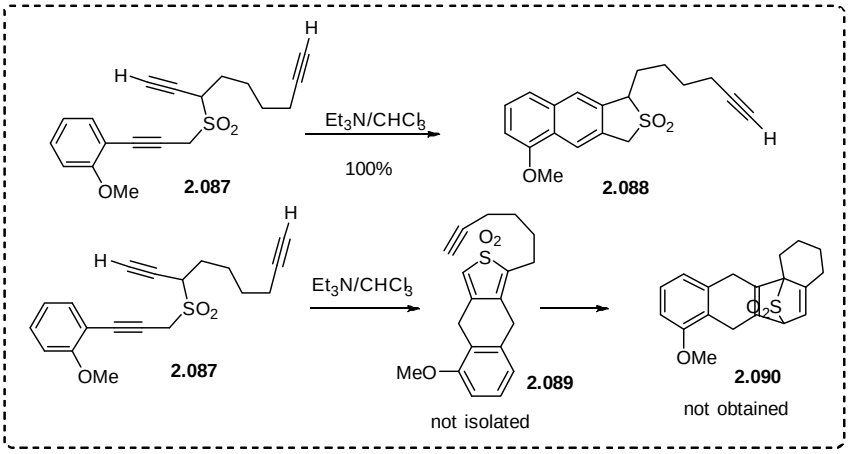

Scheme 2.13: Attempt to trap thiofene dioxide derivatives as proposed by Feldman *et al.*

In case of ethers, deuterium is expected at C-9 position *via* 1,3-D shift from C-11 to C-9 considering the aromatic nature of furan ring. Another 1,3-D shift from C-9 to C-1 will lead to the final product. However, the extent of deuterium at C-9 and C-1 will depend upon the concertedness of migration along with exchange with nondeuterated solvents. For anionic IMDAR mechanism, one can expect deuterium at C-9 considering the probability of an anionic 1,3-D shift from C-11 to C-9 in **2.082**. Such an anionic H shift was mentioned by Kudoh *et al.*[38] although no evidences to

support this were proposed. The appearance of deuterium at C-1 was explained by migration of ring junction anion to C-1 through a π-network followed by quenching with d_6-DMSO (**Scheme 2.12**).

2.4 D. Results of GB reaction of deuterated substrates

With all these informations in hand we then synthesized various pentadeuterated phenyl based bis-propargyl ethers and sulfones and subjected them to GB reaction condition. The starting materials were wisely chosen for deuterium transfer experiment as the corresponding products were either formed exclusively for unsymmetrical bis-propargyl ether (**2.060 D**) or *via* the involvement of phenyl ring for the unsymmetrical sulfone (**2.062 C**) where possibilities of participation of both the rings arise.[39,47] The outcome of the reaction is shown in **Figure 2.02**. The possibility of exchange at C-1 and C-3 still remained here. However any trace of deuterium at these positions could only arise from migrations only as the reaction was carried out in non-deuterated solvents.

The percentage of D incorporation was calculated from intensity of proton signals in ^{1}H-NMR spectrum which was further supported by the signal reduction in ^{13}C and DEPT-135 NMR spectrum of deuterated compounds as compared to their protiated counterpart. The result of GB cyclization with deuterated compounds is shown in **Figure 2.02** followed by the comparative ^{1}H and ^{13}C NMR spectra of GB cyclization products in **Figure 2.03-2.07**.

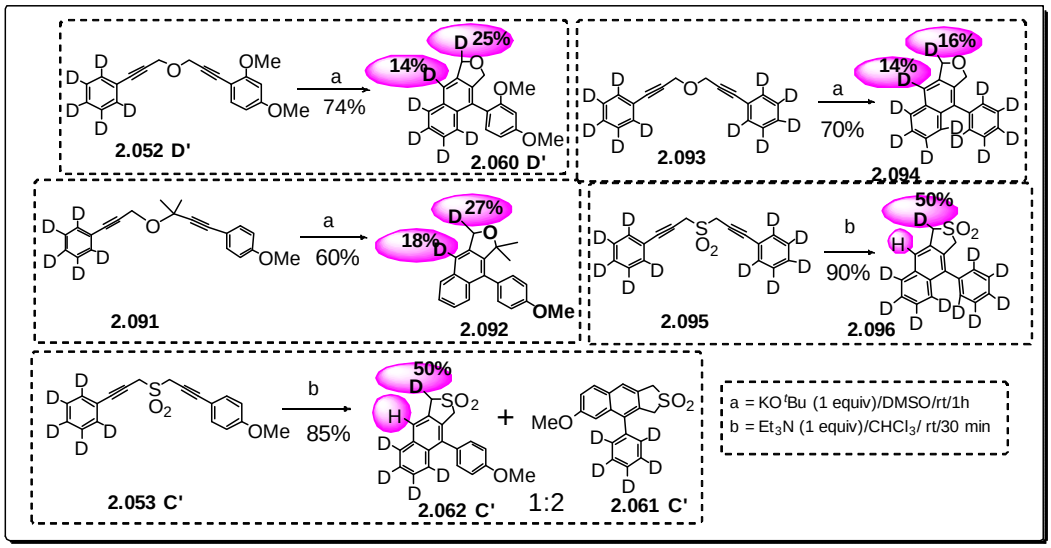

Figure 2.02: Results of GB cyclization with deuterated substrates

2.4 D.1. Comparative ^{1}H and ^{13}C NMR spectra of GB cyclization products

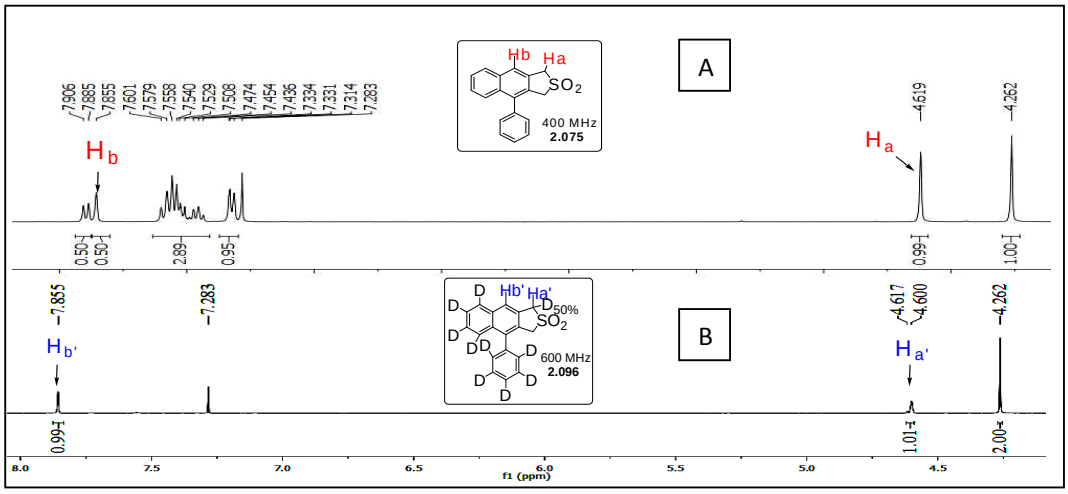

Figure 2.03: ^{1}H NMR comparison of sulfone **2.075/2.096**; integrations for the peaks at H-9 (shown here as H_b and $H_{b'}$) in both spectra **A** and **B** indicated no deuterium incorporation. Integration of C1-methylene δ ≈ 4.61 in spectrum **B** indicated ~50% D-incorporation

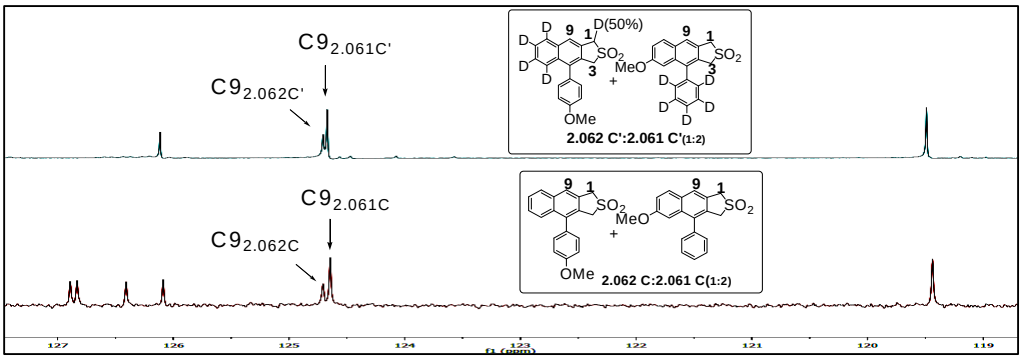

Figure 2.04: ^{13}C NMR comparison of C-9 peak showing no change of signal intensity

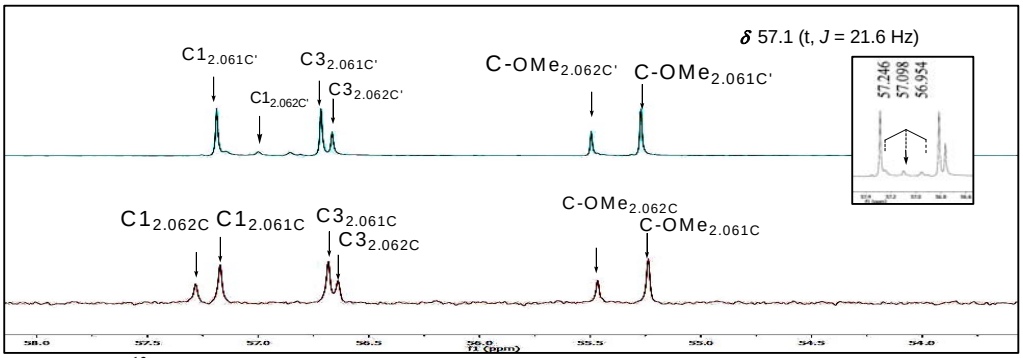

Figure 2.05: ^{13}C NMR comparison of C-1 peak showing $C1_{2.062\ C'}$ as a small triplet slightly overshadowed by the strong singlet for $C1_{2.061\ C'}$

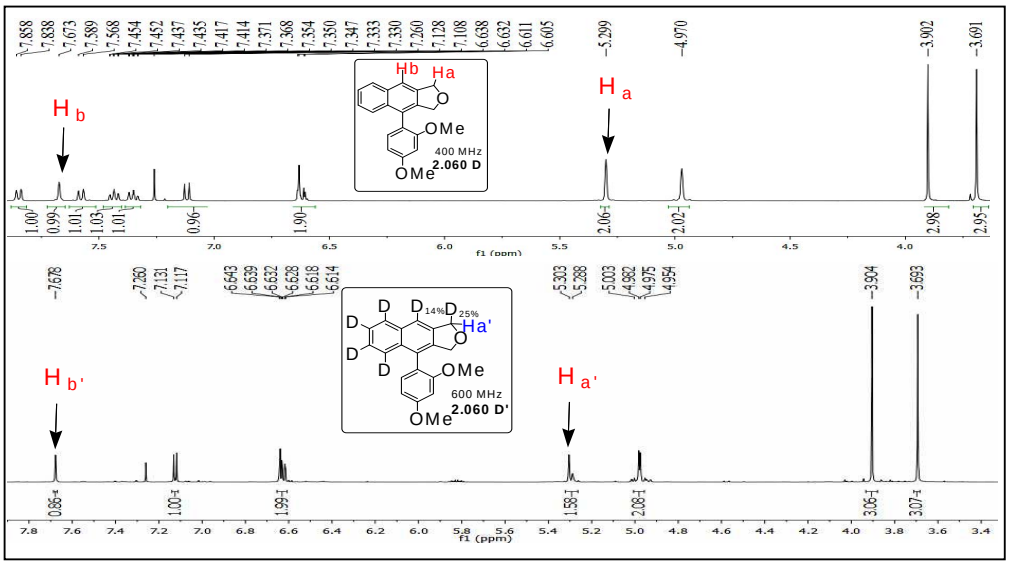

Figure 2.06: ^{1}H NMR comparison of ether; integration for the peak at H-9 (shown here as H_b and $H_{b'}$) is reduced for $H_{b'}$

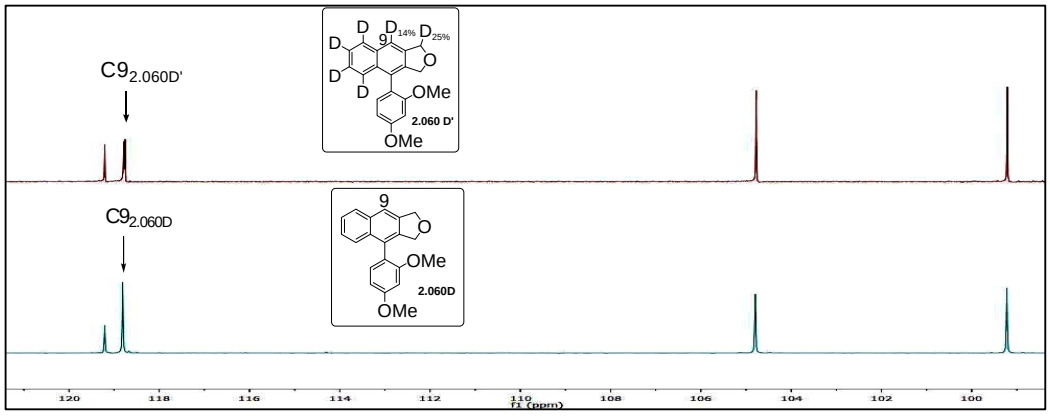

Figure 2.07: ^{13}C NMR comparison of C-9 peak showing reduced signal intensity

The extent of deuterium at C-9 and C-1 are different in case of sulfones and ethers and that point out the involvement of two different mechanistic pathways for GB cyclization in these two systems. For sulfones the extent of deuterium at C-1 was observed to be ~50% (**Figure 2.03**, **2.05**) and that indicates a concerted 1,5 D shift from C-11 to C-1. No deuterium was observed at C-9 (**Figure 2.04**) that discards 1,3-D shift from C-11 to C-9 and also the involvement of thiofene dioxide intermediates that are nonaromatic[48] in nature. As there are geometric constraints associated with sigmatropic 1,5-D shift, its concerted nature can be well explained by deprotonation and reprotonation through an intramolecular pathway. The absence of deuterium at C-

9 with reactions performed in $CDCl_3/Et_3N$ with protiated bis-propargyl sulfones also ruled out involvement of normal or anionic [4+2] cycloaddition pathway for cyclization of bis-propargyl sulfones and indicates a diradical pathway involving bis-allenes.

In case of ethers a low but considerable amount of deuterium (~14%) was observed at C-9 (**Figure 2.06**, **2.07**). The presence of deuterium at C-9 indicates an anionic 1,3-D shift[49] from C-11 to C-9 which turns out to be a minor pathway as indicated by the low level of deuterium at C-9 position and the major path is the quenching of anion by DMSO. A similar observation was made for the corresponding dimethyl bis-propargyl ether **2.091** which can only undergo cyclization *via* mono-allene. A varying degree of D (~16-27%) was observed at C-1 position that may be attributed with the possible exchange with solvent. The appearance of deuterium at C-1 arises from intramolecular 1,5 D migration from C-11 to C-1. All these observations are in agreement of anionic IMDAR mechanism as proposed by Kudoh *et al*. The presence of deuterium at C-9 and C-1 position can also be explained by radical mechanism of GB cyclization on basis of 1,3 prototopic shifts. Unlike sulfones it must be noted that the radical pathway of GB reaction involving bis-allene gives rise to furan which is aromatic for bis-propargyl ethers.

2.4 E. ^{2}H NMR spectra of deuterated GB cyclization products

To further confirm the presence of deuterium at C-9 and C-1 position of GB cyclization products deuterium NMR was carried out. It has the range of chemical shift similar to proton NMR but with low resolution. The spectra are shown below (**Figure 2.08**).

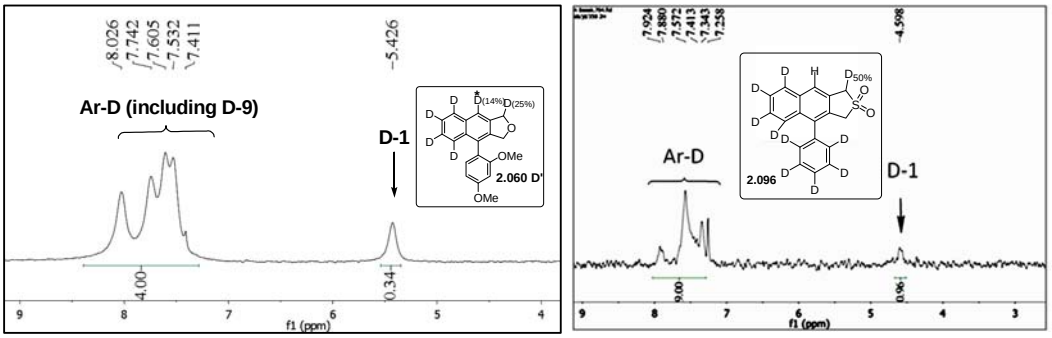

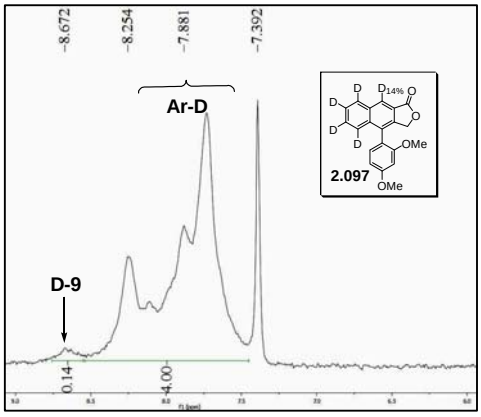

Figure 2.08: ^{2}H NMR (92.1 MHz) spectra of deuterated products; *determined from ^{1}H-spectra

In case of sulfone **2.096** the peak at δ 4.59 and for ether **2.060 D'** the broad peak at δ 5.43 corresponded to the presence of deuterium at C-1. The peak for C-9 D was masked due to the spectral broadness of other aromatic deuteriums in both ether **2.060 D'** and sulfone **2.096** if any. For sulfones C-9 D was not expected considering the radical mechanism of cyclization and 1,5-D shift from C-11 to C-1 as discussed earlier. However, the presence of deuterium at C-9 in ether **2.060 D'** was clearly visible in the corresponding lactone due to the deshielding effect. The peak shifted to δ 8.67 (compound **2.097**). The lactone was synthesized by oxidising the dihydrofuran derivative **2.060 D'** with IBX in DMSO.

2.4 F. Exploiting GB reaction mechanism by LA-LDI mass spectrometry

We used the recently developed label-assisted laser desorption mass spectrometry to detect the formation of allenic intermediates. Since polyaromatic labels are used in LA-LDI MS[50], we used naphthalene based bis-propargyl sulfone **2.102** and ether **2.098** to detect them by matrix free LDI MS. To perform the experiment, GB reaction was carried out in presence of methanol anticipating that the mono-allene and bis-allene intermediates could be trapped by an external nucleophile MeOH (**Figure 2.09**) that was used in large excess.

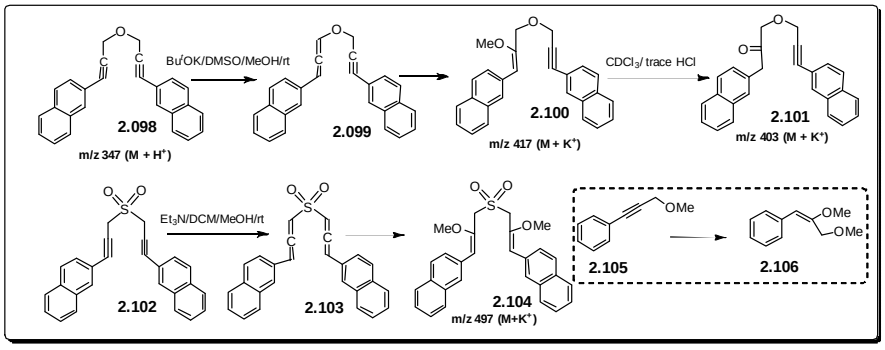

Figure 2.09: Trapping of mono-allene and bis-allene intermediates during GB cyclization

In case of ether a peak corresponding to the mono methoxy adduct **2.100** at m/z 417 ($M+K^+$) was observed. No peaks for double adduct at m/z 449 was detected that supports the formation of mono-allene in case of ethers. The mono methoxy adduct **2.100** was kept in $CDCl_3$ containing trace HCl which was sufficient to convert the vinyl ether to the corresponding ketone **2.101** for which a peak at m/z 403 was observed. As GB cyclization proceeds *via* intramolecular quenching of diradical, external quenching by MeOH was insignificant. The high sensitivity of LA-LDI MS was able to detect the peaks for methanol adduct. To support the experiment the mono methoxy alkyne **2.105** was treated with KO^{t}Bu in DMSO/MeOH (7:1) where we could isolate the mono methoxy adduct **2.106** in decent yield (70%). In contrast to the ethers, the analysis of crude reaction mixture of sulfones showed a peak for dimethanol adduct **2.104** at m/z 497 ($M+K^+$) along with a peak at m/z 433 ($M+K^+$) for the GB product (**Figure 2.10**). No peak at m/z 465 for the mono methanol adduct product was observed that further supported the formation of bis-allene during the course of GB reaction. Here a point to note that we did not observe any H$^\cdot$ abstracted product from MeOH as the intermediate diradical underwent intramolecular self quenching unlike in Bergman cyclization. Finally, EPR studies as discussed below proved the radical intermediacy only in case of sulfones and not for ethers.

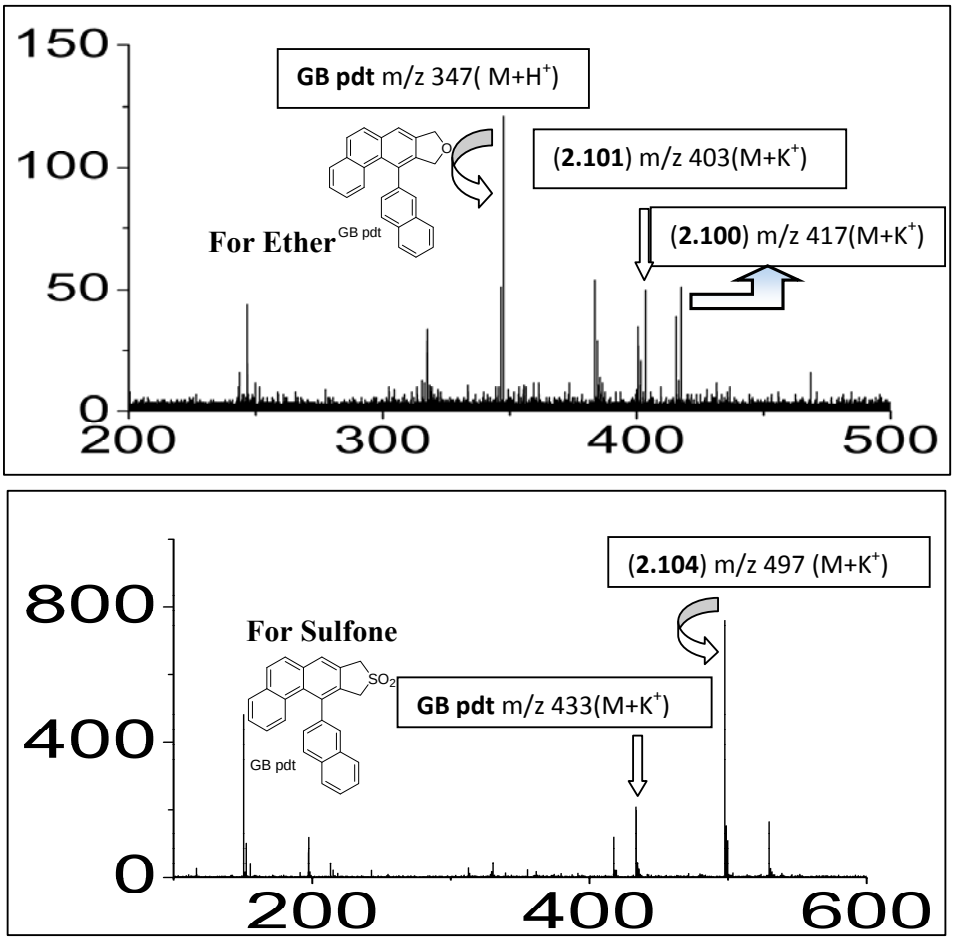

Figure 2.10: LA-LDI MS spectra of intermediates of GB cyclization

2.4 G. EPR Studies

The EPR spectra of bis-propargyl ethers **2.052 D**, **2.098** and sulfones **2.053 B**, **2.102** (**Figure 2.11**) were recorded by carrying out the reactions under appropriate conditions after purging the solutions with Ar gas for 5 min to remove the dissolved oxygen. The bases were used according to the heteroatom substitution without or in presence of TEMPO according to the requirements. For sulfones **2.053 B**, **2.102** we observed a nice stable EPR signal (**Figure 2.12**) at room temperature with isotopic *g* value of 2.004. The *g* value was found to be close to TEMPO (*g* = 2.0036) and thus indicating the presence of organic radical in case of sulfones.[51-53] The fact was further supported by quenching experiment where the EPR signal disappeared after recording the signal by purging with O_2 for 2-4 min.

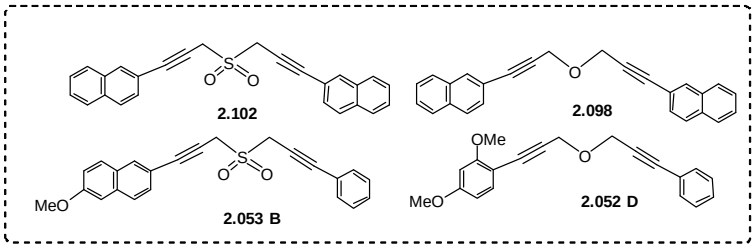

Figure 2.11: Compounds used in EPR

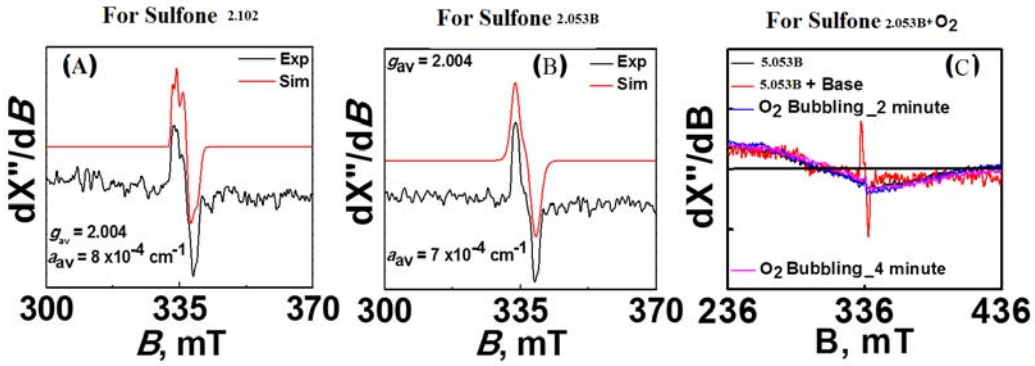

Figure 2.12: X band (9.44 GHz) EPR spectra of a mixture of sulfone and Et_3N in $CHCl_3$ at room temperature. Condition: X-band microwave frequency (GHz), 9.44; modulation frequency (kHz), 100; modulation amplitude (G), 140.0; and microwave power, 0.998 [μW]. Spectra (**A**) is for bis-naphthyl substituted bis-propargyl sulfone **2.102**; (**B**) is for sulfone **2.053 B** and (**C**) is for a solution of sulfone **2.053 B** purging with O_2 gas at room temperature. All the solutions of samples in dry $CHCl_3$ contained Et_3N as base. EXP and SIM represent experimental and simulation spectra, respectively.

A hyperfine splitting of the EPR signal for sulfones was expected and observed accordingly for compound **2.102**. However the spectral broadness did not allow us to calculate the hyperfine splitting constant (A value) due to the strong spin delocalization within the aromatic core and the benzylic proton[51a-c] as well as strong spin-spin exchange[51d-e]. Similar is the case for compound **2.053 B**. The strong nucleophilic/electrophilic nature of the radical under the influence of electron donor/acceptor substituent in the aromatic core may also be a probable reason of weak hyperfine coupling of compound **2.053 B**.[51b] However, the hyperfine splitting was resolved in the simulated spectra. Thus, the best fit to the experimental data provided the parameters g_{av} = 2.004 and hyperfine coupling constant, $A_{av} = 8 \times 10^{-4}$ cm^{-1} for

compound **2.102** and compound **2.053 B** shows same *g* value with a slightly weaker hyperfine coupling constant $A_{av} = 7 \times 10^{-4}$ cm^{-1}. Both the experimental and simulated spectra of compound **2.102** shows the average triplet EPR signal for the two radicals under the coupling influence of two separate hydrogens attached to the radical bearing carbons. However, at this stage it is difficult to clearly explain the splitting pattern or the exact interactions with our available experimental setup.[51a] It may be mentioned that at this stage we are also unable to quantify the spin. However, a correlation could be made examining the area of absorbance (Integration of the first-derivative EPR and integration again) of sample and that of TEMPO. This gave the relative spin concentration which is mentioned in **Table 2.02**. As the sample would generate diradical, understanding the exact spin state is not conclusive at this stage and need further study.

	EPR Absorbance area	**Concentration (mM)**	No. of spin	***g***	g_{av} (Simulated)	A_{av} (Simulated)
Tempo	938	1.00		2.013	----	----
2.102	620	1.69	0.39	2.0034	2.004	8×10^{-4} cm^{-1}
2.053 B	861	1.78	0.52	2.0037	2.004	7×10^{-4} cm^{-1}

Table 2.02: EPR data table of sulfones **2.102**, **2.053 B** and Tempo

[For **2.102**, the spin concentration = 0.39 = 39% spin generated; Similarly, for **2.053 B**, the spin concentration = 0.52 = 52% spin generated with respect to standard's spin, TEMPO]

To check whether the observed signal has any interaction with a stable organic radical like TEMPO we monitored the signal intensity of a fixed concentration of TEMPO in presence of the reaction mixture of compound **2.102**. It is well known that TEMPO gives a triplet EPR signal with an isotropic hyperfine splitting a_N = 15.5 G and g_0 = 2.0055 as was reported by Talsi *et.al*[51d,53]. However, in our experimental condition at room temperature TEMPO exhibited a single line EPR spectrum with a center *g* value of 2.013 which possibly due to high concentration of the TEMPO. We observed a reduction of EPR signal intensity by 17% of a solution containing the compound **2.102** (1.7 mM), Et_3N and TEMPO (0.5/1.0 eq) in $CHCl_3$ in comparison to the signal intensity of a 0.5/1.0 mM of TEMPO in $CHCl_3$. In case of sulfone **2.053 B**,

the signal intensity of TEMPO was reduced by 41% (**Figures 2.13 A** and **2.13 B**) (**Table 2.03**). All these observations point out an antiferromagnetic interaction between TEMPO and our GB diradical during reaction.[54] In case of bis-propargyl ethers **2.098** and **2.052 D**, no EPR signals were observed under GB reaction conditions (KO^{t}Bu/DMSO) indicating that the GB pathway mainly follows a non-radical pathway**.**

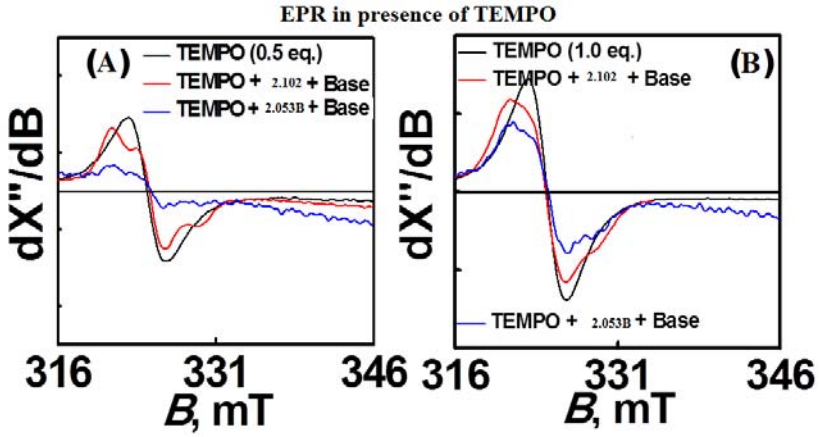

Figure 2.13: (**A**) and (**B**): X band (9.44 GHz) EPR spectra of a mixture of TEMPO and sulfones **2.102** and **2.053 B** and Et_3N in $CHCl_3$, Condition: X-band microwave frequency (GHz), 9.44; modulation frequency (KHz), 100; modulation amplitude (G), 140.0; and microwave power, 0.998 [μW]

	EPR Absorbance area	**Δ_{EPR} Absorbance area**	**% decrease in spin concentration of TEMPO**
Tempo (1mM)	938	----	----
Tempo + **2.102** (1:1)	738	155	17%
Tempo + **2.053 B** (1:1)	563	375	40%
Tempo (2mM)	1983	----	----
Tempo + **2.102** (1:1)	1635	348	18%
Tempo + **2.053 B** (1:1)	1178	805	41%

Table 2.03: Effect of Sample's spin on the spin of Tempo.

2.4 H. Spectral Characterizations

The structure elucidation as well as the extent of deuterium at different position of the compounds was mainly done on the basis of NMR spectroscopy. The ^{1}H NMR spectrum recorded at 400 MHz in $CDCl_3$ for the cyclized product **2.060 D** showed a doublet at δ 7.85 with J = 8.0 Hz corresponding to the hydrogen H_7 that appeared in deshielding region of aromatic ring followed by a singlet for peri hydrogen H_3 at δ 7.67. The aromatic proton H_4 appeared as doublet due to coupling interaction with H_5 at δ 7.58 with J = 8.4 Hz. The other aromatic hydrogens on naphthalene ring H_5 and H_6 appeared at δ 7.44 and 7.35 as doublet of a triplet with J = 10.4 Hz, 0.8 Hz. The aromatic protons H_8, H_9, H_{10} on dimethoxy ring appeared upfield due to electron donating nature of dimethoxy group. The proton H_8 appeared at δ 7.12 as doublet with J = 8.0 Hz and the doublet of doublet for H_9 and doublet for H_{10} merged between δ 6.64-6.60. The methylene hydrogens H_1 and H_2 appeared as singlet at δ 5.30 and 4.97 respectively (**Figure 2.14**). The OMe protons appeared as singlet at δ 3.90 and 3.69. The COSY spectrum recorded in d_6-DMSO for compound **2.060D** (**Figure 2.15**) was also in conformity of the peaks assigned in ^{1}H NMR spectrum.

In case of ^{1}H NMR spectrum of duterated dihydroisofuran derivative **2.060 D'**, recorded at 600 MHz in $CDCl_3$ the aromatic protons H_4-H_7 was totally replaced by deuterium and 86% of hydrogen corresponding to H_3 appeared at δ 7.68 as a singlet. The aromatic protons H_8 appeared at δ 7.12 as doublet with J = 8.4 Hz followed by H_{10} as doublet at δ 6.64 with J = 2.4 Hz. The other aromatic proton H_9 appeared as a doublet of doublet at δ 6.62 with J = 8.4 Hz, 2.4 Hz. The methylene protons H_1 corresponding to 75% of hydrogen appeared as multiplet in between δ 5.30-5.29 followed by H_2 that also appeared as multiplet in between δ 5.00-4.95. The OMe protons appeared as singlet at δ 3.90 and 3.69 (**Figure 2.14**). The peak corresponding to C-9 carbon appeared at δ 118.8 in ^{13}C NMR spectrum and the intensity of the peak was reduced compared to its protiated substrate **2.060 D** which can be explained by C-H NOE effect. The HRMS spectrum showed peak at 311.1568 (calcd 311.1580) and 312.1628 (calcd 312.1643) corresponding to [M+H$^+$] and [M-D+H$^+$].

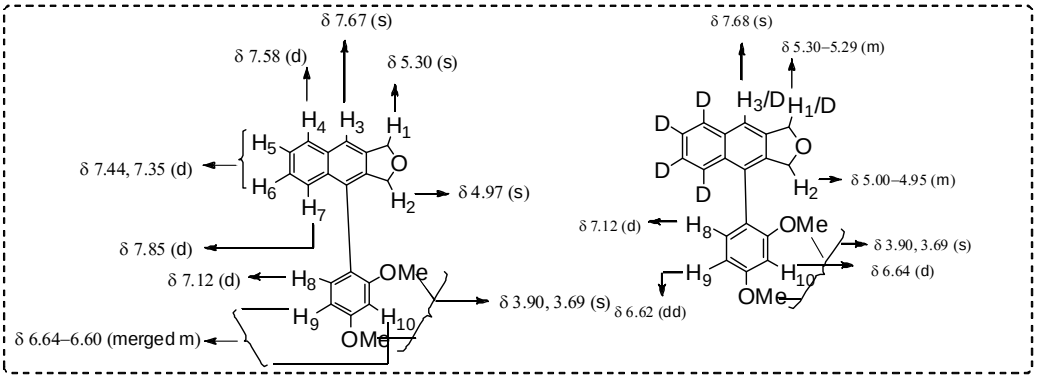

Figure 2.14: ^{1}H-NMR assignment of compound **2.060 D** and **2.060 D'**

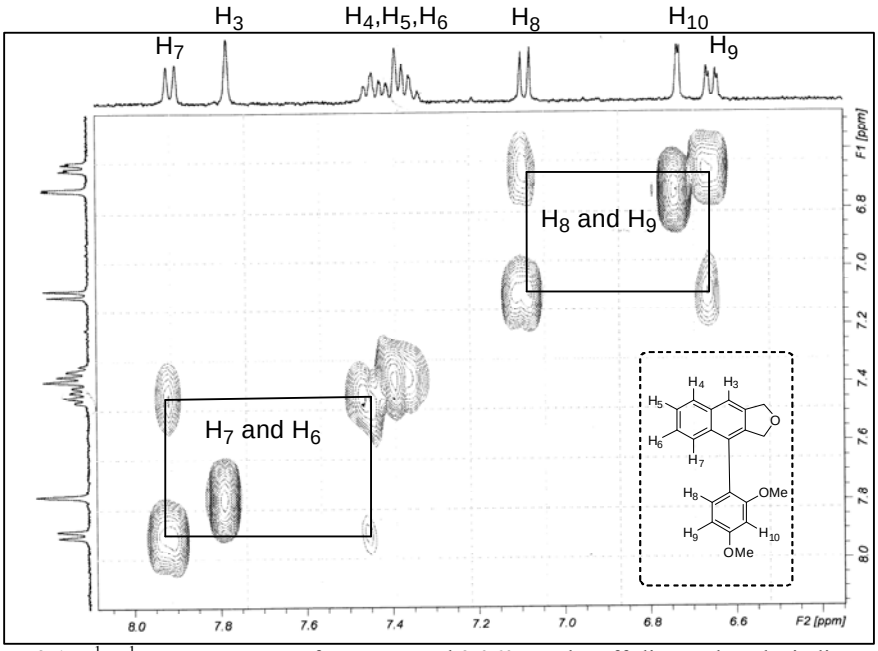

Figure 2.15: ^{1}H-^{1}H cosy spectrum for compound **2.060 D**. The off-diagonal peaks indicate the coupling interaction between the mentioned protons.

2.5 Conclusion

- We have shown the GB reaction mechanism to be system dependent and provided strong support for anionic intramolecular [4+2] cycloaddition reaction mechanism for ethers involving mono-allene and a diradical mechanism for Garratt-Braverman cyclization of bis-propargyl sulfones involving bis-allene.

- We have performed reactions with deuterium labeled substrates and the outcome of the study reinforces our proposed pathway of two different mechanisms.

- We have trapped the intermediate mono-allene for ethers and bis-allenes for sulfones with an external nucleophile MeOH and the adducts have been identified by LA-LDI mass spectrometry.

- We have been successful of recording EPR signals that suggested the involvement of radical intermediates for GB reaction with sulfones.

2.6 Experimental Details

2.6.1 General Experimental

All ^{1}H-NMR and ^{13}C-NMR spectra were obtained with 200 MHz, 400 MHz and 600 MHz NMR instruments in $CDCl_3$ unless mentioned otherwise. The following abbreviations are used to describe peak patterns where appropriate: s = singlet, d = doublet, t = triplet, q = quartet, m = multiplet, app. = apparently and b = broad signal. All coupling constants (*J*) are given in Hz. Mass spectra were recorded in ESI+ mode (ion trap). IR spectra were recorded as thin films and bands are expressed in cm^{-1}. The LA-LDI experiments were carried out using MALDI-TOF Mass Spectrometer. UV laser: smart beam II laser, 355 nm wavelength; laser rep rate 2000 Hz, reflector mode. The mass spectra were recorded in positive ion mode. For ^{2}H NMR the compounds were dissolved in distilled $CHCl_3$ with 1 drop of CD_3CN (δ 2.1) as internal standard.

All the dry solvents used for reactions were purified according to the standard protocols. Dimethyl sulfoxide (DMSO), N, N-dimethylformamide (DMF), triethylamine (Et_3N) were distilled from calcium hydride. All the solvents for column chromatography were distilled prior to use. In most of the column chromatographic purifications, ethyl acetate (EA/EtOAc) and petroleum ether (PE) of boiling range 60-80 °C were used as eluents. Columns were prepared with silica gel (Si-gel, 60-120 and 230-400 mesh, SRL).

2.6.2 General procedure for synthesis of compounds and their spectral data

General procedure for the synthesis of sulfones (2.053 A-D, 2.053 C′, 2.095)

To the ice cold solution of crude sulfide (1 mmol) in THF:MeOH (10:2, total volume 20 mL), was added oxone (767 mg, 2.5 eq) and a few drops of water and the reaction was allowed to stir at nitrogen atmosphere. After 1 h the ice was taken off to convert sulfoxide (intermediate) into sulfone fully and the reaction was kept 12 h at room temperature. The reaction mixture was then diluted with water, extracted with ethyl acetate and the organic layer was washed with saturated brine solution and the combined organic layer was dried by addition of anhydrous sodium sulfate. The solvent was removed by rotor and the crude residue was purified by column chromatography (Si- gel, petroleum ether-ethyl acetate mixture as eluent).

For compound **2.053 A** see at page no. 215 in chapter 6.

2-Methoxy-6-[3-(3-phenyl-prop-2-yne-1-sulfonyl)-prop-1-ynyl]-naphthalene (2.053 B)

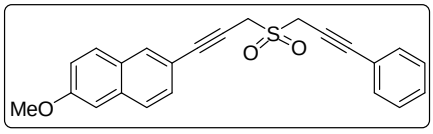

State: yellow solid; m.p. 109 - 110 °C; **yield**: 76%; ^{1}H NMR (600 MHz, Chloroform-*d*) δ 7.96 (s, 1H), 7.70 (d, *J* = 1.2 Hz, 2H), 7.53 - 7.49 (m, 3H), 7.40 - 7.34 (m, 3H), 7.19 (d, *J* = 11.4 Hz, 1H), 7.13 (s, 1H), 4.39 - 4.38 (merged s, 4H), 3.95 (s, 3H); ^{13}C NMR (150 MHz, Chloroform-*d*) δ 158.9, 134.8, 132.4, 132.3, 129.6, 129.5, 129.0, 128.6, 128.4, 127.2, 121.6, 119.9, 116.4, 106.0, 88.8, 88.2, 76.2, 75.6, 55.6, 44.9, 44.8; HRMS: Calcd for $C_{23}H_{18}NaO_3S^+$ $[M+Na]^+$ 397.0874 found 397.0874.

1-Methoxy-4-[3-(3-phenyl-prop-2-yne-1-sulfonyl)-prop-1-ynyl]-benzene (2.053 C)

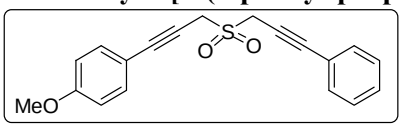

State: white solid; m.p. 110 - 111 °C; **yield**: 72%; ^{1}H NMR (400 MHz, Chloroform-*d*) δ 7.50 (d, 2H, *J* = 6.8 Hz, 2H), 7.43 (d, *J* = 8.4 Hz, 1H), 7.38 - 7.32 (m, 4H), 6.85 (d, *J* = 8.8 Hz, 2H), 4.31 (s, 2H), 4.30 (s, 2H), 3.82 (s, 3H); ^{13}C NMR (50 MHz, Chloroform-*d*) δ 160.5, 133.8, 132.2, 129.4, 128.6, 121.6, 114.2, 113.6, 88.3, 88.1, 76.2, 74.7, 55.5, 44.9, 44.6; HRMS: Calcd for $C_{19}H_{17}O_3S^+$ $[M+H]^+$ 325.0898 found 325.0912.

2,4-Dimethoxy-1-[3-(3-phenyl-prop-2-yne-1-sulfonyl)-prop-1-ynyl]-benzene (2.053 D)

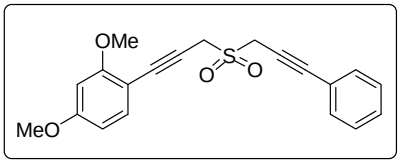

State: pale yellow solid; m.p. 127 - 128 °C; **yield**: 71%; ^{1}H NMR (400 MHz, Chloroform-*d*) δ 7.49 (d, 2H, *J* = 7.6 Hz, 2H), 7.36 - 7.31 (m, 4H), 6.46 - 6.43 (bm, 2H), 4.40 (s, 2H), 4.33 (s, 2H), 3.82 (merged s, 6H); ^{13}C NMR (100 MHz, Chloroform-*d*) δ 162.2, 162.1, 134.7, 132.3, 129.4, 128.6, 111.3, 105.1, 100.2, 98.6, 87.9, 85.1, 78.7, 76.4, 56.0, 55.7, 45.3, 44.2; HRMS: Calcd for $C_{20}H_{19}O_4S^+$ $[M+H]^+$ 355.1004 found 355.1003.

1-Methoxy-4-[3-(3-(1,2,3,4,5-^{2}H$_5$) phenyl-prop-2-yn-1-sulfonyl) prop-1-ynyl]-benzene (2.053 C′)

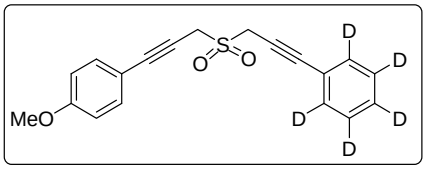

State: white solid; m.p. 119 - 120 °C; **yield**: 70%; ^{1}H NMR (400 MHz, Chloroform-*d*) δ 7.43 (d, *J* = 8.0 Hz, 2H), 6.85 (d, *J* = 8.0 Hz, 2H), 4.32 (s, 2H), 4.31 (s, 2H), 3.82 (s, 3H); ^{13}C NMR (100 MHz, Chloroform-*d*) δ 160.6, 133.8, 131.9 (t, *J* = 24.0 Hz), 129.0 (t, *J* = 25.0 Hz), 128.1 (t, *J* = 25.0 Hz), 121.5, 114.3, 113.6, 88.3, 88.1, 76.2, 74.7, 55.6, 44.9, 44.7; HRMS: Calcd for $C_{19}H_{12}D_5O_3S^+$ $[M+H]^+$ 330.1207 found 330.1194.

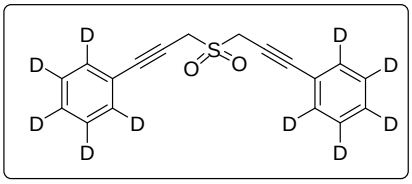

(Sulfonylbis(prop-1-yne-3,1-diyl))(2,3,4,5,6-^{2}H$_5$)dibenzene (2.095)

State: pale yellow crystalline solid; m.p. 108 - 109 °C; **yield**: 85%; ^{1}H NMR (400 MHz, Chloroform-*d*) δ 4.33; ^{13}C NMR (50 MHz, Chloroform-*d*) δ 131.8 (t, *J* = 24.5 Hz), 129.0 (t, *J* = 24.5 Hz), 128.1 (t, *J* = 24.5 Hz), 121.4, 88.2, 76.1, 44.8; HRMS: Calcd for $C_{18}H_5D_{10}O_2S^+$ $[M+H]^+$ 305.1415 found 305.1423.

General procedure for the O-propargylation: Synthesis of bis-propargyl ethers (2.052 A-D, 2.052 D′, 2.091, 2.093)

To an ice-cold solution of NaH (2 eq, 60% suspension in mineral oil) in dry DMF, the alcohol (1 mmol) was added dropwise after diluting it with dry DMF (10 mL) and the reaction was stirred for 30 min at ice cold temperature under N_2 atmosphere. After the alkoxide was generated, respective propargyl bromides (1.0 eq) **2.056 A-D** diluted with dry DMF (5 mL) were added dropwise by maintaining the ice-cold temperature and the mixture was stirred for 1 h. After completion of reaction, the mixture was

quenched by saturated aqueous NH_4Cl and extracted by ethyl-acetate. The organic layer was washed with brine solution and the combined organic layer was dried with anhydrous sodium sulfate. The solvent was removed and the crude residue was purified by column chromatography (Si- gel, petroleum ether-ethyl acetate mixture as eluent).

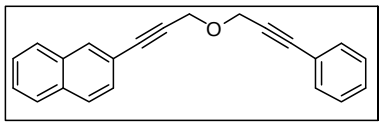

2-[3-(3-Phenyl-prop-2-ynyloxy)-prop-1-ynyl]-naphthalene (2.052 A)

State: brown liquid; **yield**: 61%; IR (neat) ν_{max} 3061, 2926, 2851, 2232, 1723, 1493, 1079, 754 cm^{-1}; ^1H NMR (400 MHz, Chloroform-*d*) δ 8.06 (s, 1H), 7.86 - 7.81 (m, 3H), 7.56 - 7.52 (m, 5H), 7.37 - 7.36 (bs, 3H), 4.65 (s, 2H), 4.64 (s, 2H); ^{13}C NMR (50 MHz, Chloroform-*d*) δ 133.0, 131.9, 128.7, 128.6, 128.5, 128.2, 127.9, 126.9, 126.7, 122.7, 119.9, 87.3, 87.0, 84.9, 84.6, 57.7; MS: m/z = 297.12 $[M+H]^+$.

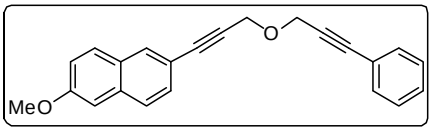

2-Methoxy-6-[3-(3-phenyl-prop-2-ynyloxy)-prop-1-ynyl]-naphthalene (2.052 B)

State: gummy liquid; **yield**: 60%; IR (neat) ν_{max} 3066, 2971, 2851, 2223, 1628, 1488, 1079, 759 cm^{-1}; ^1H NMR (400 MHz, Chloroform-*d*) δ 7.96 (s, 1H), 7.72 - 7.69 (m, 2H), 7.54 (app s, 3H), 7.37 - 7.35 (comp, 3H), 7.19 (d, *J* = 8.0 Hz, 1H), 7.12 (s, 1H), 4.64 (s, 4H), 3.92 (s, 3H); ^{13}C NMR (50 MHz, Chloroform-*d*) δ 158.5, 134.4, 131.9, 131.8, 129.4, 129.1, 128.6, 128.4, 126.9, 122.6, 119.5, 117.4, 105.8, 87.5, 86.9, 84.6, 84.1, 57.7, 57.5, 55.4; MS: m/z = 327.13 $[M+H]^+$.

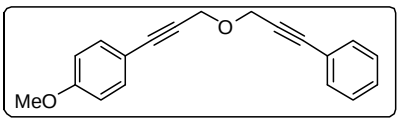

1-Methoxy-4-[3-(3-phenyl-prop-2-ynyloxy)-prop-1-ynyl]-benzene (2.052 C)

State: yellow viscous liquid; **yield**: 60%; IR (neat) ν_{max} 3061, 2972, 2851, 2232, 1620, 1482, 1049, 754 cm^{-1}; ^1H NMR (400 MHz, Chloroform-*d*) δ 7.51 - 7.50 (bm, 2H), 7.44 (d, *J* = 8.4 Hz, 2H), 7.34 (bs, 3H), 6.86 (d, *J* = 8.4 Hz, 2H), 4.57(s, 4H), 3.79 (s, 3H); ^{13}C NMR (100 MHz, Chloroform-*d*) δ 159.9, 138.3, 133.4, 131.9, 128.4, 122.6, 116.5, 114.7, 114.0, 86.8, 84.7, 83.2, 57.6, 57.4, 55.3; MS: m/z = 277.12 $[M+H]^+$.

2,4-Dimethoxy-1-[3-(3-phenyl-prop-2-ynyloxy)-prop-1-ynyl]-benzene (2.052 D)

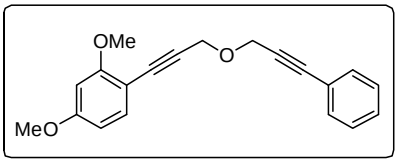

State: yellow liquid; **yield**: 65%; IR (neat) ν_{max} 3016, 2931, 2851, 2227, 1613, 1508, 1079, 764 cm^{-1}; ^1H NMR (400 MHz, Chloroform-*d*) δ 7.47 - 7.45 (m, 2H), 7.36 (d, *J* = 8.0 Hz, 2H), 7.32 - 7.30 (m, 2H), 6.45 (app d, *J* = 4.0 Hz, 1H), 6.43 (s, 1H), 4.58 (s, 2H), 4.56 (s, 2H), 3.86 (s, 3H), 3.81 (s, 3H); ^{13}C NMR (100 MHz, Chloroform-*d*) δ 161.6, 161.5, 134.8, 131.9, 128.4, 122.8, 104.9, 104.4, 98.6, 87.1, 86.7, 84.9, 83.4, 57.9, 57.4, 55.9, 55.6; MS: m/z = 307.13 $[M+H]^+$.

2,4-dimethoxy-1-(3-((3-(1,2,3,4,5-$^2H_5$) phenylprop-2-yn-1-yl)oxy)prop-1-yn-1-yl)benzene (2.052 D′)

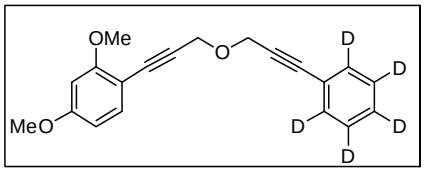

State: yellow liquid; **yield**: 67%. ^1H NMR (400 MHz, Chloroform-*d*) δ 7.36 (d, *J* = 8.0 Hz, 1H), 6.44 (d, *J* = 8.0 Hz, 1H), 6.43 (s, 1H), 4.58 (s, 2H), 4.56 (s, 2H), 3.85 (s, 3H), 3.81 (s, 3H); ^{13}C NMR (50 MHz, Chloroform-*d*) δ 161.6, 161.5, 134.7, 131.5 (t, *J* = 24.5 Hz) 127.9 (2C, s merged with t, *J* = 24.4 Hz), 122.5, 104.9, 104.3, 98.5, 87.1, 86.7, 84.8, 83.4, 57.9, 57.4, 55.9, 55.5; HRMS: Calcd for $C_{20}H_{14}D_5O_3^+$ $[M+H]^+$ 312.1643; found 312.1640.

1-Methoxy-4-[3-methyl-3-(3-(2,3,4,5,6-$^2H_5$)phenyl-prop-2-ynyloxy)-but-1-ynyl]-benzene (2.091)

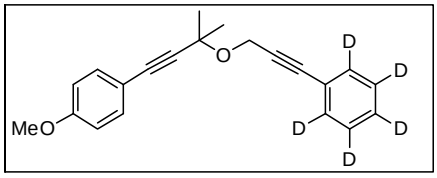

State: yellow liquid; **yield**: 67%; ^1H NMR (600 MHz, Chloroform-*d*) δ 7.40 (d, *J* = 9 Hz, 2H), 6.86 (d, *J* = 8.4 Hz, 2H), 4.60 (s, 2H), 3.83 (s, 3H), 1.65 (s, 6H); ^{13}C NMR (150 MHz, Chloroform-*d*) δ 159.8, 133.4, 114.9, 114.3, 114.1, 89.2, 86.6, 85.5, 85.2, 72.0, 55.5, 53.5, 29.3; HRMS: Calcd for $C_{21}H_{16}D_5O_2^+$ $[M+H]^+$ 310.1850 found 310.1851.

(Oxybis(prop-1-yne-3.1-diyl)) (2,3,4,5,6-$^2H_5$)dibenzene (2.093)

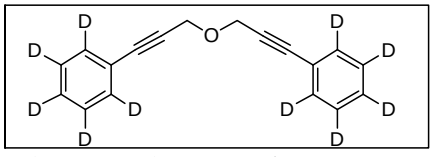

State: yellow liquid; **yield**: 65%; ^1H NMR (400 MHz, Chloroform-*d*) δ 4.57 (s, 2H); ^{13}C NMR (50 MHz, Chloroform-*d*) δ 131.6 (t, *J* = 28.5 Hz), 128.1 (2×merged t, *J* = 24.0 Hz), 122.5, 86.9, 84.6, 57.6; HRMS: Calcd for $C_{18}H_5D_{10}O^+$ $[M+H]^+$ 257.1745 found 257.1740.

General procedure for the N-propargylation: Synthesis of bis-propargyl sulfonamides (2.054 A-D)

To an ice-cold solution of 3-phenyl propargylamine-*p*-toluenesulfonamide derivatives (1 mmol) in dry DMF (5 mL), was added dry K_2CO_3 (2 eq) and stirred. After that, 1.1 equivalent of the respective propargyl bromides (**2.056 A-D**) was added dropwise as a solution in DMF (1 mL) by maintaining the temperature in ice and the reaction mixture was allowed to stir at room temperature for 4 h. It was then quenched by slow addition of NH_4Cl solution and then partitioned between water and ethyl acetate. The organic layer was then evaporated and dried (Na_2SO_4). Silica gel column chromatography furnished the desired product with ethyl acetate-pet ether as eluent.

4-Methyl-*N*-(3-naphthalen-2-yl-prop-2-ynyl)-*N*-(3-phenyl-prop-2-ynyl)-benzenesulfonamide (2.054 A)

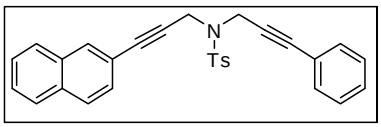

State: yellow solid; **yield**: 70%; IR (neat) ν_{max} 3061, 2926, 2856, 2237, 1603, 1493, 1363, 1169, 754 cm^{-1}; ^1H NMR (400 MHz, Chloroform-*d*) δ 7.87 - 7.81 (m, 4H), 7.33 (app d, *J* = 4.0 Hz, 2H), 7.52 - 7.50 (m, 2H), 7.28 - 7.26 (m, 7H), 7.15 (app d, *J* = 4.0 Hz, 1H), 4.53 (s, 2H), 4.52 (s, 2H), 2.31 (s, 3H); ^{13}C NMR (100 MHz, Chloroform-*d*) δ 143.9, 135.4, 132.9, 132.8, 131.8, 131.7, 131,6, 129.7, 128.6, 128.5, 128.3, 128.2, 128.1, 127.9, 127.8, 127.7, 127.5, 126.9, 126.7, 122.2, 119.5, 86.3, 85.9, 82.0, 81.8, 37.8, 37.7, 21.5; MS: m/z = 450.14 $[M+H]^+$.

***N*-[3-(6-Methoxy-naphthalene-2-yl)-prop-2-ynyl]-4-methyl-*N*-(3-phenyl-prop-2-ynyl)-benzene sulfonamide (2.054 B)**

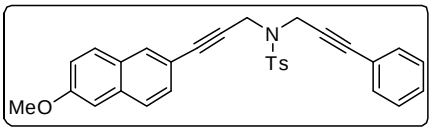

State: gummy oil; **yield**: 73%; IR (neat) ν_{max} 3051, 2966, 2926, 2856, 2232, 1633, 1488, 1348, 1163, 1094, 759 cm^{-1}; ^1H NMR (400 MHz, Chloroform-*d*) δ 7.82 (d, *J* = 8.0 Hz, 2H), 7.64 - 7.60 (m, 3H), 7.30 - 7.24 (m, 8H), 7.21 - 7.09 (m, 1H), 7.08 (s, 1H), 4.48 (s, 4H), 3.92 (s, 3H), 2.30 (s, 3H); ^{13}C NMR (100 MHz, Chloroform-*d*) δ 158.5, 143.9, 135.5, 134.3, 131.8, 131.6, 129.8, 129.7, 129.3, 128.9, 128.6, 128.3, 128.2, 128.1, 127.6, 126.7, 122.3, 119.6, 117.2, 105.8, 86.4, 85.9, 81.9, 81.3, 55.4, 37.8, 37.7, 21.6; MS: m/z = 480.16 $[M+H]^+$.

***N*-[3-(4-Methoxy-phenyl)-prop-2-ynyl]-4-methyl-*N*-(3-phenyl-prop-2-ynyl)-benzenesulfonamide (2.054 C)**

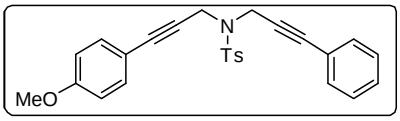

State: gummy liquid; **yield:** 69%; IR (neat) ν_{max} 3061, 2926, 2851, 2242, 1603, 1463, 1348, 1158, 1089, 749 cm^{-1}; ^1H NMR (400 MHz, Chloroform-*d*) δ 7.81 (d, *J* = 8 Hz, 2H), 7.28 - 7.21 (comp, 7H), 7.18 (d, *J* = 8.0 Hz, 2H), 6.80 (d, *J* = 8.0 Hz, 2H), 4.46 (s, 2H), 4.44 (s, 2H), 3.82 (s, 3H), 2.35 (s, 3H); ^{13}C NMR (50 MHz, Chloroform-*d*) δ 159.9, 143.9, 135.6, 133.3, 131.8, 129.7, 128.6, 128.3, 128.1, 122.4, 114.4, 113.9. 85.9, 81.9, 80.4, 55.4, 37.7, 37.6, 21.5; MS: m/z = 430.14 $[M+H]^+$.

***N*-[3-(2,4-Dimethoxy-phenyl)-prop-2-ynyl]-4-methyl-*N*-(3-phenyl-prop-2-ynyl)-benzenesulfonamide (2.054 D)**

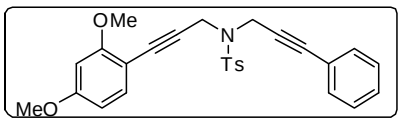

State: Viscous liquid; **yield**: 65%; IR (neat) ν_{max} 3052, 2961, 2926, 2854, 2231, 1635, 1470, 1349, 1161, 1094, 754 cm^{-1}; ^1H NMR (400 MHz, Chloroform-*d*) δ 7.79 (d, *J* = 8.0 Hz, 2H), 7.26 - 7.17 (comp, 6H), 7.06 (d, *J* = 8.0 Hz, 2H), 6.37 (app d, *J* = 8.0 Hz, 2H), 4.46 (s, 4H), 3.80 (s, 6H), 2.30 (s, 3H); ^{13}C NMR (100 MHz, Chloroform-*d*) δ 161.4, 143.7, 137.5, 135.6, 134.4, 131.7, 130.3, 129.5, 128.4, 128.2, 128.0, 122.4, 104.7, 104.1, 98.3, 85.6, 84.2, 82.4, 81.9, 55.8, 55.5, 37.9, 37.3, 21.5; MS: m/z = 460.15 $[M+H]^+$.

General procedure for the Garratt-Braverman Cyclization: Synthesis of aryl naphthalenes

For ethers (2.059/2.060 A-D, 2.060 D´, 2.092, 2.094)

To an ice-cold solution of the bis-propargyl ethers (0.2 mmol) in dry DMSO (5 mL) was added KO^{t}Bu (1.2 eq) and the reaction was allowed to stir at room temperature for 1 h. After completion of the reaction, confirmed by TLC, it was quenched with NH_4Cl solution and extracted with ethyl acetate. The organic layer was dried over anhydrous sodium sulfate and evaporated to get the crude product which was purified by column chromatography with hexane-ethyl acetate mixture as eluent. The ratio of the products was determined from crude reaction mixtures.

11-Phenyl-8,10-dihydro-9-oxa-cyclopenta[*b*]phenanthrene (major) (2.059 A), 4-Naphthalen-2-yl-1,3-dihydro-naphtho[2,3-*c*]furan (minor) (2.060 A) (2.059 A:2.060 A = 2:1)

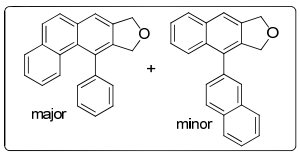

State: pale yellow sticky mass; **yield**: 86 mg, 97%; IR (neat) ν_{max} 2924, 2854, 1657, 1462, 1051, 753 cm^{-1}; ^1H NMR (400 MHz, Chloroform-*d*) δ 8.00 - 7.68 (comp, 10H, major + minor), 7.59 - 7.34 (comp, 13H, major + minor), 7.12 (td, *J* = 8.0, 4.0 Hz, 1H, major), 5.38 (s, 2H, major), 5.34 (s, 2H, minor), 5.12, 5.04 (ABq, *J* = 12.0 Hz, 2H, minor), 4.96 (s, 2H, major); ^{13}C NMR (100 MHz, Chloroform-*d*) (major + minor) δ 142.6, 139,7, 137.7, 137.4, 137.2, 135.7, 133.7, 133.6, 133.5, 132.8, 132.5, 131.9, 130.8, 130.1, 129.6, 128.8, 128.5, 128.4, 128.3, 128.2, 127.9, 127.7, 127.6, 127.5, 126.5, 126.4, 125.9, 125.8, 125.7, 125.2, 120.3, 74.0,73.9, 73.4, 72.9; MS: m/z = 297.12 $[MH^+]$. HRMS: Calcd. for $C_{22}H_{15}O^+$ $[M-H]^+$ 295.1123 found 295.1046, Calcd. for $C_{21}H_{15}^+$ $[M-CO]^+$ 267.1174 found 267.1086.

4-(6-Methoxy-naphthalen-2-yl)-1,3-dihydro-naphtho[2,3-*c*]furan (major) (2.060 B), 3-Methoxy-11-phenyl-8,10-dihydro-9-oxa-cyclopenta[*b*]phenanthrene (minor) (2.059 B) (2.060 B:2.059 B = 1:2)

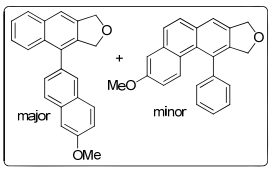

State: yellow gummy mass; **yield:** 94%; IR (neat) ν_{max} 2924, 2852, 1608, 1460, 1049, 751 cm^{-1}; ^1H NMR (400 MHz, Chloroform-*d*) δ 7.88 (t, *J* = 8.0 Hz, 2H, major), 7.78 - 7.72 (m, 6H, minor), 7.65 (d, *J* = 8.0 Hz, 1H, minor), 7.55 - 7.44 (m, 5H, major, 1H, minor), 7.38 (d, *J* = 8.0 Hz, 1H, minor), 7.33 (d, *J* = 8.0 Hz, 2H, major), 7.25 (d, *J* = 8.0 Hz, 2H, major), 7.21 (t, *J* = 4.0 Hz, 1H, minor), 6.72 (dd, *J* = 8.0 Hz, 4 Hz, 1H, minor), 5.35 - 5.30 (m, 4H, major + minor), 5.09, 5.02 (ABq, *J* = 12.0 Hz, 2H, major), 4.92 (s, 2H, minor), 3.98 (s, 3H, major), 3.88 (s, 3H, minor); ^{13}C NMR (50 MHz, Chloroform-*d*) (major + minor) δ 158.2, 157.5, 142.7, 137.9, 137.3, 136.6, 134.1, 133.9, 133.5, 132.9, 132.7, 132.2, 129.8, 129.3, 129.1, 128.5, 128.4, 128.3, 127.7, 127.2, 126.0, 125.9, 125.8, 120.5, 119.5, 118.9, 115.3, 109.0, 105.9, 74.1, 73.6, 73.2, 55.6, 55.4; MS: m/z = 327.13 $[MH^+]$; HRMS: Calcd. for $C_{23}H_{17}O_2^+$ $[M-H]^+$ 325.1229 found 325.1157, Calcd. for $C_{22}H_{17}O^+$ $[M-CO]^+$ 297.1279 found 297.1206.

4-(4-Methoxy-phenyl)-1,3-dihydro-naphtho[2,3-*c*]furan (major) (2.060 C), 6-Methoxy-4-phenyl-1,3-dihydro-naphtho[2,3-*c*]furan (minor) (2.059 C) (2.059 C:2.060 C = 1:8)

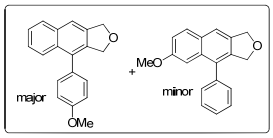

State: gummy yellow solid; **yield**: 95%; IR (neat) ν_{max} 2923, 2853, 1634, 1462, 1053, 752 cm^{-1}; ^1H NMR (400 MHz, Chloroform-*d*) δ 7.86 (d, *J* = 8.0 Hz, 1H, major), 7.72 (d, *J* = 8.0 Hz, 1H, major), 7.67 (s, 1H, major), 7.46 (t, *J* = 8.0 Hz, 1H, major), 7.38 (t, *J* = 8.0 Hz, 1H, major), 7.29 (d, *J* = 8.0 Hz, 2H, major), 7.04 (d, *J* = 8.0 Hz, 2H, major), 5.29 (s, 2H, major), 5.27 (s, 2H, minor), 5.03 (s, 2H, major), 5.00 (s, 2H, minor), 3.90 (s, 6H, major + minor); ^{13}C NMR (50 MHz, Chloroform-*d*) (major + minor) δ 159.3, 137.8, 137.2, 133.9, 132.5, 132.3, 130.8, 130.5, 128.3, 125.9, 125.8, 125.7, 118.7, 114.2, 73.6, 73.2, 55.5; MS: m/z = 277.12 [M+H^+]; HRMS: Calcd. for $C_{19}H_{15}O_2^+$[M-H]$^+$ 275.1072 found 275.0965.

4-(2,4-Dimethoxy-phenyl)-1,3-dihydro-naphtho[2,3-*c*]furan (major) (2.060 D), 6,8-Dimethoxy-4-phenyl-1,3-dihydro-naphtho[2,3-*c*]furan (minor) (2.059 D) (2.059 D:2.060 D = 1:10)

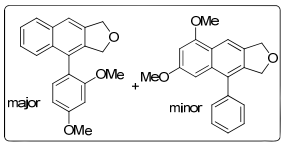

State: pale yellow gummy solid; **yield**: 94%; ^1H NMR (400 MHz, Chloroform-*d*) δ 7.85 (d, *J* = 8.0 Hz, 1H, major), 7.67 (s, 1H, major), 7.58 (d, *J* = 12 Hz, 1H, major), 7.44 (td, *J* = 8.0, 4.0 Hz, 1H, major), 7.35 (app td, *J* = 8.0, 4.0 Hz, 1H, major), 7.12 (d, *J* = 8.0 Hz, 1H, major), 6.64 (m, 1H, major), 6.61 (d, *J* = 4.0 Hz, 1H, major), 6.56 (s, 1H, minor), 6.52 (s, 1H, minor), 5.30 (s, 4H, major + minor), 4.98 (app s, 4H, major + minor), 3.90 (s, 6H, major + minor), 3.69 (s, 6H, major + minor); MS: m/z = 307.13 [M+H^+]; HRMS: Calcd. for $C_{20}H_{17}O_3^+$ [M-H]$^+$ 305.1178 found 305.1096.

4-(2,4-dimethoxyphenyl)-1,3-dihydro(5,6,7,8-$^2H_5$) naphtho [2,3-*c*] furan (2.060 D´)

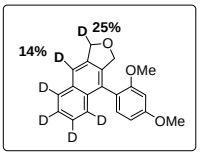

State: sticky mass; yield: 74%. ^1H NMR (600 MHz, Chloroform-*d*) δ 7.70 (s, 0.86H, 0.14D), 7.15 (d, *J* = 8.4 Hz, 1H), 6.66 (d, *J* = 2.4 Hz, 1H), 6.64 (dd, *J* = 8.4 Hz, 2.4 Hz, 1H), 5.32 - 5.31 (m, 1.5H, 0.5D), 5.04 - 4.96 (m, 2H), 3.92 (s, 3H), 3.71 (s, 3H); ^{13}C NMR (150 MHz, Chloroform-*d*) δ 161.0, 158.2, 139.5, 138.1, 137.6, 137.5, 133.7, 132.5, 132.0, 129.0, 119.2, 118.8, 118.7, 114.3, 104.7, 99.2, 73.6, 73.3 (t, *J* = 25.8 Hz), 55.7, 55.6; HRMS:

Calcd for $C_{20}H_{14}D_5O_3^+$ $[M+H]^+$ 312.1643 found 312.1628, Calcd for $C_{20}H_{15}D_4O_3^+$ $[M+H]^+$ 311.1580 found 311.1568.

4-phenyl-1,3-dihydro-(5,6,7,8-$^2H_5$)naphtho[2,3-*c*]furan (2.094)

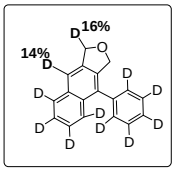

State: gummy mass; **yield**: 70%. ^{1}H NMR (600 MHz, Chloroform-*d*) δ 7.72 (s, 0.86H, 0.14D), 5.32 (s, 1.65H, 0.35D), 5.04 (s, 2H); ^{13}C NMR (150 MHz, Chloroform-*d*) δ 138.1, 137.8, 137.0, 133.8, 132.7, 131.9, 129.2 (t, *J* = 24.1 Hz), 128.3 (t, *J* = 24.0 Hz), 125.6 - 125.1 (m), 118.9, 73.6, 73.1; HRMS: Calcd for $C_{18}H_5D_{10}O^+$ $[M+H]^+$ 257.1745 found 257.1731, Calcd for $C_{18}H_6D_9O^+$ $[M+H]^+$ 256.1683 found 256.1675.

9-(4-Methoxy-phenyl)1,1-dimethyl-1,3-dihydro-(5,6,7,8-$^2H_5$)naphtho[2,3-*c*]furan (2.092)

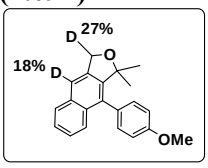

State: sticky mass; **yield**: 60%; ^{1}H NMR (400 MHz, Chloroform-*d*) δ 7.66 (s, 0.82H, 0.18D), 7.20 (d, *J* = 12.6 Hz, 2H), 7.02 (d, *J* = 12.6 Hz, 2H), 5.18 (app s, 1.73H, 0.27D), 3.90 (s, 3H), 2.17 (s, 6H); ^{13}C NMR (100 MHz, Chloroform-*d*) δ 159.2, 143.3, 139.5, 138.4, 133.8, 133.2, 133.0, 132.0, 129.5, 119.0, 114.3, 113.5, 86.4, 69.3, 55.5, 53.6, 31.1, 29.9; HRMS: Calcd for $C_{21}H_{16}D_5O_2^+$ $[M+H]^+$ 310.1850 found 310.1833, Calcd for $C_{21}H_{17}D_4O_2^+$ $[M+H]^+$ 309.1789 found 309.1804.

General procedure for the GB rearrangement of sulfonamides (2.063/2.064 A-D)

The amines (0.3 mmol) **2.054 A-D** were dissolved in dry toluene (10 ml) and 1.0 eq of DBU was added into it. The mixture was then heated to reflux for 12 h. The solvent was then removed and the crude was taken for ^{1}H NMR analysis. In some cases the major product was further isolated pure from the reaction mixture.

11-Phenyl-9-(toluene-4-sulfonyl)-9,10-dihydro-8*H*-9-aza-cyclopenta[*b*]phenanthrene (major) (2.063 A), 4-Naphthalen-2-yl-2-(toluene-4-sulfonyl)-2,3-dihydro-1*H*-benzo[*f*]isoindole (minor) (2.064 A) (2.063 A:2.064 A = 1.9:1)

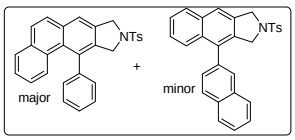

State: light brown sticky mass; **yield**: 80%; IR (neat) ν_{max} 2924, 2856, 1598, 1448, 1346, 1163, 1097, 748 cm^{-1}; ^{1}H NMR (400 MHz, Chloroform-*d*) δ 7.99 (t, *J* = 8.0 Hz, 1H,

major), 7.84 - 7.58 (complex, 20H, major + minor), 7.56 - 7.25 (comp, 10H, major + minor), 7.08 (t, *J* = 8.0 Hz, 1H, major), 4.87 (s, 2H, major), 4.84 (s, 2H, minor), 4.48 - 4.58 (m, 2H, minor), 4.44 (s, 2H, major), 2.40 (s, 6H, major + minor); ^{13}C NMR (50 MHz, Chloroform-*d*) δ 143.9, 142.0, 136.3, 135.3, 134.3, 133.8, 133.6, 130.6, 130.0, 128.7, 128.5, 128.4, 128.0, 127.8, 127.7, 127.5, 127.4, 126.7, 126.2, 125.5, 122.1, 120.9, 54.3, 54.1, 53.3, 21.7; MS: m/z = 450.14 $[M+H]^+$; HRMS: Calcd. for $C_{29}H_{23}NNaO_2S^+$ 472.1347 found 472.1344.

3-Methoxy-11-phenyl-9-(toluene-4-sulfonyl)-9,10-dihydro-8*H*-9-aza-cyclopenta[*b*]phenanthrene (major) (2.063 B), 4-(6-Methoxy-naphthalen-2-yl)-2-(toluene-4-sulfonyl)-2,3-dihydro-1*H*-benzo[*f*]isoindole (minor) (2.064 B) (2.063 B:2.064 B = 2.4:1)

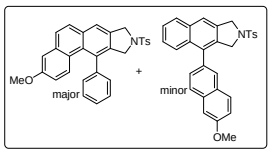

State: gummy solid; **yield**: 75%; ^{1}H NMR (400 MHz, Chloroform-*d*) δ 7.89 (d, *J* = 8.0 Hz, 1H, minor), 7.85 (d, *J* = 8.0 Hz, 1H, minor), 7.75 (d, *J* = 8.0 Hz, 2H, major, 3H, minor), 7.69 - 7.62 (m, 3H, major, 3H minor), 7.57 - 7.52 (m, 3H, major), 7.45 (app d, *J* = 9.6 Hz, 1H, major, 1H, minor), 7.37 - 7.25 (m, 4H, major, 5H, minor), 7.19 (d, *J* = 2.4 Hz, 1H, major), 6.72 (dd, *J* = 8.4 Hz, 2 Hz, 1H, major), 4.85 (s, 4H, major + minor), 4.52 - 4.54 (m, 2H, minor), 4.43 (s, 2H, major), 4.02 (s, 3H, minor), 3.88 (s, 3H, major), 2.41 (s, 6H, major + minor); MS: m/z = 480.16 $[M+H]^+$; HRMS: Calcd. for $C_{30}H_{26}NO_3S^+[M+H]^+$ 480.1633 found 480.1614.

3-Methoxy-11-phenyl-9-(toluene-4-sulfonyl)-9,10-dihydro-8*H*-9-aza-cyclopenta[*b*]phenanthrene (2.063 B)

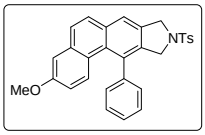

State: pale yellow solid; **yield**: 76 mg, 52%**;** IR (neat) ν_{max}, 2922, 2851, 1628, 1480, 1349, 1161, 1092, 750 cm^{-1}; ^{1}H NMR (400 MHz, Chloroform-*d*) δ 7.73 (d, *J* = 8.0 Hz, 2H), 7.67 - 7.61 (m, 3H), 7.56 - 7.50 (m, 3H), 7.42 (d, *J* = 9.6 Hz, 1H), 7.30 (d, *J* = 8.0 Hz, 2H), 7.24 - 7.22 (m, 2H), 7.17 (d, *J* = 2.8 Hz, 1H), 6.69 (dd, *J* = 9.6 Hz, 2.8 Hz, 1H), 4.84 (s, 2H), 4.40 (s, 2H), 3.86 (s, 3H), 2.39 (s, 3H); ^{13}C NMR (50 MHz, Chloroform-*d*) δ 157.7, 143.9, 142.1, 136.4, 135.3, 134.6, 133.9, 133.4, 132.9, 130.1, 129.3, 128.6, 128.5, 128.1, 128.0, 127.9, 127.8, 127.6, 124.9, 122.2, 115.5, 109.1, 55.5, 54.4, 54.2, 21.7); MS: m/z = 480.16 $[M+H]^+$; HRMS: Calcd. for $C_{30}H_{26}NO_3S^+$ $[M+H]^+$ 480.1633 found 480.1614.

4-(4-Methoxy-phenyl)-2-(toluene-4-sulfonyl)-2,3-dihydro-1*H*-benzo[*f*]isoindole (major) (2.064 C), 6-Methoxy-4-phenyl-2-(toluene-4-sulfonyl)-2,3-dihydro-1*H*-benzo[*f*]isoindole (minor) (2.063 C) (2.063 C:2.064 C = 1:4.9)

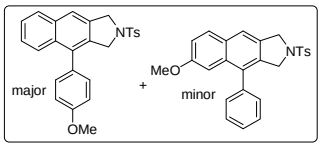

State: gummy solid; **yield**: 73%; IR (neat) ν_{max} 2924, 2856, 1662, 1465, 1352, 1162, 1093, 755 cm^{-1}; ^1H NMR (400 MHz, Chloroform-*d*) δ 7.80 (d, *J* = 8.0 Hz, 1H, major), 7.75 (d, *J* = 8.0 Hz, 2H, major), 7.60 (app d, *J* = 8.0 Hz, 2H, major), 7.43 (t, *J* = 8.0 Hz, 1H, major), 7.35 (app t, *J* = 8.0 Hz, 1H, major), 7.30 (d, *J* = 8.0 Hz, 2H, major), 7.18 (d, *J* = 12.0 Hz, 2H, major), 7.03 (d, *J* = 12.0 Hz, 2H, major), 6.85 (d, *J* = 2.4 Hz, 1H, minor), 4.79 (s, 2H, major), 4.77 (s, 2H, minor), 4.50 (s, 2H, major), 4.46 (s, 2H, minor), 3.91 (s, 3H, major), 3.69 (s, 3H, minor), 2.39 (s, 6H, major + minor); ^{13}C NMR (50 MHz, Chloroform-*d*) δ 159.5, 143.9, 134.5, 133.9, 132.3, 130.7, 130.0, 129.5, 129.1, 128.1, 127.9, 126.2, 126.1, 120.6, 114.4, 100.2, 55.6, 53.8, 53.4, 21.7; MS: m/z = 430.14 $[M+H]^+$; HRMS: Calcd. for $C_{26}H_{23}NNaO_3S^+$ $[M+Na]^+$ 452.1296 found 452.1293.

4-(2,4-Dimethoxy-phenyl)-2-(toluene-4-sulfonyl)-2,3-dihydro-1*H*-benzo[*f*]isoindole (major) (2.064 D), 6,8-Dimethoxy-4-phenyl-2-(toluene-4-sulfonyl)-2,3-dihydro-1*H*-benzo[*f*]isoindole (minor) (2.063 D) (2.063 D:2.064 D = 1:4):

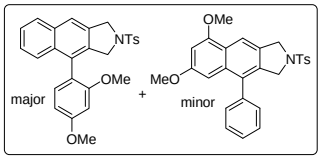

State: sticky mass; **yield**: 76%; ^1H NMR (400 MHz, DMSO-d_6) δ 7.93 (s, 1H, minor), 7.85 (d, *J* = 8.0 Hz, 1H, major), 7.74 - 7.68 (complex, 5H, major, 2H, minor), 7.40 - 7.24 (complex, 3H, major, 7H, minor), 7.01 (d, *J* = 8.0 Hz, 1H, major), 6.74 (s, 1H, major), 6.67 (d, *J* = 8.0 Hz, 1H, major), 6.60 (s, 1H, minor), 6.33 (s, 1H, minor), 4.73 (s, 2H, major), 4.69 (s, 2H, minor), 4.34 - 4.19 (m, 4H, major + minor), 3.92 (s, 3H, minor), 3.85 (s, 3H, major), 3.57 (app s, 6H, major + minor), 2.48 (s, 6H, major + minor), 2.35 (s, 3H, minor), 2.32 (s, 3H, major); MS: m/z = 460.15 $[M+H]^+$; HRMS: Calcd. for $C_{27}H_{26}NO_4S^+$ $[M+H]^+$ 460.1583 found 460.1509.

4-(2,4-Dimethoxy-phenyl)-2-(toluene-4-sulfonyl)-2,3-dihydro-1*H*-benzo[*f*]isoindole (2.064 D)

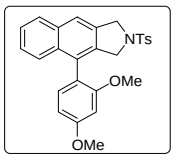

State: pale yellow solid; **yield**: 60%; IR (neat) ν_{max}, 2922, 2852, 1604, 1461, 1349, 1161, 1032, 754 cm^{-1}; ^1H NMR (400 MHz, Chloroform-*d*) δ 7.81 (d, *J* = 8.0 Hz, 1 H), 7.78 (d, *J* = 8.0 Hz, 1 H), 7.72 (d, *J* = 8.0 Hz, 2 H), 7.60 (s, 1 H), 7.50 (d, *J* = 8.0 Hz, 1 H), 7.41 (t, *J* = 8.0 Hz, 1 H), 7.34 - 7.28 (m, 2 H), 7.01 (d, *J* = 8.0 Hz, 1 H), 6.61 (app d, *J* = 7.6 Hz, 2 H), 4,81 - 4.75 (m, 2 H), 4.46 (s, 2 H), 3.91 (s, 3 H), 3.64 (s, 3 H), 2.38 (s, 3 H); ^{13}C NMR (50 MHz, Chloroform-*d*) δ 161.2, 158.0, 143.8, 134.8, 134.2, 133.8, 133.7, 132.6, 131.9, 130.8, 129.9, 128.1, 127.9, 126.7, 126.0, 125.9, 120.7, 118.4, 105.0, 99.2, 55.7, 53.9, 53.6, 21.7; MS: m/z = 460.15 $[M+H]^+$; HRMS: Calcd. for $C_{27}H_{26}NO_4S^+$ $[M+H]^+$ 460.1583 found 460.1509.

For sulfones (2.061/2.062 A-D, 2.061/2.062 C′, 2.096)

To a solution of sulfone (0.05 mmol) in dry $CHCl_3$ (1 mL) was added Et_3N (1 eq) and the solution was stirred at room temperature for 30 min. It was then quenched with NH_4Cl and extracted with DCM. The organic layer was dried over anhydrous sodium sulfate and evaporated to get the crude product that was purified by column chromatography with hexane−ethyl acetate mixture (5:1) as eluent.

The ratio of the products was determined from crude reaction mixtures.

For **2.061 A/2.062 A** see at page no. 216 in chapter 6.

3-methoxy-11-phenyl-8,10-dihydrophenanthro[2,3-*c*]thiofene 9,9-dioxide (Major) (2.061 B) + 4-(6-methoxynaphthalen-2-yl)-1,3-dihydronaphtho[2,3-*c*]thiofene 2,2-dioxide (Minor) (2.062 B) (5.16:1)

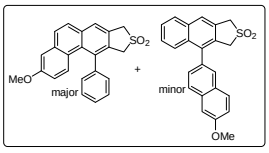

State: yellow sticky solid; **yield**: 90%; ^1H NMR (400 MHz, Chloroform-*d*) δ 7.82 (s, 1H, major), 7.70 (s, 2H, major), 7.58 - 7.52 (m, 3H, major), 7.42 (d, *J* = 9.6 Hz, 1H), 7.28 (app d, *J* = 8.0 Hz, 2H), 7.20 (d, *J* =2.8 Hz, 1H), 6.73 (dd, *J* = 9.6 Hz, 2.8 Hz, 1H), 4.62 (s, 2H major, 2H minor), 4.28 (dd, *J* = 16.8 Hz, 26.2 Hz, 2H minor), 4.15 (s, 2H, major), 3.99 (s, 3H,minor), 3.88 (s, 3H,major). ^{13}C NMR (100 MHz, Chloroform-*d*) δ 158.0, 142.3, 137.6, 135.6, 132.8, 130.9, 130.3, 129.3, 129.2, 128.7, 128.6, 128.4, 128.0, 127.6, 126.0, 124.6, 115.8, 109.3, 57.8, 57.7, 55.5; HRMS: Calcd for $C_{23}H_{19}O_3S^+$ $[M+H]^+$ 375.1055 found 375.1079.

6-Methoxy-4-phenyl-1,3-dihydro-naphtho [2,3-*c*] thiofene 2,2-dioxide (Major) (2.061 C)+ 4-(4-Methoxy-phenyl)-1,3-dihydro-naphtho [2,3-*c*] thiofene 2,2-dioxide (Minor) (2.062 C) (2:1)

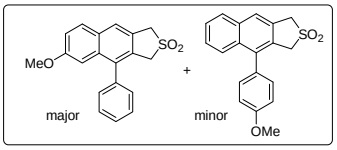

State: yellow sticky solid; **yield**: 85%; ^{1}H NMR (400 MHz, Chloroform-*d*) δ 7.86 (d, *J* = 8.0 Hz, 1H, minor), 7.80 (s, 1H, minor), 7.76 (d, *J* = 8.8 Hz, 1H, major), 7.74 (s, 1H, major), 7.61 (d, *J* = 8.8 Hz, 1H, minor), 7.55 - 7.41 (m, 3H major, 2H minor), 7.30 (d, *J* = 6.8 Hz, 2H major), 7.21 (app t, *J* = 8.8 Hz, 1H major, 2H, minor), 7.06 (d, *J* = 8.8 Hz, 2H, minor), 6.83 (d, *J* = 2 Hz, 1H, major), 4.58 (s, 2H, minor), 4.56 (s, 2H, major), 4.25 (s, 2H, minor), 4.20 (s, 2H, major), 3.90 (s, 3H, minor), 3.70 (s, 3H, major); ^{13}C NMR (100 MHz, Chloroform-*d*) δ 159.7, 158.5, 138.0, 137.9, 136.8, 133.6, 133.4, 132.6, 129.7, 129.6, 129.5, 129.2, 129.0, 128.7, 128.6, 128.4, 128.3, 128.1, 127.0, 126.9, 124.8, 124.7, 119.5, 114.5, 104.9, 57.4, 57.3, 56.8, 56.7, 55.6, 55.3; HRMS: Calcd for $C_{19}H_{17}O_3S^+$ $[M+H]^+$ 325.0893 found 325.0912.

6,8-dimethoxy-4-phenyl-1,3-dihydronaphtho[2,3-*c*]thiofene 2,2-dioxide (Major) (2.061 D) + 4-(2,4-dimethoxyphenyl)-1,3-dihydronaphtho[2,3-*c*]thiofene 2,2-dioxide (Minor) (2.062 D) (5.16:1)

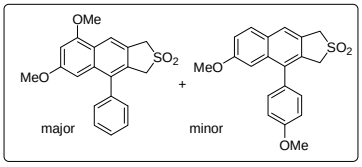

State: sticky solid; **yield**: 93%; ^{1}H NMR (400 MHz, Chloroform-*d*) δ 8.15 (s, 1H, major),7.54 - 7.46 (m, 3H, major), 7.29 (app d, *J* = 5.6 Hz, 2H, major), 6.53 (s, 1H, major), 6.39 (s, 1H, major), 4.56 (s, 2H major, 2H minor), 4.18 (s, 2H major, 2H minor), 3.99 (s, 3H major), 3.91 (s, 3H minor), 3.71 (s, 3H minor), 3.67 (s, 3H major); ^{13}C NMR (100 MHz, Chloroform-*d*) δ 159.0, 156.6, 138.3, 136.4, 134.1, 129.6, 129.2, 128.3, 125.4, 122.0, 119.4, 98.4, 96.9, 57.6, 56.9, 56.0, 55.4; HRMS: Calcd for $C_{20}H_{19}O_4S^+$ $[M+H]^+$ 355.1004 found 355.0987.

6-Methoxy-4-(1,2,3,4,5-$^{2}H_5$)phenyl-1,3-dihydro-naphtho [2,3-*c*] thiofene 2,2-dioxide (Major) (2.061 C′) + 4-(4-Methoxy-phenyl)-1,3-dihydro(5,6,7,8-$^{2}H_5$) -naphtho [2,3-*c*] thiofene 2,2-dioxide (Minor) (2.062 C′) (2:1)

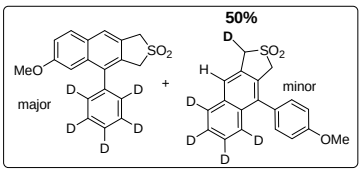

State: yellow sticky solid; **yield**: 185%; ^{1}H NMR (600 MHz, Chloroform-*d*) δ 7.81 (s, 1H, minor), 7.77 (d, *J* = 9.0 Hz, 1H, major), 7.74 (s, 1H, major), 7.22 (d, *J* = 8.4 Hz, 2H, minor), 7.19 (dd, *J* = 9.0 Hz, 2.4 Hz, 1H, major), 7.06 (d, *J* = 8.4 Hz, 2H, minor), 6.84 (d, *J* = 2.4 Hz, 1H, major), 4.56 (app s, 2H major, 1H minor, 1D minor), 4.26 (s, 2H, minor), 4.20 (s, 2H, major), 3.91 (s, 3H, minor), 3.70 (s, 3H, major); ^{13}C NMR (150 MHz, Chloroform-*d*) δ 159.7, 158.6, 138.0, 137.7, 136.8, 133.6, 133.4, 132.5, 130.9, 129.7, 129.6, 129.0, 128.6, 128.4, 126.2, 124.8, 124.7, 119.6, 114.6, 104.9, 57.3, 57.1 (t, *J* = 21.6 Hz), 56.8, 56.7, 55.6, 55.4; HRMS: Calcd for $C_{19}H_{12}D_5O_3S^+$ $[M+H]^+$ 330.1207 found 330.1213.

4-(2,3,4,5,6-$^{2}H_5$)Phenyl-1,3-dihydro-(5,6,7,8-$^{2}H_5$)naphtho[2,3-*c*]thiofene 2,2-dioxide (2.096)

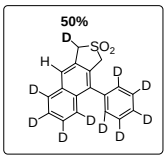

State: white solid; m.p. 177 - 178 °C; **yield**: 90%; ^{1}H NMR (600 MHz, Chloroform-*d*) δ 7.85 (s, 1H), 4.6 (app s, 1H, 1D), 4.26 (s, 2H); ^{13}C NMR (150 MHz, Chloroform-*d*) δ 138.2, 137.5, 133.3, 132.2, 129.2 (t, *J* = 25.0 Hz), 128.6 (t, *J* = 26.8 Hz), 128.6, 128.1, 127.8 (t, *J* = 24.1 Hz), 127.7 (t, *J* = 25.2 Hz), 126.6 (t, *J* = 24.6 Hz), 126.5 (t, *J* = 24.0 Hz), 126.1 (t, *J* = 24.3 Hz), 125.0, 57.0 (t, *J* = 21.75 Hz), 56.7; HRMS: Calcd for $C_{18}H_5D_{10}O_2S^+$ $[M+H]^+$ 305.1415 found 305.1402.

Oxidation to the lactone: Synthesis of Compound (2.097)

A DMSO (1 mL) solution of phthalan **2.060 D´** (10 mg, 0.025 mmol) was mixed with freshly prepared IBX (4.0 eq) and was stirred at 90 °C overnight under nitrogen. The solution was then filtered through celite and was rinsed thoroughly with ethyl acetate several times. The organic layer was then washed with water, dried over Na_2SO_4, concentrated in vacuum and the crude product was purified by column chromatography with hexane-ethyl acetate mixture (4:1) as eluent.

4-(2,4-dimethoxyphenyl)-(5,6,7,8-$^{2}H_5$)naphtho[2,3-*c*]furan-1(3*H*)-one (2.097)

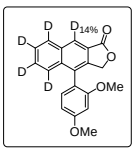

State: sticky solid; **yield**: 50%; ^{1}H NMR (600 MHz, Chloroform-*d*) δ 8.52 (s, 0.86H, 0.14D), 7.17 (d, *J* = 8.4 Hz, 1H), 6.69 - 6.67 (m, 2H), 5.24 (ABq, *J* = 15 Hz, 2H), 3.94 (s, 3H), 3.7 (s, 3H); ^{13}C NMR (150

MHz, Chloroform-*d*) δ 171.8, 161.6, 158.1, 139.9, 135.7, 133.8, 132.1, 130.8, 126.3, 123.1, 116.7, 105.1, 99.3, 70.2, 55.8, 55.7; HRMS: calcd for $C_{20}H_{13}D_4O_4^+$ $[M+H]^+$ 325.1374 found 325.1358, Calcd for $C_{20}H_{12}D_5O_4^+$ $[M+H]^+$ 326.1436 found 326.1419.

2.6.3 EPR measurement

The samples solutions were prepared in dry dichloromethane and purged with Ar gas to free from any dissolved oxygen for 5 min. Then base or TEMPO or both was added as per the requirement of the reaction and preceded for recording the EPR spectra. The radical quenching experiment was performed via purging O_2 gas to a sample solution containing Et_3N as base for 2 min and 4 minutes. Continuous-wave EPR experiments at X band (9.44 GHz) were carried out using ESR spectrometer, at center field 330 mT with a sweep width 30 mT, and a modulation frequency (kHz), 100; modulation amplitude (G), 140.0; and microwave power, 0.998 [μW] at temperature, 22 ^{O}C.

2.6.4 ^{1}H and ^{13}C NMR spectra of selected compounds

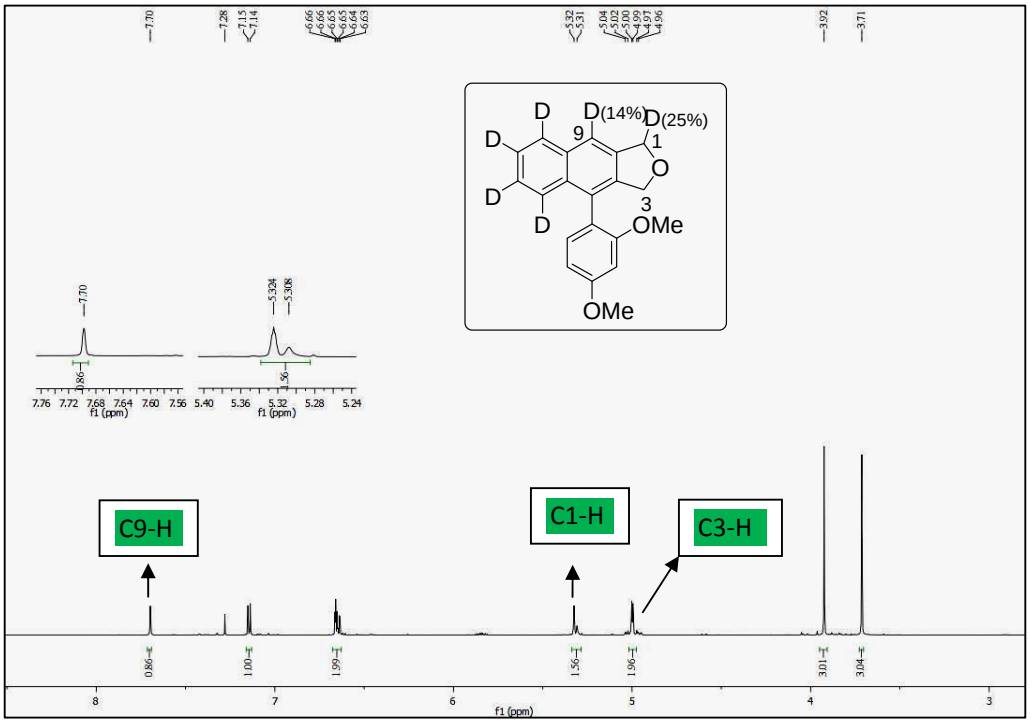

^{1}H NMR ($CDCl_3$, 600 MHz) spectrum of 2.060 D´

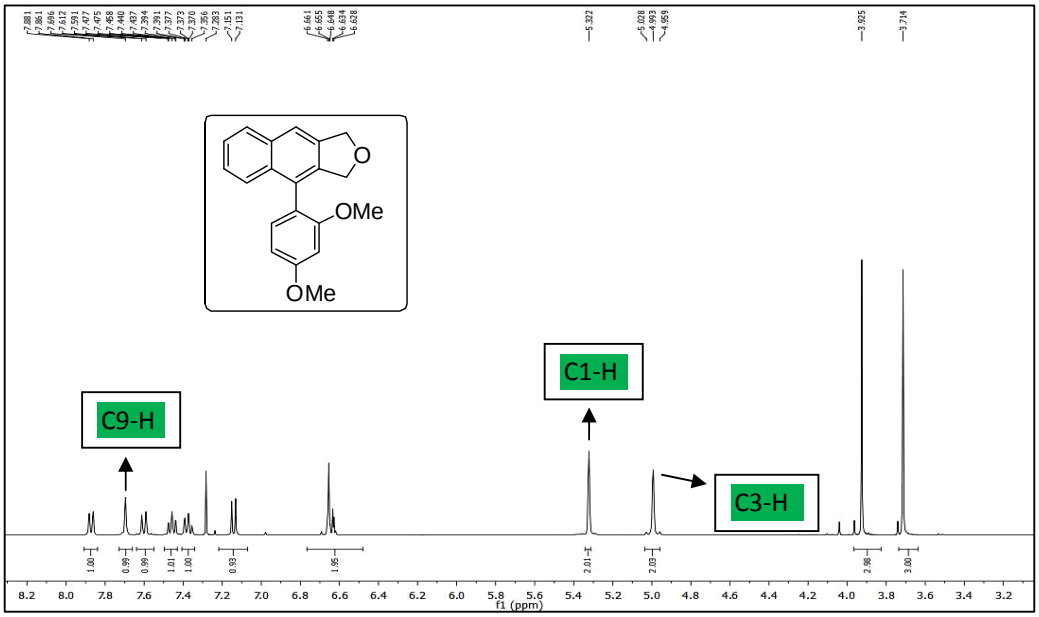

^{1}H NMR ($CDCl_3$, 400 MHz) spectrum of 2.060 D

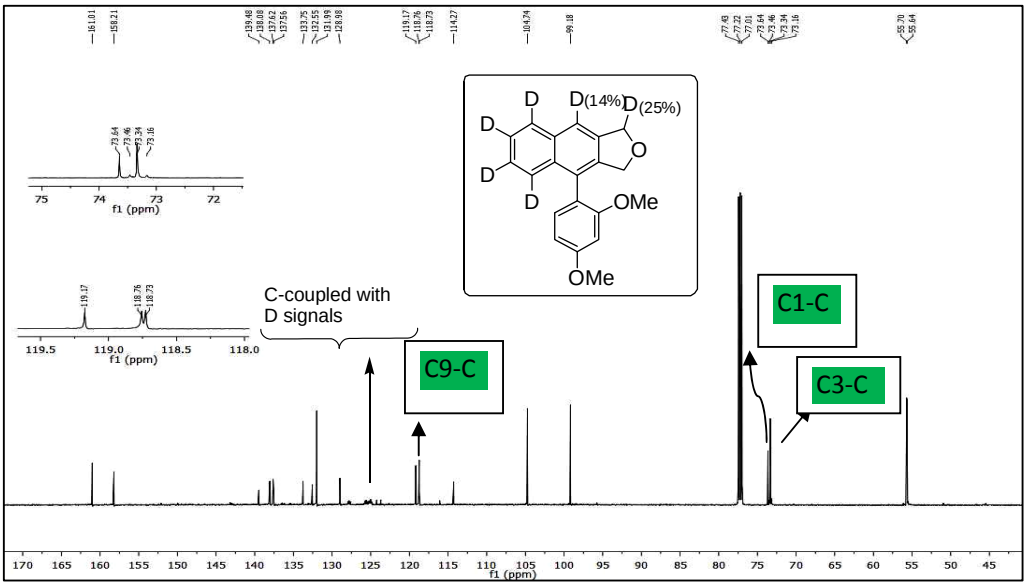

^{13}C NMR ($CDCl_3$, 150 MHz) spectrum of 2.060 D´

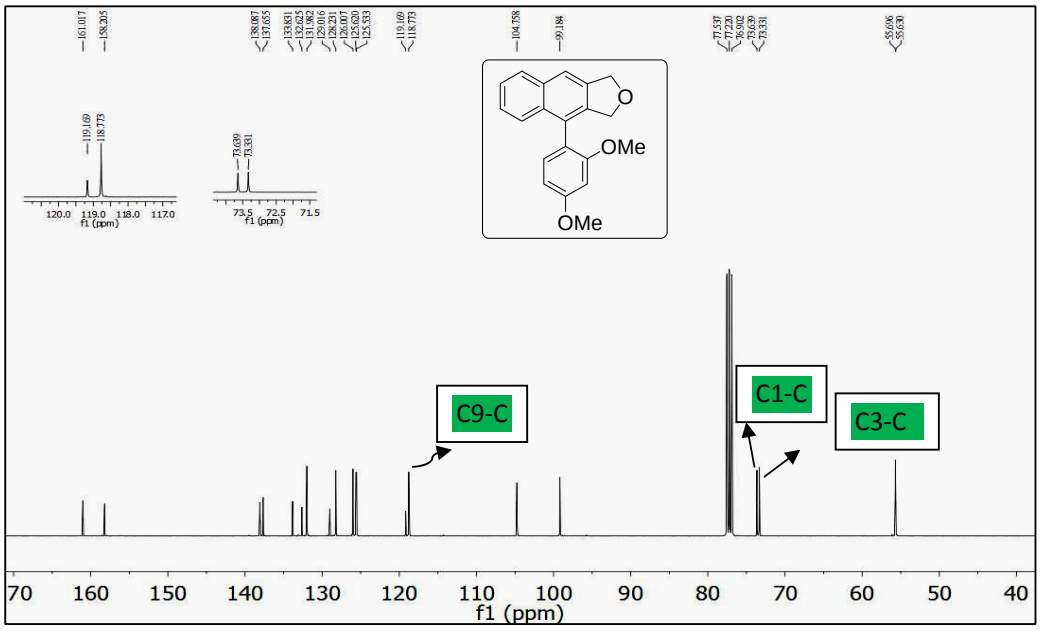

^{13}C NMR ($CDCl_3$, 100 MHz) spectrum of 2.060 D

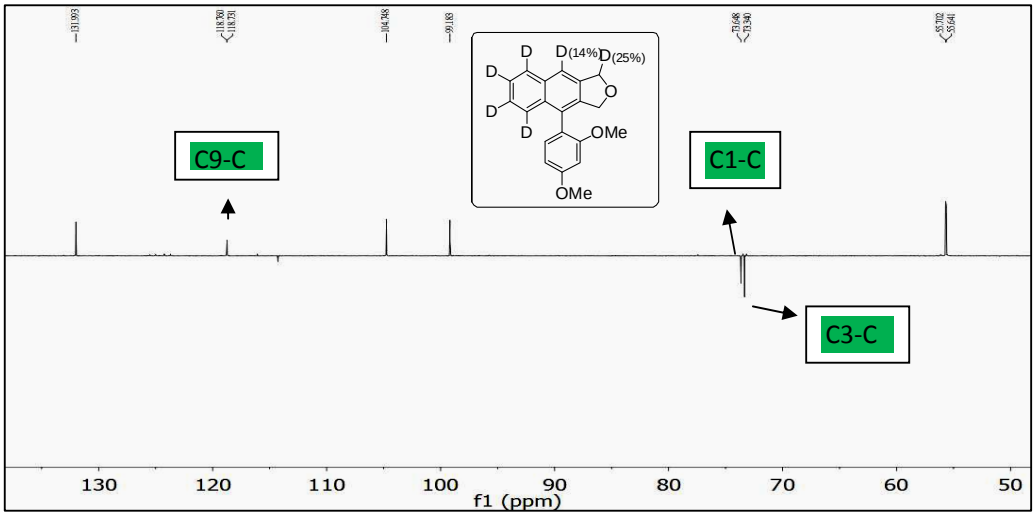

DEPT-135 NMR (150 MHz) spectrum of 2.060D´

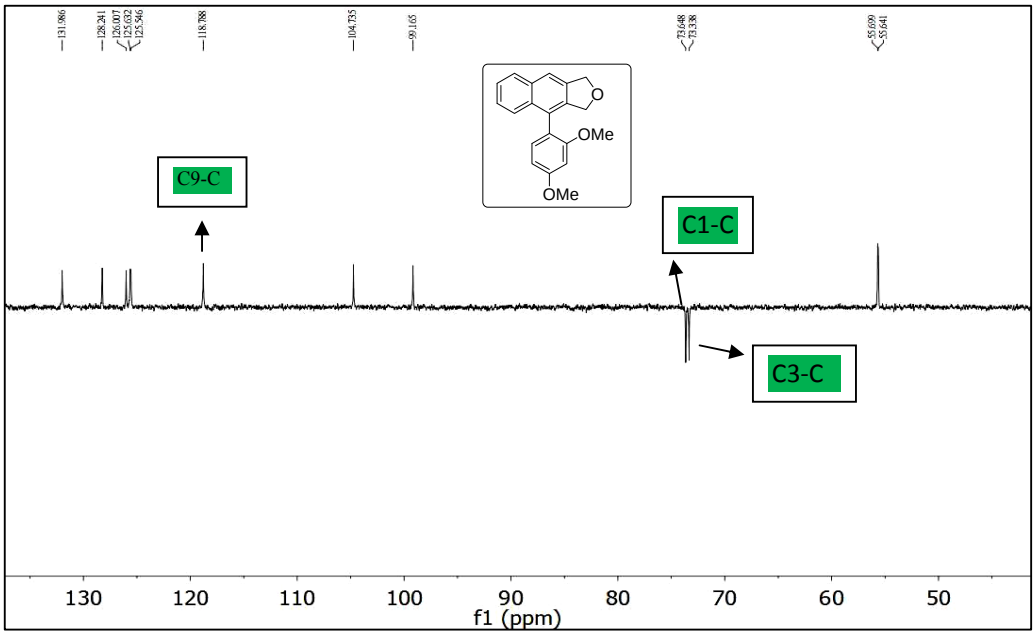

DEPT-135 NMR (50 MHz) spectrum of 2.060D

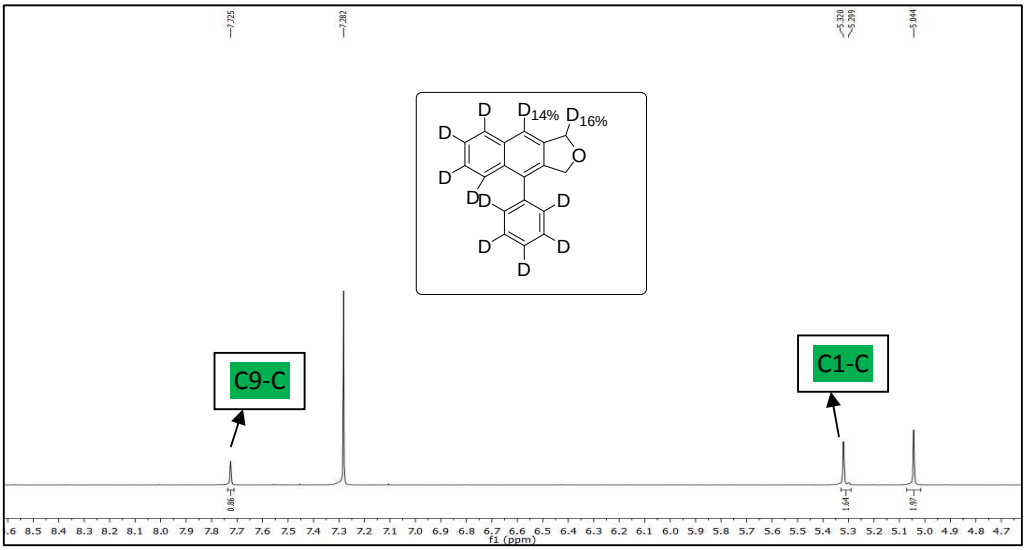

^{1}H NMR ($CDCl_3$, 600 MHz) spectrum of 2.094

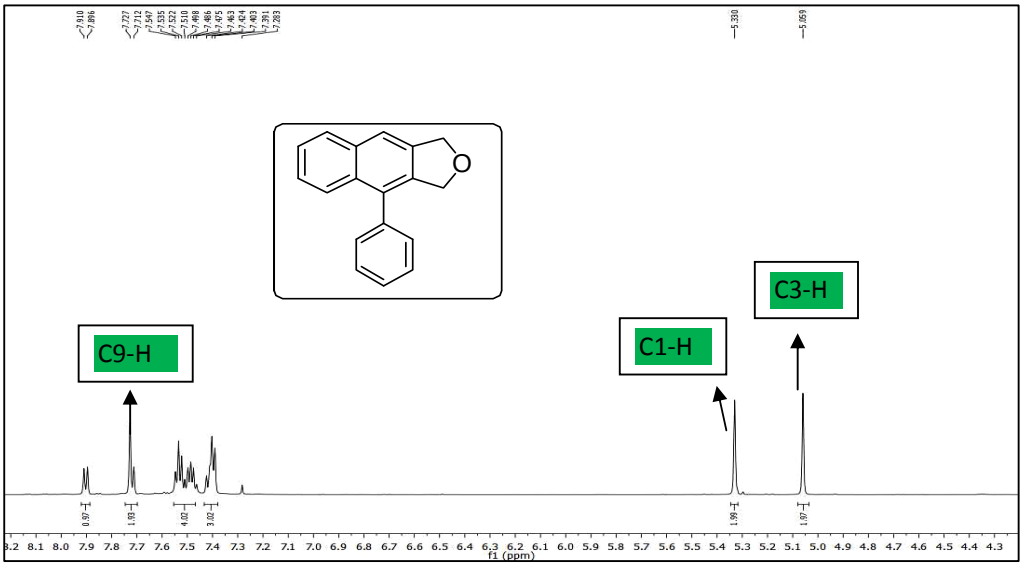

^{1}H NMR ($CDCl_3$, 600 MHz) spectrum

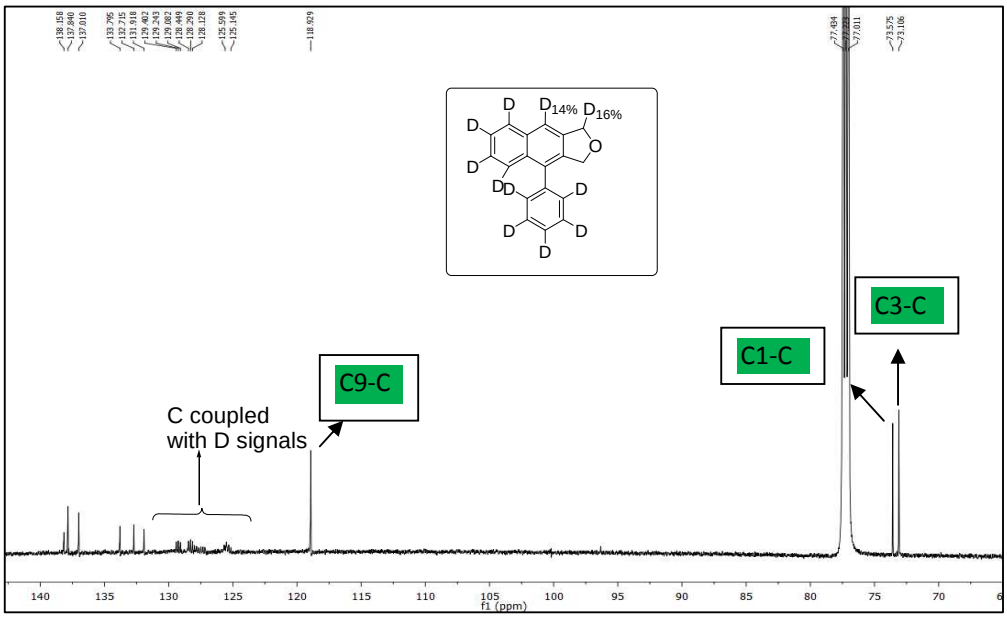

^{13}C NMR ($CDCl_3$, 150 MHz) spectrum of 2.094

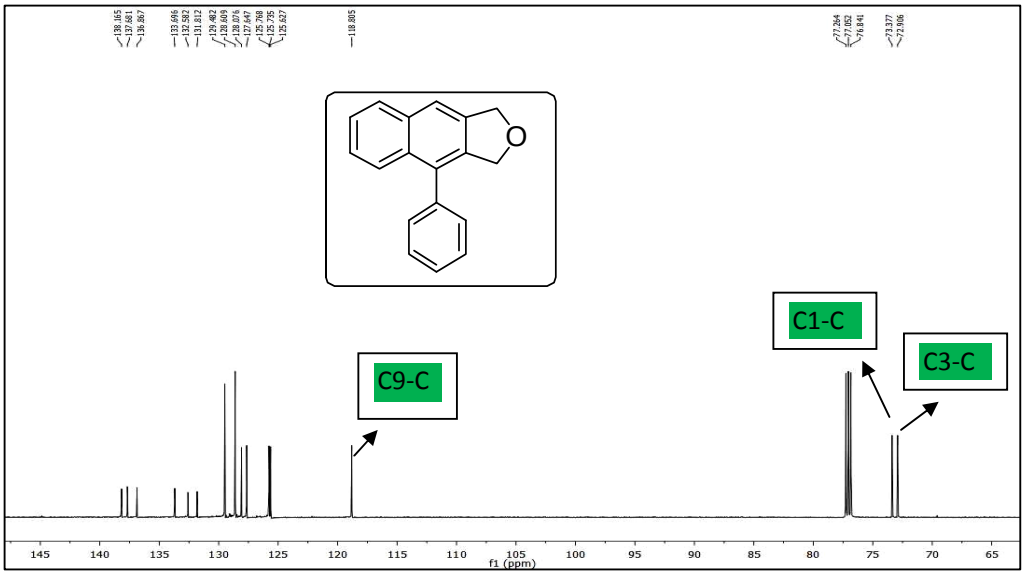

^{13}C NMR ($CDCl_3$, 150 MHz) spectrum

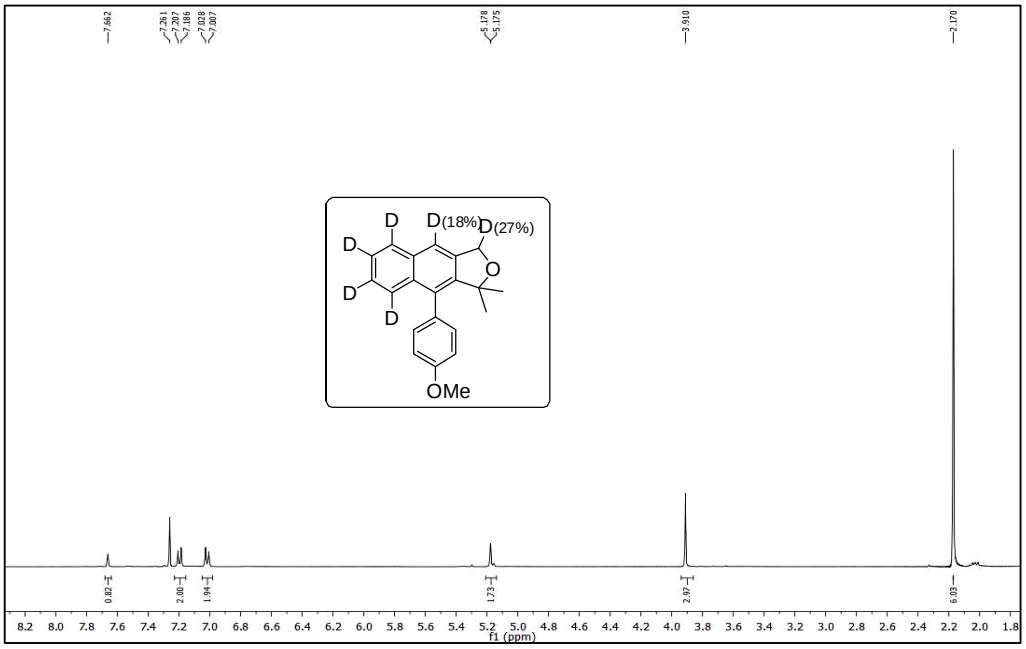

^{1}H NMR ($CDCl_3$, 400 MHz) spectrum of 2.092

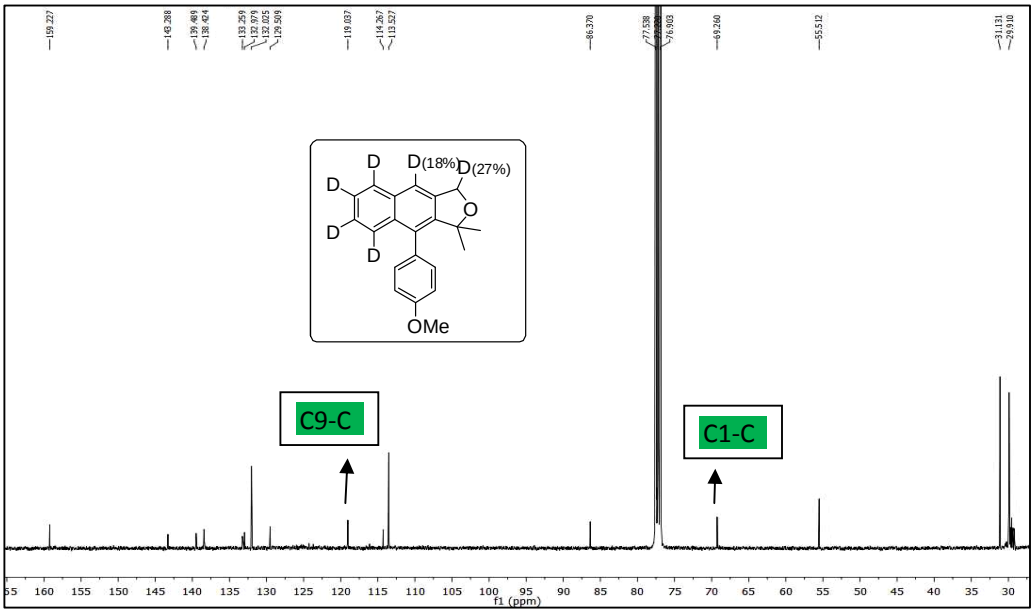

^{13}C NMR ($CDCl_3$, 100 MHz) spectrum of 2.092

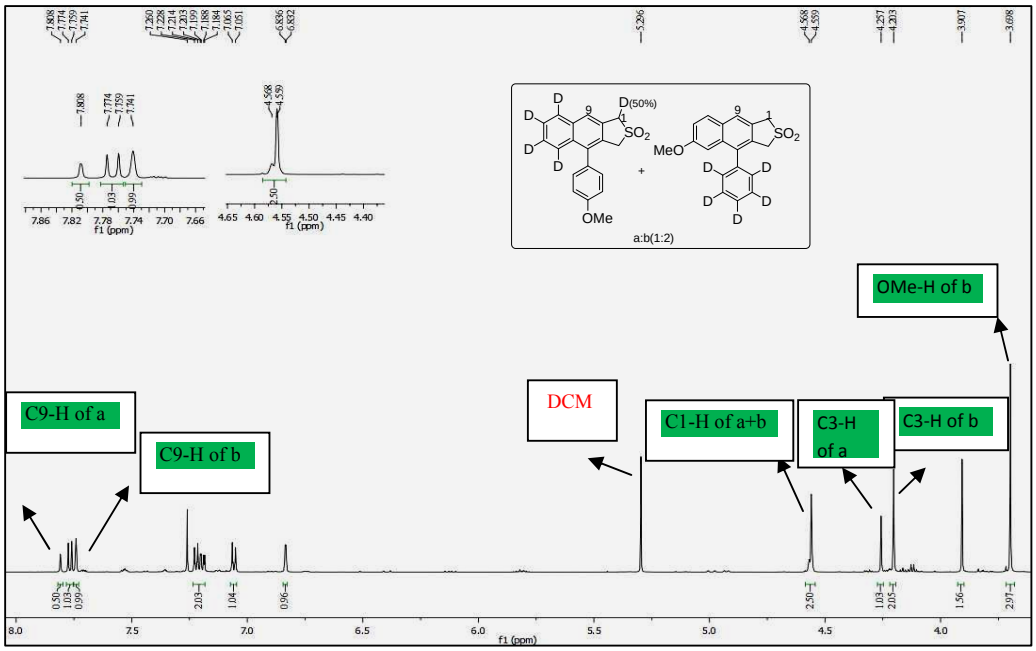

^{1}H NMR ($CDCl_3$, 600 MHz) spectrum of 2.061/2.062 C´

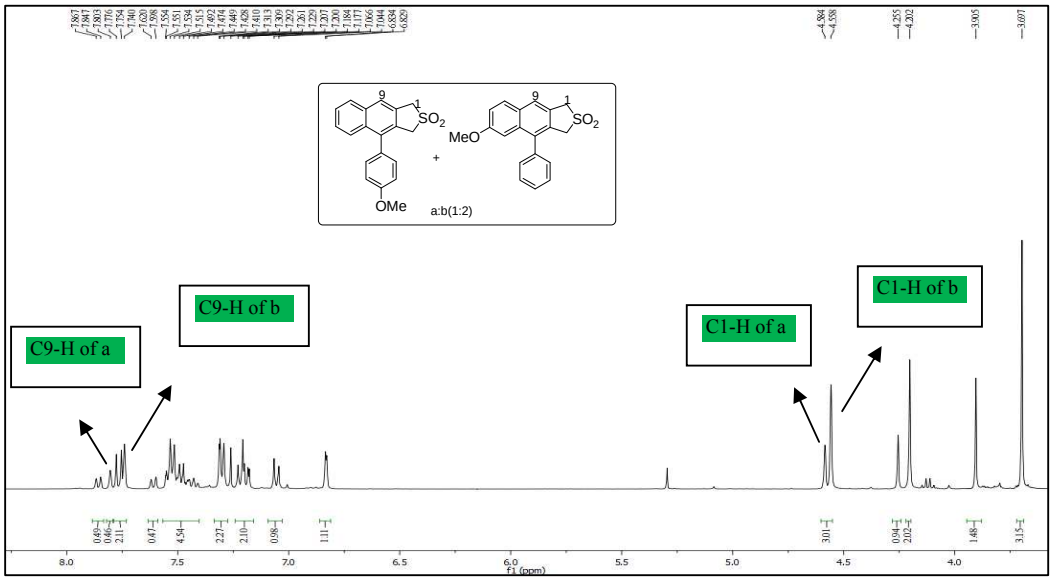

^{1}H NMR ($CDCl_3$, 400 MHz) spectrum of 2.061/2.062 C

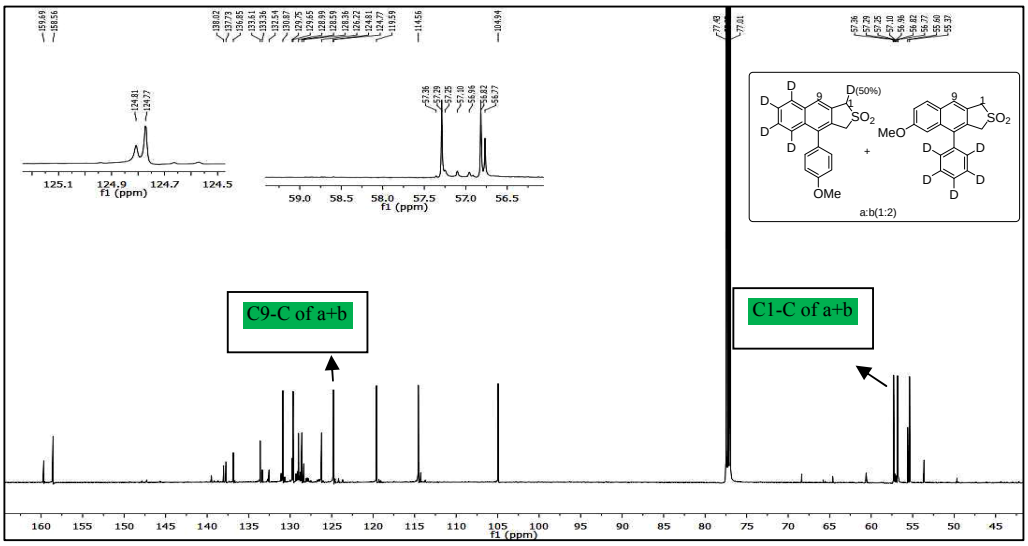

^{13}C NMR ($CDCl_3$, 150 MHz) spectrum of 2.061/2.062 C´

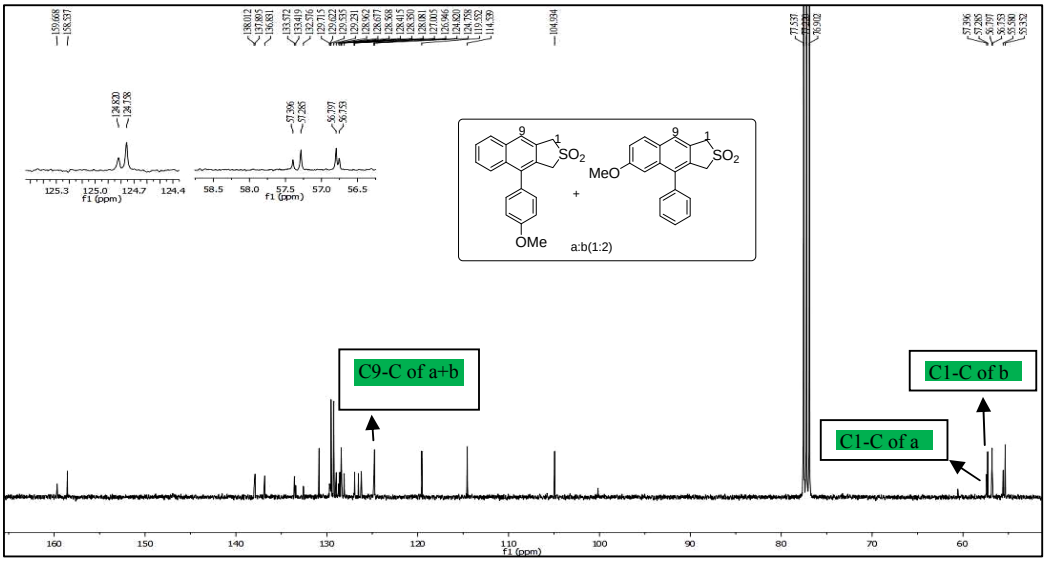

^{13}C NMR ($CDCl_3$, 100 MHz) spectrum of 2.061/2.062 C

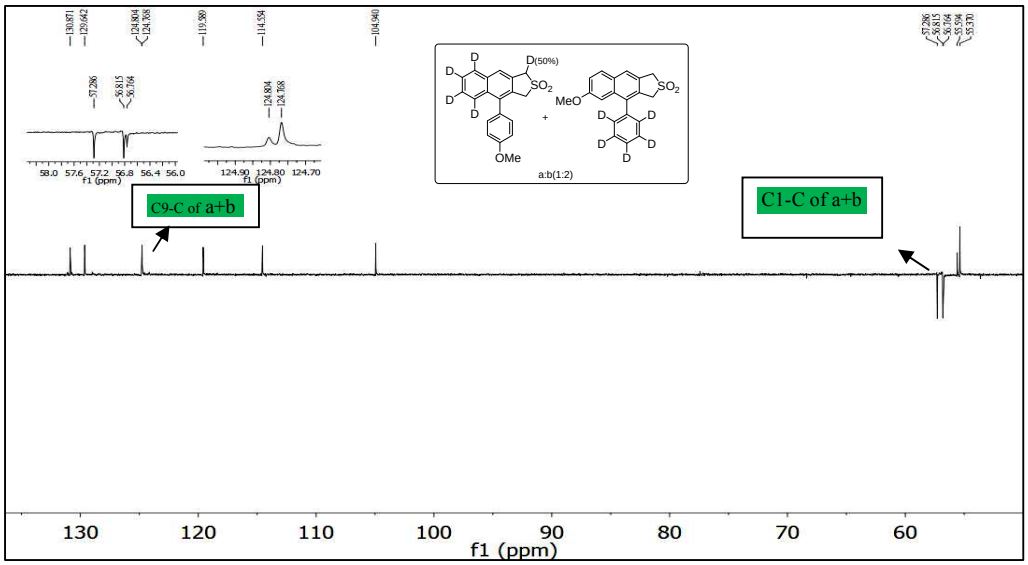

DEPT-135 NMR (150 MHz) spectrum of 2.061/2.062 C′ (2:1)

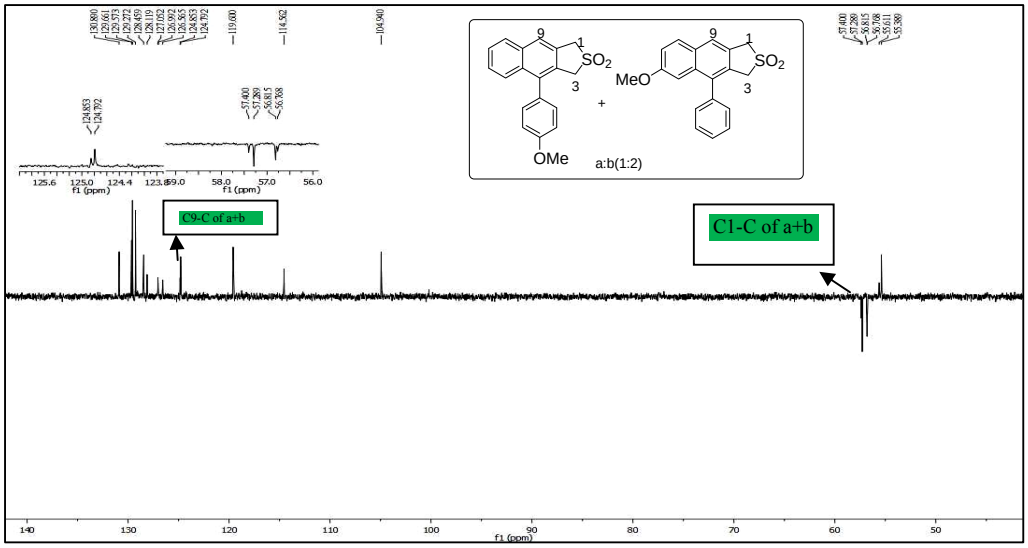

DEPT-135 NMR (100 MHz) spectrum of 2.061/2.062 C (2:1)

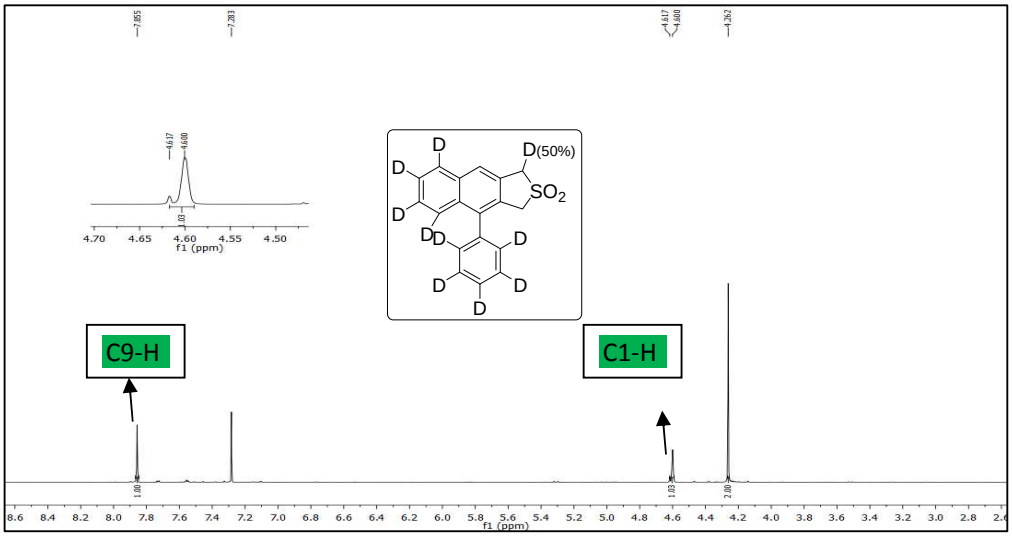

^{1}H NMR ($CDCl_3$, 600 MHz) spectrum of 2.096

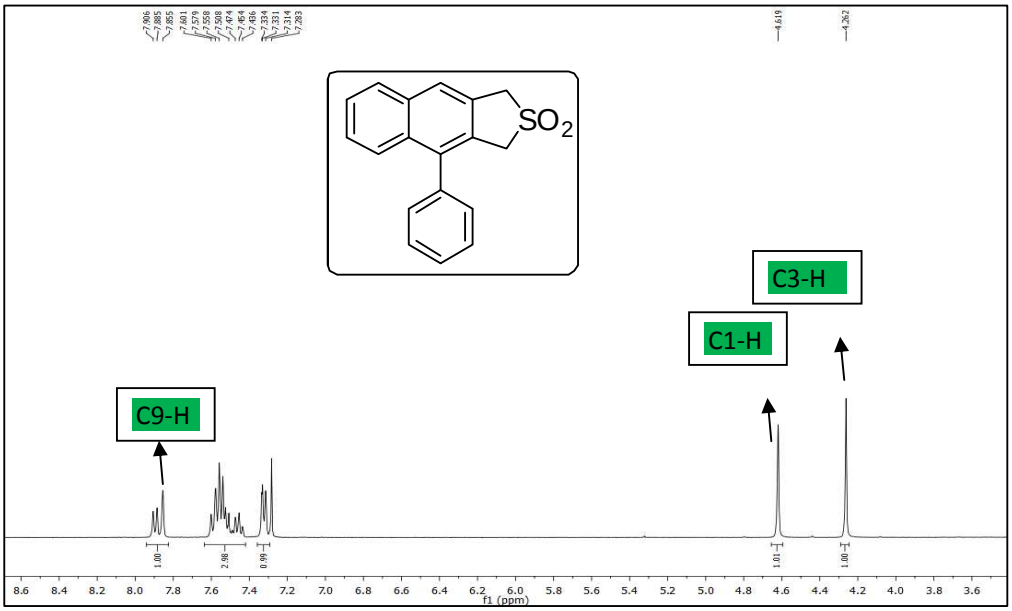

^{1}H NMR ($CDCl_3$, 400 MHz) spectrum of 2.075

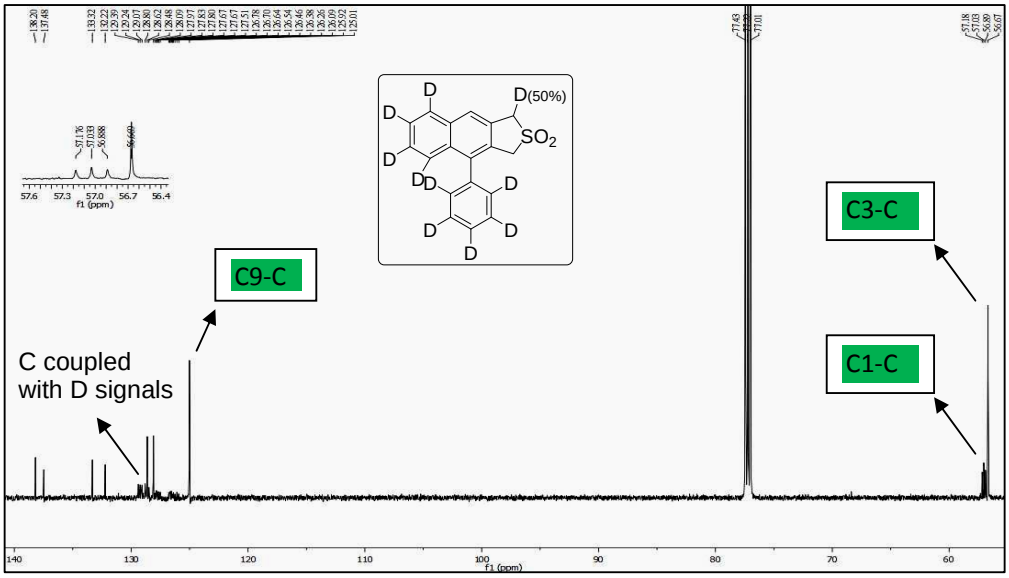

^{13}C NMR ($CDCl_3$, 150 MHz) spectrum of 2.096

^{13}C NMR ($CDCl_3$, 100 MHz) spectrum of 2.075

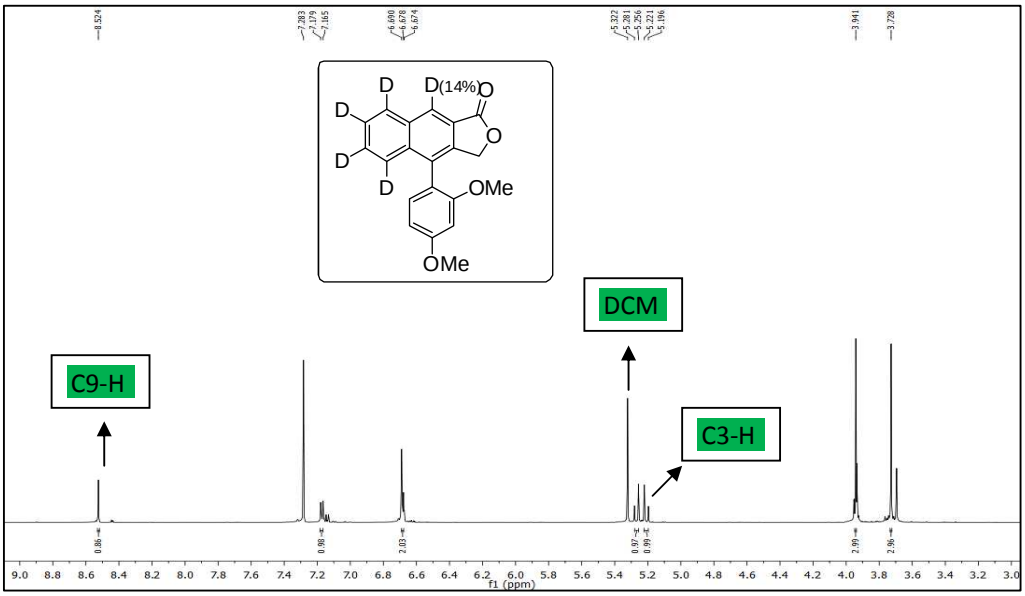

^{1}H NMR ($CDCl_3$, 600 MHz) spectrum of 2.097

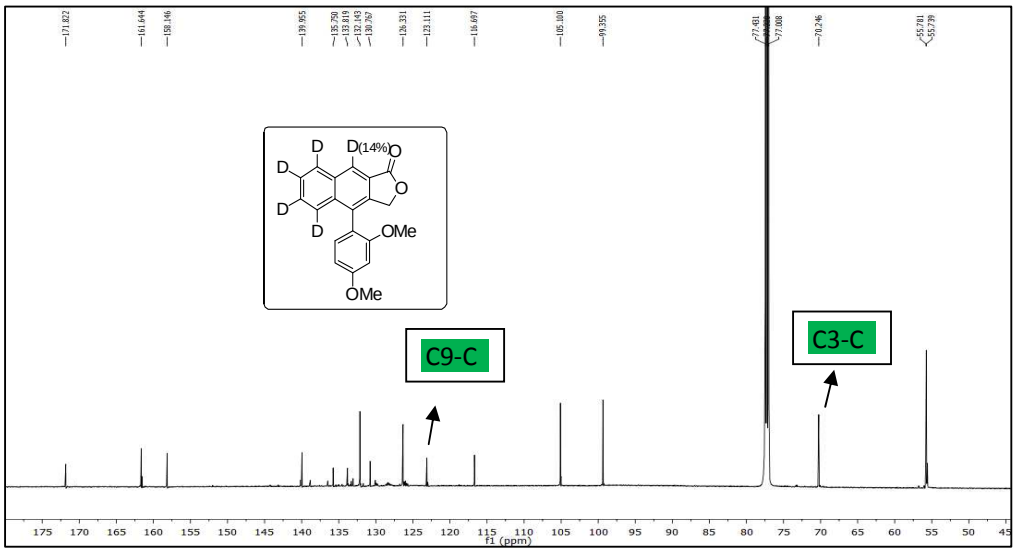

^{13}C NMR ($CDCl_3$, 150 MHz) spectrum of 2.097

Chapter 3

Support for Ionic Mechanism in Bergman Cyclization: Use of Enediyne Moiety Acting as a Photoaffinity Label in the Design of Capture Compounds for Human Carbonic Anhydrase II

3.1 Introduction

Proteomics[55] is a field in which an extensive and a large scale study of proteins is done, particularly focused on the various kinds of structures and functions of the different types of proteins. Proteins are the vital components of living organisms, as the metabolic pathways of the cells comprise mainly of proteins. The proteome is an entire set of proteins which are produced or modified by an organism or a biological system. The proteome always varies from cell to cell with time and it also varies with some specific requirements for the changes a cell wants to undergo.

As the proteome changes with time and differs from cell to cell, distinct genes are expressed in different cell types, which means that out of the different proteins present, we need to give importance to the identification of the basic set of proteins produced in a cell which contribute to the physical and chemical changes along with the genomic changes.

Thus to improve our understanding of what makes a cell function normally and what happens when struck by some disease, we need a different approach and tools such as protein capture[56] moieties and probes which will enable us to study how proteins work in isolation and the way in which they interact with other proteins, carbohydrates and DNA within a cell. Therefore to see from a broader point of view, this can be applied in research and clinical studies which enhance our understanding of the proteins and will eventually help in detecting, preventing and treating diseases.

The approach of protein capture has fascinated many scientists in the past few years and the initial protein capture agents exploited were the monoclonal antibodies[57]. Many such antibodies were produced for a number of protein targets, and they worked fine but their major drawback was that they lacked the desired level of selectivity and specificity as they targeted other proteins as well apart from the desired protein. Recently researchers have started using small molecules such as the 1,3,5 tripodal[58] benzene templates for the purpose of protein capture.

3.2 Recent developments

Recently, Fischer *et al*. have reported[59] a novel technology for the detection and isolation of protein subfamilies based on trifunctional molecular probes, which

they termed as Capture Compound Mass Spectrometry (CCMS). The capture compounds comprise three major functionalities, a selectivity function, a photo activable function and a sorting function[60]. The procedure was very simple and consisted of incubating the capture compound with the cell lysate which allow equilibrium binding to the target protein *via* the selectivity hand. Photolysis leads a cross-linking[61] with the protein. Next, with the help of sorting hand, the protein is fished out using an external bead having a functionality that recognizes the sorting hand. The CCMS technology is shown in **Figure 3.01**.

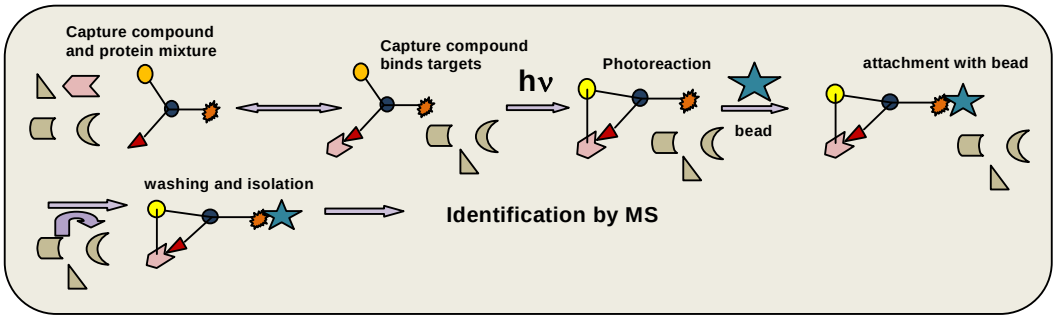

Figure 3.01: Schematic representation of capture process utilizing CCMS technology

CCMS technology can be modified in several ways if a gel base detection is wanted. Instead of a sorting hand, one can use a visualization hand (usually a fluorescence hand)[62]. From our laboratory, a 1,3,5-trisubstituted benzene template has been used to design a protein capture agent (**Figure 3.02**) which was specific in capturing HCA II and visualized in polyacrylamide gel (**Figure 3.03**).[63]

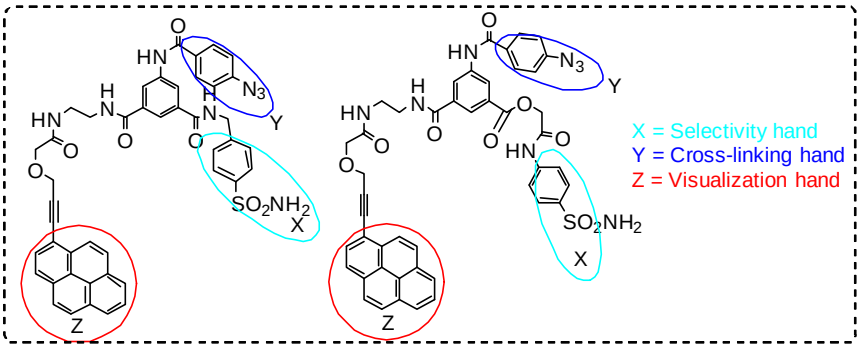

Figure 3.02: 1,3,5-trisubstituted capture molecules for HCA II

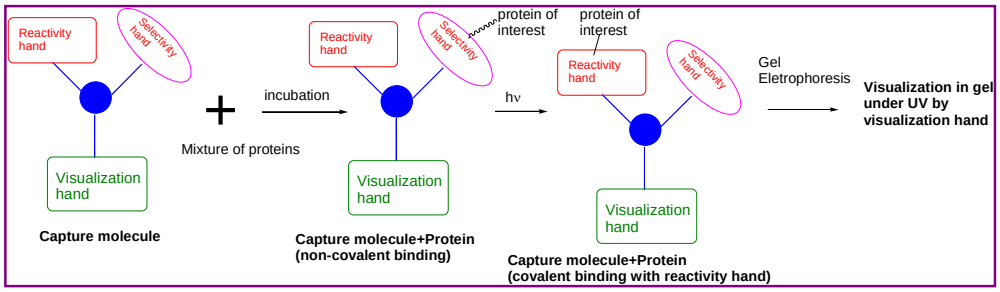

Figure 3.03: Working principle of Capture compound by using selectivity, reactivity and visualization hand.

Alternately, bioorthogonal chemistry[64] can be employed to attach the visualization hand *via* click chemistry. Utilizing a bioorthogonal approach (**Figure 3.04**) *β*-lactones showed a number of intense interactions with mouse brain and liver proteins.

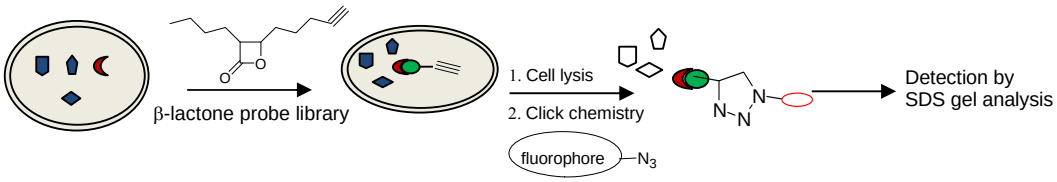

Figure 3.04: Activity based protein profiling by bioorthogonal approach by using probes with an alkyne hand for Click chemistry with and azide linked fluorophore.

3.3 Designing strategy

This project was mainly focused on human carbonic anhydrase II[65] (HCA II) which is one of the enzymes of the carbonic anhydrase family which helps in catalysing the inter conversion of CO_2 and water to bicarbonate and protons. The purpose of this project was to synthesize small molecules so that we can effectively visualize HCA II in SDS-PAGE and study it as an increase in any of its isoforms may be indicative of some diseases including hypoxia and cancer (CA IX)[66].

To synthesize the 1,2,4 tri substituted[67] aromatic enediyne based capture molecule for HCA II, we planned to attach a sulfonamide[68] moiety with a linker to the enediyne part as a selectivity hand for reversible binding with HCA II; similarly, an aryl azide moiety was attached with a linker to serve as a reacting hand *via* the formation of nitrene upon UV irradiation which was expected to be converted into azepine intermediate and would become susceptible towards nucleophilic attack by the free amines on protein surface and form covalent bond with the capture compound and a pyrene moiety for visualization purpose as it has high fluorescence quantum

yield. The structure of the target molecule **3.001** is shown in **Figure 3.05**. The linker groups with the three hands were chosen meticulously in order to maintain a distance between them and also for proper balancing of hydrophilicity and hydrophobicity. It was hoped that the enediyne framework would allow the photo cross-linking moiety, namely the azide to be in close proximity with the protein surface after the sulfonamide is anchored to the active site of HCA II.

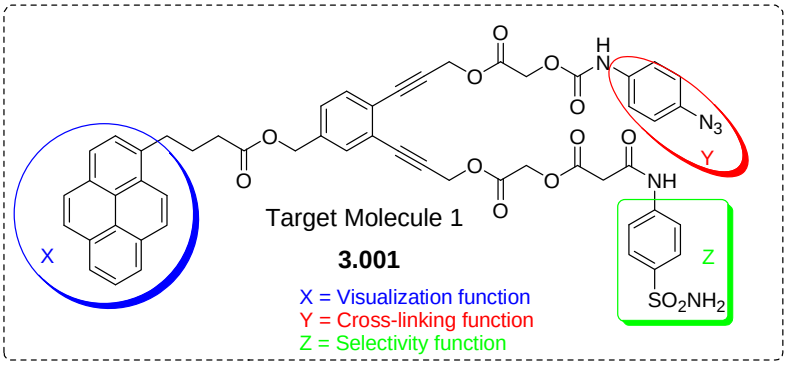

Figure 3.05: 1,2,4-trisubstituted aromatic enediyne based capture compound **3.001**

A noteworthy point here is that the enediyne moiety itself may undergo photo-Bergman cyclization[69] under UV irradiation and may give rise to a radical mediated cleavage of protein[70,71] molecule by the 1,4-diradical generated after Bergman cyclization of the enediyne. In 2007 Perrin *et al*. reported[22] H-X (X = Cl, Br, I) addition to cyclodeca-1,5-diyn-3-ene to 1-halotetrahydronaphthalene upon slight heating. The authors proposed a zwitterionic form of the 1,4-diradical generated after Bergman cyclization of the enediyne that underwent H-X addition. Thus, considering the zwitterionic form of the diradical a second possibility may be the protein itself may cross-link to the capture compound by the nucleophilic amino acids present in it. It may be mentioned that the "diradical" species derived from a photochemical route are electronically different from ground state analogues. It is possible that the zwitterionic mode is amplified in the excited state in cycloaromatization reactions.[1b] All these possibilities are shown in **Scheme 3.01**. Our next objective was to synthesize a dipodal enediyne based capture molecule **3.002** (**Figure 3.06**) with only sulfonamide and pyrene moiety and observe the ability of an enediyne moiety to act as a photoaffinity label.

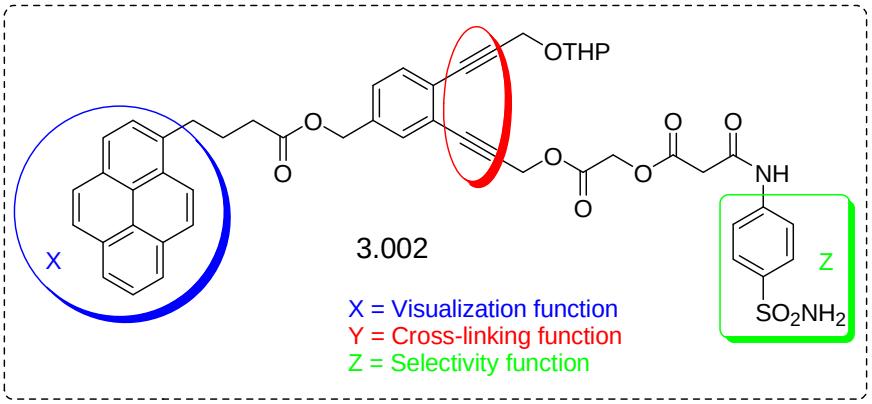

Figure 3.06: Capture compound **3.002** with enediyne as cross-linking function

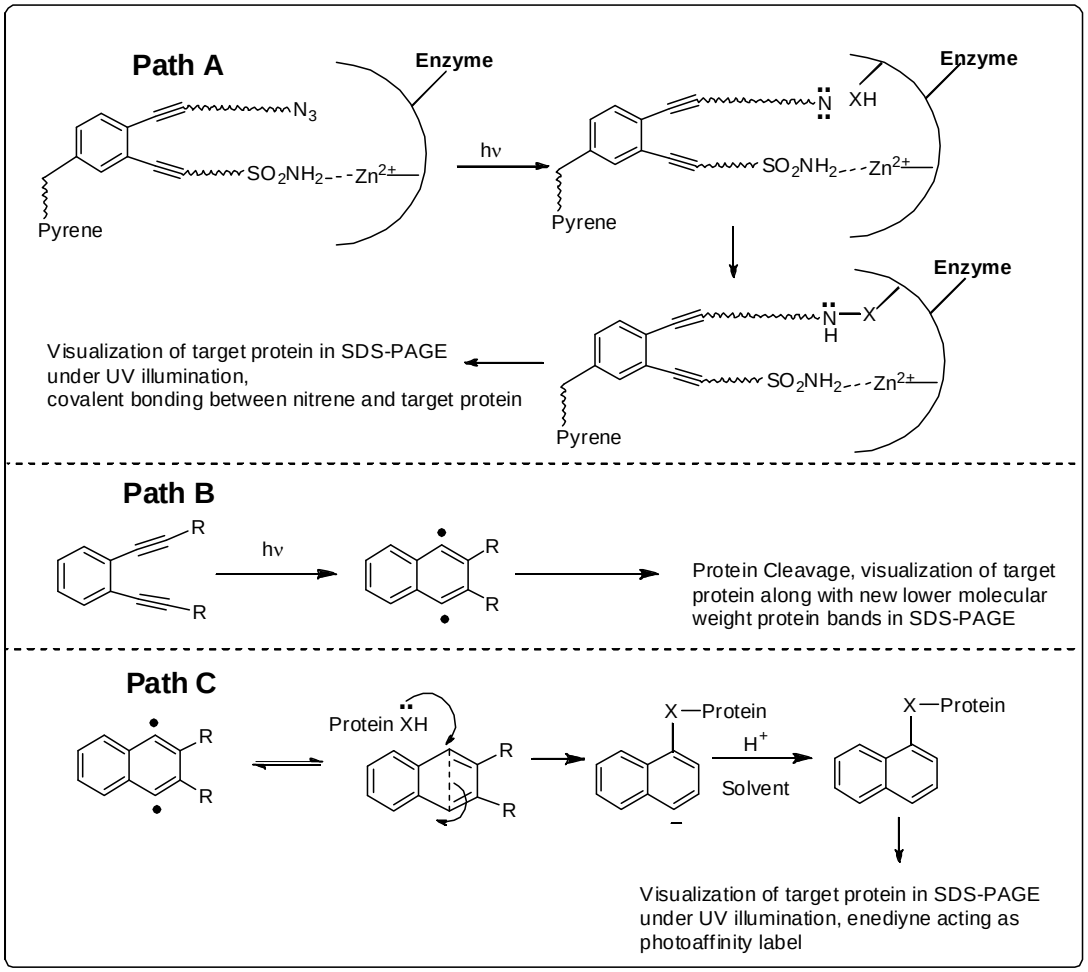

Scheme 3.01: Possible fates of capture compound with HCA II upon irradiation

3.4 Objective

To explore the possibilities of using 1,2,4-trisubstituted benzene system with an enediyne linker as a template for designing protein capture molecule we set our objectives as follows:

1. To design enediyne based capture molecule for HCA II.
2. To study the efficacy of enediyne as a linker.
3. To check the photo cross-linking ability of enediyne in view of the zwitterionic character of the diradical for Bergman cyclization.

3.5 Results and Discussion

3.5 A. 1. Synthesis of Na salt of N-(4-Sulfamoyl-phenyl)-oxalamic acid 3.005

The synthesis of **3.005** started with reaction of 4-aminobenzenesulfonamide **3.003** with ethyl malonyl chloride in presence of anhydrous K_2CO_3 in dry THF to afford the amide **3.004**. The amide as then stirred in NaOH solution at room temperature to attain hydrolysis of the ester functionality and compound **3.005** was obtained as white solid after repeated purification from DCM+MeOH+Hexane (**Scheme 3.02**).

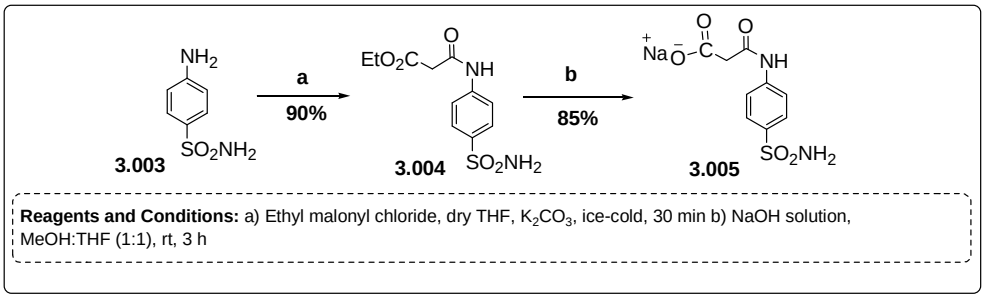

Scheme 3.02: Synthesis of Na salt of N-(4-Sulfamoyl-phenyl)-oxalamic acid **3.005**

3.5 A. 2. Synthesis of 4-(bromomethyl)-1,2-diiodobenzene 3.010

The synthesis of **3.010** was achieved by following some earlier reported protocols.[72] Firstly, 4-amino benzoic acid **3.006** was diazotised and subsequent

treatment with KI afforded 4-iodobenzoic acid **3.007**. Mono iodination of **3.007** yielded compound **3.008** which was eventually reduced to its corresponding alcohol **3.009**. The alcohol was then treated with PBr_3 in dry DCM followed by quenching the reaction with aqueous solution of $NaHCO_3$ resulted the formation of the bromide **3.010** (**Scheme 3.03**).

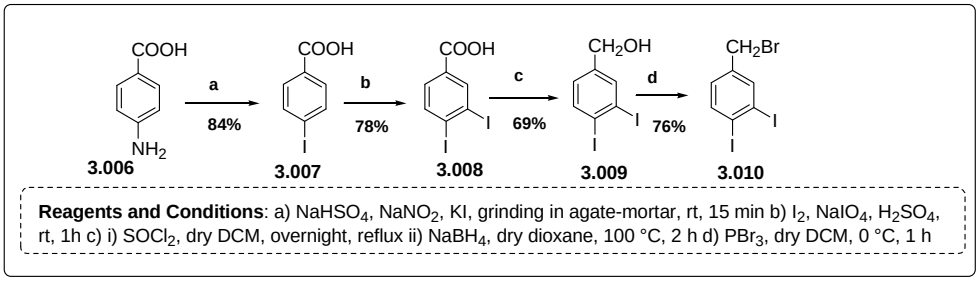

Scheme 3.03: Synthesis of 4-(bromomethyl)-1,2-diiodobenzene **3.010**

3.5 A. 3. Synthesis of Capture compounds

The synthesis of the capture compounds started with assembling the three hands namely reactivity, selectivity and visualization hand with the 1,2,4-substituted benzene template. At first, 3,4-diiodo benzyl bromide **3.010** was reacted with K-salt of pyrene butyric acid to get the ester **3.011**. It was then made to undergo Sonogashira coupling[3a,3b] to get the mono-propargylated alcohol **3.012**. The reaction was performed carefully by maintaining the temperature from initial 0 °C to ultimately 25 °C over a period of 3 h to get only the mono coupled product **3.012**. At this stage the product was a mixture of inseparable regioisomers (**3.012 a** + **3.012 b**) which were carried forward for the next sequence of reactions. A second Sonogashira coupling with mono-THP protected propargyl alcohol furnished **3.013**. Reaction of **3.013** with bromoacetyl chloride followed by esterification with Na salt of *p*-azido benzoic acid in dry DMF incorporated the reactivity hand (compound **3.014**). The THP group was then removed and the alcohol **3.015** was esterified similarly with bromoacetyl chloride followed by Na salt of malonyl sulfanilamide **3.005** to afford compound **3.001** (**Scheme 3.04**). The dipodal capture compound **3.002** without any azide moiety was synthesized from the alcohol **3.013** by following a similar esterification protocol (**Scheme 3.05**). The yields of individual steps and the reaction conditions are shown in the corresponding schemes.

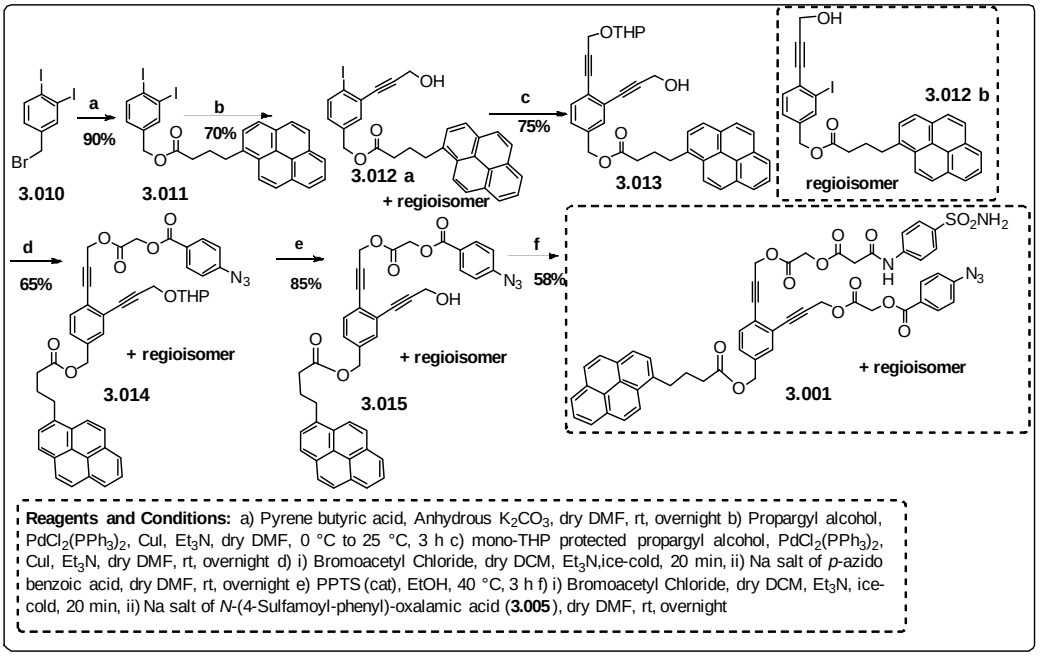

Scheme 3.04: Synthesis of target molecule **3.001**

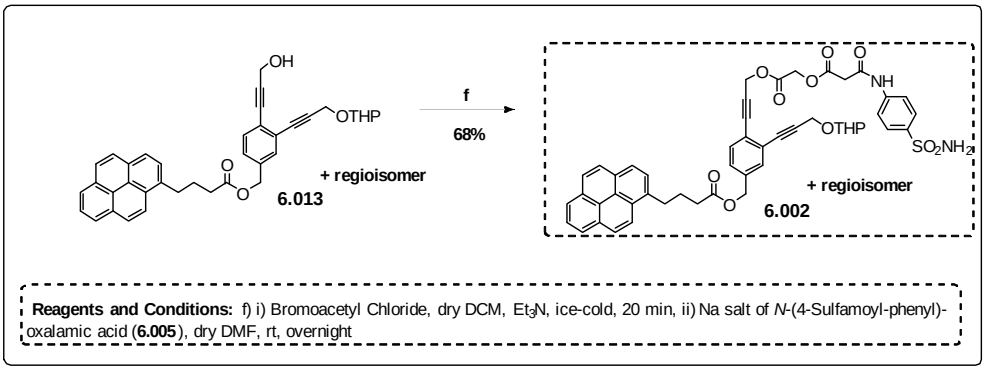

Scheme 3.05: Synthesis of target molecule **3.002**

3.5 B. Spectral Characterization

The structure of both the capture compounds synthesized were in good agreement with NMR and HRMS data. The tentative assignments of various protons are shown in **Figure 3.07**. The IR spectra of compound **3.001** showed a peak at 2120 cm^{-1} indicating the presence of azide functionality. The final confirmation of the structures came from mass spectral analysis that showed molecular ion peak at

1010.2346 (calcd 1010.2319) and 891.2540 (calcd 891.2564) for compound **3.001** and **3.002** respectively.

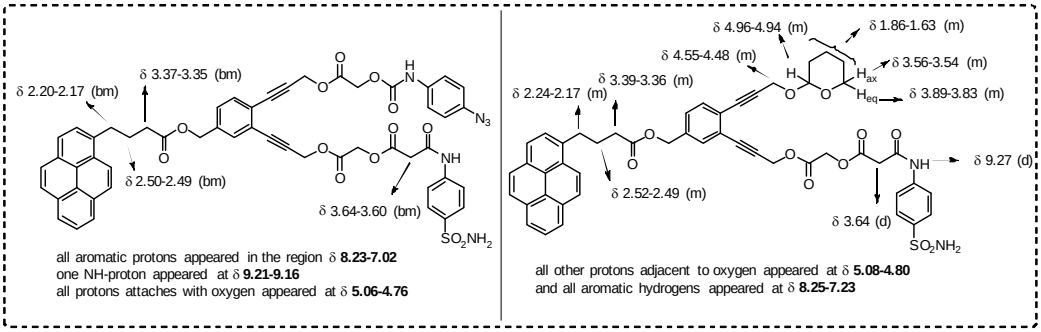

Figure 3.07: Spectral assignments of capture molecule **3.001** and **3.002**

3.5 C. Determination of Minimum Energy conformations of Compound 3.001 and 3.002

The energy minimized conformations of the compounds were determined by using the software, Avogadro and is given in **Figure 3.08**. From the structures it is clearly visible that the visualization hand pyrene moiety is pointing away from the sulfonamide and possibly in this way avoiding the steric crowding when the sulfonamide moiety binds to the active site of HCA II and thus validating our designing of the capture compounds.

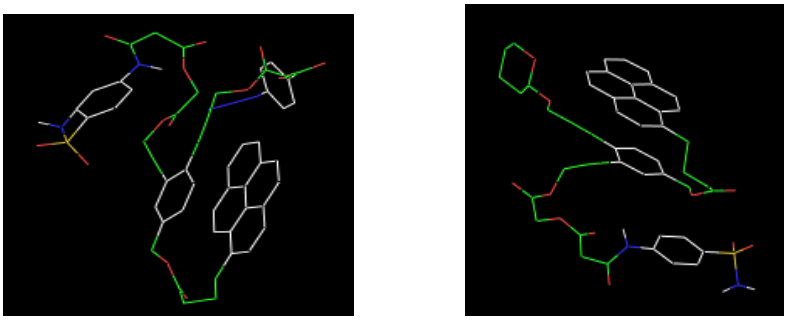

A **B**

Figure 3.08: Energy minimized structures of compound **3.001** (**Figure 3.08 A**) and compound **3.002** (**Figure 3.08 B**)

3.5 D. Determination of IC_{50} values for capture compounds

The binding as well as inhibition potentials of the synthesized capture compounds with HCA II (**Figure 3.09**) were first determined. Thus, the absorbance at

405 nm (absorbance of *p*-nitrophenol from hydrolysis of *p*-nitrophenol acetate) was determined for a mixture of different concentrations of compound **3.001** and **3.002** along with a fixed concentration of PNPA (2 mM) as substrate and 14 μM (working concentration) of HCA II in a microplate spectrophotometer. Both the compounds were observed to inhibit HCA II with compound **3.001** having a lower IC_{50} value of 1.89 μM as against 10.76 μM for compound **3.002**. It was reported earlier that azides may act as inhibitors[73] of HCA II and to verify, the inhibitory potential of compound **3.014** was checked similarly and was observed to remain neutral against HCA II.

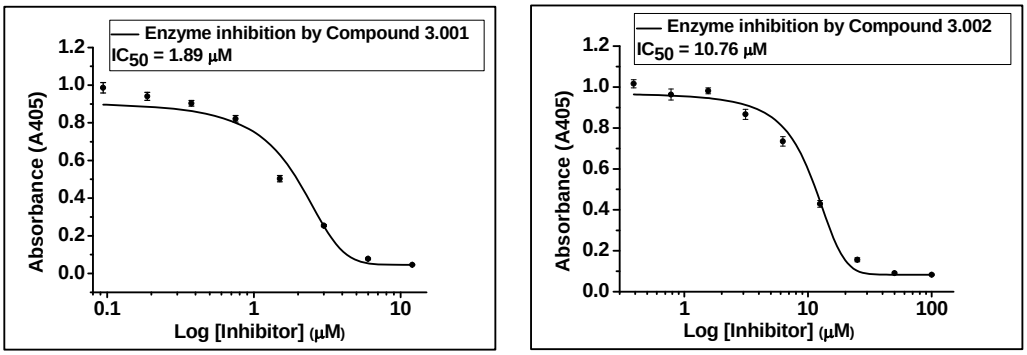

Figure 3.09: IC_{50} determinations of compound **3.001** and compound **3.002**, 50 mM HEPES (pH 7.2) was used for the measurements.

3.5 E. Capture Experiment

After getting an idea of inhibition concentrations of the capture compounds we aimed towards the capture experiment of HCA II with our synthesized compounds. Compound **3.001** was first evaluated. Thus a fixed concentration of HCA II (40 μM) with different concentrations of compound **3.001** (**Table 3.01**) were incubated for 20 min and then irradiated for 60 min with light of wavelength ≥ 300 nm and then directly run on a polyacrylamide gel. Exposure of the gel to the UV-transilluminator clearly showed the fluorescence band for the protein at the expected region which was further confirmed by staining the gel with Coomassie blue (**Figure 3.10 M**). The experiment was repeated with Compound **3.002** (**Figure 3.10 N**) and Compound **3.014**. Analysis of the gel pictures showed that compound **3.002** was also able to capture protein with similar efficiencies whereas compound **3.014** without any sulfonamide moiety failed to show any cross-linking[74] (**lane 1**, **Figure 3.10 O**). The results validated our concept of protein capture and visualization by small molecules

and also demonstrated that the azide functionality is not mandatory to be present in order to generate cross-links as revealed by the capturing of HCA II by compound **3.002**. The enediyne moiety can perform the role of photoaffinity labeling under UV irradiation. Thus pathway C involving photo Bergman cyclization followed by nucleophilic addition as shown in **Scheme 3.01** seemed to be the process happening under UV-light. To check whether UV irradiation is necessary to induce cross-links, a separate experiment was performed by carrying out the incubation of HCA II with compound **3.002** without any photo irradiation and then directly run on a polyacrylamide gel. Exposure of the gel to the UV-transilluminator showed without photo-irradiation the capture experiment was not successful. There was no spot visible under UV-transilluminator (**lane 1, Figure 3.10 P**) and the presence of proteins can be seen upon Coomassie stain of the same gel (**Figure 3.10 P**). This further confirms the capture process requires photo-irradiation.

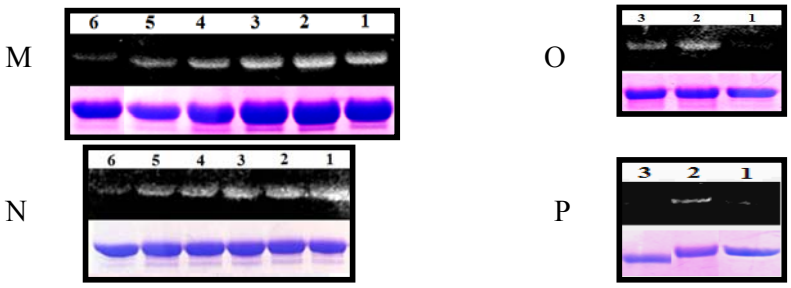

Figure 3.10: Results of gel electrophoresis analysis of HCA II capture by compound **3.001** and **3.002** (total volume of reaction mixture: 50 µl) at different concentrations, as visualised by UV (upper panel) and Coomassie blue (lower panel). (**M):** Gel image of incubation and photo-irradiation with HCA II (40 µM) and Compound **3.001** (**N**): Gel image of incubation and photo-irradiation with HCA II (40 µM) and Compound **3.002** (**O**) Gel image of comparison between Compound **3.001**, **3.002** and **3.014** at 10 µM concentration incubated and photo-irradiated with 20 µM HCA II, lanes 1, 2, 3 represent incubation and photo-irradiation with compound **3.014**, **3.002**, **3.001** respectively and (**P**): Gel image shows enhancement of protein capture, lane 2 represents incubation and photo-irradiation of compound **3.002** (100 µM) with HCA II (20 µM), lane 1 represents only incubation of compound **3.002** (100 µM) with HCA II (20 µM) without photo-irradiation whereas lane 3 represents photo-irradiation with DMSO (2%) and HCA II (20 µM). HEPES buffer (pH 7.2) was used for capture experiment.

Lane	HCA II concentration (µM)	Compound Concentration (µM)	DMSO concentration
1	40	20 (compound **3.001**)	---
2	40	10 (compound **3.001**)	---
3	40	5 (compound **3.001**)	---
4	40	2.5 (compound **3.001**)	---
5	40	1.75 (compound **3.001**)	---
6	40	---	2 % (as control)
1	40	40	---
2	40	20 (compound **3.002**)	---

3	40	10 (compound **3.002**)	---
4	40	5 (compound **3.002**)	---
5	40	2.5 (compound **3.002**)	---
6	40	---	2 % (as control)

Table 3.01: Contents in different lanes of gel images in **Figure 3.10 M** and **3.07 N**

After confirming the capture efficiency we then turned our attention to check the selectivity of our designed probes. Thus the entire process of incubation and irradiation was repeated with compound **3.001** and **3.002** with a mixture of three proteins namely BSA, HCA II and lysozyme. The fluorescence band corresponding to HCA II was only visible under UV-transilluminator, whereas the Coomassie blue staining of the same gel showed the presence of all three proteins (**Figure 3.11**). The bands corresponding to BSA and lysozyme also showed some amounts of photo-degradation as pyrene based compounds are known to possess such degrading ability.[75]

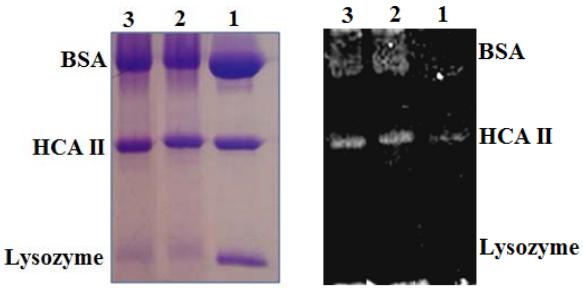

Figure 3.11: Capture experiment with a mixture of proteins, namely lysozyme, HCA II and BSA. Lane 2 and 3 represents incubation and photo-irradiation with mixture of proteins (20 μM each) and Compound **3.002** and **3.001** (20 μM) respectively and lane 1 indicates incubation and photo-irradiation with DMSO (2%) and protein mixture (20 μM each) as control.

3.5 F. MALDI MS study

To further confirm the occurrence of cross-linking, the incubated and photo-reacted mixture was directly analyzed on a MALDI mass spectrometer. As the native HCA II itself gave rise to a broad peak at 28000-31000 Da, the peak corresponding to the captured protein was masked. We next performed MALDI-MS of tryptic digestion of the proteins cross-linked with **3.001** and **3.002** and were compared with that for the native protein digestion (**Figure 3.13**). Trypsin hydrolyzes the protein at the carboxyl side of the amino acids lysine or arginine, except when either is followed by proline. The peptides or the amino acids with basic side chains then get protonated and appear in MALDI. The native protein HCA II showed some specific bands after trypsin digestion and was confirmed by comparing it with the reported values given in **Figure 3.12**

Mass fragment	Peptide Sequence
2141	YDPSLPLSVSYDQATSLR
2063	LNNGHAFNVEFDDSQDK
1581	YAAELHLVHWNTK
1169	SADFTNFDPR
1141	HNGPEHWHK
935	GGPLDGTYR

Figure 3.12: Expected fragments $[M+H]^+$ from tryptic digest of HCA II

Apart from the expected digestion fragments[76] (**Figure 3.12**) the cross-linked proteins showed additional bands (m/z 2914 and 2668 for compound **3.001** and m/z 2912, 2667 and 2929 for compound **3.002**) which were absent in the MALDI MS of the tryptic digested fragments of native HCA II. The origin of these additional peaks along with probable structures are mentioned in **Figure 3.14**.

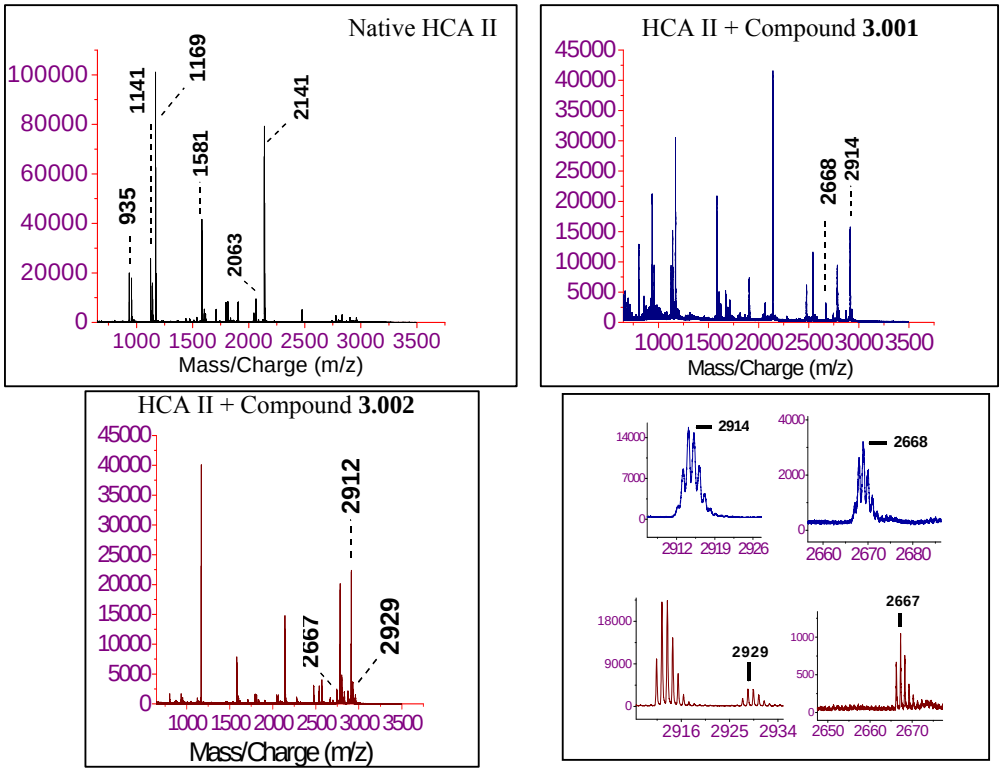

Figure 3.13: MALDI-MS spectra of tryptic digestion of native HCA II and HCA II + Capture compounds

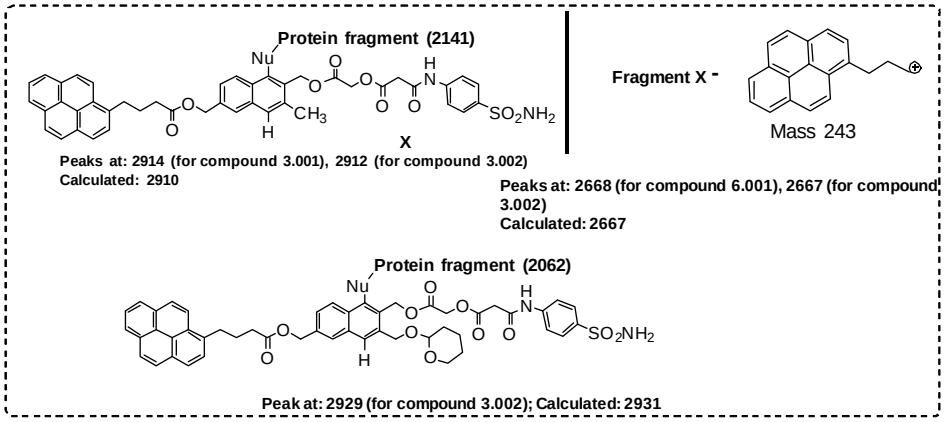

Figure 3.14: Probable structures of mass fragments in MALDI

It was apprehended that the fragment "**YDPSLPLSVSYDQATSLR**" (containing amino acids 40-58) (Mol. Wt. 2141) with four serine and two lysine residues has the favorable position for cross-linking[77] and we obtained the highest intensity peak at ~ 2912 for captured protein in MALDI. To confirm it molecular docking experiment was performed that too indicated the close proximity of this residue with compound **3.002.** Thus both the compounds **3.001**, **3.002** showed potential of capturing HCA II which could be demonstrated by our fluorescence based technology. Here a point to note that at this stage we were unable to confirm the nature of cross-linking of compound **3.001** with the protein was either through diradical or *via* the nitrene formation.

3.6 Conclusion

- We have successfully synthesized two enediyne based protein capture agents and have shown that a 1,2,4-trisubstituted benzene can be used as a template for designing capture compound.

- The capture of HCA II by these probes has been demonstrated by gel electrophoresis and MALDI MS studies.

- The capture experiments demonstrated the photo cross-linking ability of enediyne possibly occurred *via* the addition of nucleophilic amino acid to the partial zwitterionic form of the diradical generated through photo Bergman cyclization.

3.7 Experimental Details

3.7.1 General Experimental

General experimental procedures are same as described at page no. 59 in Chapter 2.

3.7.2 General procedure for synthesis of compounds and their spectral data

Synthesis of compound 3.004

To an ice-cold solution of 4-amino benzenesulfonamide (500 mg, 2.90 mmol) **3.003** in dry THF (20 ml) was added anhydrous K_2CO_3 (1002 mg, 7.25 mmol) followed by dropwise addition of ethyl malonyl chloride (0.34 ml, 3.48 mmol) under inert atmosphere. The reaction was then allowed to stir for 30 min at ice-cold temperature and then quenched with water and extracted with ethylacetate (20 ml×3). The combined organic layer was then washed with brine, dried with anhydrous sodium sulfate and evaporated to give the crude product **3.004** that was purified by repeated precipitation from a mixture of DCM-MeOH-Hexane.

***N*-(4-Sulfamoyl-phenyl)-malonamic acid ethyl ester (3.004)**

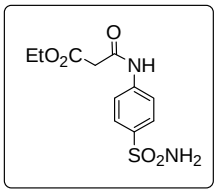

State: colorless solid; m.p. 182 - 183 °C; **yield**: 748 mg, 90%; ^{1}H NMR (400 MHz, DMSO-d_6) δ 10.52 (s, 1H), 7.78, 7.73 (ABq, 4H, *J* = 8.2 Hz), 7.27 (s, 2H), 4.12 (q, 2H, *J* = 6.8 Hz), 3.50 (s, 2H), 1.20 (t, 3H, *J* = 6.8 Hz); ^{13}C NMR (100 MHz, DMSO-d_6) δ 167.5, 164.7, 141.7, 138.7, 126.8, 118.7, 60.7, 43.7, 14.0; HRMS: Calcd for $C_{11}H_{15}N_2O_5S^+$ $[M+H]^+$ 287.0702 found 287.0701.

Synthesis of compound 3.005

A solution of NaOH (105.2 mg, 2.63 mmol in 1.0 ml of water) was added into a MeOH+THF (1:1) (15 ml) solution of *N*-(4-Sulfamoyl-phenyl)-malonamic acid ethyl ester **3.004** (500 mg, 1.75 mmol) and the mixture was stirred at room temperature for 3 h within which all the starting materials disappeared as visualized by thin layer chromatography. The solvent was then evaporated and the crude product was purified by repeated precipitation from DCM-MeOH-Hexane. The Na-salt was then dried in vacuum and used directly for next step.

Sodium (4-Sulfamoyl-phenylcarbamoyl)-acetate (3.005)

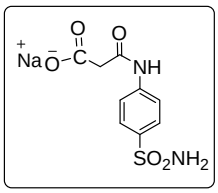

State: colorless solid; **yield**: 416 mg, 85%; ^{1}H NMR (600 MHz, DMSO-d_6) δ 12.10 (bs, 1H), 7.73 (s, 4H), 7.07 (bs, 2H), 3.03 (s, 2H); ^{13}C NMR (150 MHz, DMSO-d_6) δ 170.9, 168.9, 142.1, 138.1, 126.7, 118.4, 45.9; HRMS: Calcd for $C_9H_9N_2Na_2O_5S^+$ $[M+Na]^+$ 303.0027 found 303.0021.

Synthesis of compound 3.011

4-bromomethyl-1,2-diiodo-benzene **3.010** was prepared by following a reported procedure. To a solution of **3.010** (400 mg, 0.95 mmol) in dry DMF (10 ml) was added anhydrous K_2CO_3 (197 mg, 1.42 mmol) followed by pyrene butyric acid (274 mg, 0.95mmol) under N_2 atmosphere and the mixture was stirred at room temperature overnight. The reaction was then quenched by addition of water and extracted with ethyl acetate (15 ml×2). The combined organic layer was then washed with brine, dried over anhydrous sodium sulfate, concentrated and the crude product was purified by column chromatography by using hexane-ethyl acetate as eluent.

4-Pyrene-1-yl-butyric acid 3,4-diiodo-benzyl ester (3.011)

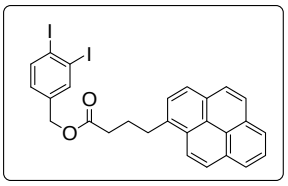

State: gummy mass; **yield**: 537 mg, 90%; ^{1}H NMR (600 MHz, Chloroform-*d*) δ 8.23 - 8.18 (m, 3H), 8.10 - 8.03 (m, 5H), 7.80 - 7.78 (m, 2H), 7.64 (d, *J* = 7.8 Hz, 1H), 6.74 (dd, *J* = 8.4 Hz, 1.8 Hz, 1H), 3.32 (t, *J* = 7.2 Hz, 2H), 2.48 (t, *J* = 7.2 Hz, 2H), 2.25 - 2.20 (m, 2H); ^{13}C NMR (150 MHz, Chloroform-*d*) δ 172.5, 138.9, 138.2, 137.1, 135.1, 131.0, 130.5, 129.6, 128.4 (×2), 127.2 (×2), 127.0, 126.5, 125.6, 124.7 (×2), 124.6, 122.9, 108.0, 107.4, 64.0, 33.4, 32.2, 26.3; HRMS: Calcd for $C_{27}H_{21}I_2O_2^+$ $[M+H]^+$ 630.9631 found 630.9632.

Synthesis of compound 3.012a/b

To a degassed solution of pyrene butyric acid ester **3.011** (300 mg, 0.48 mmol) in dry DMF (10 ml) was added propargyl alcohol (0.026 ml, 0.48 mmol), $PdCl_2(PPh_3)_2$ (10 mg, 0.014 mmol), dry Et_3N (0.1 ml, 0.72 mmol) and CuI (19 mg, 0.096 mmol) under inert atmosphere at 0 °C and the mixture was stirred at 25 °C for 3 h. The temperature and time should be carefully maintained in order to obtain the mono propargylated product exclusively. The reaction was then quenched by addition

of a saturated solution of NH_4Cl and the crude products were extracted in ethyl acetate (10 ml×2). The ethyl acetate layer was then dried over anhydrous sodium sulfate, evaporated and the purified product was obtained *via* column chromatography by using hexane-ethyl acetate as eluent.

4-Pyrene-1-yl-butyric acid 4-(3-hydroxy-prop-1-ynyl)-3-iodo-benzyl ester + 4-Pyrene-1-yl-butyric acid 3-(3-hydroxy-prop-1-ynyl)-4-iodo-benzyl ester (3.012a/b)

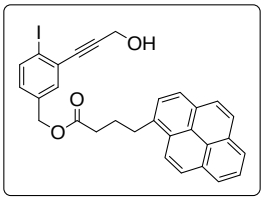

State: buff colored sticky solid; **yield**: 186 mg, 70%; ^{1}H NMR (600 MHz, Chloroform-*d*) δ 8.26 - 8.23 (m, 1H), 8.16 (t, *J* =6.6 Hz, 2H), 8.11 - 8.06 (m, 2H), 8.02 - 7.98 (m, 3H), 7.83 (d, *J* = 7.8 Hz, 1H), 7.78 (d, *J* = 8.4 Hz, 1H), 7.44 - 7.42 (m, 1H), 6.95 (d, *J* = 9.6 Hz, 1H), 5.02 - 5.00 (m, 2H), 4.52 (t, *J* = 14.4 Hz, 2H), 3.38 (t, *J* = 7.2 Hz, 2H), 2.52 - 2.49 (m, 2H), 2.23 - 2.19 (m, 2H); ^{13}C NMR (150 MHz, Chloroform-*d*) δ 173.3 (×2), 139.0, 138.2, 137.8, 136.2, 135.6, 135.5, 132.8, 132.4, 131.5, 131.0, 130.1, 129.5, 129.4, 129.1, 128.8, 127.6, 127.5, 126.9, 126.0, 125.2, 125.1, 124.9, 123.3, 100.9, 100.4, 91.8, 91.7, 87.3 (×2), 65.1, 64.8, 51.7 (×2), 33.9 (×2), 32.8, 26.8 (×2); HRMS: Calcd for $C_{30}H_{24}IO_3^+$ $[M+H]^+$ 559.0770 found 559.0775.

Synthesis of compound 3.013

To a degassed solution of compound **3.012** (200 mg, 0.34 mmol) and mono-THP protected propargyl alcohol in dry DMF (8 ml) was added $PdCl_2(PPh_3)_2$ (7 mg, 0.01 mmol), dry Et_3N (0.07 ml, 0.51 mmol) and CuI (13 mg, 0.068 mmol) under N_2 atmosphere at room temperature and the mixture was stirred overnight. The reaction mixture was then poured into ethyl acetate (15 mL) and the organic layer was washed with saturated NH_4Cl solution and brine (30 mL each), dried over anhydrous Na_2SO_4. Evaporation of solvent left an oily residue from which the product was isolated by column chromatography (Silica-gel, petroleum ether-ethyl acetate mixture as eluent).

4-Pyrene-1-yl-butyric acid 4-(3-hydroxy-prop-1-ynyl)-3-[3-(tetrahydro-pyran-2-yloxy)-prop-1-ynyl]-benzyl ester + 4-Pyrene-1-yl-butyric acid 3-(3-hydroxy-prop-1-ynyl)-4-[3-(tetrahydro-pyran-2-yloxy)-prop-1-ynyl]-benzyl ester (3.013)

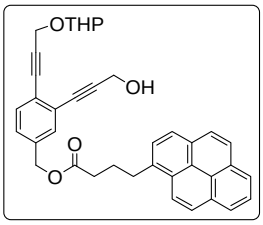

State: yellow gummy mass; **yield**: 153 mg, 75%; ^{1}H NMR (600 MHz, Chloroform-*d*) δ 8.23 (d, *J* = 9.0 Hz, 1H), 8.15 (t, *J* = 7.2 Hz, 2H), 8.08 (t, *J* = 8.4 Hz, 2H), 8.01 - 7.97 (m, 3H), 7.81 (d, *J* = 7.8 Hz, 1H), 7.43 - 7.37 (m, 2H), 7.21 - 7.19 (m, 1H), 5.22 (merged m, 1H), 5.05 (s, 2H), 4.99 - 4.50 (m, 4H), 3.86 (t, *J* = 10.8 Hz, 1H), 3.63 - 3.61 (m, 1H), 3.36 (t, *J* = 7.2 Hz, 2H), 2.49 (t, *J* = 7.2 Hz, 2H), 2.23 - 2.18 (m, 2H), 1.85 - 1.53 (m, 6H); ^{13}C NMR (150 MHz, Chloroform-*d*) δ 173.3, 136.5, 136.2, 135.6, 131.9, 131.7, 131.5, 131.3, 131.0 (×2), 130.1, 128.8, 128.0, 127.8, 127.6 (×2), 127.5, 126.9, 126.4, 126.0, 125.9, 125.7, 125.2 (×2), 125.1 (×2), 123.3, 95.5, 92.8, 92.7, 89.3, 89.2, 85.0, 83.7, 65.3, 61.6, 54.7, 54.6, 51.5 (×2), 33.9, 32.8, 31.7, 30.1, 26.8, 25.5, 22.8; HRMS: Calcd for $C_{38}H_{35}O_5^+$ $[M+H]^+$ 571.2485 found 571.2484.

Synthesis of compound 3.014

Compound **3.013** (100 mg,0.18 mmol) was dissolved in dryDCM (5 ml) and dry Et_3N (0.05 ml, 0.36 mmol) followed by bromoacetyl chloride (0.03 ml, 0.27 mmol) was added at ice cold temperature and the reaction was stirred at ice cold condition for 20 min. After that the reaction was quenched by addition of water and extracted with DCM (10 ml×2). The combined organic layer was washed with brine, dried over anhydrous Na_2SO_4 and evaporated under vacuum. The crude bromoacetylated product was then dissolved in dry DMF (5 ml) and Na-salt of *p*-azido benzoic acid (100 mg, 0.54 mmol) was added to it and the reaction mixture was stirred at room temperature overnight. The reaction was then quenched with water and the crude product **3.014** was extracted in ethyl acetate (10 ml×3). The ethyl acetate layer was washed with brine, dried over anhydrous Na_2SO_4, concentrated and purified by column chromatography by using hexane-ethyl acetate as eluent.

4-Azido-benzoic acid 3-{4-(4-pyrene-1-yl-butyryloxymethyl)-2-[3-(tetrahydro-pyran-2-yloxy)-prop-1-ynyl]-phenyl}-prop-2-ynyloxycarbonylmethyl ester + 4-Azido-benzoic acid 3-{5-(4-pyrene-1-yl-butyryloxymethyl)-2-[3-(tetrahydro-pyran-2-yloxy)-prop-1-ynyl]-phenyl}-prop-2-ynyloxycarbonylmethyl ester (3.014)

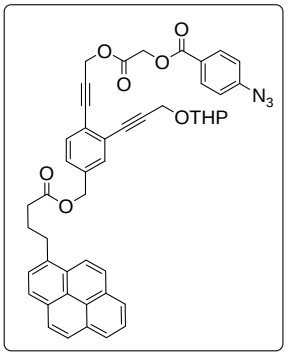

State: brown gummy mass; **yield**: 88 mg, 65%; ^{1}H NMR (600 MHz, Chloroform-*d*) δ 8.25 (dd, *J* = 9.3 Hz, 2.4 Hz, 1H), 8.16 (t, *J* = 7.2 Hz, 2H), 8.11 - 8.07 (m, 4H), 8.02 - 7.98 (m, 3H), 7.84 (dd, *J* = 7.8 Hz, 1.2 Hz, 1H), 7.45 (bs, 1H), 7.42 (dd, *J* = 8.4 Hz, 3.0 Hz, 1H), 7.25 - 7.21 (m, 1H), 7.09 - 7.06 (m, 2H), 5.07 - 5.06 (merged s, 4H), 4.97 - 4.96 (m, 1H), 4.93 - 4.90 (merged s, 2H), 4.56 - 4.49 (m, 2H), 3.88 - 3.84 (m, 1H), 3.57 - 3.54 (m, 1H), 3.39 (t, *J* = 7.8 Hz, 2H), 2.51 (t, *J* = 6.6 Hz, 2H), 2.25 - 2.20 (m, 2H); ^{13}C NMR (150 MHz, Chloroform-*d*) δ 173.3, 167.4, 165.2 (×2), 136.9, 136.4, 135.7, 132.6, 132.5, 132.0 (×2), 131.9, 131.8, 131.6, 131.1, 130.2, 129.0, 128.5, 128.0, 127.7 (×2), 127.6, 126.9, 126.1, 125.3, 125.2, 125.1, 125.0 (×2), 123.4, 119.2, 119.1, 96.7, 90.2, 90.1, 86.5, 86.4, 85.6, 83.9, 65.4, 62.1, 61.2 (×2), 54.8 (×2), 53.6, 34.0, 32.9, 31.8, 26.9, 25.6, 22.8, 19.0; HRMS: Calcd for $C_{47}H_{40}N_3O_8^+$ $[M+H]^+$ 774.2815 found 774.2820.

Synthesis of compound 3.002

To an ice-cold solution of compound **3.013** (50 mg, 0.09 mmol) in dry DCM (3 ml) was added dry Et_3N (0.03 ml, 0.18 mmol) followed by bromoacetyl chloride (0.01 ml, 0.135 mmol) and the reaction was allowed to stir at ice cold temperature for 20 min. The reaction was then quenched with water and after performing usual work up procedure the crude bromoacetylated product was isolated. It was then dissolved in dry DMF (3 ml) and Na salt of *N*-(4-Sulfamoyl-phenyl)-oxalamic acid **3.005** (75.6 mg, 0.27 mmol) was added into it under inert atmosphere and the reaction was stirred overnight at room temperature. The reaction was then quenched by diluting the reaction mixture with water and ethyl acetate. The water layer was extracted with ethyl acetate (10 ml) thrice and the combined organic layer was washed with brine, dried over anhydrous Na_2SO_4, concentrated and the crude product **3.002** was purified by column chromatography by using hexane-ethyl acetate as eluent.

4-Pyren-1-yl-butyric acid 4-(3-{2-[2-(4-sulfamoyl-phenylcarbamoyl)-acetoxy]-acetoxy}-prop-1-ynyl)-3-[3-(tetrahydro-pyran-2-yloxy)-prop-1-ynyl]-benzyl ester + 4-Pyren-1-yl-butyric acid 3-(3-{2-[2-(4-sulfamoyl-phenylcarbamoyl)-acetoxy]-

acetoxy}-prop-1-ynyl)-4-[3-(tetrahydro-pyran-2-yloxy)-prop-1-ynyl]-benzyl ester (3.002)

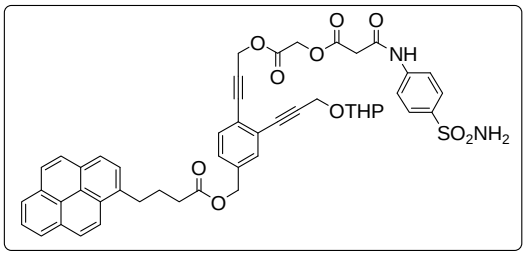

State: yellow sticky mass; **yield**: 52 mg, 68%; ^{1}H NMR (600 MHz, Chloroform-*d*) δ 9.27 (d, *J* = 12.0 Hz, 1H), 8.25 - 8.23 (m, 1H), 8.17 - 8.15 (m, 2H), 8.11 - 8.07 (m, 2H), 8.02 - 7.98 (m, 3H), 7.83 - 7.81 (m, 3H), 7.71 (app d, *J* = 8.4 Hz, 2H), 7.44 - 7.39 (m, 2H), 7.23 (d, *J* = 8.4 Hz, 1H), 5.08 - 5.05 (merged s, 4H), 4.96 - 4.94 (m, 1H), 4.85 (s, 1H), 4.80 (s, 1H), 4.55 - 4.48 (m, 2H), 3.89 - 3.83 (m, 1H), 3.64 (d, *J* = 16.8 Hz, 2H), 3.56 - 3.54 (m, 1H), 3.39 - 3.36 (m, 2H), 2.52 - 2.49 (m, 2H), 2.24 - 2.17 (m, 2H), 1.86 - 1.63 (m, 6H); ^{13}C NMR (150 MHz, Chloroform-*d*) δ 173.4 (×2), 168.1, 168.0, 167.7 (×2), 163.0, 147.3, 141.7, 139.5, 137.5, 137.2, 136.5, 135.7, 132.6 (×2), 131.9, 131.8, 131.6, 131.1, 130.2, 128.9, 128.6, 128.0, 127.8, 127.7, 127.6, 127.0, 126.9, 125.3, 125.2, 125.1, 125.0, 123.4 (×2), 120.1, 114.3, 96.8, 90.1 (×2), 86.0 (×2), 85.9 (×2), 84.0, 65.3, 62.2, 61.5, 54.8, 54.5, 34.0, 32.9, 32.1, 31.6, 29.6, 26.9, 22.9, 19.1; ν_{max}(KBr, cm^{-1}): 3122, 3031, 2960, 2874, 1751, 1597, 1281, 1159, 1135, 845, 768; λ_{max} (CH_3CN): 236 (35030 M^{-1} cm^{-1}), 263 (27636 M^{-1} cm^{-1}), 273 (31515M^{-1} cm^{-1}), 326 (8484 M^{-1} cm^{-1}), 341 (13333 M^{-1} cm^{-1}), 396 (363 M^{-1} cm^{-1}); HRMS: Calcd for $C_{49}H_{45}N_2O_{11}S^+$ $[M+H]^+$ 891.2564 found 891.2540.

Synthesis of compound 3.001

Compound **3.015** (40 mg, 0.06 mmol) was dissolved in dry DCM and to it was added dry Et_3N (0.02 ml, 0.12 mmol) followed by bromoacetyl chloride (0.01 ml, 0.10 mmol) in ice cold temperature and stirred at ice cold condition for 20 min. The reaction was quenched with water and extracted with DCM (5 ml×3). The crude product isolated after following usual work up procedure was dissolved in dry DMF (2 ml) and Na salt of *N*-(4-Sulfamoyl-phenyl)-oxalamic acid **3.005** (50 mg, 0.18 mmol) was added into it and the reaction mixture was stirred at room temperature overnight. After that the reaction mixture was quenched by addition of water, extracted the crude product **3.001** in ethyl acetate (5 ml×3) and the combined organic layer was washed with brine, dried over anhydrous Na_2SO_4, concentrated and purified

by column chromatography by using DCM-MeOH as eluent. The product was then purified further by repeated precipitation from DCM-Hexane.

4-Azido-benzoic acid 3-[5-(4-pyrene-1-yl-butyryloxymethyl)-2-(3-{2-[2-(4-sulfamoyl-phenylcarbamoyl)-acetoxy]-acetoxy}- prop-1-ynyl)-phenyl]-prop-2-ynyloxy carbonylmethyl ester + 4-Azido-benzoic acid 3-[4-(4-pyrene-1-yl-butyryloxymethyl)-2-(3-{2-[2-(4-sulfamoyl-phenylcarbamoyl)-acetoxy]-acetoxy}-prop-1-ynyl)-phenyl]-prop-2-ynyloxy carbonylmethyl ester (3.001)

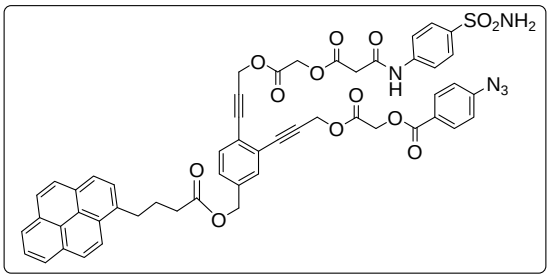

State: brown solid; **yield**: 25 mg, 58%; ^{1}H NMR (600 MHz, Chloroform-*d*) δ 9.21 - 9.16 (bm, 1H), 8.23 - 8.22 (m, 1H), 8.16 - 8.14 (m, 2H), 8.09 - 7.96 (m, 6H), 7.82 - 7.64 (m, 6H), 7.43 - 7. 37 (m, 2H), 7.24 - 7.22 (m, 1H), 7.03 - 7.02 (m, 2H), 5.06 - 4.76 (m, 10H), 3.64 - 3.60 (bm, 2H), 3.37 - 3.35 (bm, 2H), 2.50 - 2.49 (m, 2H), 2.20 - 2.17 (bm, 2H); ^{13}C NMR (150 MHz, Chloroform-*d*) δ 173.4 (×2), 167.7, 167.5, 165.4, 165.3, 163.1, 145.7, 145.6, 141.7, 141.6, 139.5, 137.4, 137.2, 137.1, 135.7, 132.7, 132.6, 132.0, 131.8, 131.6, 131.1, 130.2, 128.9, 128.5 (×2), 127.7 (×2), 127.6, 127.0, 126.1, 125.3, 125.2, 125.0, 123.7, 123.4, 120.4, 120.0, 119.2, 116.1, 114.3, 87.0, 86.9 (×2), 86.8, 85.4, 85.3, 85.1 (×2), 65.2, 61.2 (×2), 53.9, 53.6, 33.9, 32.8, 29.9, 26.9; ν_{max}(KBr, cm^{-1}): 3123, 3035, 2961, 2929, 2870, 2120, 1752, 1597, 1410, 1282, 1160, 1138, 846, 767; λ_{max} (CH_3CN): 238 (36125 M^{-1} cm^{-1}), 264 (28500 M^{-1} cm^{-1}), 273 (33125 M^{-1} cm^{-1}), 326 (9375 M^{-1} cm^{-1}), 341 (14375 M^{-1} cm^{-1}), 399 (750 M^{-1} cm^{-1}); HRMS: Calcd for $C_{53}H_{41}N_5NaO_{13}S^+$ $[M+Na]^+$ 1010.2319 found 1010.2294.

3.7.3 Capture experiment protocol

The HCA II concentration was kept at 40 μM and the total volume was made up to 50 μL with buffer (50 mM HEPES; pH 7.2). HCA II and capture compounds (C1: 1.75–20 μM; C2: 2.5-40 μM) in DMSO were mixed by vortexing followed by centrifugation. For comparing C1, C2, and C3 (10 μM), the HCA II was kept constant at 20 μM concentration. The compounds were incubated with proteins for 20 min at room temperature, then photo-irradiated (UV λ≥ 300 nm, 15 watts each

× 5 bulbs, 30 pulses, each pulse has a duration of 120 sec) in a 96 well plate followed by SDS-PAGE and trypsin digestion for mass spectrometric analysis.

3.7.4 Trypsin digestion and Matrix Assisted Laser Desorption Ionization Spectrometry (MALDI analyses)

The molecular mass of the protein-capture compound complex was determined by mass spectrometry after digesting the protein bands with Trypsin. In brief, protein bands were chopped from SDS-PAGE and emerged in 100 µl of 100 mM ammonium bicarbonate and 100 % acetonitrile in 1:1 (V/V). The samples were agitated occasionally for 30 min. Another 500 µl of acetonitrile was added to each of the sample followed by 15 min incubation at room temperature. Total volume of liquid supernatant was decanted and the gel pieces were air dried for 15 min. 40 µl of Trypsin (200 ng, sequencing grade, Roche Life Science) was added to each samples and kept for 1h 30 min in ice and then in 37 °C for overnight. Total solutions were taken in fresh tubes and lyophilized. For mass spectrometric studies, the lyophilized samples were dissolved in 10 µl of 0.1 % Trifluro acetic acid and 2 µL from the solution was mixed thoroughly with 2 µL of HCCA (α- cyano-4-hydroxycinnamic acid) as matrix. From the mixture, 2 µL was spotted onto 384 well stainless steel MALDI plate and allowed to be air dried prior to MALDI analysis by the ultraFlextrene MALDI Time-of-Flight Mass Spectrophotometer in positive ion mode. The instrument was calibrated for the mass range 600-3500 Da using a standard calibration kit that contains Bradykinin, Angiotensin II, Angiotensin I, Substance_P, Bombesin, Renin_substrate, ACTH_clip (1-17), ACTH_clip (18-39), Somatostatin. By using this kit whole mass range was calibrated in positive ion mode. UV Laser: Smartbeam II (N_2, NdYag), 355 nm wavelength, Laser rep rate 2 KHz, Reflector mode.

3.7.5 SDS-polyacrylamide gel electrophoresis

For SDS-polyacrylamide gel analysis, the samples were mixed with 6X Laemmli buffer (1X buffer composition was 63 mM Tris-HCl ((pH 6.8), 2% SDS, 10% glycerol, 0.1% 2-mercaptoethanol and 0.01% Bromophenol blue) (U. K. Laemmli, Cleavage of structural proteins during the assembly of the head of bacteriophage T4. *Nature* 1970, **227**, 680-685) and heated at 95 °C for 5 min. 20 µL

sample from each mixture was loaded in each well of 12% discontinuous SDS-PAGE (Mini-PROTEAN 3, Multi casting chamber, BioRad Instruments). The electrophoresis was done under denaturing condition. The stacking and resolving gels were composed of 5% (w/v) and 12% (w/v) acrylamide with Tris (pH 6.8 and pH 8.8) respectively, and 0.1% SDS. The composition of electrophoresis buffer was 0.025 M Tris, 0.2 M glycine, pH 8.3 and 0.1% SDS. An electric potential of 160 volt was applied to run the gel until the bromphenol blue dye reached the end of the resolving gel. The gel was visualized under UV light in UVP gel documentation system. The position of the fluorescent bands was confirmed by staining the gels with 0.1% (w⁄v) Coomassie Brilliant Blue R-250 in 50% (v⁄v) methanol and 10% (v⁄v) acetic acid and destained with methanol⁄acetic acid.

3.7.6 ^{1}H and ^{13}C NMR spectra of selected compounds

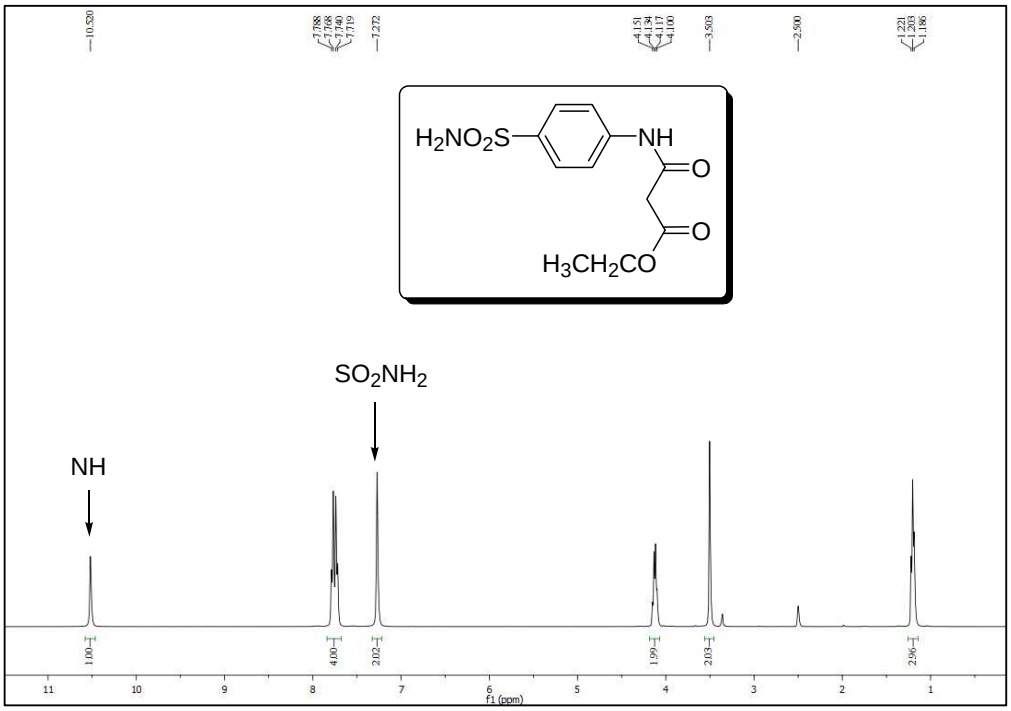

^{1}H NMR (DMSO-d_6, 600 MHz) spectrum of 3.004

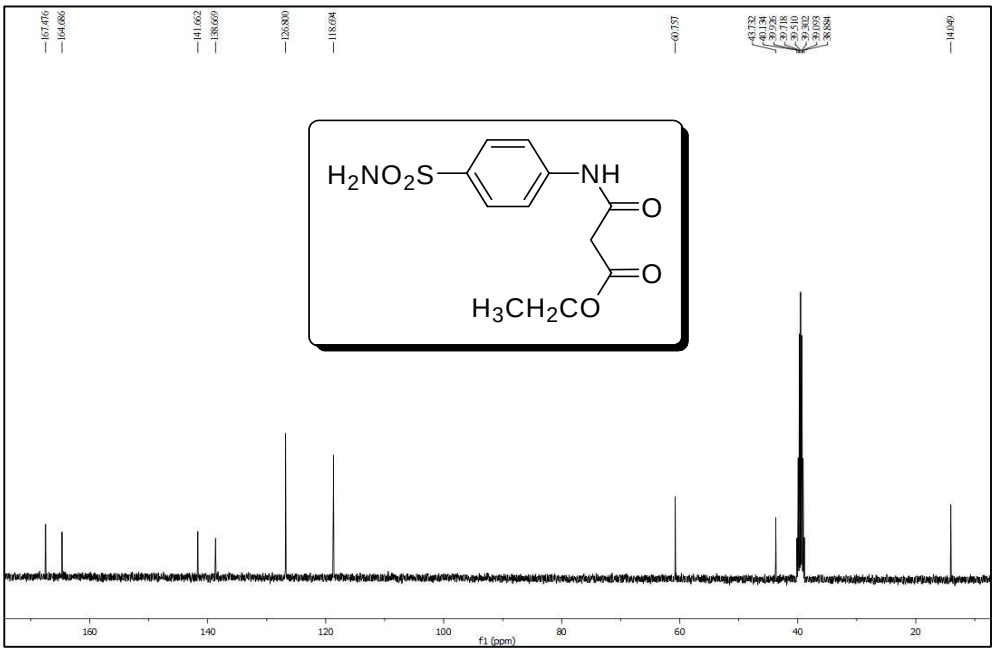

^{13}C NMR (DMSO-d_6, 150 MHz) spectrum of 3.004

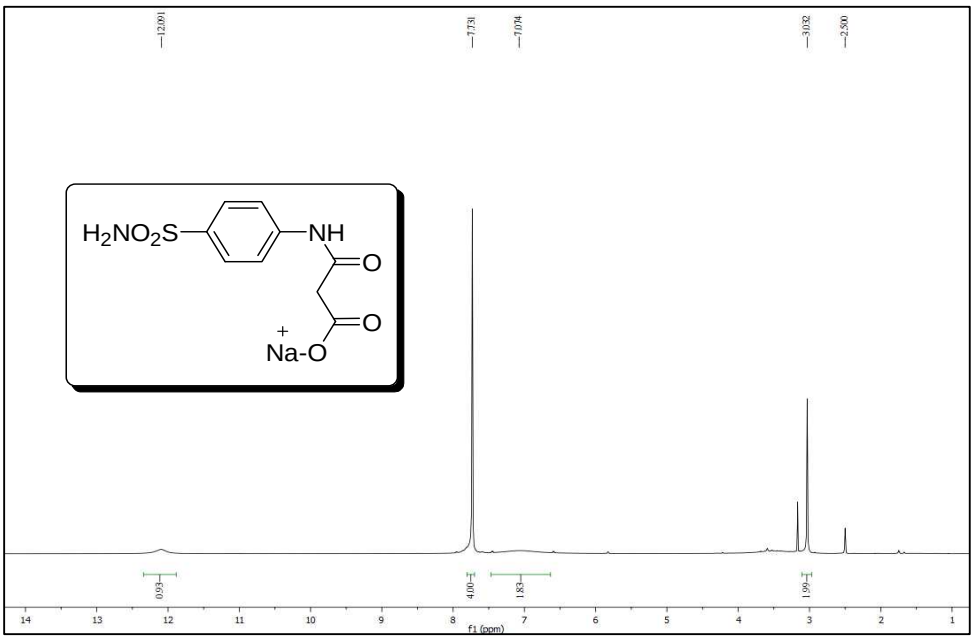

^{1}H NMR (DMSO-d_6, 600 MHz) spectrum of 3.005

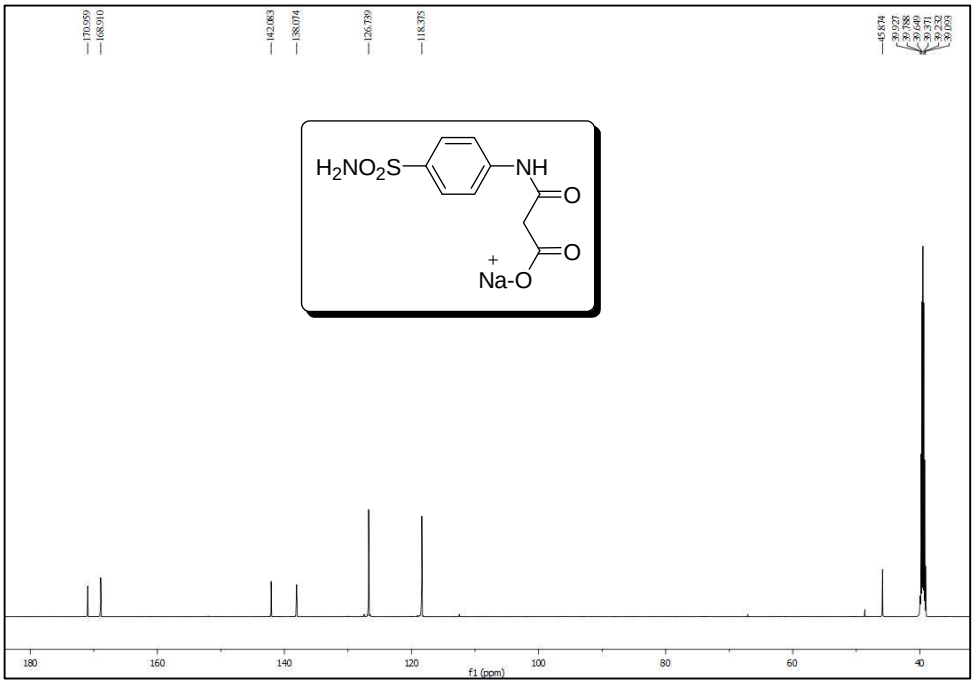

^{13}C NMR (DMSO-d_6, 150 MHz) spectrum of 3.005

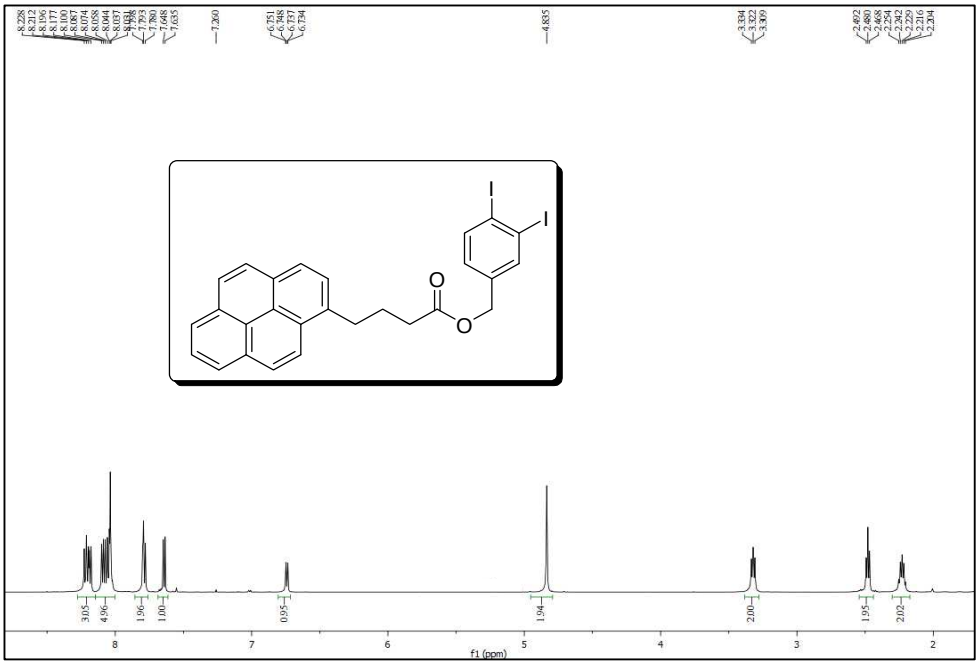

^{1}H NMR ($CDCl_3$, 600 MHz) spectrum of 3.011

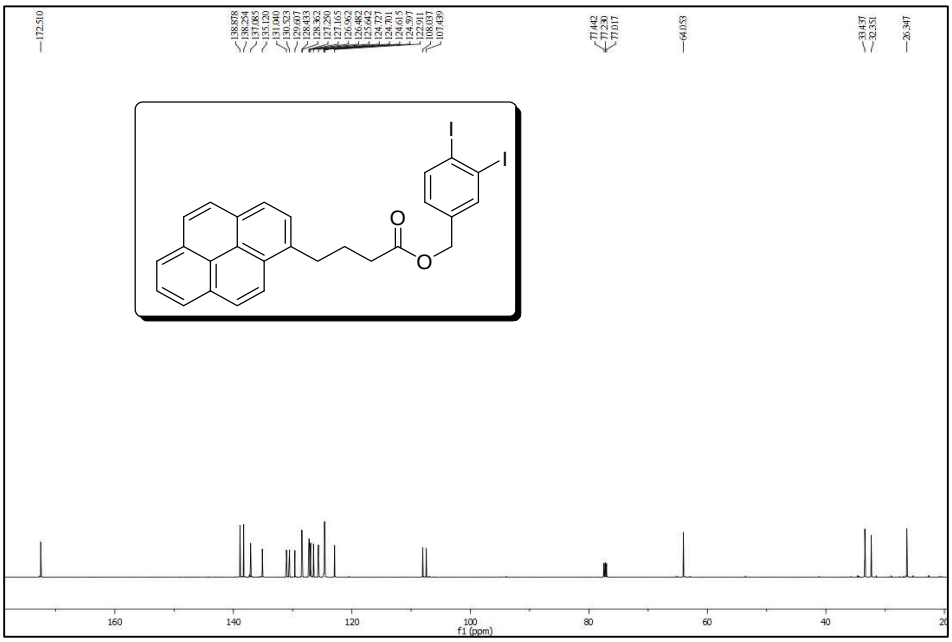

^{13}C NMR ($CDCl_3$, 150 MHz) spectrum of 3.011

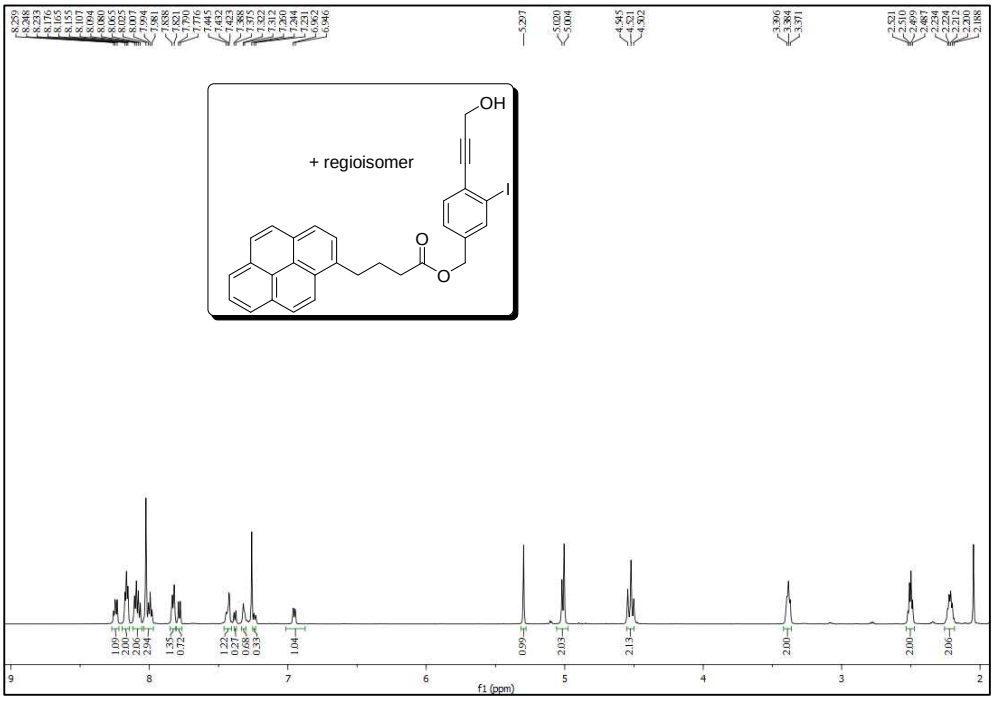

^{1}H NMR ($CDCl_3$, 600 MHz) spectrum of 3.012

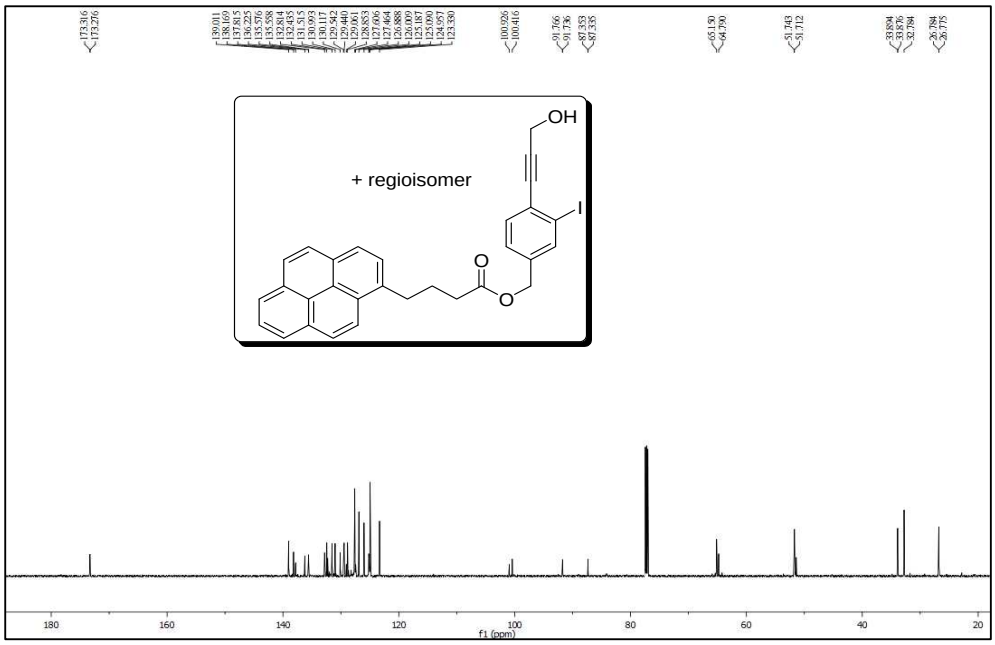

^{13}C NMR ($CDCl_3$, 150 MHz) spectrum of 3.012

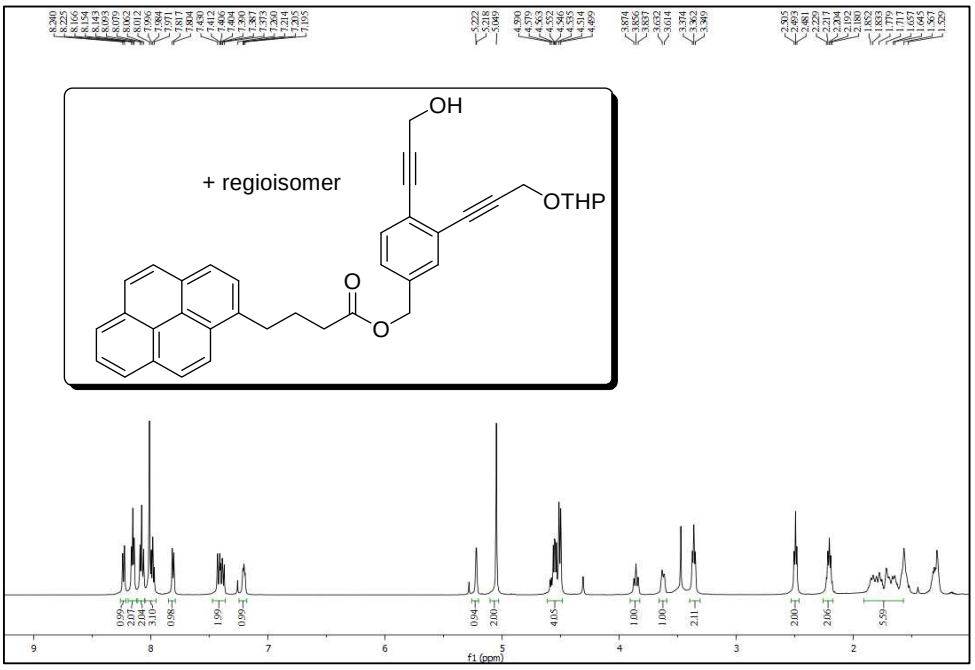

^{1}H NMR ($CDCl_3$, 600 MHz) spectrum of 3.013

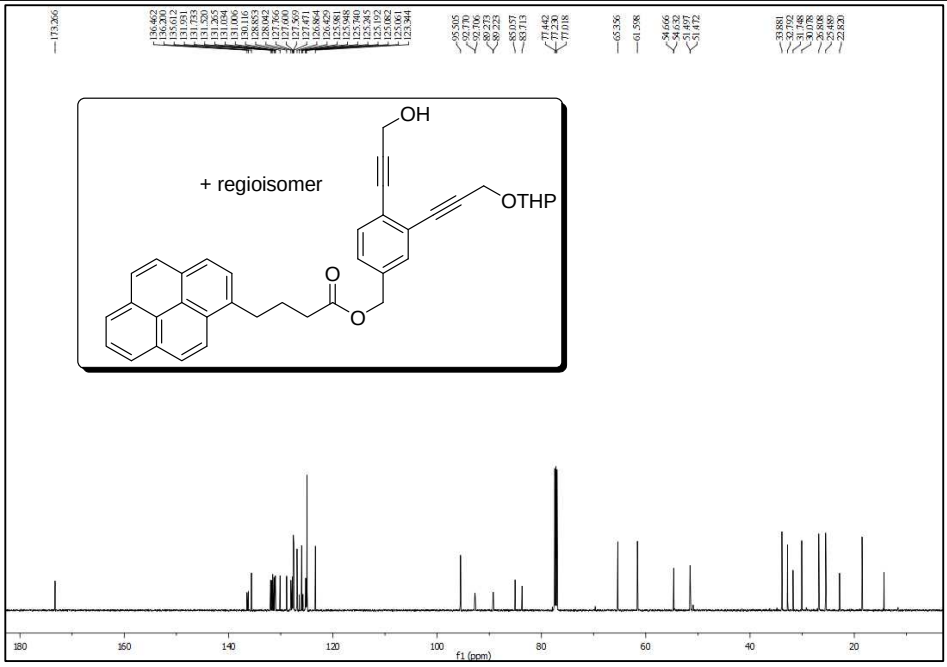

^{13}C NMR ($CDCl_3$, 150 MHz) spectrum of 3.013

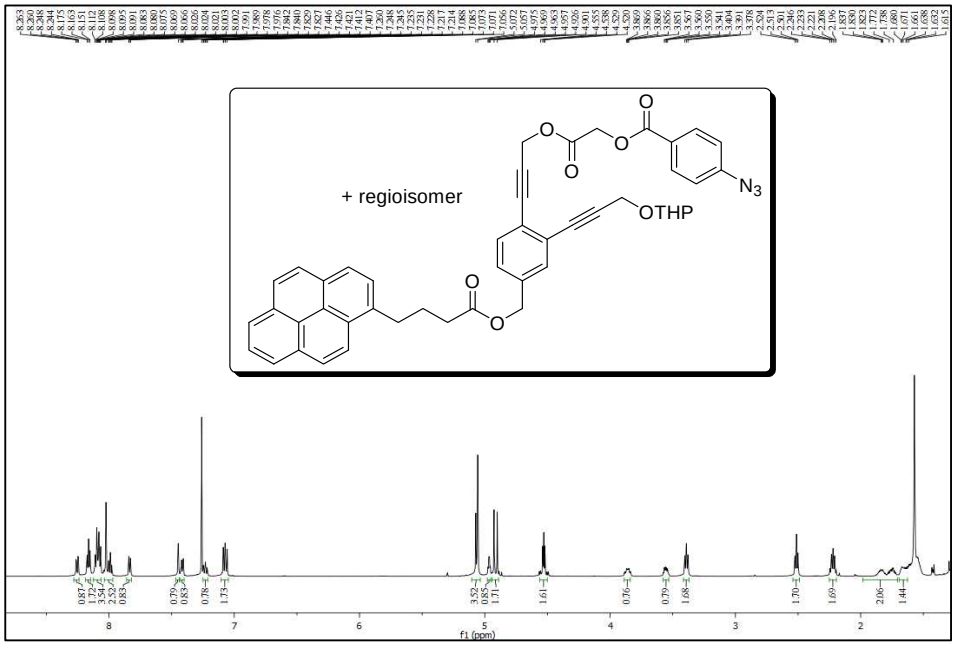

^{1}H NMR ($CDCl_3$, 600 MHz) spectrum of 3.014

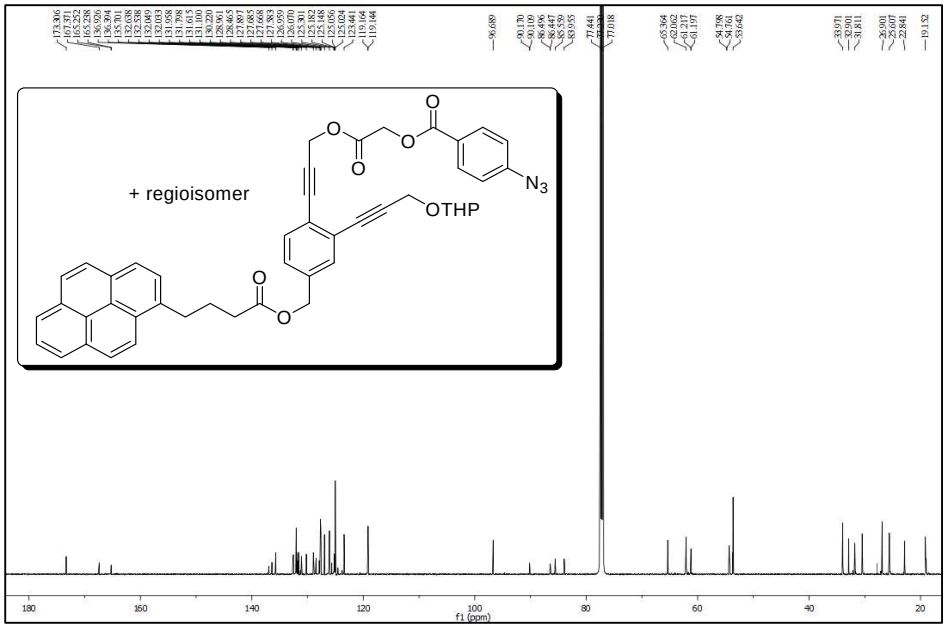

^{13}C NMR ($CDCl_3$, 150 MHz) spectrum of 3.014

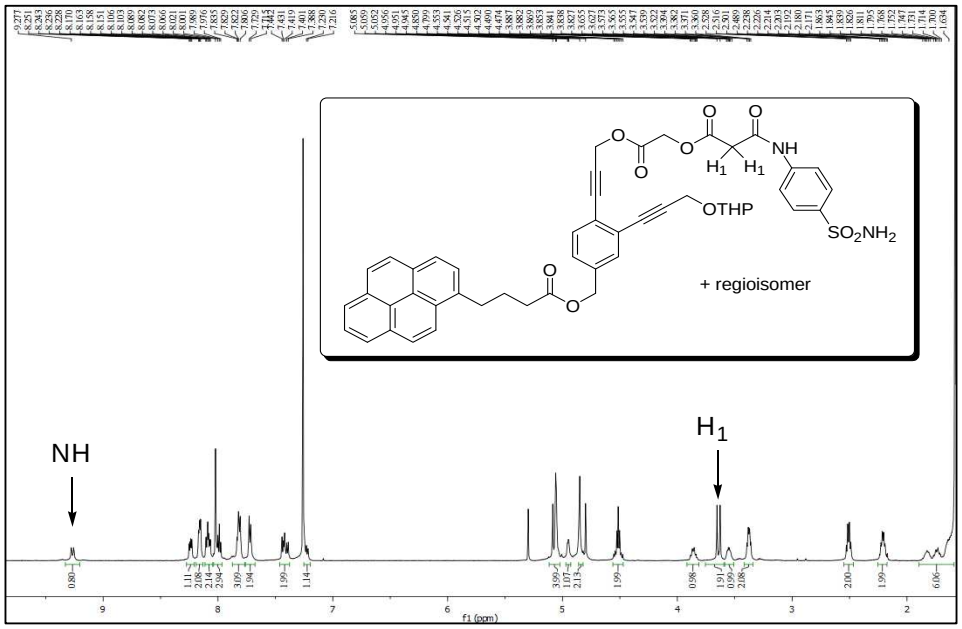

^{1}H NMR ($CDCl_3$, 600 MHz) spectrum of 3.002

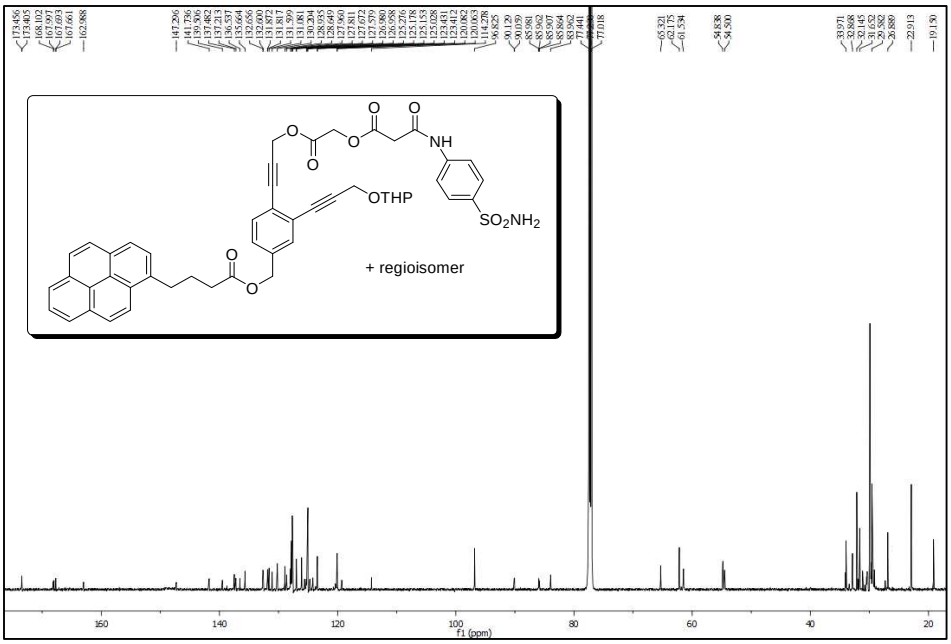

^{13}C NMR ($CDCl_3$, 150 MHz) spectrum of 3.002

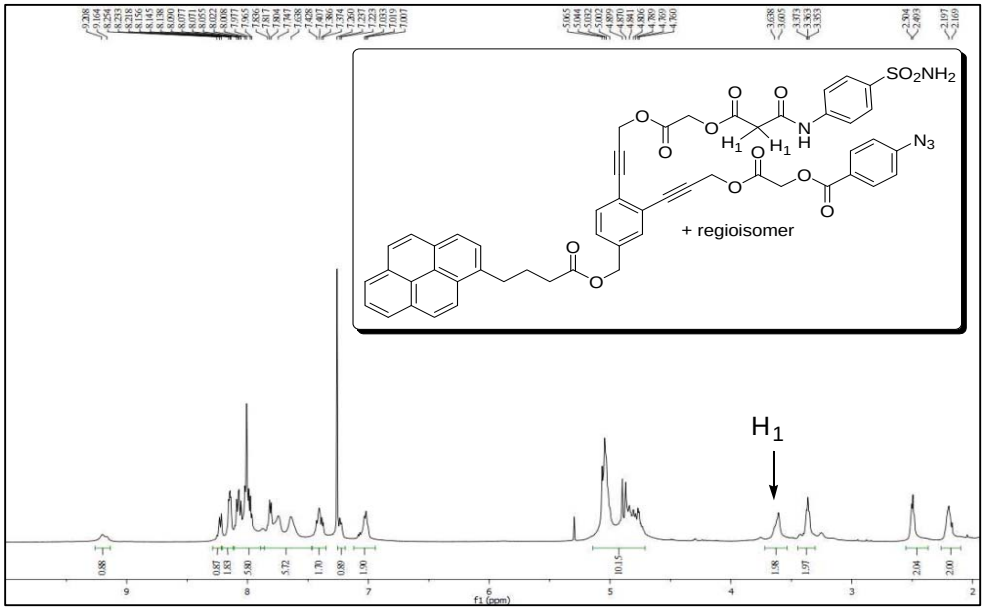

^{1}H NMR ($CDCl_3$, 600 MHz) spectrum of 3.001

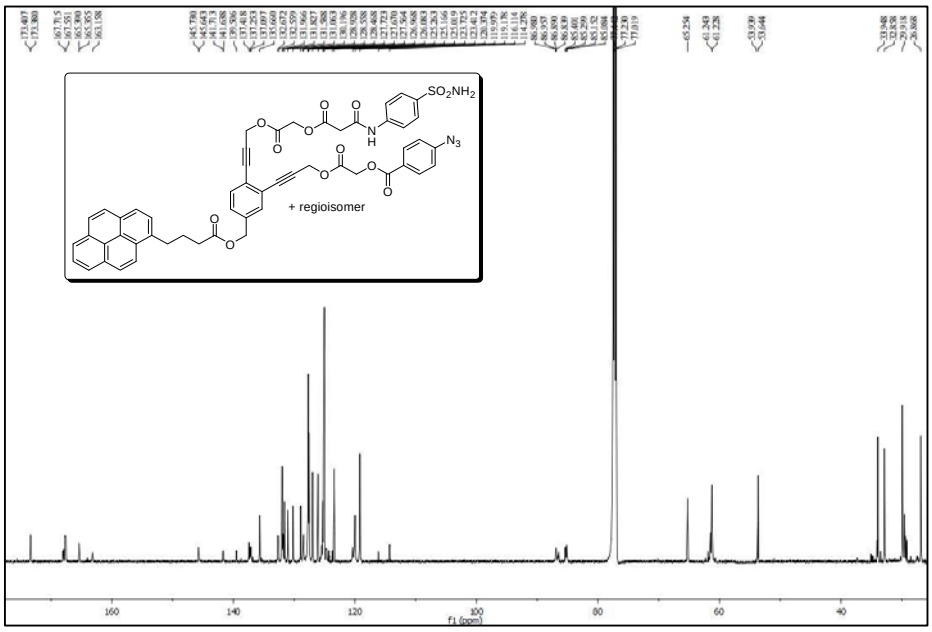

^{13}C NMR ($CDCl_3$, 150 MHz) spectrum of 3.001

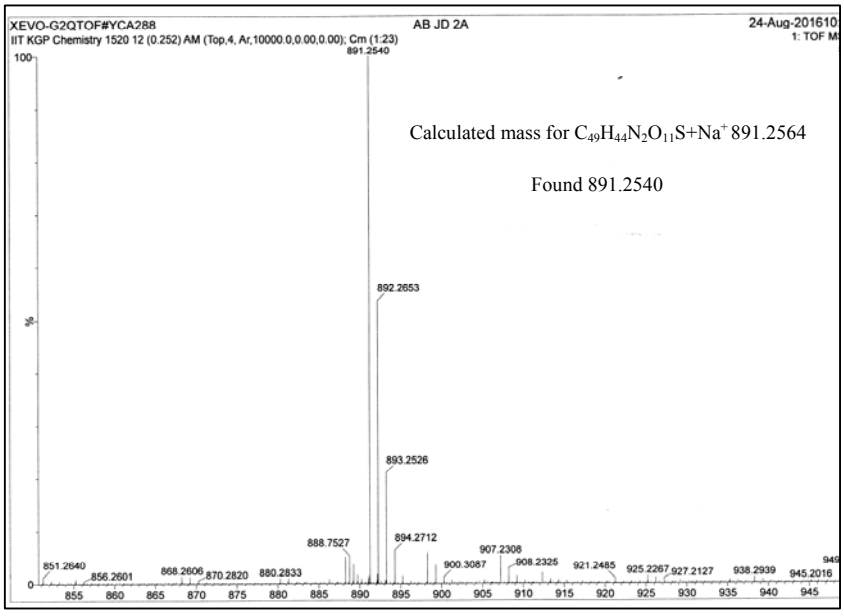

HRMS Spectrum of Compound 3.002

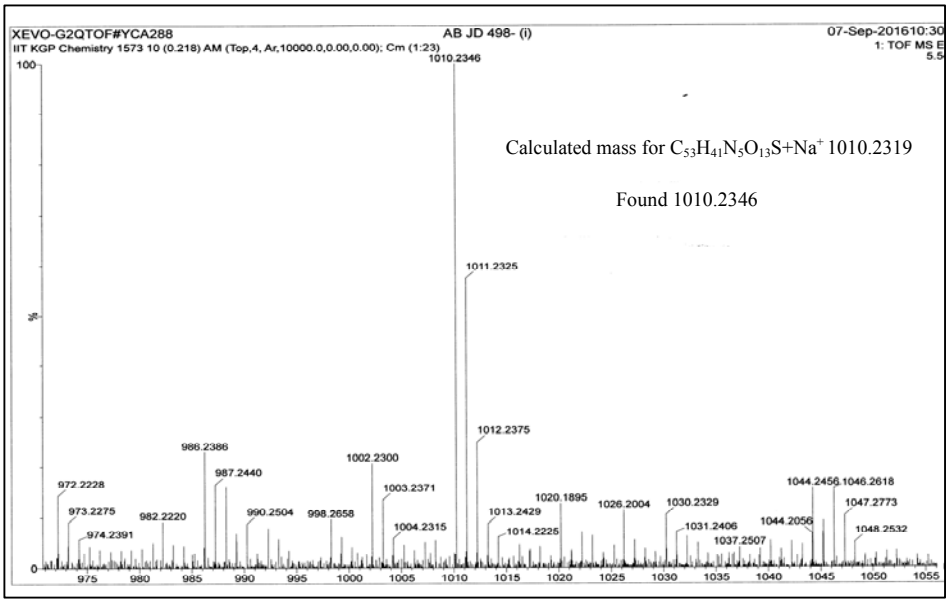

HRMS Spectrum of Compound 3.001

3.7.7 Docked image of Compound 3.002 with HCA II

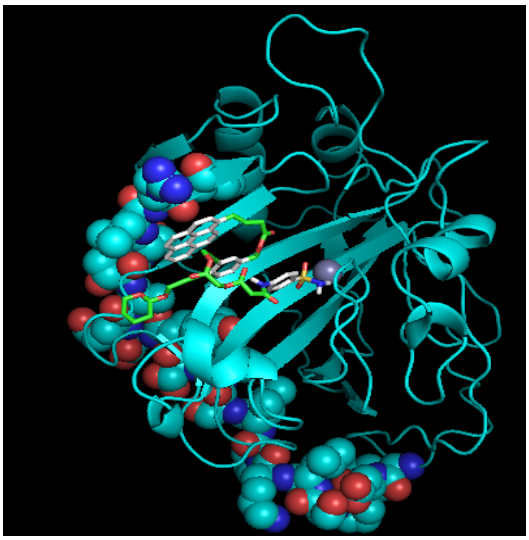

The grey sphere represents Zn atom. The amino acid residues from 40-58 (protein portion as sphere, mass fragment 2141 in tryptic digestion of HCA II) is close to the molecule; hence we obtained a major peak at 2912/2914 after photo cross-linking of enediyne with the protein.

Chapter 4

Shifting the Reactivity of Bis-Propargyl Ethers from Aryl Naphthalenes to 3,4-Disubstituted Furans via 1,5-H shift Pathway

4.1 Introduction

Base mediated rearrangement of bis-propargyl precursors has now been established as a fertile ground of designing novel synthons convenient for synthesis of complex molecular structures.[40] The reaction is popularly known as Garratt-Braverman (GB) cyclization[4a,32,33,34,78] and involves the formation of two new C-C bonds.(**Scheme 4.01**)

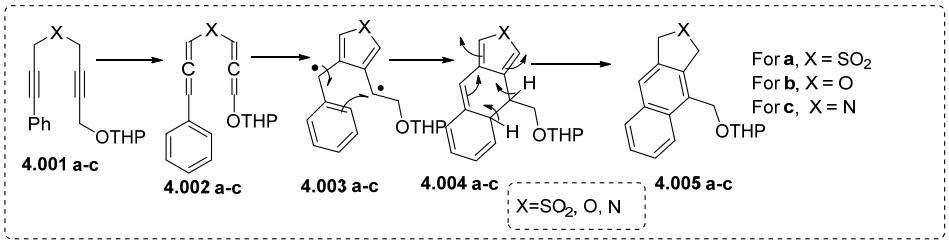

Scheme 4.01: Garratt-Braverman cyclization of aryl substituted bis-propargyl systems

Likewise the mechanism, the outcome of the reaction depends upon the nature of substituent in the propargyl arm as well as the reaction condition. In case of an unsubstituted bis-propargyl precursor **4.006**, a dimeric product **4.007** is formed whereas for *t*-butyl substitution **4.010,** an intramolecular quenching of diradical *via* cyclobutane ring formation to **4.011** is observed.[32,4a] For substrates with aryl or vinyl substitution like in **4.012,** the aryl or vinyl double bond participates in cyclization to form naphthalene or benzene fused heterocyclic systems **4.013** and for substrates with alkyl substituted acetylenic terminus as in **4.008,** a 3,4-disubstituted heterocycle **4.009** is formed *via* a 1,5-H shift process (**Scheme 4.03**) to internally quench the diradical. [79] All these possibilities are shown schematically as follows (**Scheme 4.02**).

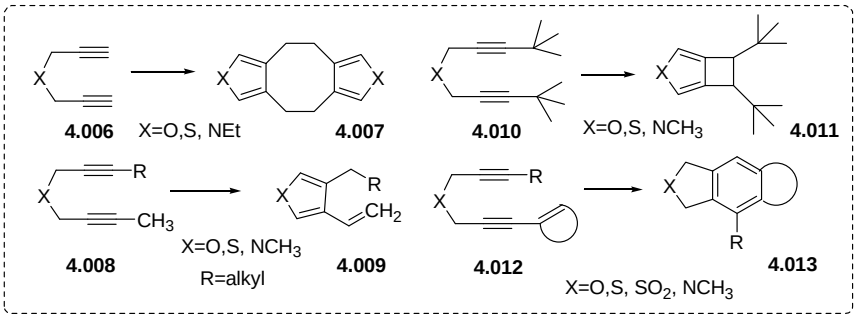

Scheme 4.02: Reactivity of differentially substituted bis-propargyl systems

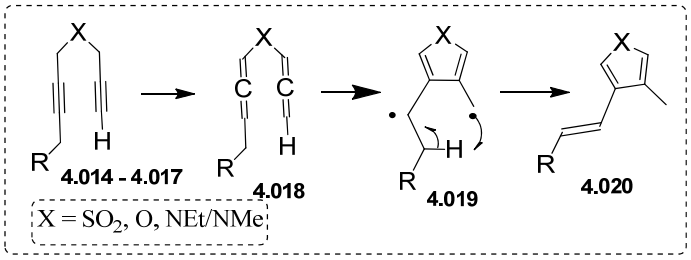

Scheme 4.03: 1,5-H shift for alkyl substituted acetylenic termini

Thus, for alkyl substituted acetylenic substrates, the 1,5-H shift becomes predominant if there is no involvement of aryl or vinyl double bond. If there is a possibility of involvement of both alkyl and aryl functionality then GB cyclization pathway becomes predominant as that would create a more stable aromatic ring than less stable heterocyclic ring which is the end product for 1,5-H shift process. It is thus a challenge to shift the reaction from GB to 1,5-H shift process. Here we have restricted our discussion for bis-propargyl ethers only as in that case we have been able to obtain a fair amount of success to tilt the preference from GB cyclization mode to 1,5-H shift pathway. Eventually, the 1,5-H shift products are 3,4-disubstituted furans, which are important synthons[80] and are also present in numerous biologically active compounds[81]. For example, furan and its derivatives can serve as an easily available building block for structurally diverse molecules (**Figure 4.01**) as they can undergo wide range of reactions including cycloaddition with a dienophile, hydrolysis to 1,4-dicarbonyl compounds **4.024**, oxidation or reduction to dihydro and tetrahydrofuran derivatives.

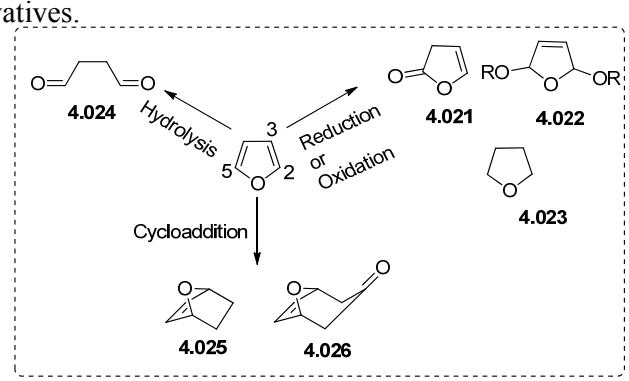

Figure 4.01: Synthetic diversity with furan

In addition, compound **4.027** with 3,4-disubstitution exhibits bioactivity by inhibiting PGH_1 formation (**Figure 4.02**). It may undergo facile [4+2] cycloaddition with oxygen to produce endoperoxide **4.028** that may exhibit PGH_1 agonist activity.[81]

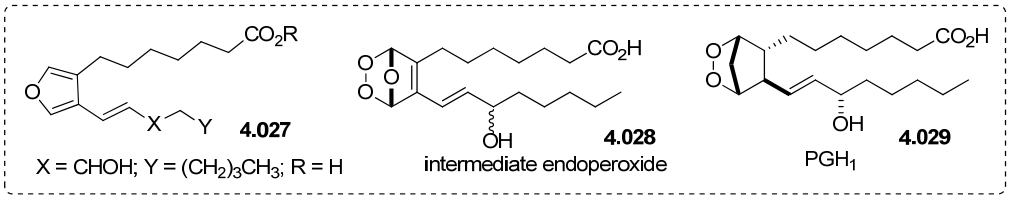

Figure 4.02: 3,4-disubstituted furans as inhibitor

It is well known that furan shows a preference towards electrophilic substitution at 2/5-position (α) as the intermediate formed by electrophilic attack at C-2/C-5 is stabilized by charge delocalization to a greater extent than the intermediate from C-3 attack. Thus, it appears to be a great challenge to synthesize 3,4-disubstituted furans relevant in pharmacology.

Hence, by combining these two criteria, herein we report strategies to tilt preference of reactivity of bis-propargyl ethers from GB cyclization to 1,5-H shift process. This will ensure synthesis of 3,4-disubstituted furans in a convenient pathway. The reaction operates in mild condition and comprises easily available starting materials like bis-propargyl ethers.

Here, we have discussed the mechanism of 1,5-H shift process for bis-propargyl ethers to synthesize 3,4-disubstituted furans *via* radical pathway. The bis-propargyl ethers are shown to follow a [4+2] cycloaddition mechanism involving the mono-allene[82] in the previous chapter. However, for bis-propargyl ethers with ethereal substitution at the acetylenic termini, the cycloaddition mechanism gives rise to the formation of a strained 6-membered ring **4.031 a/b** (**Scheme 4.04**) and the corresponding pathway must be associated with higher energy of activation.

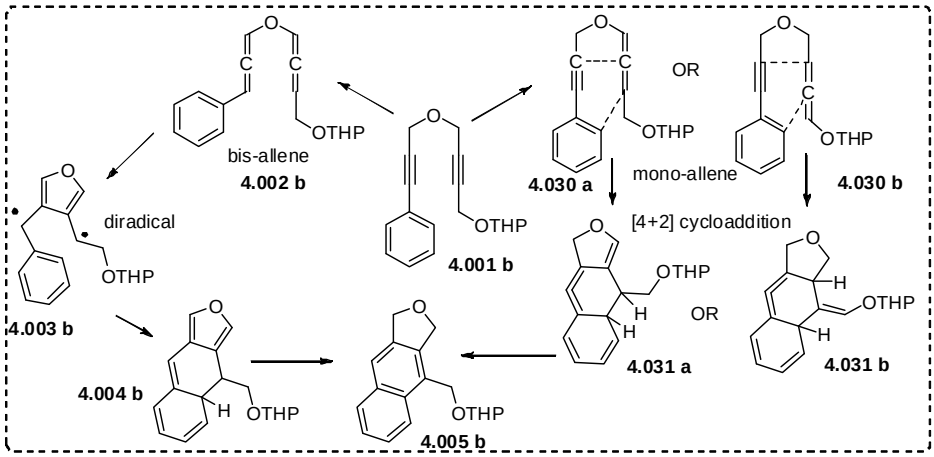

Scheme 4.04: Reaction Mechanism *via* mono-allene and bis-allene pathway

Thus, the mono-allene formed will choose to undergo second isomerization to bis-allene followed by diradical formation rather than [4+2] cycloaddition pathway.

4.2 Objective

We realized the biological importance of furan moiety and synthetic relevance of base mediated rearrangement of bis-propargyl ethers. To tilt the preference from GB to 1,5-H shift pathway to achieve furan moiety it was necessary to come across the parameters that assist in shifting the reactivity. It was comprehended that in order to maximize the outcome of 1,5 H-shift product than the vinyl double bond participation in GB cyclization we have to weaken the C-H bond participating in 1,5-H shift *i.e.* somehow the radical adjacent to it must be stabilized and also another strategy may be to use different aryl systems with varying resonating energy or double bond fixation as to involve in GB cyclization the involved aryl system has to lose its resonance stability. Now greater the loss of resonance energy during GB cyclization greater the reaction will shift towards 1,5-H shift process. All these possibilities are shown in **Scheme 4.05**.

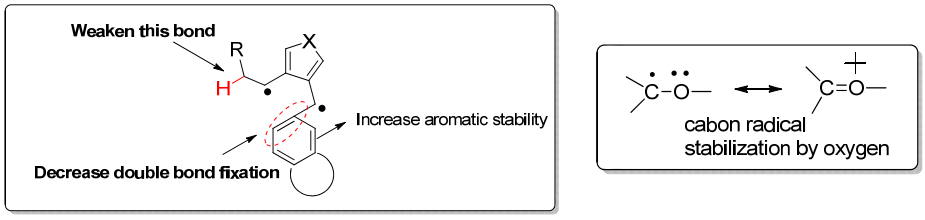

Scheme 4.05: Strategies to tilt the preference towards 1,5-H shift pathway

Taking all these aspects into consideration we set our objectives as follows:

- Synthesize various bis-propargyl ethers of general structure **A**.

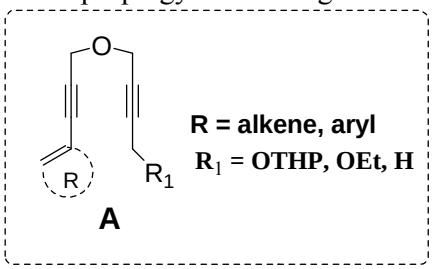

- Alter the **R** group from phenyl, substituted phenyl to vinyl functionality to validate the effect of resonance stability during the course of reaction.

- Vary the alkyl part with different alkoxy substitutions (OTHP, OEt) anticipating that the incipient radical formed during H migration would be stabilized by the adjacent oxygen atom of alkoxy groups.
- Shift the preference to 1,5-H shift pathway from Garratt-Braverman cyclization to synthesize 3,4-disubstituted furans.

4.3 Previous Work

In 1975 Garratt *et al.* illustrated base catalyzed rearrangement of bis-propargyl ethers **4.032** to heterocylic molecule **4.037**.[32] As discussed earlier the outcome of rearrangement depended upon the substituents at the acetylenic end as well as the reaction conditions. In case of bis (3-phenyl-2-propargyl) ether **4.032**, treatment with 14% KO^{t}Bu in presence of *t*-butyl alcohol gave rise to aryl naphthalene product **4.037** whereas treatment with KO^{t}Bu in THF at 20 °C for 10 min afforded a furan derivative **4.036** that was confirmed by ^{1}H-NMR spectral analysis (**Scheme 4.06**). It was converted to the aryl naphthalene product **4.037** by treatment of base under vigorous condition for a prolonged reaction time. The reaction was believed to proceed by a bis-allene intermediate **4.033** that dimerized to diradical **4.034** followed by cyclization and prototropic rearrangement. The formation of diradical was further supported by the rearrangement of unsubstituted and *t*-butyl substituted bis-propargyl compounds **4.038** and **4.040** to the furan derivatives **4.039** and **4.041**.

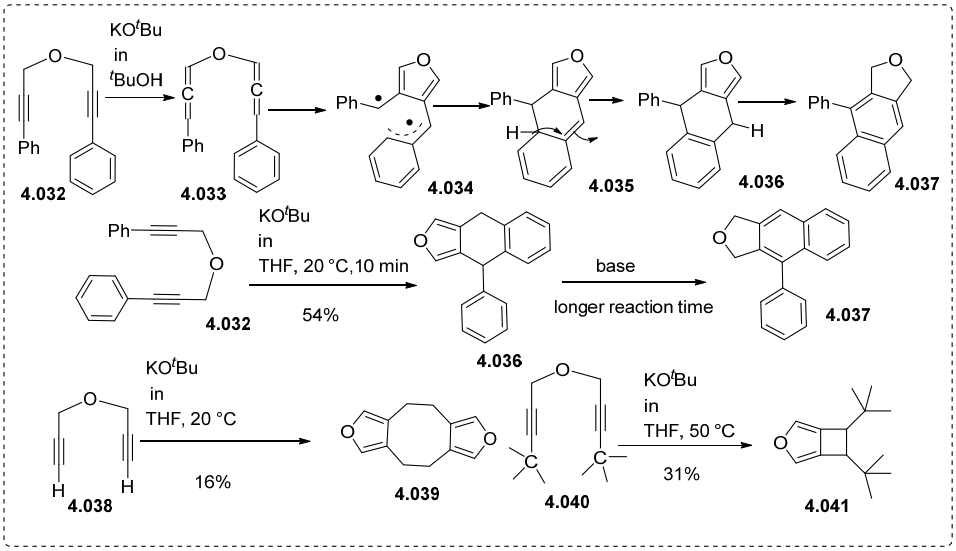

Scheme 4.06: Base mediated rearrangement of bis-propargyl ethers proposed by Garratt *et al*.

In 1990 Braverman and his co-workers reported the formation of 3-isopropenyl-4-isopropylfuran **4.045** upon treatment of ether **4.042** with MeLi at -35 °C (**Scheme 4.07**).[34] The reaction proceeded *via* 1,5-H shift of the intermediate bis(*γ*,*γ*-dimethylallenyl) ether which they were unable to isolate.

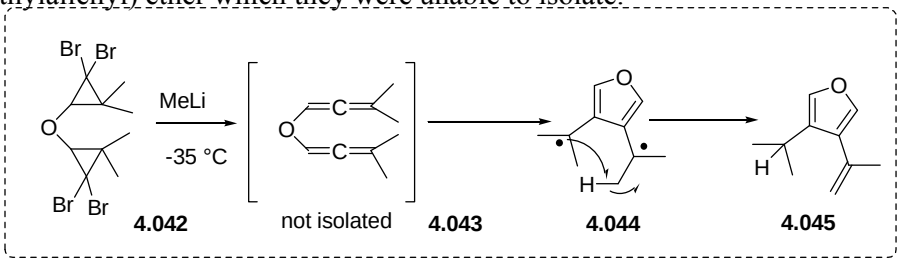

Scheme 4.07: 1,5-H shift pathway for bis-allenic ether as proposed by Braverman *et al*.

For classical synthesis of 3,4-disubstituted furans the process starts generally with the preparation of 3,4-bis(tri butylstanny1)furan **4.048** *via* Diels Alder reaction of an oxazole **4.047** and alkyne **4.046**. It was then converted into different derivatives *via* Pd catalyzed Stille reaction. In 1992 Wong *et al*. reported the synthesis of various 3,4-disubstituted furans using **4.048** as a starting material although the reaction suffered from low yield of initial cycloaddition product (**Scheme 4.08**).[83]

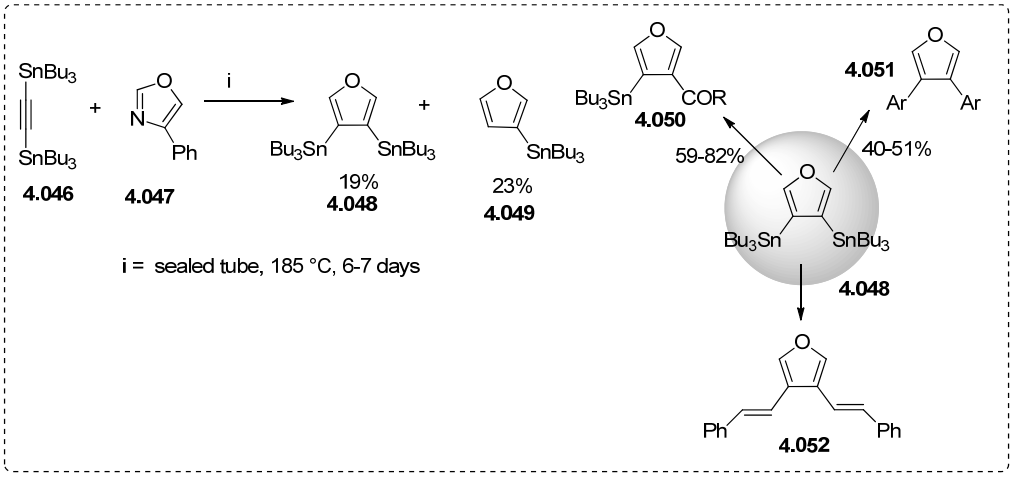

Scheme 4.08: Synthesis of 3,4-disubstituted furans as proposed by Wong *et al*.

In 2007 Kudoh *et al.* reported the formation of 3,4-disubstituted furans as a minor product (**Scheme 4.09**) during anionic intramolecular Diels Alder reaction of 4-oxahepta-1,6-diynes **4.001 a**, **4.053** having a benzene ring and an aliphatic substituent appended at the acetylenic terminus.[38] The major product was the cycloadduct in each individual cases along with the furan derivatives as a minor by product.

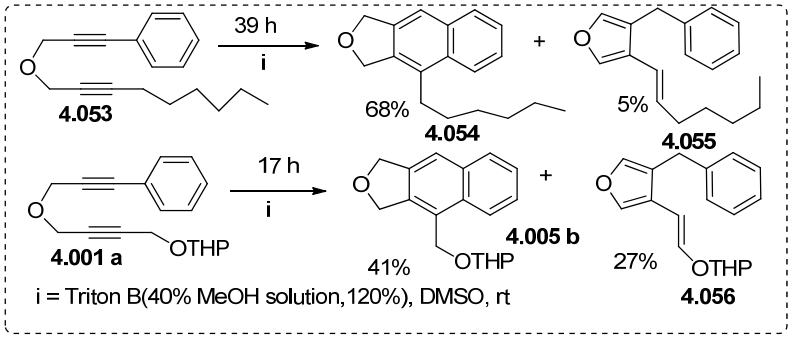

Scheme 4.09: Anionic IMDAR of 1-Phenyl-6-alkyl-4-oxahepta-1,6-diynes

4.4 Results and Discussion

4.4 A. Synthesis of Bis-propargyl ether derivatives 4.062 A-E

The synthesis of bis-propargyl ethers **4.062 A-E** started with selective mono-THP protection of 2-butyne-1,4-diol **4.057**. The reaction was carried out in presence of 0.5 equiv of DHP and catalytic amount of PPTS. The resulting partially protected alcohol **4.058** was O-alkylated with various aryl propargyl bromides **4.061 A-E** in presence of NaH in dry DMF. The bromides were obtained from the corresponding alcohol **4.060 A-E** which in turn were prepared *via* Sonogashira coupling from the aryl iodides **4.059 A-E** under standard Pd(0) mediated conditions. The synthetic protocol is shown in **Scheme 4.10**.

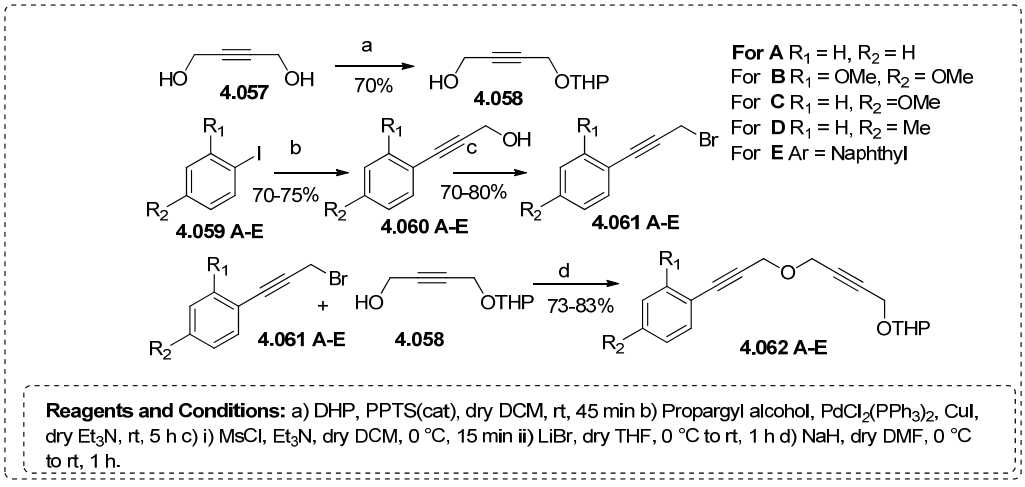

Scheme 4.10: Synthesis of target bis-propargyl ethers

4.4 B. Synthesis of Bis-propargyl ether derivative 4.062 F

The unsymmetrical bis-propargyl ether 2-((4-(prop-2-yn-1-yloxy)but-2-yn-1yl)oxy)tetrahydro-2*H*-pyran **4.064** was synthesized by following the similar multistep protocol starting from mono-THP protected butyne-1,4-diol and propargyl bromide **4.063**. The alkyne was then made to undergo Sonogashira coupling with vinyl bromide under degassed condition to obtain the enyne derivative **4.062 F** (**Scheme 4.11**). The self-coupling of the alkyne was suppressed by carefully maintaining an inert atmosphere throughout the reaction.

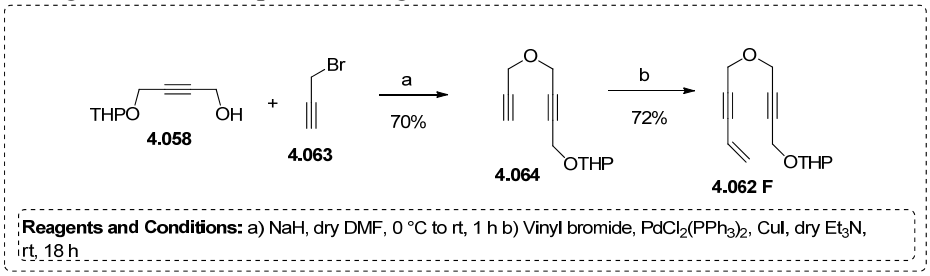

Scheme 4.11: Synthesis of target bis-propargyl ethers

4.4 C. Synthesis of Bis-propargyl ether derivative 4.066

The synthesis started with the formation of bis-propargyl ether derivative **4.062 A** and subsequent deprotection of alcohol with catalytic amount of PPTS in ethanol at 40 °C to the bis-propargyl alcohol **4.065**. It was then treated with NaH to get the alkoxide followed by ethyl iodide that successfully led to the formation of bis-propargyl ether analogue **4.066** (**Scheme 4.12**).

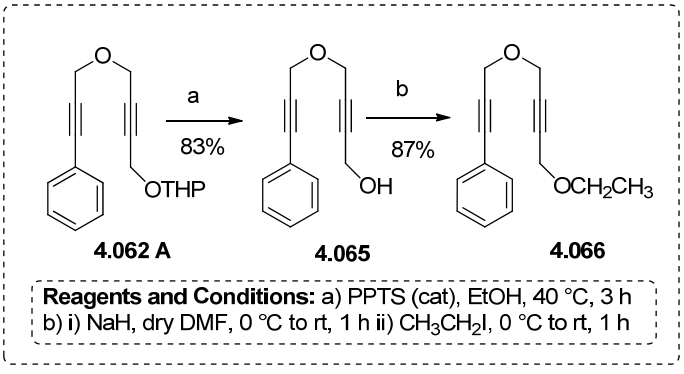

Scheme 4.12: Synthesis of target bis-propargyl ethers

4.4 D. Synthesis of Bis-propargyl ether derivative 4.068

The bis-propargyl ether with methyl group attached in one acetylenic termini was prepared by following the same Williamson ether synthesis protocol (**Scheme**

4.13) starting from 3-phenyl propargyl bromide **4.061 A** and commercially available but-2-yn-1-ol **4.067**.

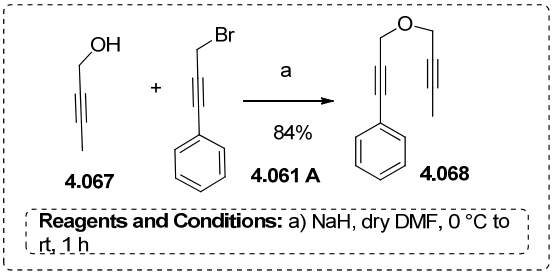

Scheme 4.13: Synthesis of target bis-propargyl ethers

4.4 E. Base mediated rearrangement of bis-propargyl ethers 4.062 A-F, 4.066, 4.068

After successfully synthesizing the bis-propargyl ethers appended with various aliphatic moieties and an aromatic ring we proceeded to determine their reactivity profile under basic condition. Unlike the bis-propargyl sulfones which require stirring with Et_3N as base[39], the rearrangement of bis-propargyl ethers was achieved by treating a DMSO solution of ethers with 1.2 equiv of KO^{t}Bu at room temperature for 1 h (**Scheme 4.14**). The reaction was then quenched with NH_4Cl and the crude products were extracted in ethyl acetate. The ratio of GB cyclized products and 3,4-disubstituted furans from 1,5-H shift pathway was determined by analyzing the integration values of the corresponding peaks in ^{1}H-NMR spectrum of crude reaction mixture. The products were then purified by column chromatographic separation and the structure of the compounds was determined by NMR and HRMS analysis. A representative stacked spectrum of ^{1}H NMR of one of the bis-propargyl precursors and 3,4-disubstituted furans is shown in **Figure 4.03**.

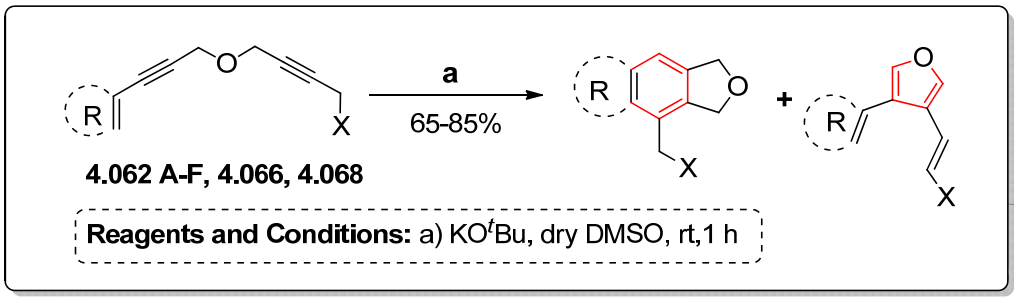

Scheme 4.14: Base mediated rearrangement of bis-propargyl ethers

The results of GBC and 1,5-H shift are compiled in **Figure 4.04**.

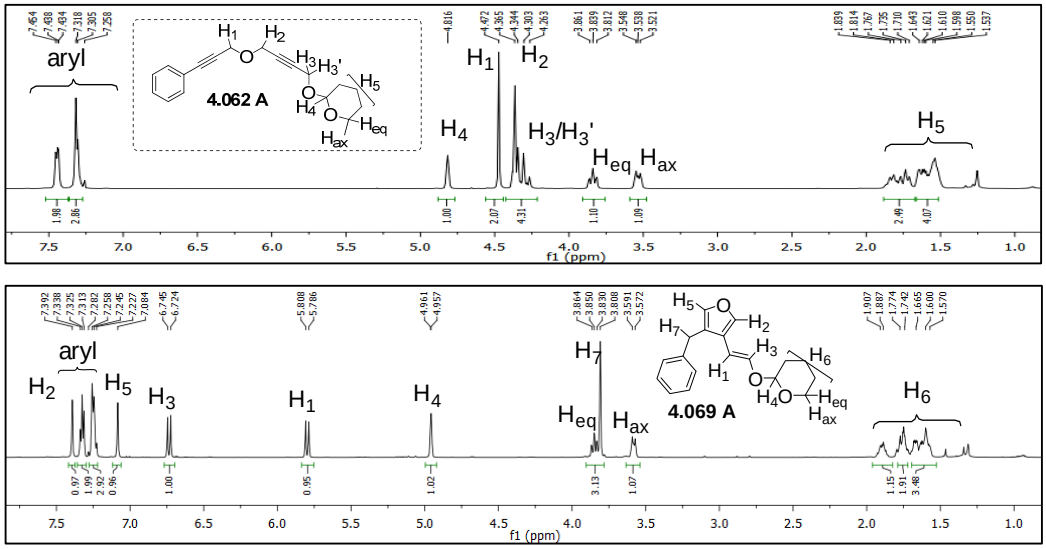

Figure 4.03: Comparative ^{1}H NMR spectra of bis-propargyl precursor **4.062 A** (400 MHz) and 1,5-H shift product **4.069 A** (600 MHz)

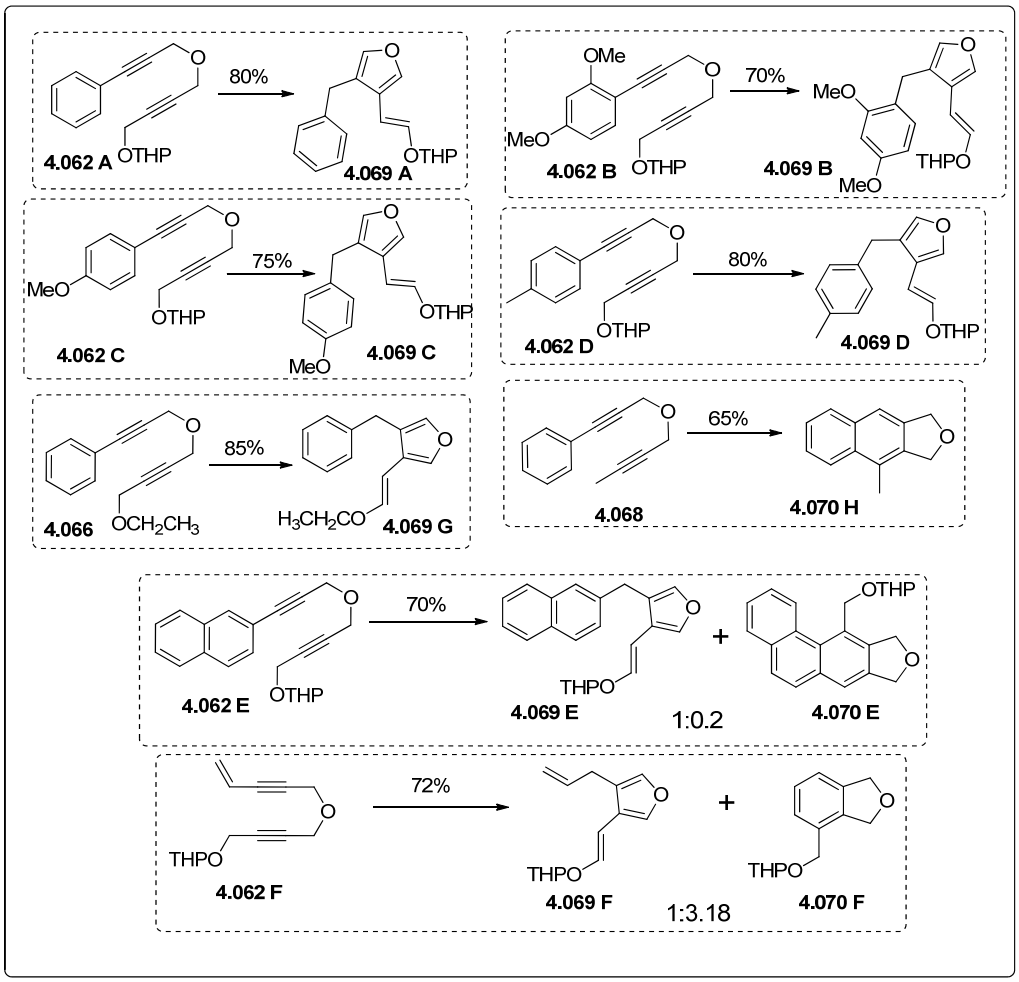

Figure 4.04: Results of base treatment of various bis-propargyl ethers

4.4 F. Explanation of Product Distribution

There are several interesting aspects associated with the results of base mediated rearrangement of bis-propargyl ethers to reach aryl naphthalene products or 3,4-disubstituted furans *via* GBC or 1,5-H shift pathway respectively. The explanations here are given based on diradical formation of bis-propargyl ethers (**Scheme 4.15**). In case of phenyl or substituted phenyl the reaction led to exclusive formation of 1,5-H shift product **4.069 A-D**, **4.069 G**. The presence of ethereal oxygen played the main role here by stabilizing the adjacent carbon radical. For bis-propargyl ether analogue **4.068**, replacing the ethereal moiety with methyl substitution forced the reaction entirely to follow GBC pathway to **4.070 H**. The higher loss of aromaticity/delocalization energy during GBC was also reflected from the formation of both GB and 1,5-H shift products from naphthyl and vinyl analogues of bis-propargyl ether **4.062 E** and **4.062 F**. As naphthalene has lower aromatic stabilization energy than phenyl, substitution of phenyl ring with naphthalene led to the formation of GB cyclized product **4.070 E** in a minor ratio (1:0.2; 1,5-H shift vs GB). For vinyl system **4.062 F**, no such issue of loss of aromaticity arises and the major product turned out to be from GBC **4.070 F** (3.18:1; 1,5-H shift vs GB). This phenomenon also validates our assertion that lesser sacrifice of aromaticity during self-quenching of diradical *via* GB pathway may allow the GB product to be formed.

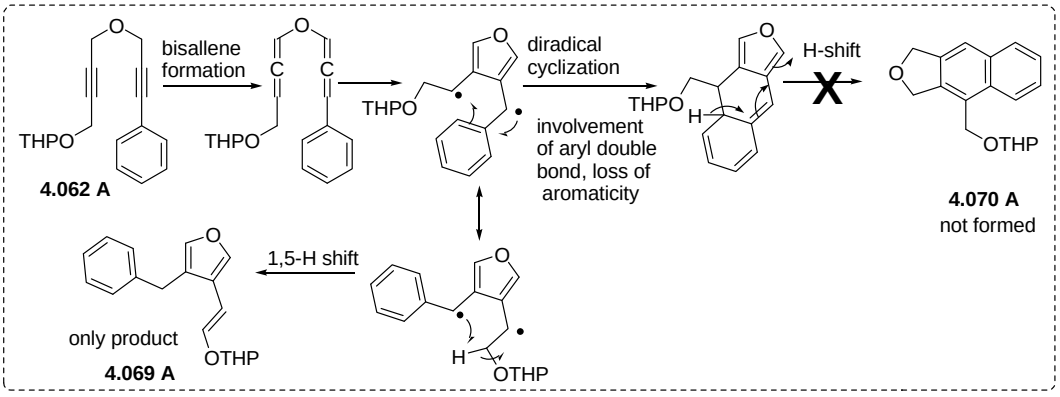

Scheme 4.15: Radical mechanism of 1,5-H shift and GB cyclization of bis-propargyl ether precursors

4.4 G. Equilibration of vinyl ethers; *E* to *Z* isomerization

The geometry of the double bond of 3,4-disubstituted furans were confirmed to be *E* (trans) from the coupling constant value of vinyl hydrogens H_6 and H_7 and it appeared to be 12.6 Hz. During chromatographic purification of 2,4-dimethoxy

phenyl substituted furan derivative **4.069 B** the ^{1}H-NMR of the crude product did not match the spectrum obtained after purification of the compound (**Figure 4.05**).

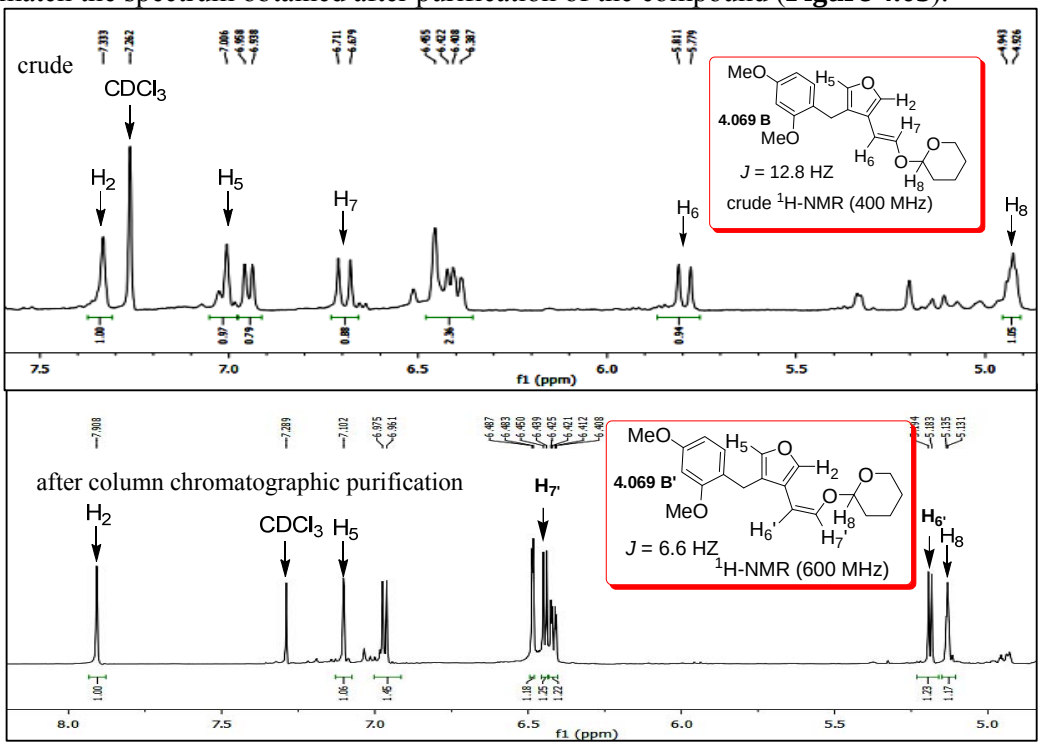

Figure 4.05: Representative ^{1}H-NMR spectra of trans and cis 1,5-H shift product

A thorough analysis of the ^{1}H-NMR spectrum revealed that the product isolated after purification was the *Z* (cis) isomer of the vinyl ether and the coupling constant value of vinyl hydrogens $H_{6'}$ and $H_{7'}$ was calculated to be 6.6 Hz with an upfield shift of δ value. To further generalize the fact, one of the vinyl ether analogues with unsubstituted furan ring **4.069 A** was kept in $CDCl_3$ and the *E* to *Z* isomerization was monitored by ^{1}H-NMR spectroscopy (**Figure 4.06**). The isomerization took 5-6 days for completion. The spectrum is attached below for better clarification.

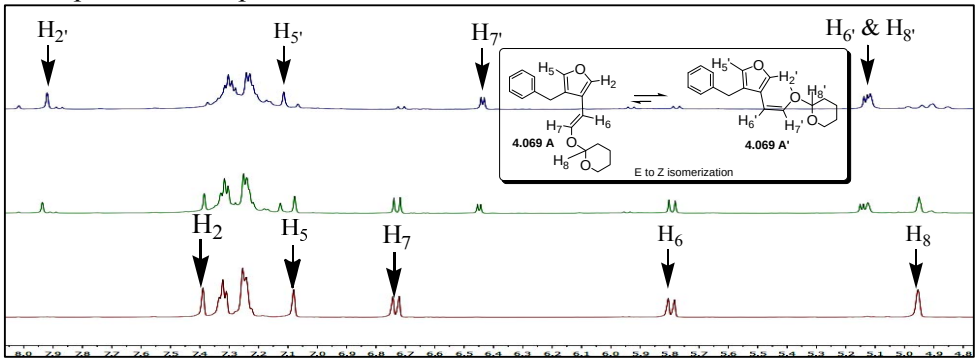

Figure 4.06: Equilibration between *E* and *Z* isomers monitored by ^{1}H NMR (600 MHz)

As, the furans synthesized were liquid in nature the assignment of ^{1}H-NMR signals were carried out mainly by observing the through space interactions of protons by recording the NOESY spectrum of the corresponding compounds and the same has been described later. This type of unusual *E* to *Z* isomerization at room temperature indicated higher stability of *Z* isomer and we then were curious to decipher it. In a recent JOC paper of 2014, Schmittel *et al*. reported the formation of both *E* and *Z* isomers **4.074** and **4.073** of 1,5-H shift product from thermolysis of ene-diallene **4.071** (**Scheme 4.16**) experimentally as well as by theoretical calculations.[79b]

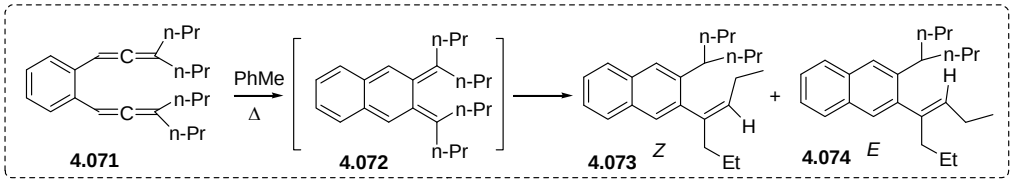

Scheme 4.16: Thermolysis of ene-diallene no producing *E* and *Z* as proposed by Schmittel *et al*.

In 2006 Sander and his co-workers reported an *ab initio* and matrix isolation study of furan-formic acid dimers.[84] Their model compounds had H-bonding interaction involving furan H-2 and formic acid oxygen. Based on these references we then proposed an intramolecular C-H···O hydrogen bond involving the furan H-2 and oxygen of vinyl ether functionality that gave the extra stability to the *Z* form and the probable cause of rapid equilibration of *E* to *Z* configuration. We also have done energy minimization of the two isomers that too pointed out the presence of intramolecular H-bond. Our next target was to validate our assumption of intramolecular H-bond involving furan H-2 by any available experimental techniques. Petrova *et al.* in 2011 showed upfield shift of hydrogen in $CDCl_3$ vs d_6-DMSO involved in C-H···O bonding in their study of conformations of 1,4-dihydropyridine derivatives.[85] Thus, ^{1}H-NMR of the two configurations were recorded separately in two different solvent like $CDCl_3$ followed by d_6-DMSO. To our surprise, ^{1}H-NMR taken separately in $CDCl_3$ and then in d_6-DMSO showed a slight upfield shift ($\Delta\delta \approx 0.1$) of the furan H-2 in the *Z*-isomer. On the other hand, all other furan hydrogens (H-2 in *E* isomer and H-5 of both *E* and *Z* isomers) showed a downfield shift of $\Delta\delta > 0.2$, indicating the possibility of involvement of H-2 in the *Z* isomer in intramolecular H-bonding (**Figure 4.07**). Being a polar aprotic solvent, DMSO was able to form intermolecular H-bond with furan hydrogens available except H-2 which was involved in intramolecular H-bond with ethereal oxygen. As a result, H-2 in *E* isomer

and H-5 of both *E* and *Z* isomers of furan ring showed downfield shift in NMR spectrum.

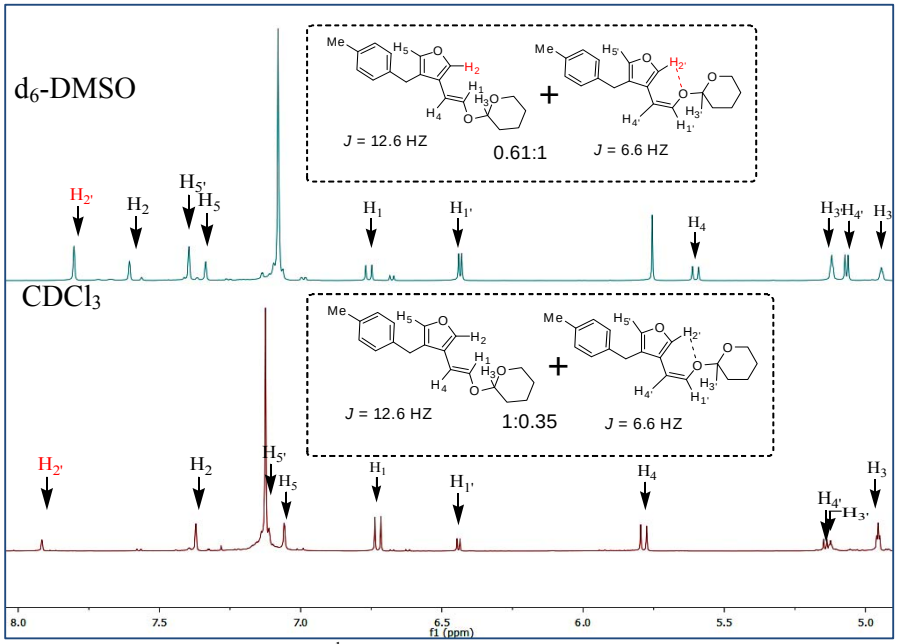

Figure 4.07: Representative ^{1}H-NMR (600 MHz) comparison of **4.069 D** (**E**+**Z**)

4.4 H. Spectral characterizations

The structure of final products *i.e.* 3,4-disubstituted furans was fully characterized with the help of NMR and HRMS analysis. Characteristic features of furan derivatives **4.069 D**, **4.069 E** and GB product **4.070 F** are mentioned below.

In the ^{1}H-NMR spectrum of compound **4.069 D** recorded in 400 MHz NMR in $CDCl_3$, H_a of furan ring appeared as singlet at δ 7.35. The deshielding effect of adjacent vinyl ether functionality made H_a to experience more external magnetic field and as a consequence it was shifted downfield than H_b. All other aromatic hydrogens of *p*-tolyl ring merged as singlet at δ 7.11 due to their equivalent magnetic environment. The H-2 or H_b of furan ring appeared as singlet at δ 7.04. The vinylic hydrogen H_e appeared as doublet at δ 6.71 due to coupling with H_d which appeared slight upfield at δ 5.77 as doublet with J = 12.8 Hz indicating the trans geometry of the compound. The H_e hydrogen experienced electron withdrawing inductive effect of oxygen and shifted downfield whereas H_d experienced electron donating + R effect of oxygen and accordingly shifted upfield in the NMR spectrum. The hydrogen attached to asymmetric centre of tetrahydropyran moiety H_f appeared as broad singlet at δ 4.96. The equatorial proton H_g/H_e appeared as multiplet at δ 3.85 - 3.81 whereas the

axial hydrogen H_g/H_e shifted upfield at δ 3.57-3.55 as it resided in the shielded region of C-C bond anisotropy and appeared as multiplet due to germinal coupling as well as vicinal coupling with H_f and H_j. The benzylic hydrogen H_c appeared as singlet as δ 3.73 and the three methyl protons of tolyl group appeared as singlet as δ 2.33. The rest of the protons of tetrahydropyran moiety H_h, H_i, H_j appeared as multiplet at 1.75 - 1.57. **Figure 4.08** shows the ^{1}H-NMR assignment of 1,5-H shift and GBC product **4.069 D** and **4.070 F**. Mass spectrum of **4.069 D** showed peak at m/z 321.1467 corresponding to $[M+Na]^+$ (calcd mass 321.1462).

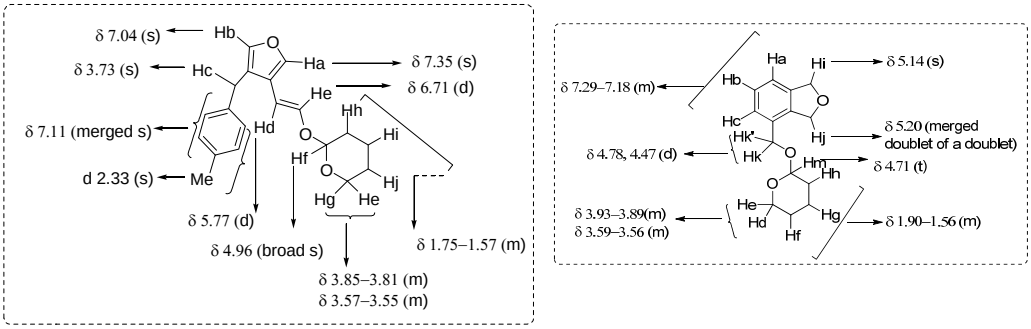

Figure 4.08: ^{1}H-NMR assignment of compound **4.069 D** and **4.070 F**

For the ^{1}H NMR (600 MHz) of compound **4.069 E** in d_6-DMSO the aromatic protons appeared as multiplet in between δ 7.87 - 7.81 and 7.49 - 7.44 whereas H_e appeared as doublet at δ 7.38 with J = 8.4 Hz. The furan hydrogens, H_b came at δ 7.68 and H_a appeared at δ 7.65 as singlet. The downfield appearance of H_b may be associated with the greater intermolecular H bonding of DMSO with H_b compared to H_a. In case of vinylic hydrogens, H_d appeared as doublet at δ 6.77 and H_c came upfield at 5.64 as doublet with J = 12.6 Hz. The benzylic protons appeared at δ 3.92 as singlet and the protons on tetrahydropyran moiety followed the same trend (**Figure 4.10**). The assignment of peaks was further verified by NOESY spectrum analysis (**Figure 4.09**). The peak at 357.1471 in HRMS spectrum corresponded to $[M+Na]^+$ (calcd mass 357.1462) and was in agreement with the structure.

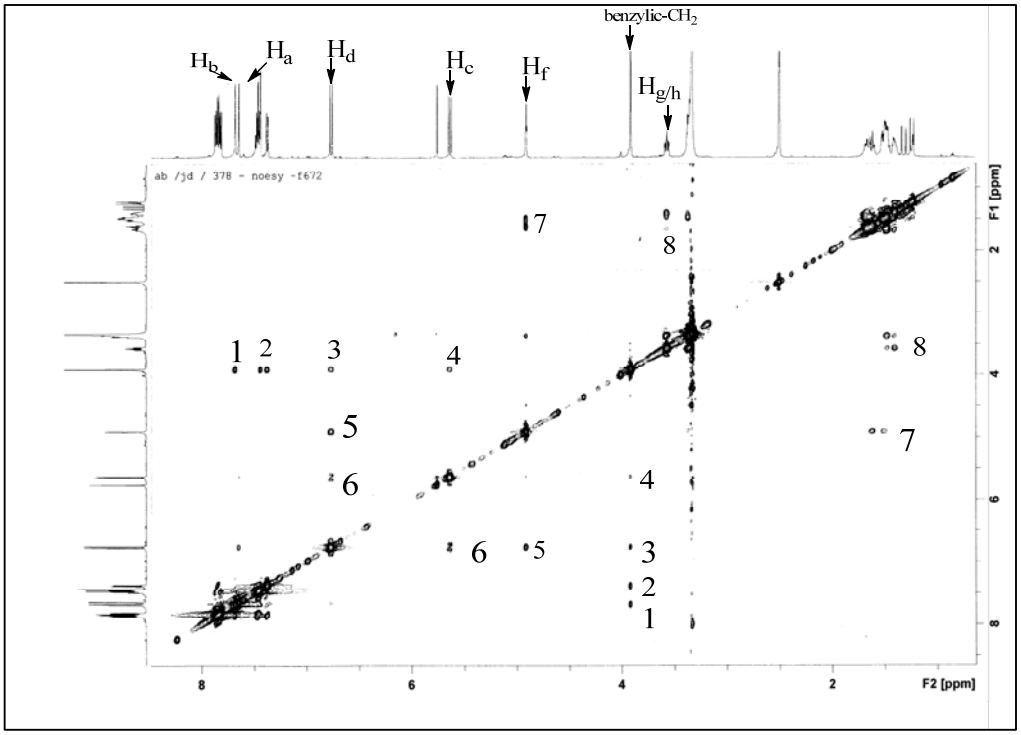

Figure 4.09: NOESY spectrum of compound **4.069 E** [d_6-DMSO, 600 MHz], the cross peaks appeared due to through space interactions are shown by numbers.

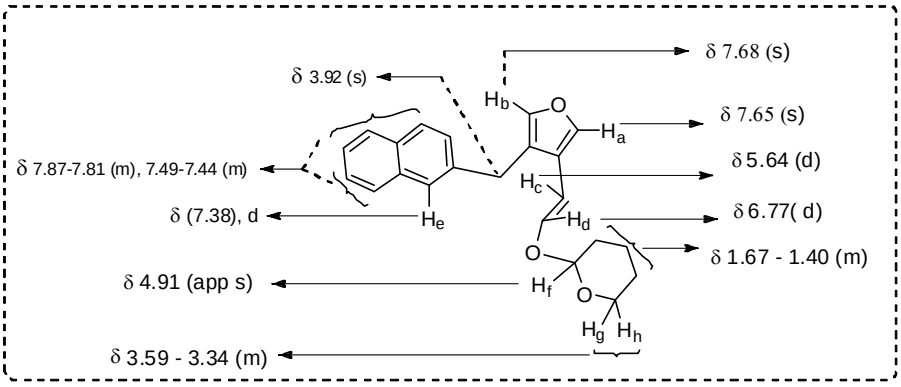

Figure 4.10: ^{1}H-NMR assignment of compound **4.069 E**

The NMR (600 MHz, $CDCl_3$) spectrum of the GB product **4.070 F** (**Figure 4.11**) was compared in details with other similar compounds prepared earlier from our laboratory. In the ^{1}H NMR of **4.070 F** the aromatic hydrogens on aryl ring appeared as multiplet at δ 7.29 - 7.18. The methylene protons H_j came as merged doublet of doublet at δ 5.20 and H_i appeared as singlet at δ 5.14. The two benzylic protons H_k and $H_{k'}$ appeared as doublet at δ 4.78 and 4.47 with J = 12.6 Hz. The proton attached

to the asymmetric carbon of tetrahydropyran moiety H_m appeared as triplet at δ 4.71 with J = 3.0 Hz and H_e and H_d appeared at 3.93 - 3.89 (equatorial) and 3.59-3.56 (axial) as multiplet. The rest of protons H_h, H_g, H_f appeared at δ 1.9-1.56 as multiplet. The compound **4.070 F** showed peak at m/z 257.1154 in the mass spectra corresponding to $[M+Na]^+$ (calcd mass 257.1149).

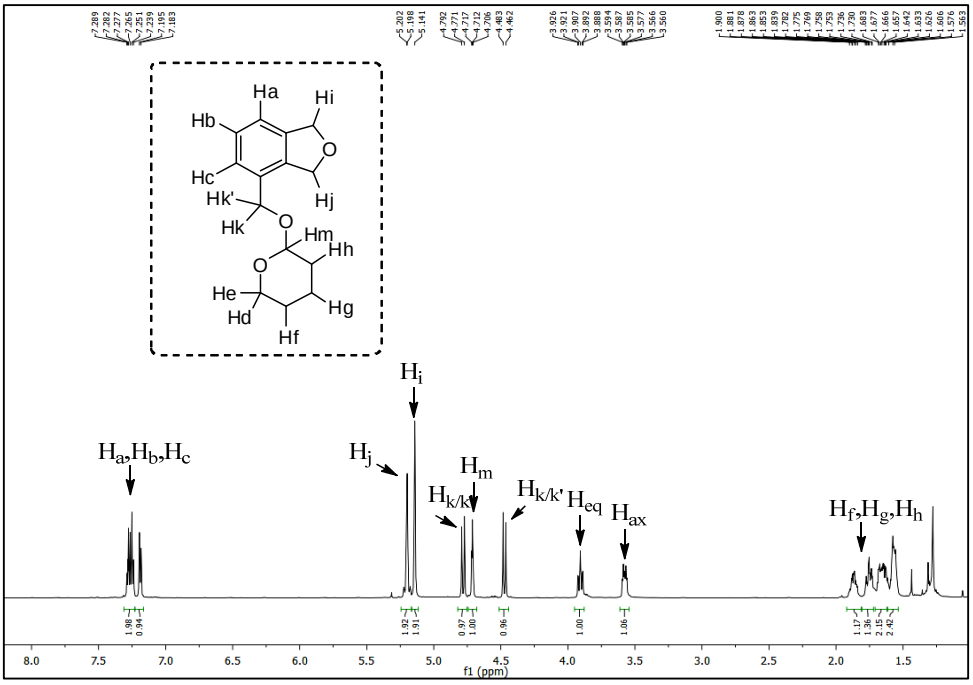

Figure 4.11: ^{1}H-NMR spectrum of compound **4.070 F**

Structure assignments of all other furan derivatives and GBC products were done similarly as described earlier. All the structures were in good agreement with the NMR and mass spectral data.

4.5 Conclusion

- We have been successful in shifting the reactivity towards 1,5 H-shift mode from the usual GB pathway for bis-propargyl ethers.
- The parameters controlling the reactivity have been identified.

- We have been able to synthesize 3,4-disubstituted furans whose synthetic utility will be explored in future along with a more elaborate study on *E* to *Z* isomerization.

4.6 Experimental details

4.6.1 General experimental

General experimental procedures are same as described at page no. 59 in Chapter 2.

4.6.2 General procedure for synthesis of compounds and their spectral data

General procedure for O-propargylation: Synthesis of compounds (4.062 A-E, 4.064, 4.066, 4.068)

The procedure is same as described at page no. 61 in Chapter 2.

Preparation of (4.062 F) *via* Sonogashira Coupling

To a solution of vinyl bromide (4 equiv) and **4.064** (1 mmol) in dry degassed Et_3N (10 mL), $PdCl_2(PPh_3)_2$ (3 mol %) and CuI (20 mol %) were added sequentially under inert atmosphere and the mixture was allowed to stir at room temperature for 18 h. The mixture was then extracted with ethyl acetate and the organic layer was washed with saturated solution of NH_4Cl and brine. The ethyl acetate layer was then dried over anhydrous sodium sulfate, evaporated and the purified product was obtained *via* column chromatography by using hexane-ethyl acetate as eluent.

2-[4-(3-Phenyl-prop-2-ynyloxy)-but-2-ynyloxy]-tetrahydro-pyran (4.062 A)

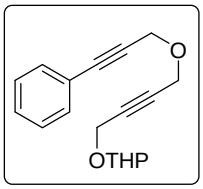

State: yellow oil; **yield**: 227 mg, 80%; IR (neat) ν_{max} 2927, 2855, 2230, 1611, 1575, 1503, 1210, 1024, 752 cm^{-1}; ^1H NMR (400 MHz, Chloroform-*d*) δ 7.45 - 7.43 (m, 2H), 7.32 - 7.26 (m, 3H), 4.82 (bs, 1H), 4.47 (s, 2H), 4.36 (s, 2H), 4.36 - 4.26 (m, 2H), 3.86 - 3.81 (m, 1H), 3.55 - 3.52 (m, 1H), 1.84 - 1.54 (m, 6H); ^{13}C NMR (50 MHz, Chloroform-*d*) δ 131.8, 128.5, 128.3, 122.5, 96.8, 86.8, 84.3, 83.0, 81.3, 62.0, 57.3, 56.9, 54.3, 30.2, 25.4, 19.0; HRMS: Calcd. for $C_{18}H_{21}O_3^+$ $[M+H]^+$ 285.1491 found 285.1494.

2-{4-[3-(2,4-Dimethoxy-phenyl)-prop-2-ynyloxy]-but-2-ynyloxy}-tetrahydro-pyran (4.062 B)

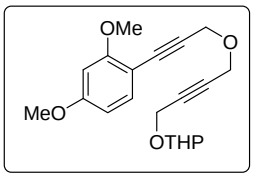

State: yellow oil; **yield**: 265 mg, 77%; IR (neat) ν_{max} 2934, 2876, 2231, 1623, 1564, 1034, 750 cm^{-1}; ^{1}H NMR (400 MHz, Chloroform-*d*) δ 7.32 (d, *J* = 8.0 Hz, 1H), 6.43 - 6.41 (m, 2H), 4.81 (t, *J* = 3.2 Hz, 1H), 4.49 (s, 2H), 4.36 (s, 2H), 4.32 - 4.25 (m, 2H), 3.83 (s, 3H), 3.81 (s, 3H), 3.86 - 3.79 (m, 1H), 3.54 - 3.51 (m, 1H), 1.83 - 1.52 (m, 6H); ^{13}C NMR (50 MHz, Chloroform-*d*) δ 161.6, 161.5, 134.8, 104.9, 104.3, 98.5, 97.0, 87.0, 83.3, 82.9, 81.7, 62.2, 57.9, 56.9, 55.9, 55.6, 54.5, 30.4, 25.5, 19.2; HRMS: Calcd. for $C_{20}H_{25}O_5^+$ $[M+H]^+$ 345.1702 found 345.1705.

2-{4-[3-(4-Methoxy-phenyl)-prop-2-ynyloxy]-but-2-ynyloxy}-tetrahydro-pyran (4.062 C)

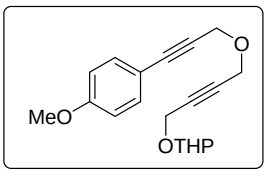

State: yellow oil; **yield**: 235 mg, 75%; IR (neat) ν_{max} 2977, 2875, 1576, 2231, 1613, 1045, 754 cm^{-1}; ^{1}H NMR (400 MHz, Chloroform-*d*) δ 7.37 (d, *J* = 8.8 Hz, 2H), 6.82 (d, *J* = 8.8 Hz, 2H), 4.81 (t, *J* = 3.6 Hz, 1H), 4.45 - 4.25 (m, 6H), 3.86 - 3.79 (m, 4H), 3.54 - 3.50 (m, 1H), 1.83 - 1.51 (m, 6H); ^{13}C NMR (50 MHz, Chloroform-*d*) δ 159.8, 133.3, 114.5, 113.9, 96.8, 86.8, 82.9, 82.8, 81.3, 61.9, 57.4, 56.8, 55.2, 54.2, 30.2, 25.3, 19.0; HRMS: Calcd. for $C_{19}H_{23}O_4^+$ $[M+H]^+$ 315.1596 found 315.1597.

2-[4-(3-*p*-Tolyl-prop-2-ynyloxy)-but-2-ynyloxy]-tetrahydro-pyran (4.062 D)

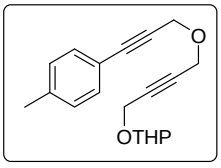

State: yellow oil; **yield**: 247 mg, 83%; IR (neat) ν_{max} 3100, 2855, 1564, 2231, 1632, 1025, 765 cm^{-1}; ^{1}H NMR (400 MHz, Chloroform-*d*) δ 7.29 (d, *J* = 7.2 Hz, 2H), 7.05 (d, *J* = 6.8 Hz, 2H), 4.77 (bs, 1H), 4.40 (s, 2H), 4.30 (s, 2H), 4.30 - 4.21 (m, 2H), 3.78 - 3.76 (m, 1H), 3.49 - 3.47 (m, 1H), 2.28 (s, 3H), 1.77 - 1.48 (m, 6H); ^{13}C NMR (100 MHz, Chloroform-*d*) δ 138.8, 131.9, 129.2, 119.6, 97.0, 87.1, 83.8, 83.2, 81.5, 62.1, 57.5, 57.0, 54.4, 30.4, 25.6, 21.6, 19.2; HRMS: Calcd. for $C_{19}H_{23}O_3^+$ $[M+H]^+$ 299.1647 found 299.1643.

2-[4-(3-Naphthalen-2-yl-prop-2-ynyloxy)-but-2-ynyloxy]-tetrahydro-pyran (4.062 E)

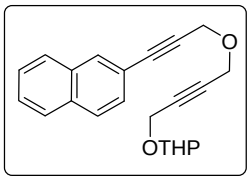

State: yellow oil; **yield**: 243 mg, 73%; IR (neat) ν_{max} 3123, 2937, 2876, 2234, 1506, 1617, 1027, 765 cm^{-1}; ^{1}H NMR (600 MHz, Chloroform-*d*) δ 8.00 (s, 1H), 7.83 - 7.79 (m, 3H), 7.52 - 7.49 (m, 3H), 4.86 (t, *J* = 3.6 Hz, 1H), 4.55 (s, 2H), 4.44 (s, 2H), 4.43 - 4.31 (m, 2H), 3.89 - 3.85 (m, 1H), 3.58 - 3.55 (m, 1H), 1.88 - 1.56 (m, 6H); ^{13}C NMR (50 MHz, Chloroform-*d*) δ 133.0, 132.9, 131.9, 128.5, 128.1, 127.9, 126.9, 126.7, 119.8, 97.0, 87.2, 84.7, 83.2, 81.4, 62.1, 57.5, 57.1, 54.4, 30.3, 25.5, 19.2; HRMS: Calcd. for $C_{22}H_{23}O_3^+$ $[M+H]^+$ 335.1647 found 335.1647.

2-(4-Pent-4-en-2-ynyloxy)-but-2-ynyloxy]-tetrahydro-pyran (4.062 F)

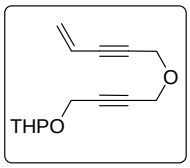

State: yellow oil; **yield**: 168 mg, 72%; IR (neat) ν_{max} 2937, 2876, 2234, 1523, 1623, 1025, 745 cm^{-1}; ^{1}H NMR (400 MHz, Chloroform-*d*) δ 5.83 (dd, *J* = 11.8 Hz, 7.2 Hz, 1H), 5.68 (dd, *J* = 11.8 Hz, 1.2 Hz, 1H), 5.52 (dd, *J* = 7.4 Hz, 1.2 Hz, 1H), 4.82 (t, *J* = 2.0 Hz, 1H), 4.38 (s, 2H), 4.37 - 4.27 (m, 4H), 3.87 - 3.83 (m, 1H), 3.57 - 3.53(m, 1H), 1.88 - 1.55 (m, 6H); ^{13}C NMR (50 MHz, Chloroform-*d*) δ 127.8, 116.6, 97.0, 85.5, 85.0, 83.1, 81.3, 62.1, 57.3, 57.0, 54.4, 30.3, 25.5, 19.1; HRMS: Calcd. for $C_{14}H_{19}O_3^+$ $[M+H]^+$ 235.1334 found 235.1332.

[3-(4-Ethoxy-but-2ynyloxy)-prop-1-ynyl]-benzene (4.066)

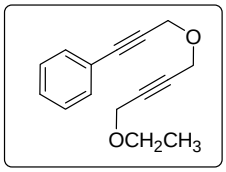

State: yellow oil; **yield**: 198 mg, 87%; IR (neat) ν_{max} 3069, 2985, 2852, 2251, 1731, 1604, 1495, 1088, 887, 761, 694 cm^{-1}; ^{1}H NMR (400 MHz, Chloroform-*d*) δ 7.45 (m, 2H), 7.32 - 7.31 (bm, 3H), 4.47 (s, 2H), 4.36 (s, 2H), 4.20 (s, 2H), 3.57 (dd, *J* = 7.2 Hz, 6.8 Hz, 2H), 1.23 (appt, *J* = 7.2 Hz, 3H); ^{13}C NMR (50 MHz, Chloroform-*d*) δ 131.8, 128.5, 128.3, 122.5, 86.8, 84.3, 83.2, 81.3, 65.5, 58.0, 57.3, 56.9, 15.0; HRMS: Calcd. for $C_{15}H_{17}O_2^+$ $[M+H]^+$ 229.1229 found 229.1223.

(3-But-2-ynyloxy-prop-1-ynyl)-benzene (4.068)

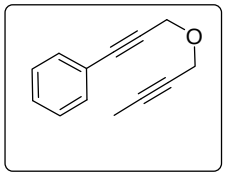

State: yellow oil; **yield**: 154 mg, 84%; IR (neat) ν_{max} 3066, 2960, 2932, 2859, 2230, 1963, 1611, 1499, 1362, 1132, 926, 894, 764, 698 cm^{-1}; ^{1}H NMR (400 MHz, Chloroform-*d*) δ 7.46 - 7.45 (bm,

2H), 7.32 - 7.31 (bm, 3H), 4.46 (s, 2H), 4.28 (apps, 2H), 1.88 (s, 3H); ^{13}C NMR (50 MHz, Chloroform-*d*) δ 131.8, 128.5, 128.3, 122.6, 86.5, 84.6, 83.2, 74.5, 57.2, 57.1, 3.6; HRMS: Calcd. for $C_{13}H_{13}O^+$ $[M+H]^+$ 185.0966 found 185.0965.

General procedure for furan ring formation: Synthesis of compounds (4.069 A-G, 4.070 E, 4.070 F, 4.070 H)

The procedure is same as described at page no. 65 in Chapter 2.

2-[2-(4-Benzyl-furan-3-yl)-vinyloxy]-tetrahydro-pyran (4.069 A)

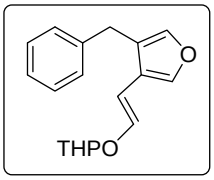

State: yellow oil; **yield**: 45 mg, 80%; IR (neat) ν_{max} 2954, 2874, 2857, 1660, 1530, 1234, 1178, 1050, 767 cm^{-1}; ^{1}H NMR (600 MHz, Chloroform-*d*) δ 7.39 (s, 1H), 7.34 - 7.31 (m, 2H), 7.28 - 7.23 (m, 3H), 7.08 (s, 1H), 6.73 (d, *J* = 12.6 Hz, 1H), 5.80 (d, *J* = 13.2 Hz, 1H), 4.96 (app s, 1H), 3.86 - 3.83 (m, 1H), 3.81 (s, 2H), 3.59 - 3.57 (m, 1H), 1.90 - 1.57 (m, 6H); ^{13}C NMR (150 MHz, Chloroform-*d*) δ 144.5, 141.0, 139.7, 138.4, 128.6, 128.4, 126.1, 123.1, 121.1, 98.7, 98.4, 62.0, 30.3, 29.6, 25.1, 18.6; HRMS: Calcd. for $C_{18}H_{21}O_3^+$ $[M+H]^+$ 285.1491 found 285.1495.

2-{2-[4-(2,4-Dimethoxy-benzyl)-furan-3-yl]-vinyloxy}-tetrahydro-pyran (4.069 B)

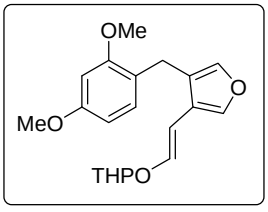

State: yellow oil; **yield**: 48 mg, 70%; IR (neat) ν_{max} 2989, 2945, 2867, 1664, 1567, 1357, 1209, 1098, 756 cm^{-1}; ^{1}H NMR (600 MHz, Chloroform-*d*) δ 7.90 (s, 1H), 7.10 (s, 1H), 6.97 (d, *J* =8.4 Hz, 1H), 6.49 (d, *J* = 2.4 Hz, 1H), 6.44 (d, *J* = 6.6 Hz, 1H), 6.42 (dd, *J* = 7.8 Hz, 2.4 Hz, 1H), 5.19 (d, *J* = 6.6 Hz, 1H), 5.13 (app t, *J* = 2.4 Hz, 1H), 3.84 (s, 3H), 3.81 (s, 3H), 3.70 (s, 2H), 3.71 - 3.70 (m, 1H), 3.62 - 3.60 (m, 1H), 1.95 - 1.69 (m, 6H); ^{13}C NMR (150 MHz, Chloroform-*d*) δ 159.3, 157.9, 142.5, 142.0, 139.7, 129.9, 122.4, 120.8, 119.6, 103.8, 98.8, 98.3, 96.2, 61.6, 55.4, 55.3, 29.6, 25.1, 22.7, 18.6; HRMS: Calcd. for $C_{20}H_{24}NaO_5^+$ $[M+Na]^+$ 367.1521 found 367.1541.

2-{4-[3-(4-Methoxy-phenyl)-prop-2-ynyloxy]-but-2-ynyloxy}-tetrahydro-pyran (4.069 C)

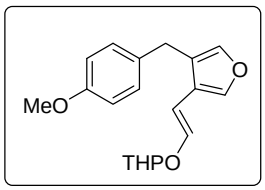

State: yellow oil; **yield**: 47 mg, 75%; IR (neat) ν_{max}. 2954, 2876, 1667, 1530, 1359, 1213, 1095, 789 cm^{-1}; ^{1}H NMR (400 MHz, Chloroform-*d*) δ 7.34 (s, 1H), 7.12 (d, *J* = 8.0 Hz, 2H), 7.02 (s, 1H), 6.83 (d, *J* = 8.0 Hz, 2H), 6.70 (d, *J* = 12.8 Hz, 1H), 5.75 (d, *J* = 12.8 Hz, 1H), 4.93 (app s, 1H), 3.84 - 3.82 (m, 1H), 3.79 (s, 3H), 3.70 (s, 2H), 3.56 - 3.54 (m, 1H), 1.87 - 1.53 (m, 6H); ^{13}C NMR (100 MHz, Chloroform-*d*) δ 158.0, 144.4, 140.9, 138.4, 131.7, 129.5, 123.6, 121.0, 113.8, 98.8, 98.4, 62.0, 55.2, 29.6, 29.5, 25.1, 18.6; HRMS: Calcd. for $C_{19}H_{23}O_4^+$ $[M+H]^+$ 315.1596 found 315.1591.

2-{2-[4-(4-Methyl-benzyl)-furan-3-yl]-vinyloxy}-tetrahydro-pyran (4.069 D)

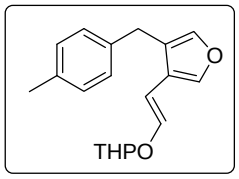

State: yellow oil; **yield:** 47 mg, 80%; IR (neat) ν_{max} 2948, 2929, 2876, 2854, 1664, 1520, 1464, 1357, 1206, 1169, 1090, 786, 745 cm^{-1}; ^{1}H NMR (400 MHz, Chloroform-*d*) δ 7.35 (s, 1H), 7.11 (s, 4H), 7.04 (s, 1H), 6.71 (d, *J* = 12.8 Hz, 1H), 5.77 (d, *J* = 12.8 Hz, 1H), 4.96 (app s, 1H), 3.85 - 3.81 (m, 1H), 3.73 (s, 2H), 3.57 - 3.55 (m, 1H), 2.33 (s, 3H), 1.75 - 1.57 (m, 6H); ^{13}C NMR (100 MHz, Chloroform-*d*) δ 144.6, 141.1, 138.5, 136.8, 135.8, 129.3, 128.7, 123.6, 121.2, 99.0, 98.6, 62.2, 30.1, 29.9, 25.3, 21.2, 18.8; HRMS: Calcd. for $C_{19}H_{22}NaO_3^+$ $[M+Na]^+$ 321.1467 found 321.1467.

2-[2-(4-Naphthalen-2-ylmethyl-furan-3-yl)-vinyloxy]-tetrahydro-pyran (4.069 E)

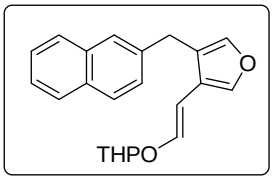

State: yellow oil; **yield:** 39 mg, 58%; IR (neat) ν_{max}.2950, 2786, 1669, 1465, 1208, 1178, 1098, 745 cm^{-1}; ^{1}H NMR (600 MHz, DMSO-d_6) δ 7.87 - 7.81 (m, 3H), 7.68 (s, 1H), 7.65 (s, 1H), 7.49 - 7.44 (m, 3H), 7.38 (d, *J* = 8.4 Hz, 1H), 6.77 (d, *J* = 12.6 Hz, 1H), 5.64 (d, *J* = 12.6 Hz, 1H), 4.91 (app s, 1H), 3.92 (s, 2H), 3.59 - 3.55 (m, 1H), 3.38 - 3.34 (m, 1H), 1.67 - 1.40 (m, 6H); ^{13}C NMR (150 MHz, Chloroform-*d*) δ 144.5, 141.1, 138.4, 137.2, 133.6, 132.2, 128.0, 127.6, 127.3, 126.8, 125.9, 125.3, 123.0, 121.1, 98.7, 98.3, 61.9, 30.5, 29.6, 25.0, 18.6; HRMS: Calcd. for $C_{22}H_{22}NaO_3^+$ $[M+Na]^+$ 357.1467 found 357.1471.

7-((tetrahydro-2H-pyran-2-yloxy)methyl)-8,10-dihydrophenanthro[2,3-c]furan (4.070 E)

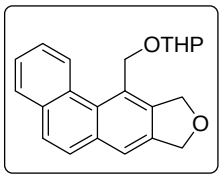

State: yellow oil; **yield:** 9 mg, 13%; IR (neat) ν_{max} 3069, 2965, 2867, 1645, 1475, 1145, 755 cm^{-1}; ^{1}H NMR (600 MHz, Chloroform-*d*) δ 8.91 (d, *J* = 9.0 Hz, 1H), 7.93 (d, *J* = 9.6 Hz, 1H), 7.74 - 7.71 (m, 3H), 7.64 - 7.63 (m, 2H), 5.50 (app s, 2H), 5.38 - 5.35 (m, 3H), 4.99 - 4.96 (m, 2H), 4.12 - 4.08 (m, 1H), 3.74 - 3.70 (m, 1H), 2.07 - 1.64 (m, 6H); ^{13}C NMR (150 MHz, Chloroform-*d*) δ 141.4, 139.3, 137.8, 133.7, 133.3, 130.5, 130.3, 128.4, 128.0, 127.4, 127.1, 126.3, 125.9, 120.8, 98.9, 73.6, 73.5, 67.7, 62.6, 30.2, 25.5, 19.4; HRMS: Calcd. for $C_{22}H_{22}NaO_3^+$ $[M+Na]^+$ 357.1467 found 357.1469.

2-[2-(4-Allyl-furan-3-yl)-vinyloxy]-tetrahydro-pyran (4.069 F)

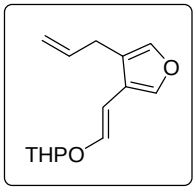

State: yellow oil; **yield:** 9 mg, 18%; IR (neat) ν_{max}.2947, 2875, 1667, 1525, 1234, 1095, 734 cm^{-1}; ^{1}H NMR (400 MHz, Chloroform-*d*) δ 7.36 (s, 1H), 7.34 (s, 1H), 6.77 (d, *J* = 12.8 Hz, 1H), 6.60 (d, *J* = 8.0 Hz, 1H), 6.13 (d, *J* = 11.2 Hz, 1H), 5.86 - 5.78 (m, 2H), 5.02 - 4.91 (m, 2H), 4.73 (app s, 1H), 3.90 - 3.84 (m, 1H), 3.60 - 3.58 (m, 1H), 2.07 - 1.67 (m, 6H); ^{13}C NMR (150 MHz, Chloroform-*d*) δ 137.7, 137.6, 136.3, 126.0, 118.4, 114.1, 99.0, 98.9, 62.2, 31.9, 30.7, 30.6, 22.7, 19.5; HRMS: Calcd. for $C_{14}H_{18}NaO_3^+$ $[M+Na]^+$ 257.1154 found 257.1154.

4-(Tetrahydro-pyran-2-yloxymethyl)-1,3-dihydro-isobenzofuran (4.070 F)

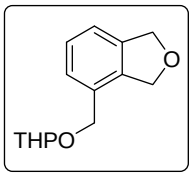

State: yellow oil; **yield:** 25 mg, 55%; IR (neat) ν_{max}.2956, 2935, 2856, 1668, 1465, 1205, 1093, 786 cm^{-1}; ^{1}H NMR (600 MHz, Chloroform-*d*) δ 7.29 - 7.24 (m, 2H), 7.19 - 7.18 (d, *J* = 7.2 Hz, 1H), 5.20 (app s, 2H), 5.14 (s, 2H), 4.78 (d, *J* = 12.6 Hz, 1H), 4.71 (t, *J* = 3.0 Hz, 1H), 4.47 (d, *J* = 12.6 Hz, 1H), 3.93 - 3.89 (m, 1H), 3.59 - 3.56 (m, 1H), 1.9 - 1.56 (m, 6H); ^{13}C NMR (150 MHz, Chloroform-*d*) δ 139.5, 137.8, 131.9, 127.5, 126.5, 120.1, 97.9, 73.5, 73.0, 67.3, 62.0, 30.5, 25.4, 19.2; HRMS: Calcd. for $C_{14}H_{18}NaO_3^+$ $[M+Na]^+$ 257.1154 found 257.1154.

3-Benzyl-4-(2-ethoxy-vinyl)-furan (4.069 G)

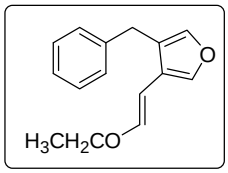

State: yellow oil; **yield:** 39 mg, 85%; IR (neat) ν_{max}.2987, 2956, 2867, 1669, 1356, 1189, 1067, 755 cm^{-1}; ^{1}H NMR (600 MHz, Chloroform-*d*) δ 7.35 (s, 1H), 7.33 - 7.31 (m, 2H), 7.24 -7.23 (m, 3H), 7.10 (s, 1H), 6.63 (d, *J* = 12.6 Hz, 1H), 5.46 (d, *J* = 12.6 Hz, 1H), 3.79 (app q, *J* = 8.4 Hz, 4H), 1.29 (dd, *J* = 7.2 Hz, 6.6 Hz, 3H); ^{13}C NMR (50 MHz, Chloroform-*d*) δ 147.8, 141.1, 139.9, 138.1, 128.7, 128.6, 126.3, 123.3, 121.6, 95.0, 65.5, 30.4, 14.9; HRMS: Calcd. for $C_{15}H_{17}O_2^+$ $[M+H]^+$ 229.1229 found 229.1213.

4-Methyl-1,3-dihydro-naphtho[2,3-c]furan (4.070 H)

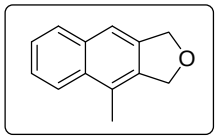

State: sticky mass; **yield:** 24 mg, 65%; IR (neat) ν_{max}.3100, 2986, 2934, 1667, 1523, 1356, 1189, 1098, 785, 747 cm^{-1}; ^{1}H NMR (600 MHz, Chloroform-*d*) δ 8.02 (d, *J* = 7.2 Hz, 1H), 7.84 (d, *J* = 8.4 Hz, 1H) , 7.57 (s, 1H), 7.53 - 7.47 (m, 2H), 5.28 (s, 2H), 5.27 (s, 2H), 2.58 (s, 3H); ^{13}C NMR (150 MHz, Chloroform-*d*) δ 137.4, 136.6, 133.5, 132.1, 128.5, 126.2, 125.5, 125.3, 123.5, 117.3, 73.5, 72.8, 15.4; HRMS: Calcd. for $C_{13}H_{13}O^+$ $[M+H]^+$ 185.0966 found 185.0968.

4.6.3 ^{1}H and ^{13}C NMR spectra of selected compounds

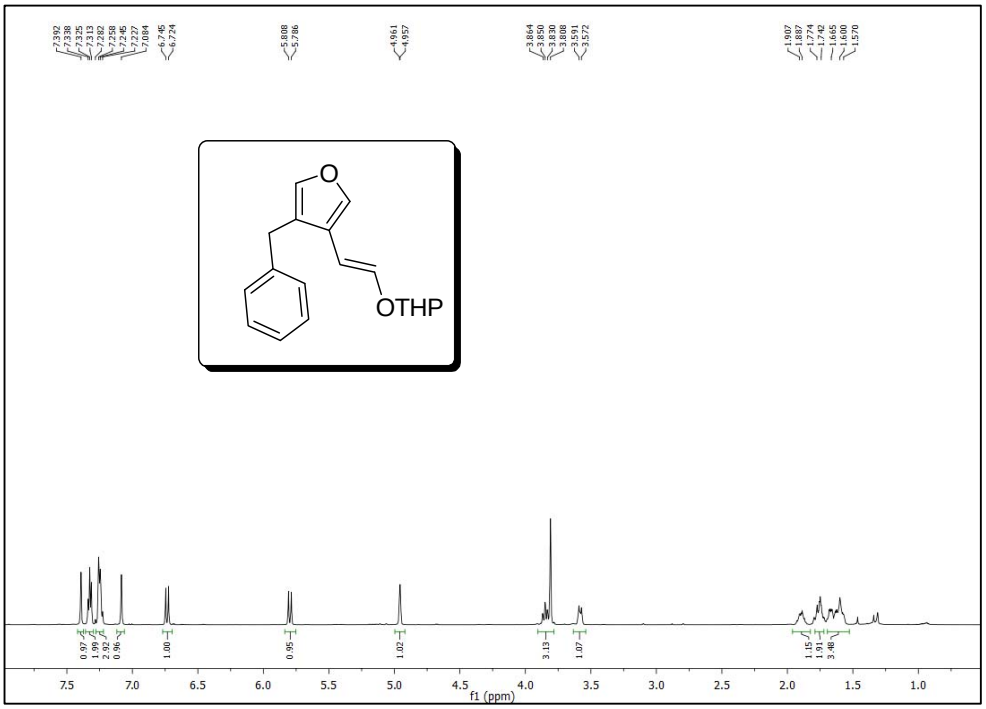

^{1}H NMR ($CDCl_3$, 600 MHz) spectrum of 4.069 A

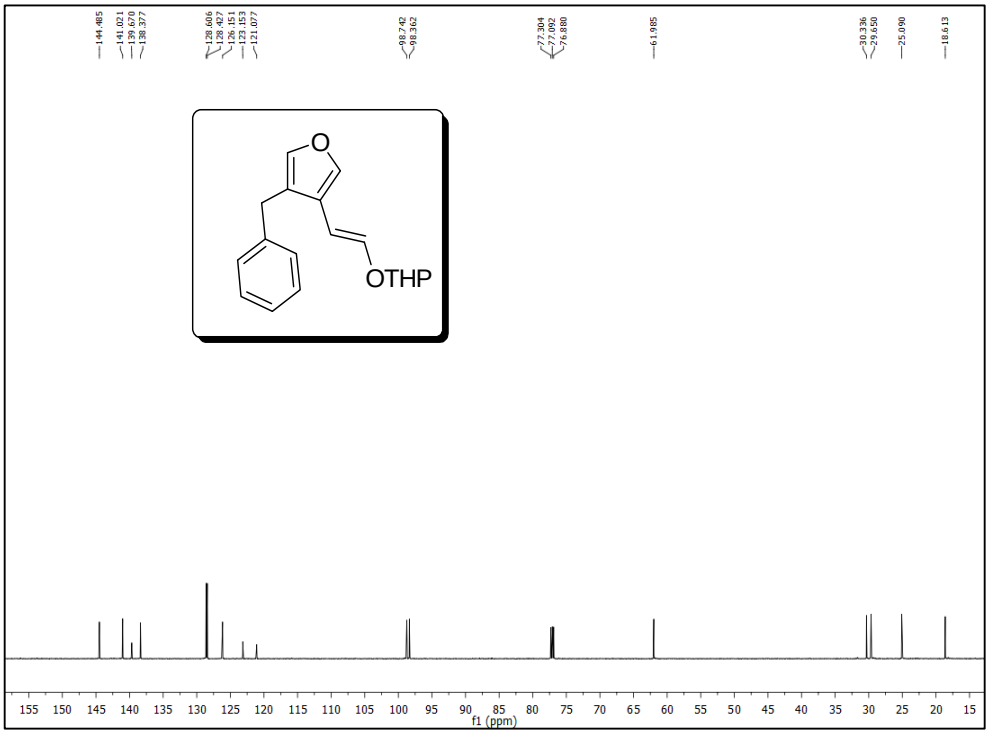

^{13}C NMR ($CDCl_3$, 150 MHz) spectrum of 4.069 A

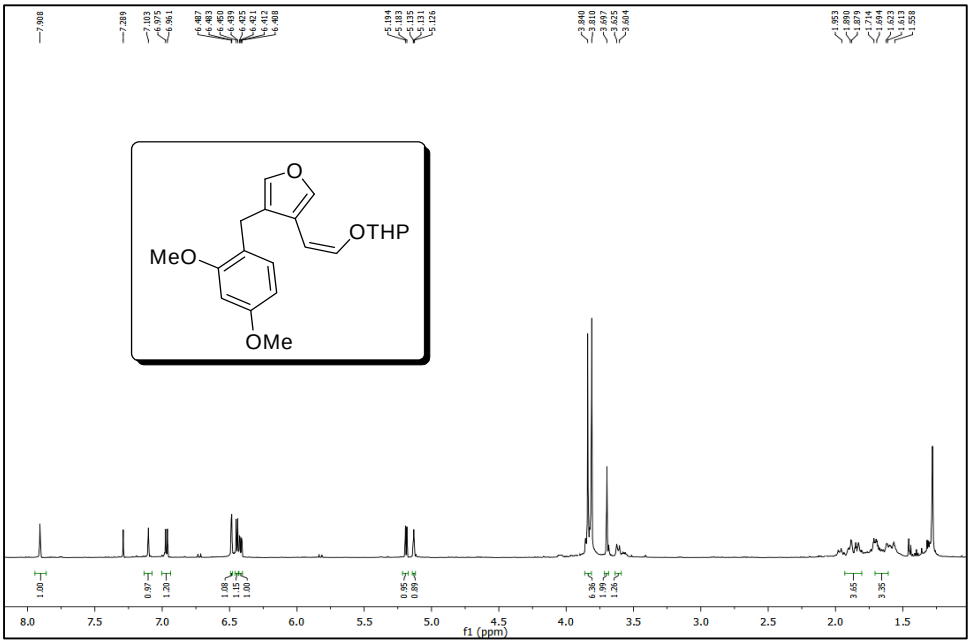

^{1}H NMR ($CDCl_3$, 600 MHz) spectrum of 4.069 B

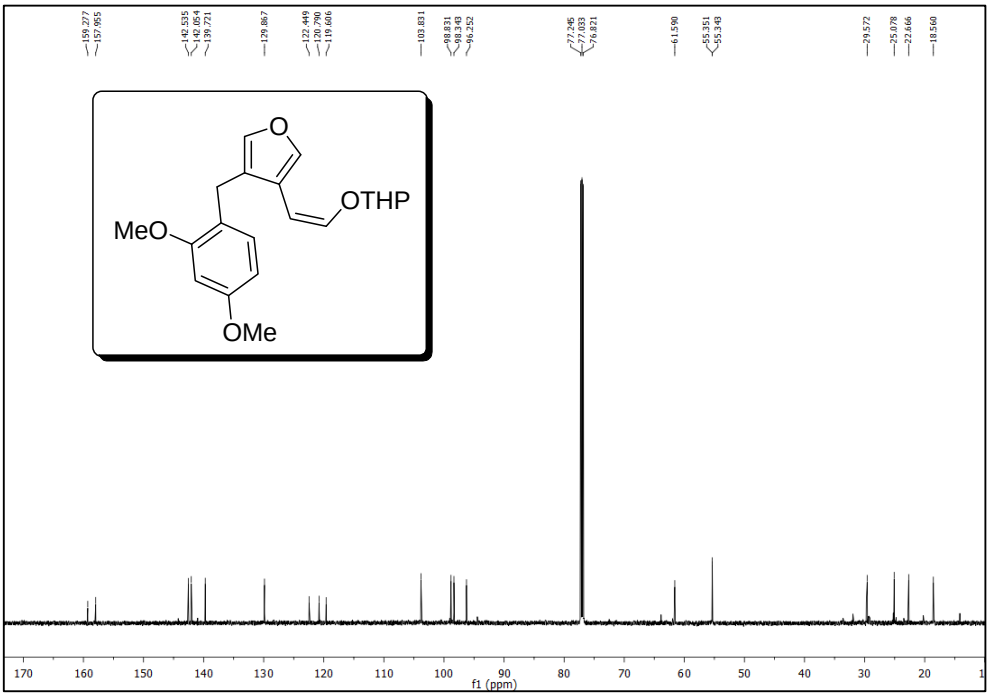

^{13}C NMR ($CDCl_3$, 150 MHz) spectrum of 4.069 B

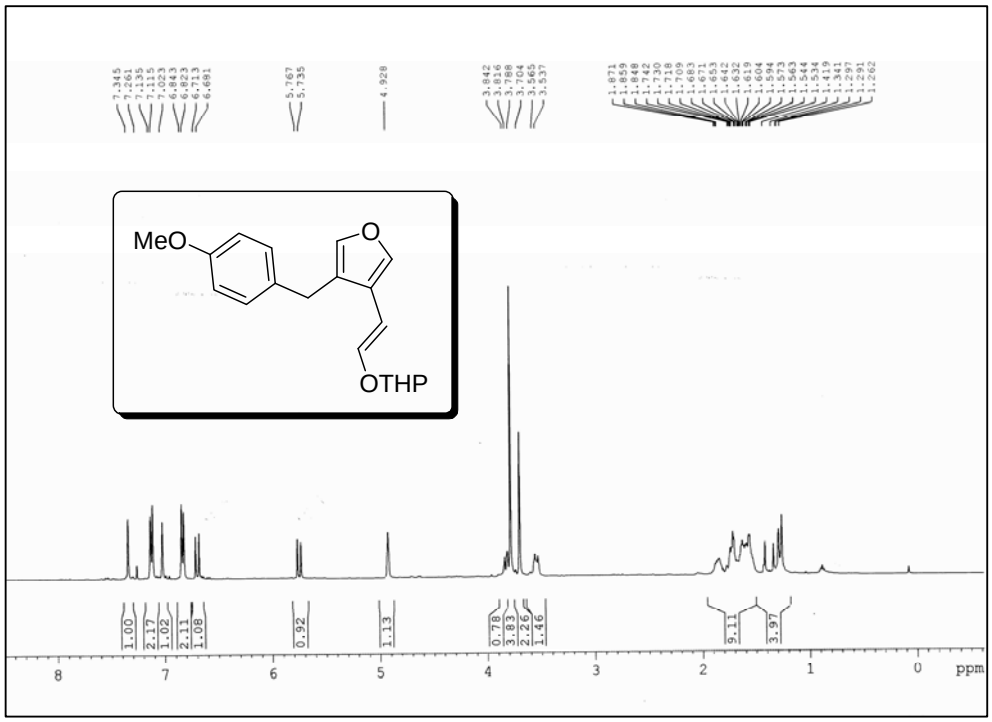

^{1}H NMR ($CDCl_3$, 100 MHz) spectrum of 4.069 C

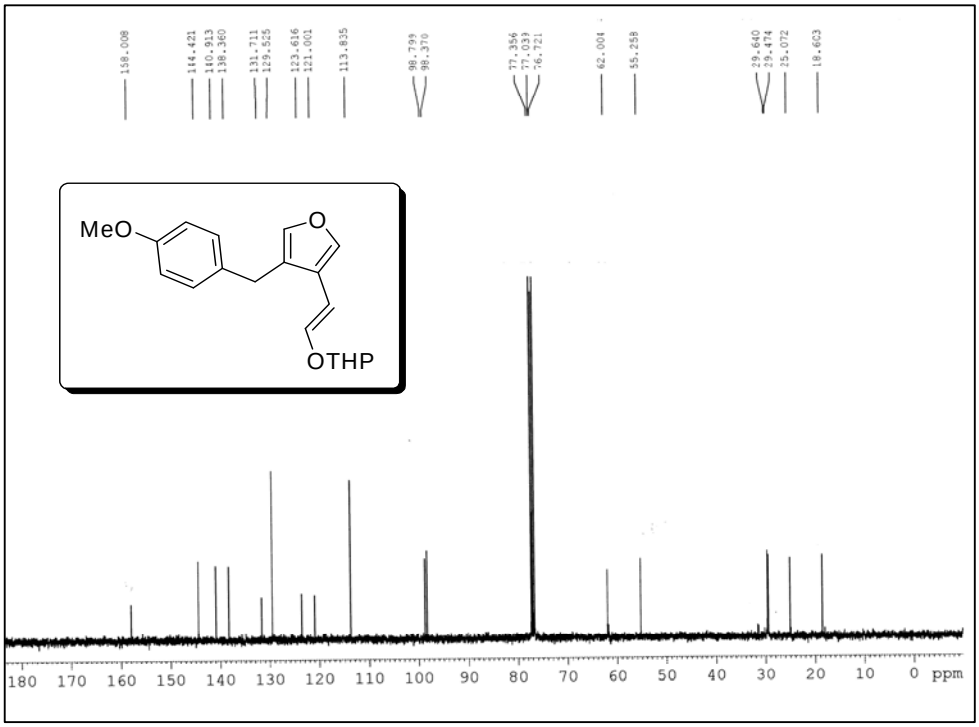

^{13}C NMR ($CDCl_3$, 100 MHz) spectrum of 4.069 C

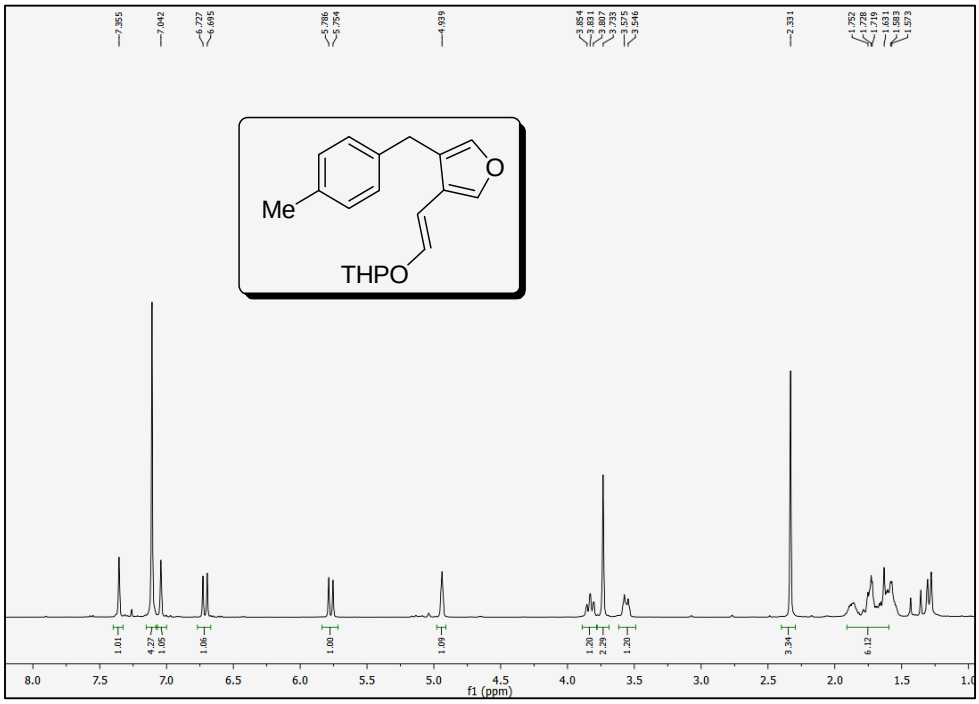

^{1}H NMR ($CDCl_3$, 400 MHz) spectrum of 4.069 D

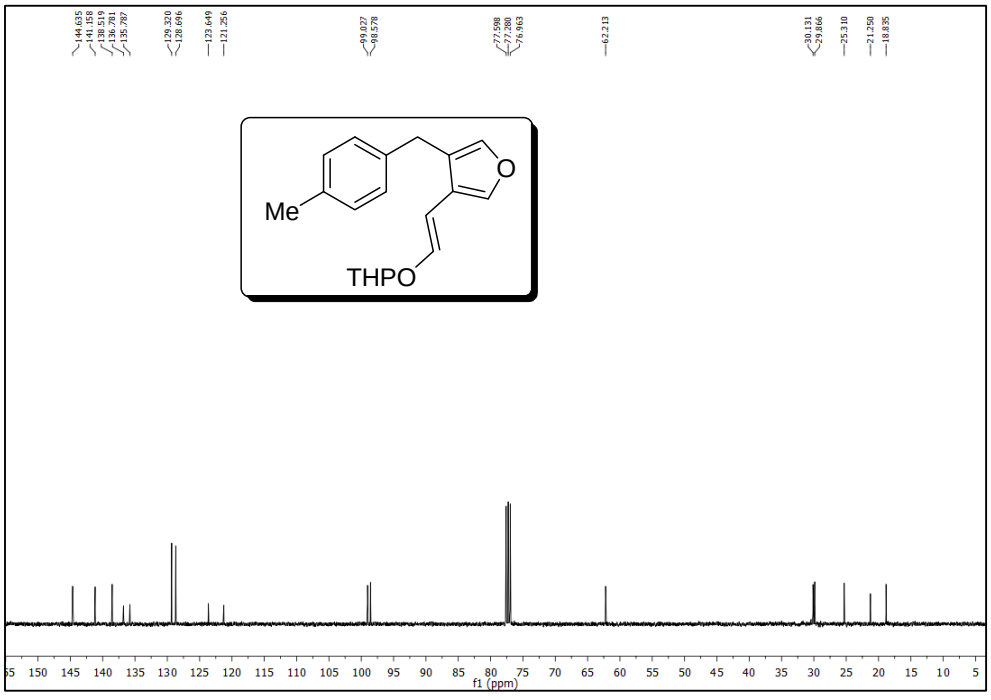

^{13}C NMR ($CDCl_3$, 100 MHz) spectrum of 4.069 D

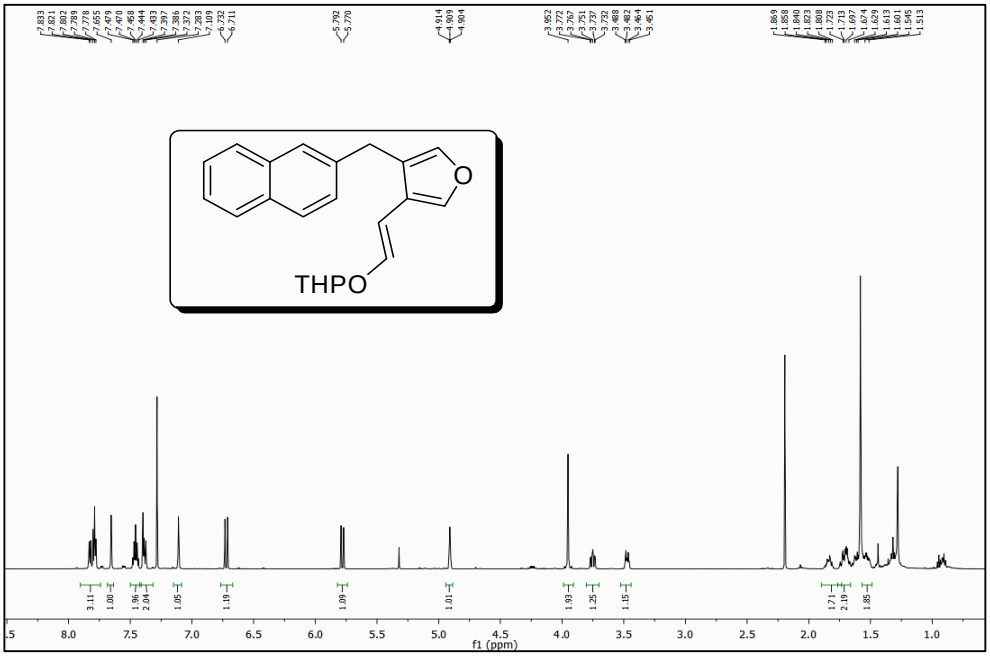

^{1}H NMR ($CDCl_3$, 600 MHz) spectrum of 4.069 E

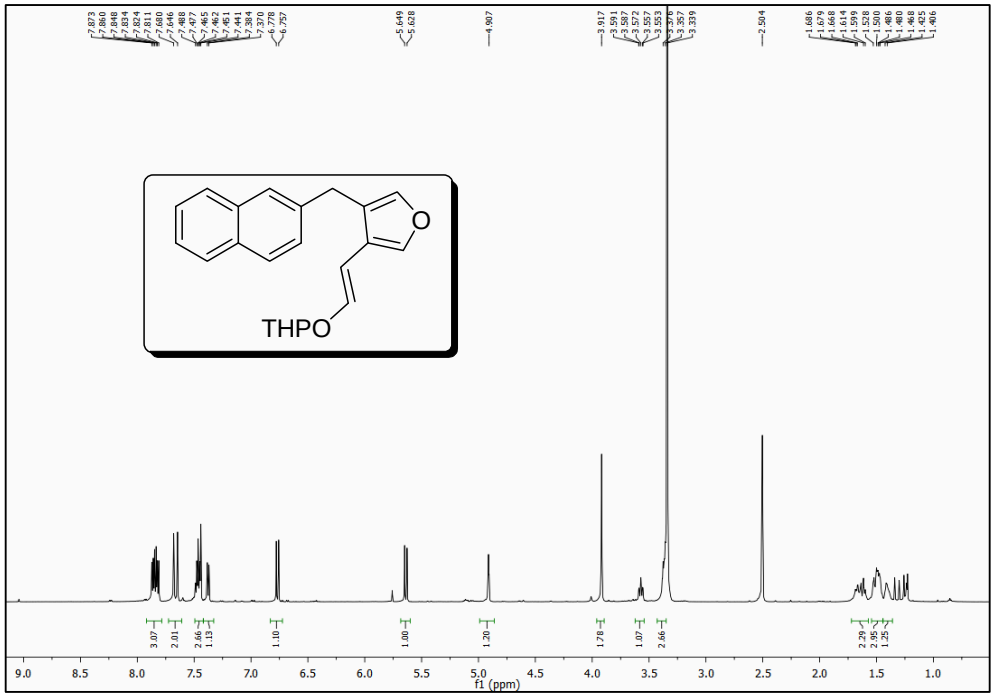

^{1}H NMR (DMSO-d_6, 600 MHz) spectrum of 4.069 E

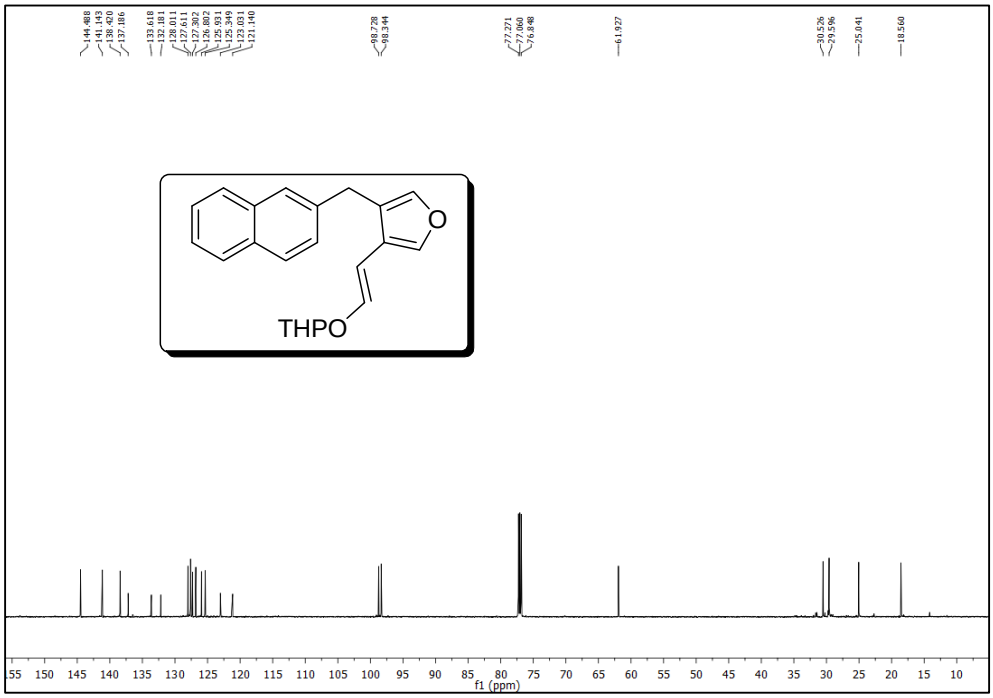

^{13}C NMR ($CDCl_3$, 150 MHz) spectrum of 4.069 E

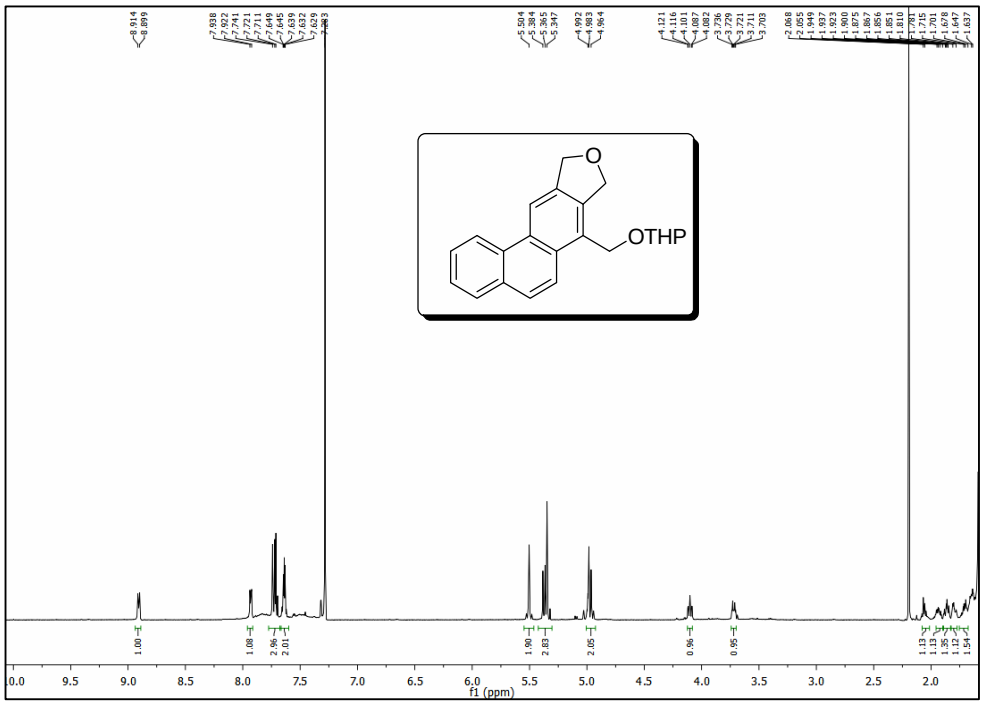

^{1}H NMR ($CDCl_3$, 600 MHz) spectrum of 4.070 E

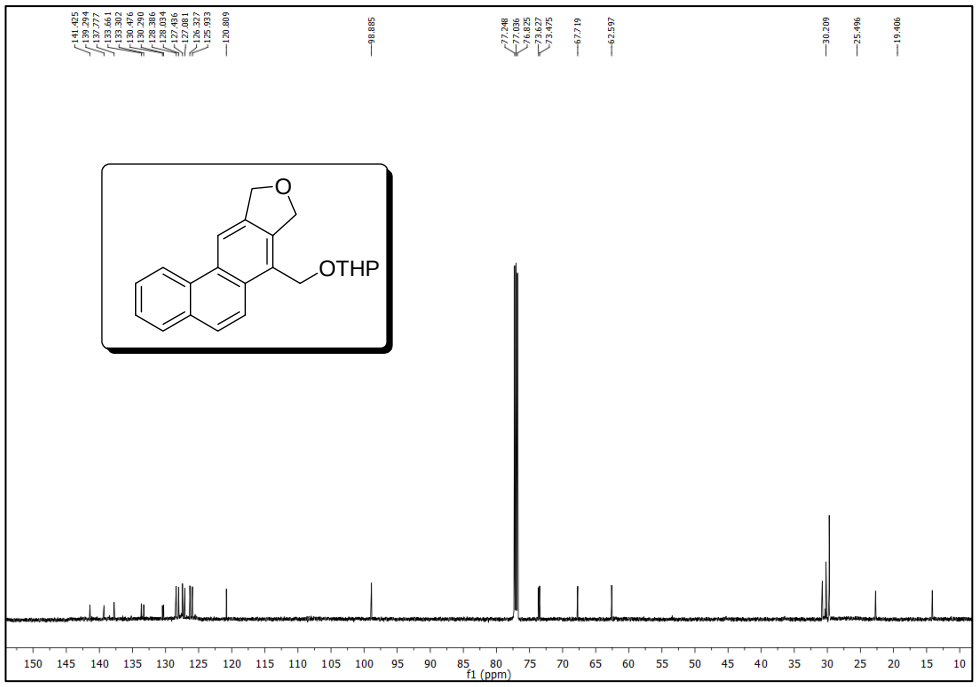

^{13}C NMR ($CDCl_3$, 150 MHz) spectrum of 4.070 E

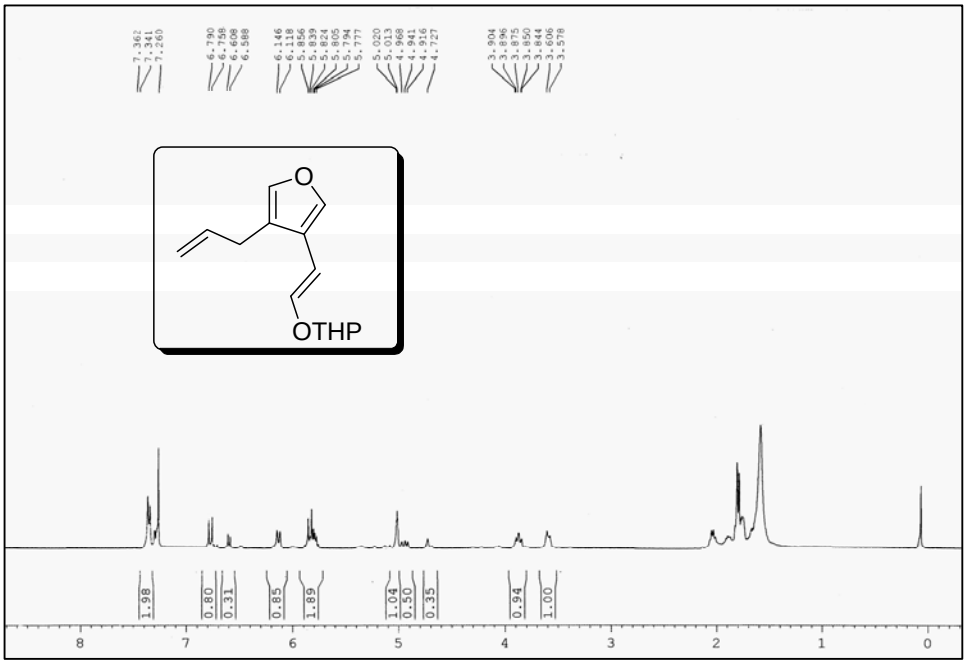

^{1}H NMR ($CDCl_3$, 400 MHz) spectrum of 4.069 F

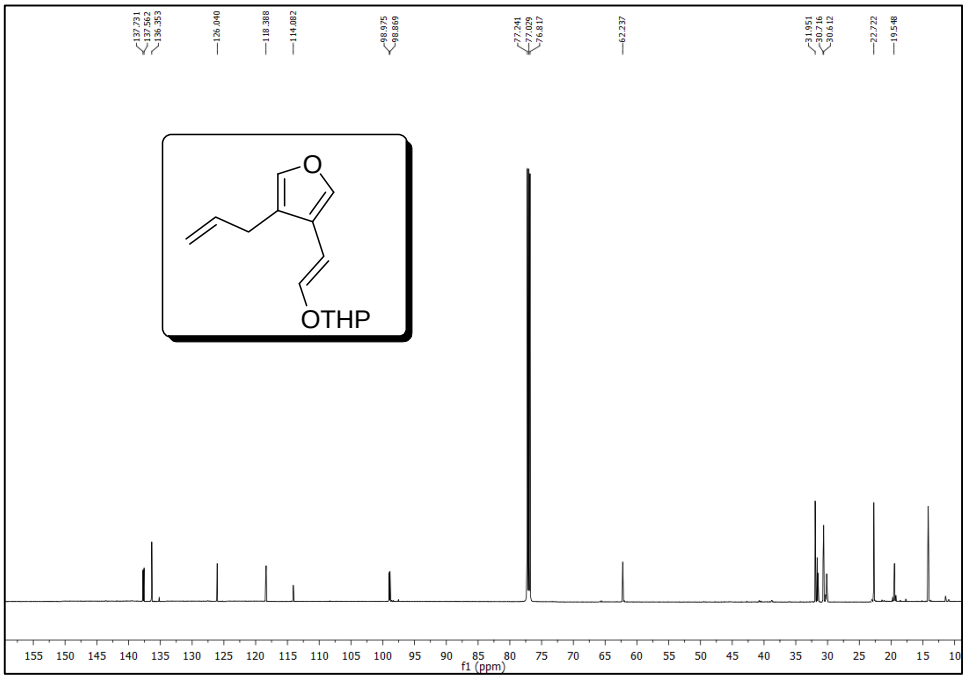

^{13}C NMR ($CDCl_3$, 150 MHz) spectrum of 4.069 F

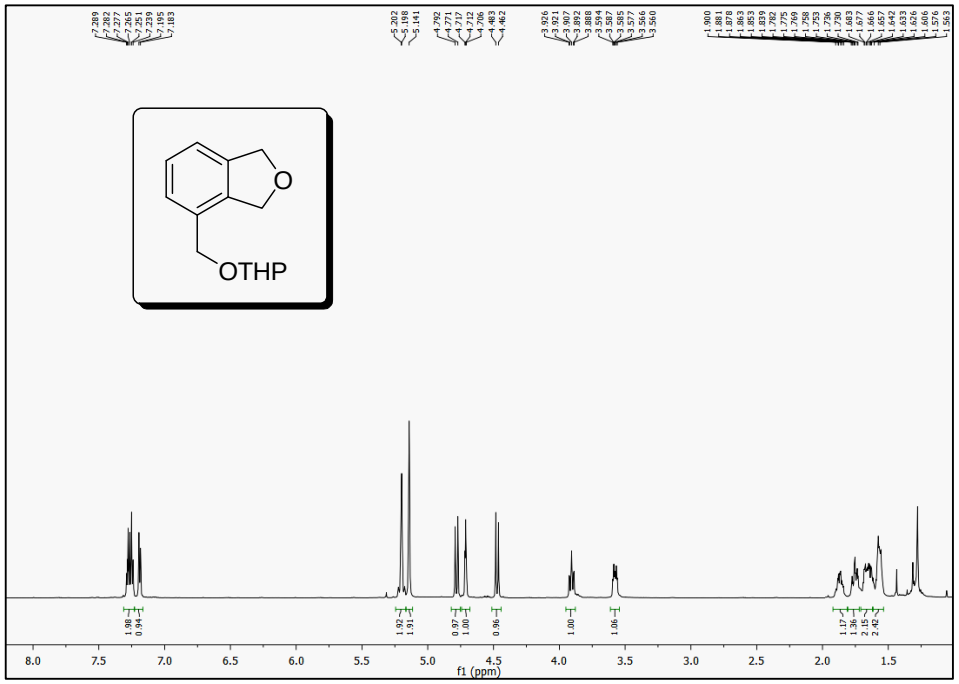

^{1}H NMR ($CDCl_3$, 600 MHz) spectrum of 4.070 F

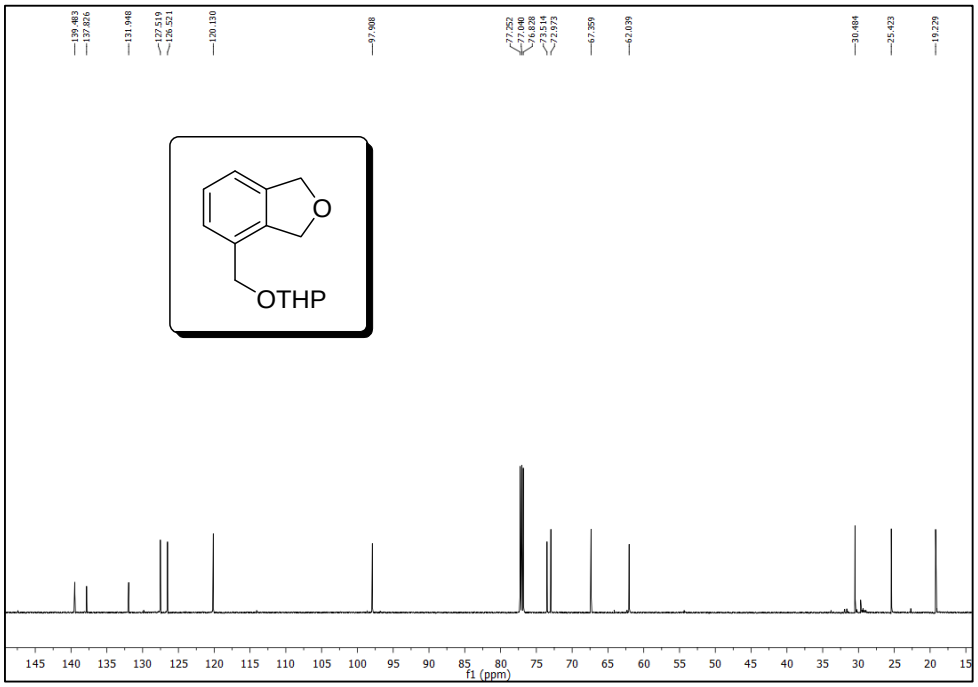

^{13}C NMR ($CDCl_3$, 150 MHz) spectrum of 4.070 F

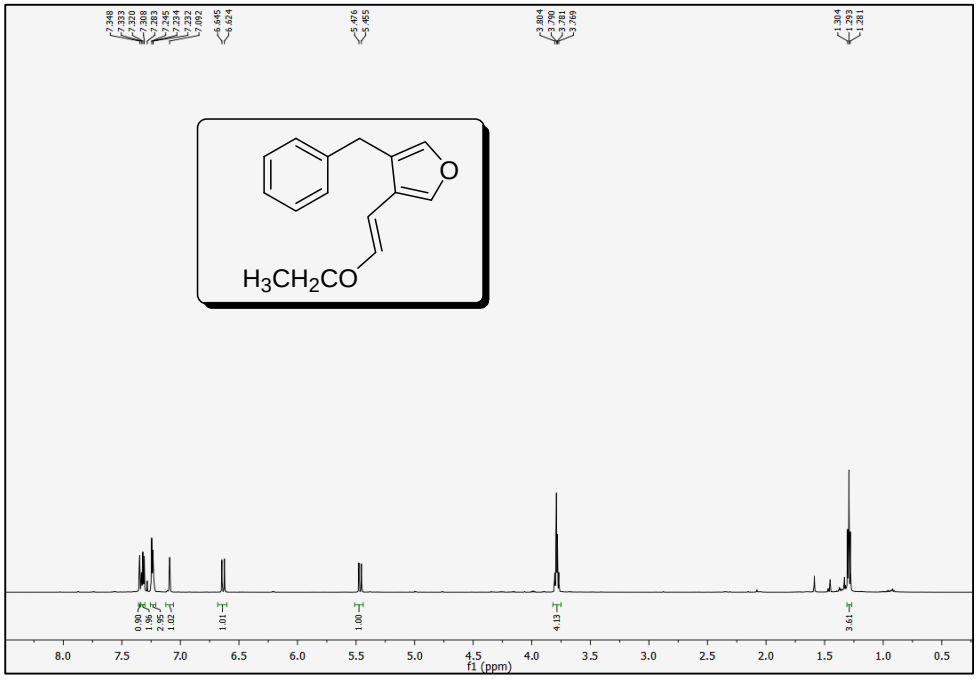

^{1}H NMR ($CDCl_3$, 600 MHz) spectrum of 4.069 G

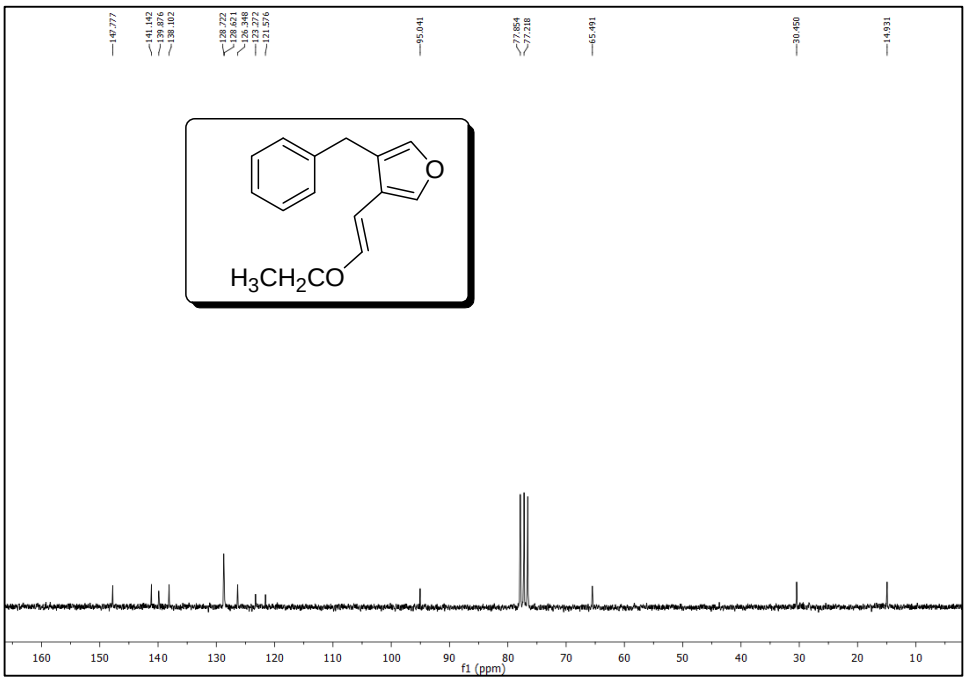

^{13}C NMR ($CDCl_3$, 50 MHz) spectrum of 4.069 G

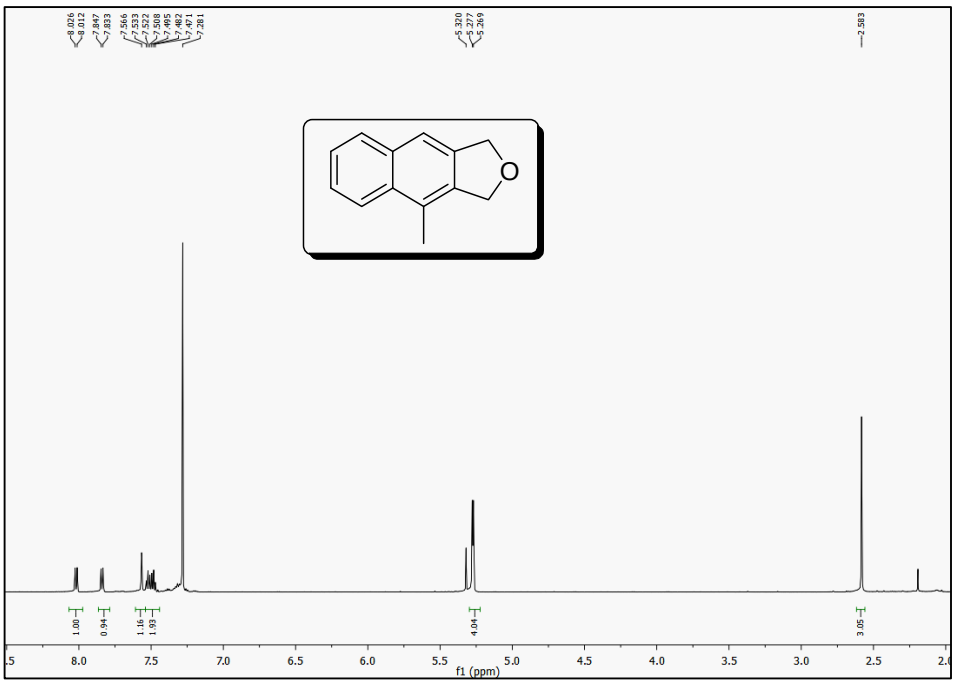

^{1}H NMR ($CDCl_3$, 600 MHz) spectrum of 4.070 H

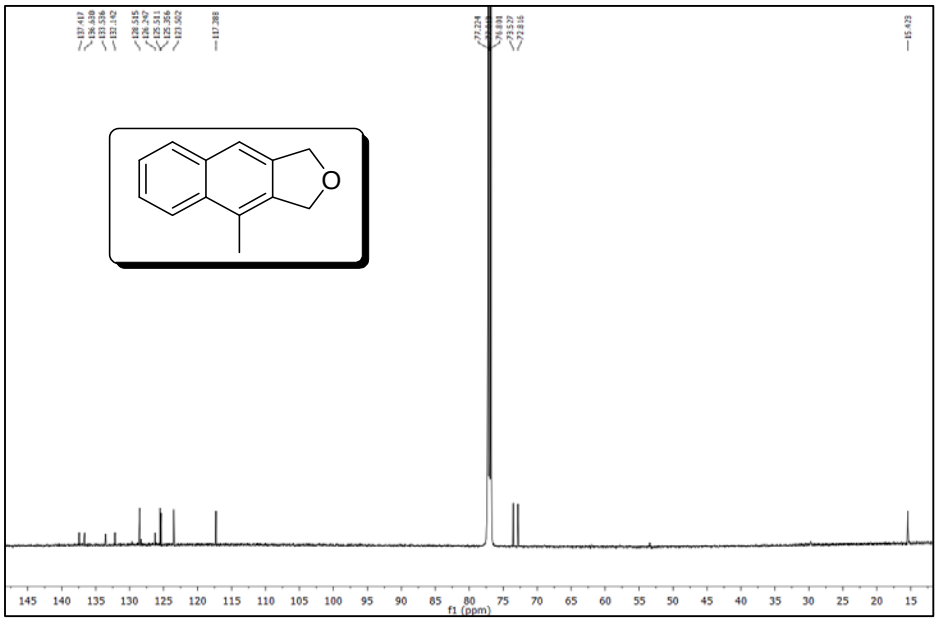

^{13}C NMR ($CDCl_3$, 150 MHz) spectrum of 4.070 H

Chapter 5

Mechanistic Studies on the Base Induced Cyclization of Propargyl Alkenyl Sulfones

5.1 Introduction

Cyclic organosulfur compounds like sulfoxides and sulfones constitute an important class of organic compounds. They appear to be useful synthetic intermediates[86] for several organic transformations and also belong to many functional cores of biologically active molecules[87] relevant in medicinal chemistry. The saturated five membered cyclic sulfones or tetrahydothiofene dioxides are known as sulfolanes whereas their unsaturated analogues are termed sulfolenes. The sulfone moieties help to increase hydrophilicity as well as the interaction with biological targets, thus making them a potent candidate for drug design. For example, the sulfone moiety in sulfolane **5.004** serves as a bioisostere of amide bonds[87a] that makes it a suitable inhibitor of HIV 1 Protease **(Figure 5.01)**. Similar is the situation for sulfolane **5.005** that executes inhibition property against viral neuraminidase[87g] responsible for the release of virus to the host cell. In case of Nifurtimox **5.002**, an antitrypanosomal, the thiomorpholine dioxide moiety serves as a Lewis base to create H-bond interaction[87h] whereas the nitro group is susceptible towards reduction and produces reactive oxygen radicals that are superoxides and destroy protozoa cells selectively. A list of biologically active cyclic sulfones is given as follows.

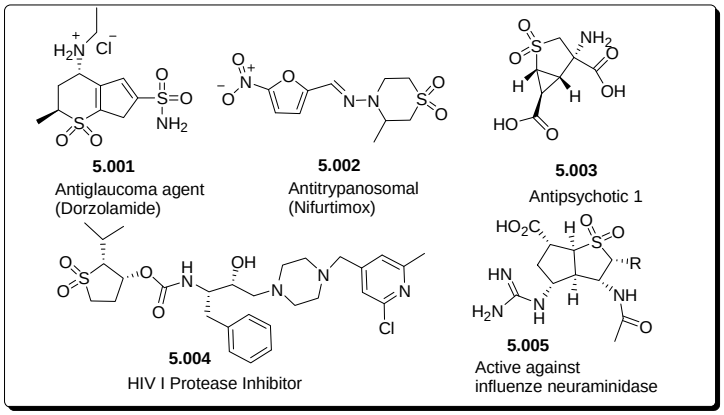

Figure 5.01: Examples of some bio-active sulfone derivatives

Apart from this, the acyclic counterpart bis(2-ethylhexyl) sulfoxide (BESO) is also applicable in extracting metals like Pd(II) based upon the strategy of soft-soft metal-ligand interaction[88] and unsubstituted sulfolane acts as dipolar aprotic solvent to form inert microemulsions as reaction media to conquer reagent incompatibility[89]. In addition to sulfolanes, sulfolenes are desirable candidates in organic synthesis as they

readily undergo alkylation reactions and the $-SO_2$ moiety can be eliminated under mild reaction condition.[90]

In this chapter, we have discussed the synthesis of cyclic sulfones that have huge applications in pharmacology.

5.2 Previous Work

Some of the well-known available methods for the synthesis of sulfolanes comprise the traditional way of oxidation of sulfides to sulfones with oxidants, cycloaddition of dienes with SO_2 as dienophile or catalytic alkylation of vinyl sulfones with organocatalysts. All these methods are associated with their own merits and disadvantages like poor catalyst recyclability, poor functional group tolerance, limited scope of substrates, high reaction temperature, poor atom economy, insolubility in organic medium etc. A couple of synthetic methodologies are available for synthesis of cyclic sulfones in literature. Few selected useful methods are described here. The synthesis either begins with cyclization followed by oxidation or vice versa.

The classical way of construction of tetrahydrothiofene or thiopyran ring was intramolecular addition of sulfur nucleophile to alkenes or alkynes in presence of an electrophilic reagent like halogens. In 1995, Turos *et al.* reported halocyclization of unsaturated benzyl sulfides **5.006**. The reaction was believed to proceed either *via* an episulfonium ion or a cyclic sulfonium ion formation (**Scheme 5.01**).[91]

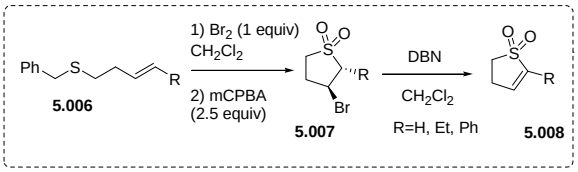

Scheme 5.01: Synthesis of cyclic sulfones by halocyclization reaction

In 1979, Quin and McPhail *et al*. reported cycloaddition of a diene **5.013** and SO_2 to fused sulfolene derivative **5.014** (**Scheme 5.02**).[92]

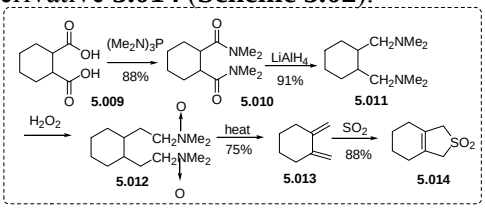

Scheme 5.02: Synthesis of cyclic sulfones by cycloaddition reaction

The easiest way of synthesizing sulfones is oxidation of sulfides to sulfoxides followed by sulfones. The disadvantages associated with the conventional oxidants like peracids, MnO_4, $NaIO_4$, SeO_2, and CrO_3 are the requirement of stoichiometric amount of oxidants that make it atom non-efficient along with the by-products. Thus Yadolahi *et al*. in 2014 reported an efficient chemoselective oxidation of sulfides **5.015** to sulfone **5.016** (**Scheme 5.03**) by environmentally benign oxidant H_2O_2 in presence of a Chromium substituted Keggin-type polyoxometalate [(*n*-$C_4H_9)_4N]_4[PW_{11}CrO_{39}].3H_2O$ (PWCr). The reaction proceeded with an oxygen transfer mechanism and had a wide window of functional group tolerance.[93]

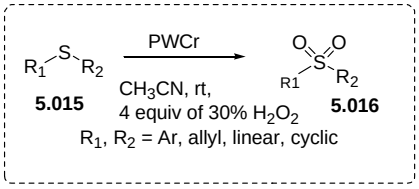

Scheme 5.03: Chemoselective oxidation of sulfides as proposed by Yadolahi *et al*.

In 2014, Chand *et al.* reported a green protocol of oxidation of sulfides **5.017** to sulfoxides **5.018** and sulfones **5.019** in water in presence of a surfactant cetyl ammonium cation (CTA) based Molybdenum catalyst $(C_{19}H_{42}N)_2[MoO(O_2)_2(C_2O_4)]\cdot H_2O$and H_2O_2 as oxidant.[94] The reaction condition was mild and had functional group tolerance (**Scheme 5.04**).

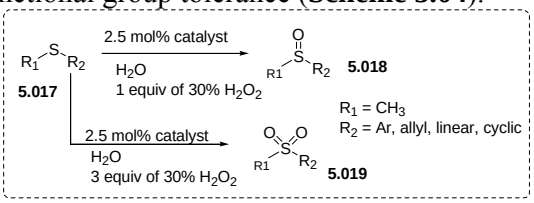

Scheme 5.04: Oxidation of sulfides as proposed by Chand *et al.*

In 2010, Ikemoto *et al*. suggested oxidation of sulfides **5.020** using aqueous solution of NaOCl in presence of a catalytic amount of imide cyanuric acid (**Scheme 5.05**). The reaction was believed to proceed by the *in situ* formation of N-chloroimide that served as both oxidising agent as well as phase transfer catalyst.[95]

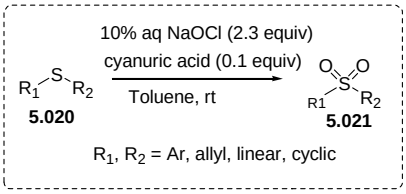

Scheme 5.05: Oxidation of sulfides as proposed by Ikemoto *et al*.

Hayashi *et al.* in 2015 proposed an asymmetric arylation of allyl sulfolenes **5.022** in presence of aryl boronic acid, a chiral Rh catalyst $[RhCl((R,R)\text{-Fc-tfb})]_2$ (Fc=Ferrocenyl) and 10 equivalent of KOH (**Scheme 5.06**). It was supposed that the reaction proceeded by isomerization of allyl to vinyl sulfones that are more electron deficient hence more reactive.[96]

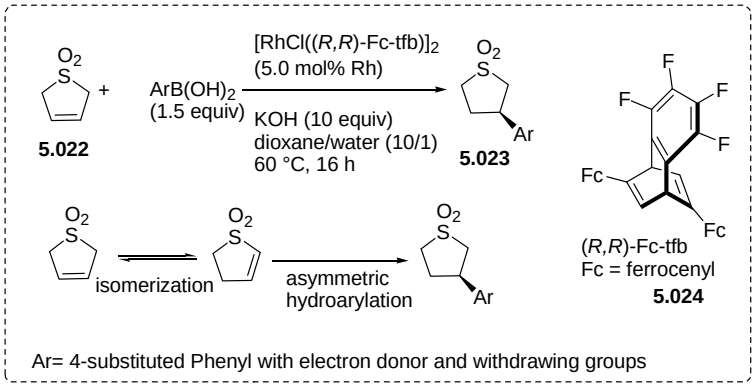

Scheme 5.06: Asymmetric arylation of allyl sulfolenes with aryl boronic acids

Braverman *et al*. in 1974 reported the thermal cyclization of Bis-γ,γ-dimethylallenyl sulfone **5.028** to 3-isopropenyl-4-isopropylthiofene-1,1- dioxide **5.029**. The bis-allene was obtained by 2,3-sigmatropic rearrangement of propargylic sulfoxylate **5.026**. The reaction was believed to proceed either *via* diradical or intramolecular ene reaction pathway (**Scheme 5.07**).[31]

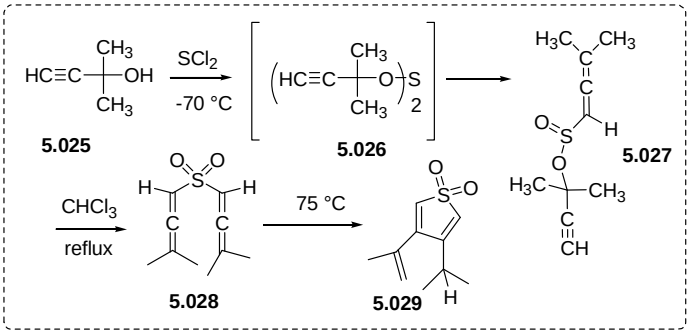

Scheme 5.07: Cyclization of Bis-γ,γ-dimethylallenyl sulfone as proposed by Braverman *et al*.

Subsequently, in 1975 Garratt *et al*. investigated the base catalyzed rearrangement of various γ-substituted bis-propargyl sufides, ethers and amines **5.030**, **5.036**, **5.038** to cyclohexane fused heterocyclic ring like thiofene, furan and pyrrole respectively (**Scheme 5.08**). In case of γ-phenyl substitution **5.030** the intermediate heterocycle further rearranged to tetrahydroheterocycle functionality **5.035**.[32]

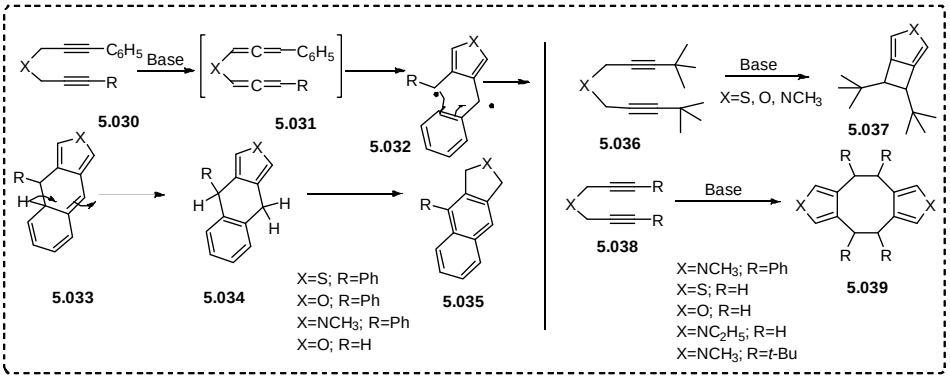

Scheme 5.08: Cyclization of bis-propargyl precursors as proposed by Garratt *et al.*

Thus, base catalyzed rearrangement of bis-propargyl sulfides, sulfoxides and sulfones was established to be a convenient pathway to synthesize sulfur containing heterocycles in quantitative yield from easily available starting materials.

In 2007 Kudoh *et al*. reported an anionic intramolecular Diels Alder reaction of differently substituted bis-propargyl ethers (**Scheme 5.09**). The outcome of the reaction was similar as revealed by Garratt and Braverman for base catalyzed cyclization of bis-propargyl ethers. They provided DFT calculations and deuterium scrambling experiment in favour of anionic IMDAR mechanism of bis-propargyl ethers.[38]

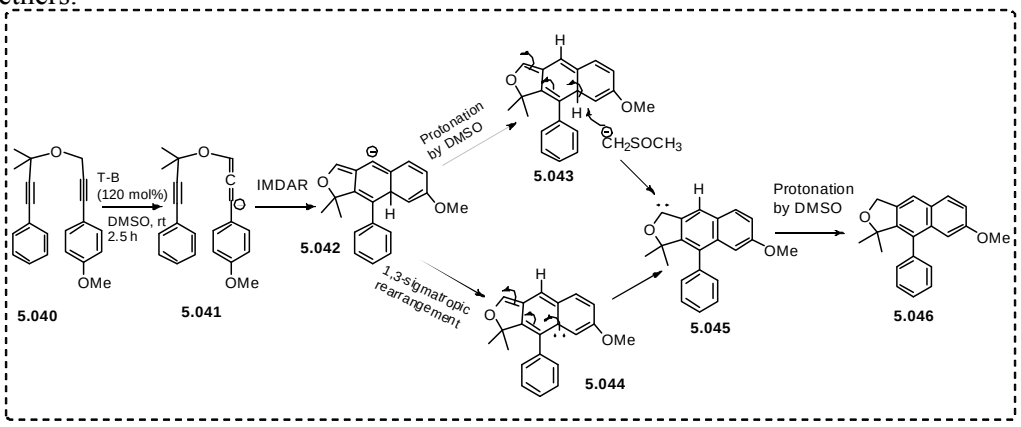

Scheme 5.09: Anionic intramolecular Diels Alder reaction (IMDAR) of bis-propargyl ethers as proposed by Kudoh *et al.*

The application of IMDAR was further extended to the propargyl alkenyl systems **5.047** where both the alkyne hand as well as the alkene functionality acted as diene for intramolecular Diels Alder reaction (**Scheme 5.10**).

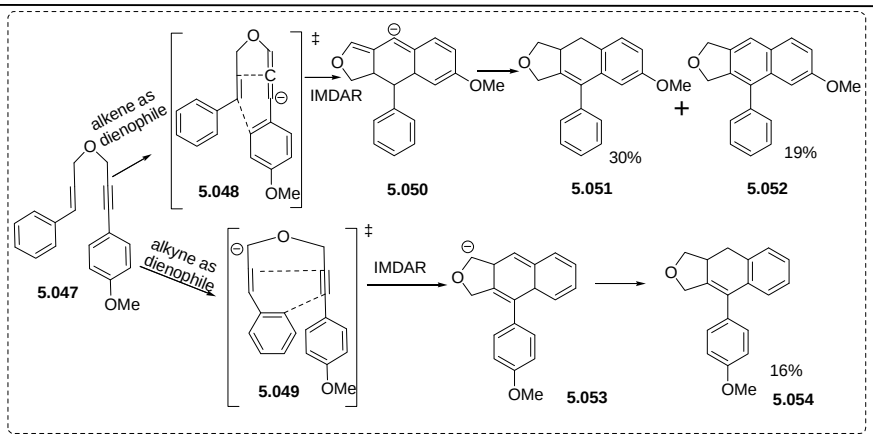

Scheme 5.10: Anionic intramolecular Diels Alder reaction of propargyl alkenyl ethers as proposed by Kudoh *et al.*

It is previously discussed that *γ*-substituted bis-propargyl sulfones serve as suitable precursors for synthesis of benzene fused sulfolanes *via* a base mediated Garratt-Braverman cyclization. Rewinding the existing differences between reactivity and selectivity profiles for bis-propargyl sulfones and ethers considering the electron-donating vinyl ether and electron withdrawing nature of sulfone moiety various propargyl alkenyl sulfones **5.055** with only phenyl substitution at the alkene hand were synthesized in our lab and the outcome of base mediated rearrangement of these sulfones were investigated. To our surprise the alkenyl propargyl sulfones **5.055** upon treatment with NaH in DMSO yielded 4,5-disubstituted *2H*-thiopyran 1,1-dioxides **5.056** instead of benzene fused sulfolanes **5.057**-**5.059** (**Scheme 5.11**).[97]

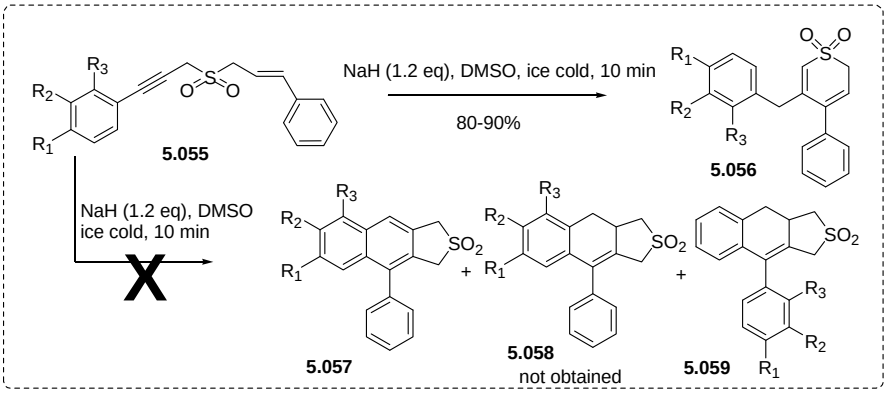

Scheme 5.11: Base mediated rearrangement of propargyl alkenyl sulfones

A 6π electrocyclization based mechanism (**Scheme 5.12**) was tentatively proposed for the formation of thiopyran dioxide moiety although no further studies were continued to support the mechanism or to expand the scope of the reaction.

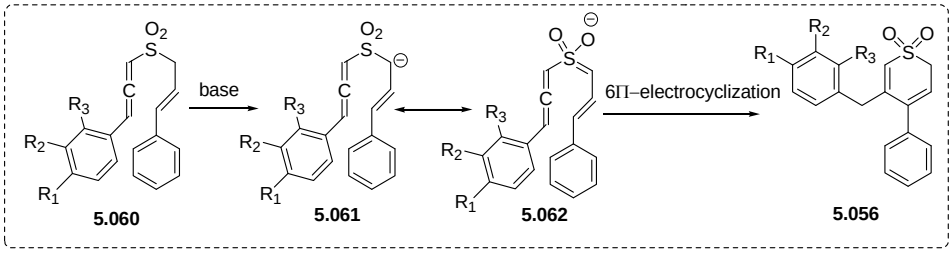

Scheme 5.12: 6π-electrocyclization mechanism of cyclization for propargyl alkenyl sulfones

5.3 Objective

Based on above observation of 6π electrocyclization of propargyl alkenyl sulfones to yield thiopyran dioxides instead of benzene or cyclohexene fused sulfolanes we then set our objectives as follows:

- Synthesize various propargyl alkenyl sulfones from commercially available starting materials having general structure **A** with substituted phenyl moiety at the alkene hand and observe the effect of substitution on the course of the reaction.(**Scheme 5.13**)

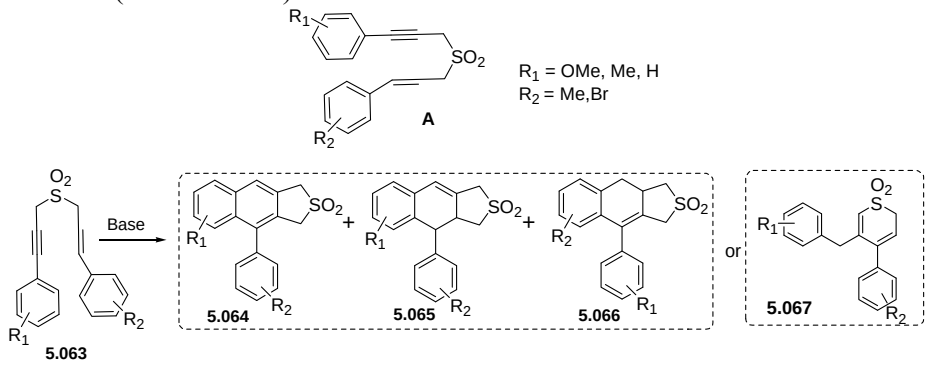

Scheme 5.13: Structure of expected sulfolanes *via* IMDAR of propargyl alkenyl sulfones

- To carry out the reaction in different solvents (polar and non-polar) and observe the effect of solvent polarity on the outcome of the reaction.

- To check the behaviour of thiopyran dioxides upon hydrogenation. One of the possible hydrogenated product tetrahydrothiopyrans are known to possess bioactivity.

- To study the behaviour of an alkenyl propargyl sulfone **5.068** with *β*-methyl cinnamyl moiety and check whether there will be any Me migration during the reaction.

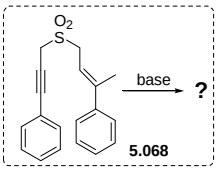

- To carry out the reaction in deuterated solvents and observe the amount of D incorporation in the product if any to further confirm the mechanism of the reaction.

- To propose a plausible mechanism that is supported by all the experimental observations.

5.4 Results and Discussion

5.4 A. Synthesis of Unsymmetrical Propargyl Alkenyl Sulfides

The key step for the synthesis of sulfolanes was the synthesis of unsymmetrical propargyl alkenyl sulfides (**Scheme 5.14**). The synthesis started with the *in situ* generation of 3-substituted prop-2-ene-1-thiols **5.070** by hydrolysis of the corresponding alkenyl thioacetates **5.069** in basic medium.[98] The thiols were then made to undergo S-propargylation immediately in presence of K_2CO_3 and 1 equiv of respective bromides **5.071** to generate the unsymmetrical propargyl alkenyl sulfides **5.072 A-F**.[99] The *β*-methyl substituted cinnamyl sulfide **5.076** was prepared by nucleophilic attack by *in situ* produced propargyl thiol **5.074** on to *β*-methyl cinnamyl bromide **5.075**. The crude sulfides were directly carried over to the next step without any chromatographic purification.

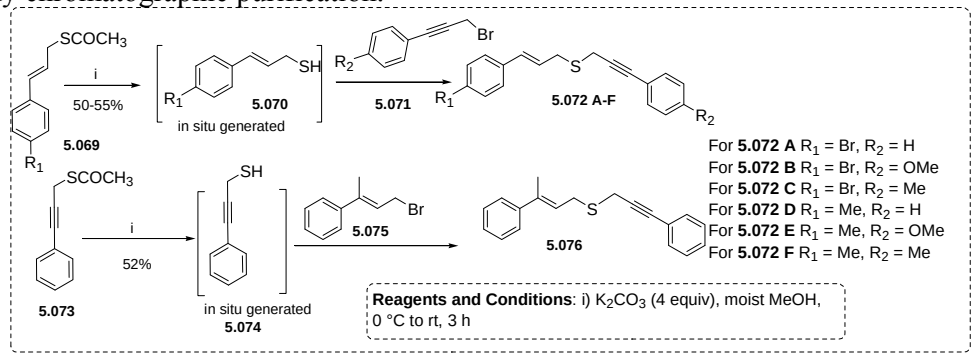

Scheme 5.14: Synthesis of Unsymmetrical Propargyl alkenyl sulfides

The synthesis of propargyl or alkenyl thioacetates **5.069**, **5.073** was accomplished by nucleophilic substitution by potassium thioacetate ($KSCOCH_3$) with the corresponding bromides **5.077, 5.078 A** in anhydrous MeOH (**Scheme 5.15**).

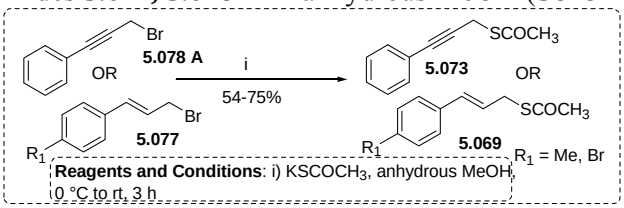

Scheme 5.15: Synthesis of propargyl or alkenyl thioacetates

Sonogashira coupling followed by mesylation and bromination with lithium bromide furnished 3-substituted propargyl bromides **5.078 A-C** and the alkenyl bromides **5.077 D-E** and **5.075** were obtained by bromination in presence of PBr_3. The 4-substituted cinnamyl alcohol derivatives **5.087** were prepared by Wittig reaction of substituted benzaldehydes and phosphonium ylide PPh_3=$CHCO_2Et$. The resulting *α,β*-unsaturated esters **5.086** were reduced to corresponding alcohol by nucleophilic hydride transfer from DIBAL-H. In case of *β*-methyl cinnamyl alcohol **5.090** the initial *α,β*-unsaturated ester **5.089** was obtained by Wittig-Horner reaction with acetophenone and more nucleophilic phosphonate stabilized carbanion of triethyl phosphonoacetate (**Scheme 5.16**).

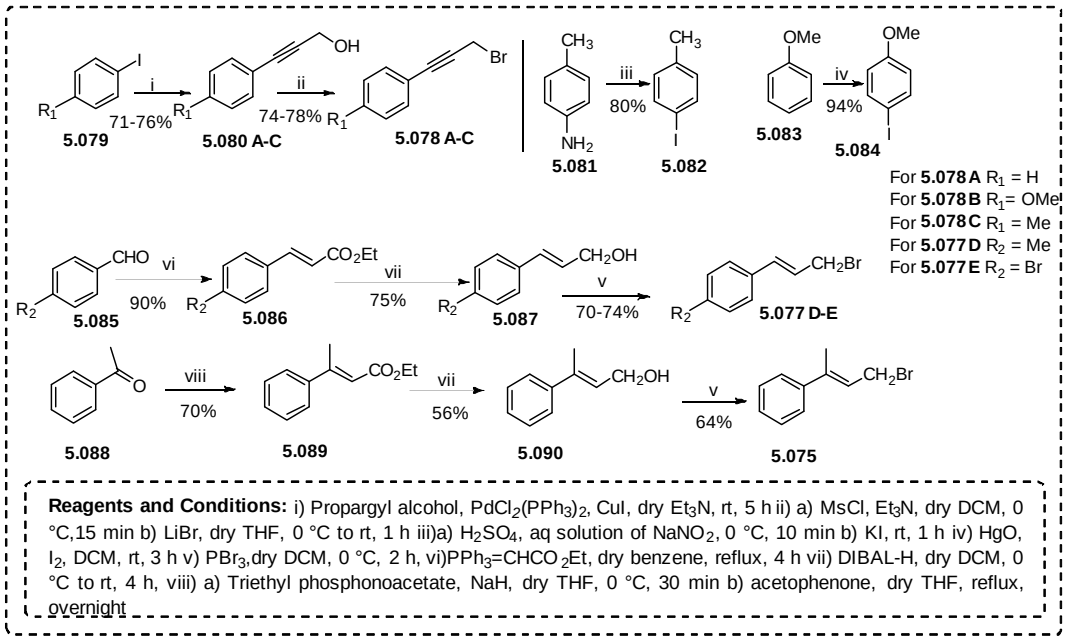

Scheme 5.16: Synthesis of propargyl and alkenyl bromides

5.4 B. Synthesis of Unsymmetrical Propargyl alkenyl Sulfones

The oxidation of sulfides **5.072 A-F**, **5.076** to the corresponding sulfones **5.091 A-F**, **5.068** was achieved by oxone whose active oxidant was potassium peroxomonosulfate ($KHSO_5$) in a mixed solvent medium of THF and methanol. The reagent gave rise to chemoselective oxidation of sulfide only without any oxidation of alkene functionality (**Scheme 5.17**).

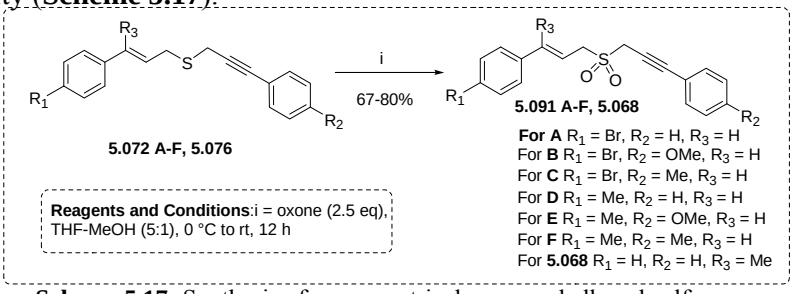

Scheme 5.17: Synthesis of unsymmetrical propargyl alkenyl sulfones

5.4 C. Base mediated cyclization of propargyl alkenyl sulfones

The p*K*a[100] of the methylene hydrogens of alkenyl and propargyl sulfones were reported to be in between 20-22. Hence, NaH (p*K*a = 35) was chosen as a base. Thus a DMSO solution of sulfone **5.091 B** was treated with 1.2 equivalent of NaH in ice-cold condition for 10 minutes that gave rise to the formation of a single distinct spot as analyzed by thin layer chromatography. The product was then purified by column chromatography and after performing NMR (**Figure 5.02**, **5.03**), COSY and HRMS analysis the product was confirmed to be 4-(4-bromophenyl)-5-(4-methoxybenzyl)-2*H*-thiopyran 1,1-dioxide **5.092 B** instead of tetrahydro thiofene-1,1-dioxide derivative **5.093 A-C** (**Scheme 5.18**) possible *via* a GB like rearrangement. The results of base mediated reaction of the substituted precursors of propargyl alkenyl sulfones appeared to be same as their unsubstituted analogues performed previously.

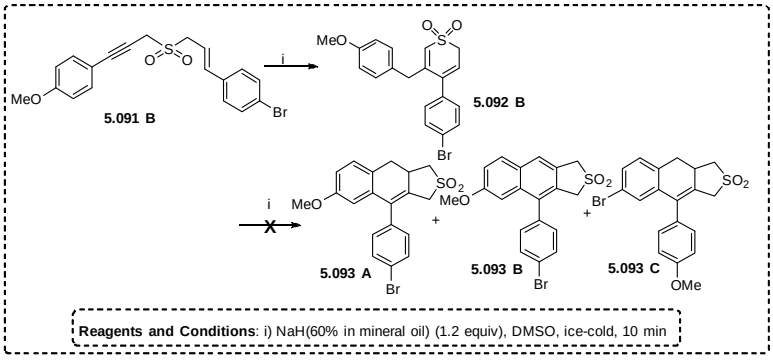

Scheme 5.18: Structure of expected tetrahydrothiofene 1,1-dioxide derivative *via* intramolecular Diels Alder reaction

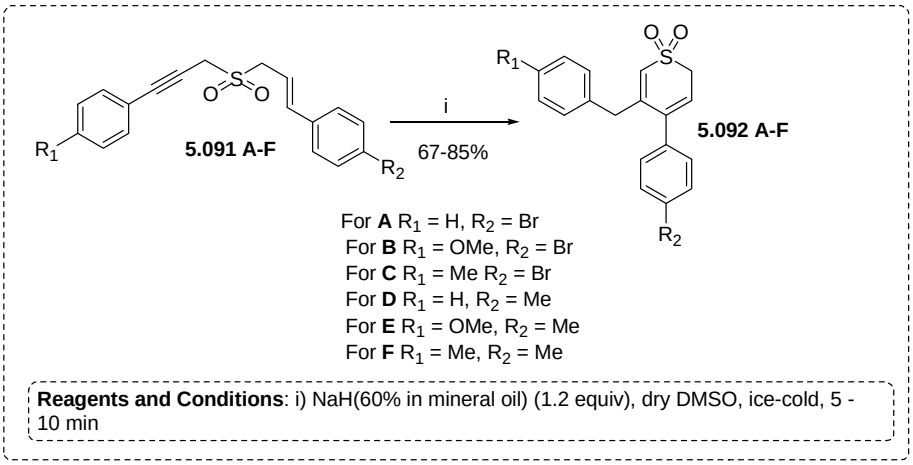

Scheme 5.19: Results of base mediated cyclization of propargyl alkenyl sulfones

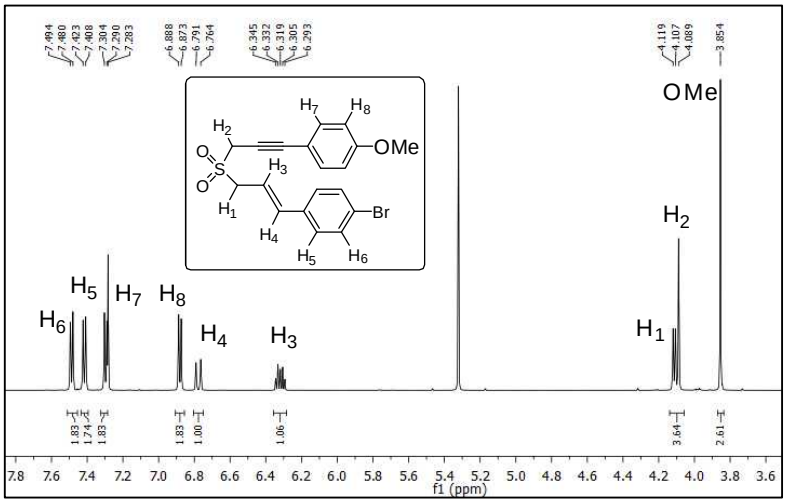

Figure 5.02: Representative ^{1}H-NMR (600 MHz) spectrum of alkenyl propargyl sulfone **5.091 B**

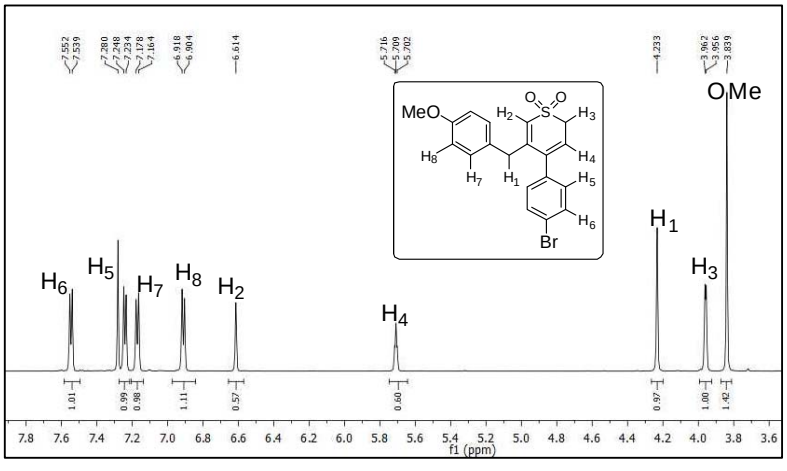

Figure 5.03: Representative ^{1}H-NMR (600 MHz) spectrum of thiopyran dioxide **5.092 B**

Similar thiopyran dioxide derivatives were obtained from moderate to decent yield upon treatment of base with analogous alkenyl propargyl sulfones **5.091 A-F** (**Scheme 5.19**). The reaction was quite general and proceeded smoothly with both electron donating and withdrawing substituents appended with alkyne part as well as the alkene moiety except for strong electron withdrawing substituent $–NO_2$. For all the substrates, the reaction did not follow intramolecular anionic Diels Alder pathway to sulfolane derivatives as proposed by Kudoh *et al*., rather it involved formation of only one new C-C bond to 2*H*-thiopyran derivatives. The outcome of base mediated cyclization to thiopyran dioxide derivatives is shown in **Figure 5.04**.

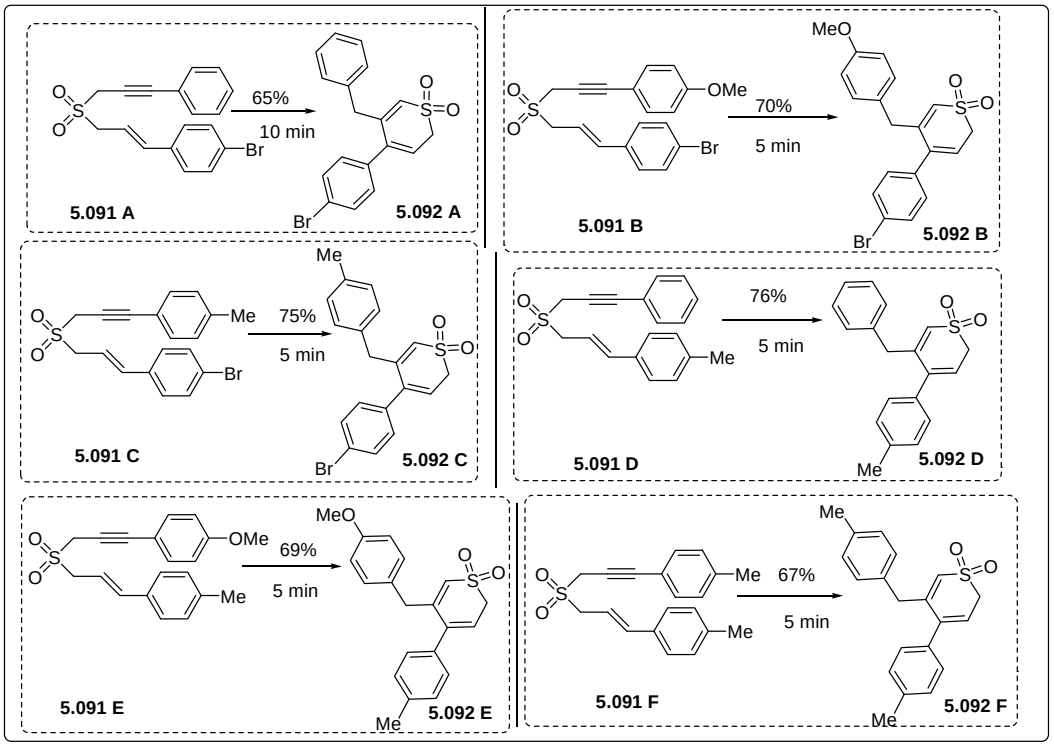

Figure 5.04: Synthesis of 4,5-disubstituted 2*H*-thiopyran 1,1 dioxides

5.4 D. Effect of solvent polarity

We had performed the reaction in non-polar solvents like dichloromethane in presence of NaH. The reaction did not proceed and the starting materials were recovered unchanged. However, we were fortunate to isolate product from reaction mixture in moderately polar solvent like THF in presence of NaH for sulfone **5.094** (**Scheme 5.20**). In contrast to the 4,5-disubstituted thiopyran dioxide **5.096**[97] as obtained in DMSO, in this case, the product was confirmed to be an exomethylene

compound **5.095** that was further characterized by single crystal X-Ray analysis. Thus the polarity of the solvent had a dramatic effect on the nature of the product and it also illustrated a possible mechanistic pathway of cyclization to thiopyran derivatives described later.

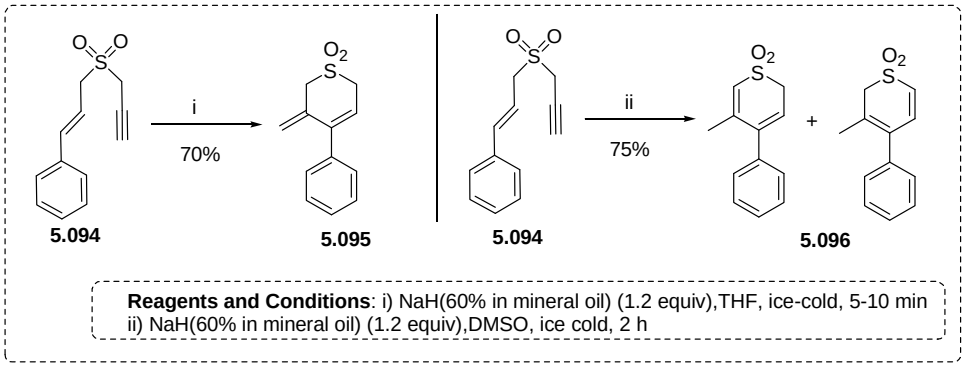

Scheme 5.20: Distinct nature of base mediated cyclization of **5.094** in THF and DMSO

5.4 E. Hydrogenation of thiopyran moiety: Synthesis of dihydro and tetrahyrothiopyran derivatives

The following two compounds where a phenyloxazolidinone moiety was attached to a thiopyran ring by a C-C bond (**Figure 5.05**) were known to possess antimicrobial property due to the presence of oxazolidinone moiety along with minimum MAO inhibitory activity.

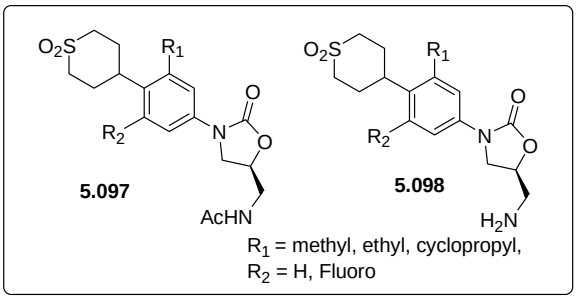

Figure 5.05: Bioactive tetrahydrothiopyran derivatives

Considering the biological activity[101] of dihydro and tetrahydrothiopyran derivatives one of the synthesized thiopyran dioxide **5.099**[97] was subjected to hydrogenation[102] in presence of 10% Pd/C catalyst in methanol (**Scheme 5.21**). The reaction gave rise to the formation of an inseparable mixture of hydrogenated products. However we were able to isolate and characterize the dihydrogenated product **5.100** (**Figure 5.06 A**) formed by selective hydrogenation of the diene. The product was isolated as a white solid after fractional crystallization of the crude reaction mixture. The mother liquor

contained an inseparable mixture of cis and trans tetrahydrothiopyran derivatives **5.101** (**Figure 5.06 B**).

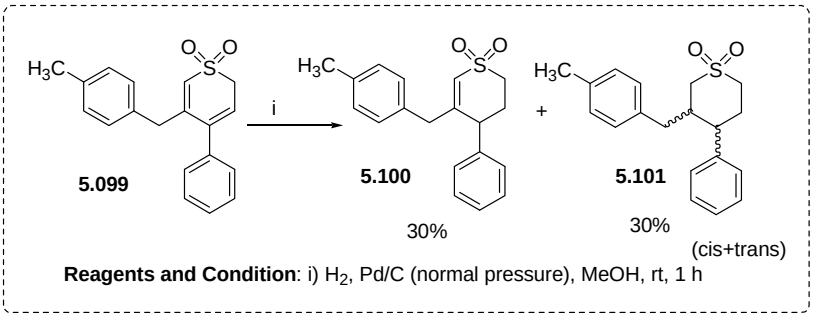

Scheme 5.21: Hydrogenation of 5-(4-Methyl-benzyl)-4-phenyl-*2H*-thiopyran 1, 1-dioxide

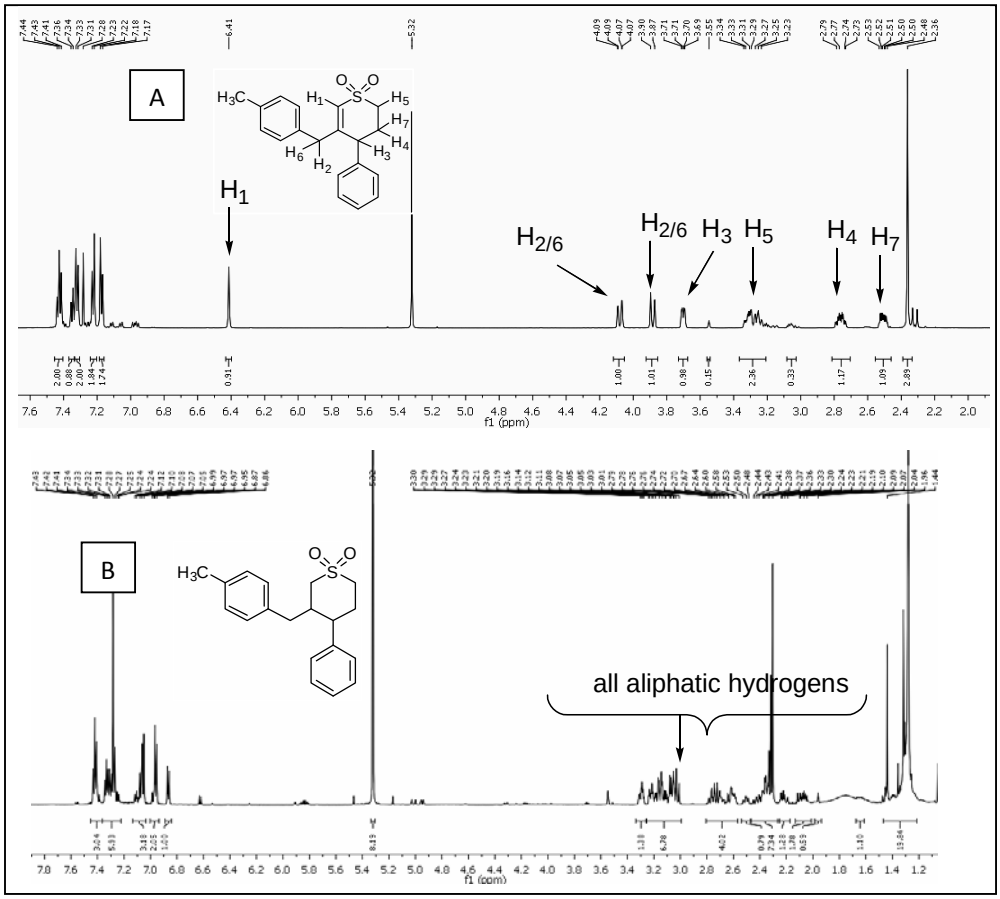

Figure 5.06: Representative ^{1}H-NMR of dihydrothiopyran **5.100** (600 MHz) and tetrahydrothiopyran **5.101** derivatives (400 MHz)

5.4 F. Mechanistic Study

Analyzing the structure of the products formed along with information gained from literature an exothermic[103] 6π-electrocyclization mechanism for the cyclization of the propargyl alkenyl sulfones to thiopyran derivatives was proposed. In 1982 Minkin *et al*. reported[104] theoretical calculations and predicted a favourable equilibrium towards electrocyclization to 2*H*-thiopyran ring involving a C=S bond (**Figure 5.07**).

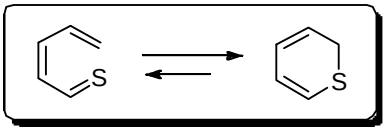

Figure 5.07: A favourable electrocyclization to 2*H*-thiopyran ring

We anticipated that due to the comparable p*K*a of the propargylic and allylic hydrogens for sulfone both the two hand underwent deprotonation simultaneously which was not the case for ethers. The isomerization of propargyl hand to allene **5.107** with concomitant sulfinate generation from alkene hand gave rise to the formation of a 1,3,5 triene **5.109** essential for electrocyclization. At this point one may argue about the nature of sulfone moiety whether it is electron withdrawing or electron delocalizing in nature. There are reports of electron accepting nature of cyclic sulfone moiety. In 1962 Corey *et al*. reported[105] the decarboxylation of optically active sulfone **5.102** (**Figure 5.08**) to completely racemic sulfone and also reported the existence of C_α-S π-bond.

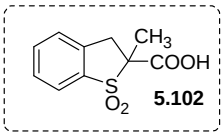

Figure 5.08: Structure of sulfone studied by Corey *et al.* for decarboxylation followed by racemization experiment

Later Namboothiri *et al*. in 2014 proposed the existence of similar C_α-S π-bond during reaction of vinyl sulfones with *α*-diazo-*β*-keto sulfones.[106] The 6π-electrocyclization mechanism to thiopyran rings is shown in **Scheme 5.22**.

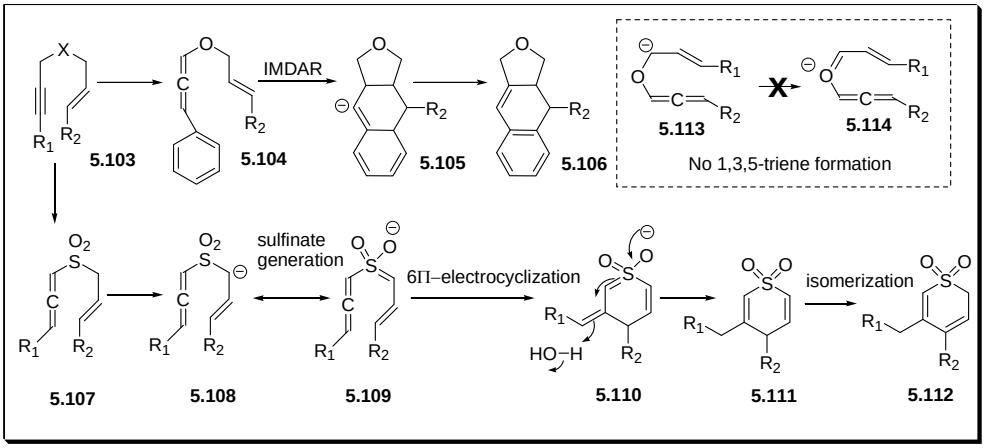

Scheme 5.22: Proposed 6π-electrocyclization mechanism

According to the mechanism proposed it comes out that 6π-electrocyclization is favourable than intramolecular Diels Alder reaction in case of alkenyl propargyl sulfones. In contrast to sulfones, ethers are unable to generate 1,3,5 triene prerequisite for 6π-electrocyclization. An alternate mechanism for cyclization of propargyl alkenyl sulfones could be a 6-exo-dig process (**Scheme 5.23**) favourable according to Baldwin's rule[107].

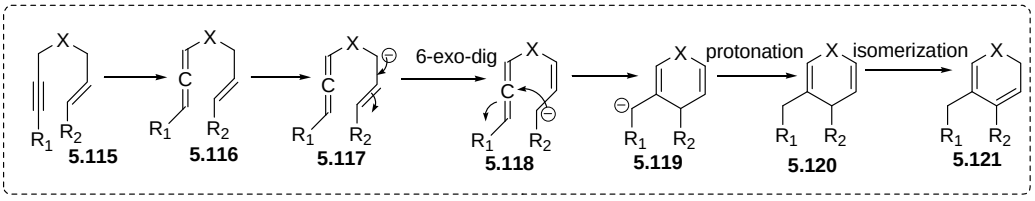

Scheme 5.23: An alternate 6-exo-dig process to thiopyran rings

The 6-exo-dig process of cyclization was discarded as we were unable to isolate any pyran derivatives from propargyl alkenyl ethers. The mechanism was further supported by the isolation of exomethylene compound **5.095** (by carrying out the reaction in THF) which could have generated by 1,3 protonation after 6π-electrocyclization (**Scheme 5.24**).

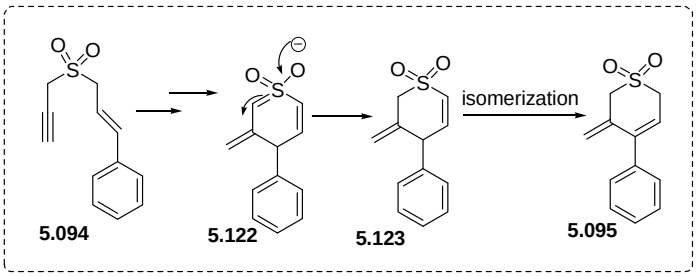

Scheme 5.24: 6π-electrocyclization mechanism in THF

To further provide additional evidences to the proposed mechanistic pathway and to gain insight about the H–shifts, we studied the base mediated outcome of propargyl alkenyl sulfone **5.068** with *β*-methyl cinnamyl moiety expecting to isolate intermediate **5.092 I**. However we could not isolate any well defined product from this reaction (**Scheme 5.25**).

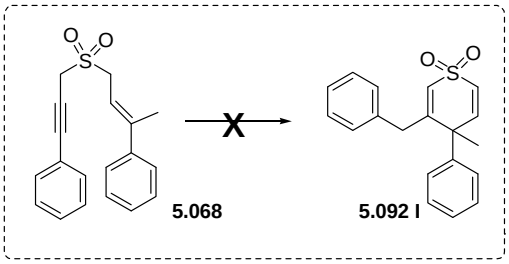

Scheme 5.25: Attempted cyclization of propargyl alkenyl sulfone **5.068**

We then performed deuterium incorporation experiment in deuterated solvents. Initially we attempted the reaction in d_4-MeOH but we were unable to reproduce the reaction in protic solvent. Later the reaction was carried out in d_6-DMSO and NaH and the reaction was quenched with H_2O. The product isolated did not contain any deuterium as revealed by ^{1}H-NMR analysis. The reaction was repeated with d_6-DMSO/NaH and quenched with D_2O. This time the product isolated was diagnosed to have deuterium at benzylic CH_2 as well as CH_2 adjacent to sulfone moiety. To confirm whether the incorporation of deuterium occurred during cyclization or after product formation followed by exchange with deuterium, we treated one of the thiopyran products **5.099** with d_6-DMSO/NaH and subsequent D_2O quenching. Deuterium was detected in same proportions at benzylic CH_2 as well as CH_2 adjacent to sulfone moiety (**Figure 5.09**). Thus, deuterium scrambling experiment remained inconclusive because of this exchange problem.

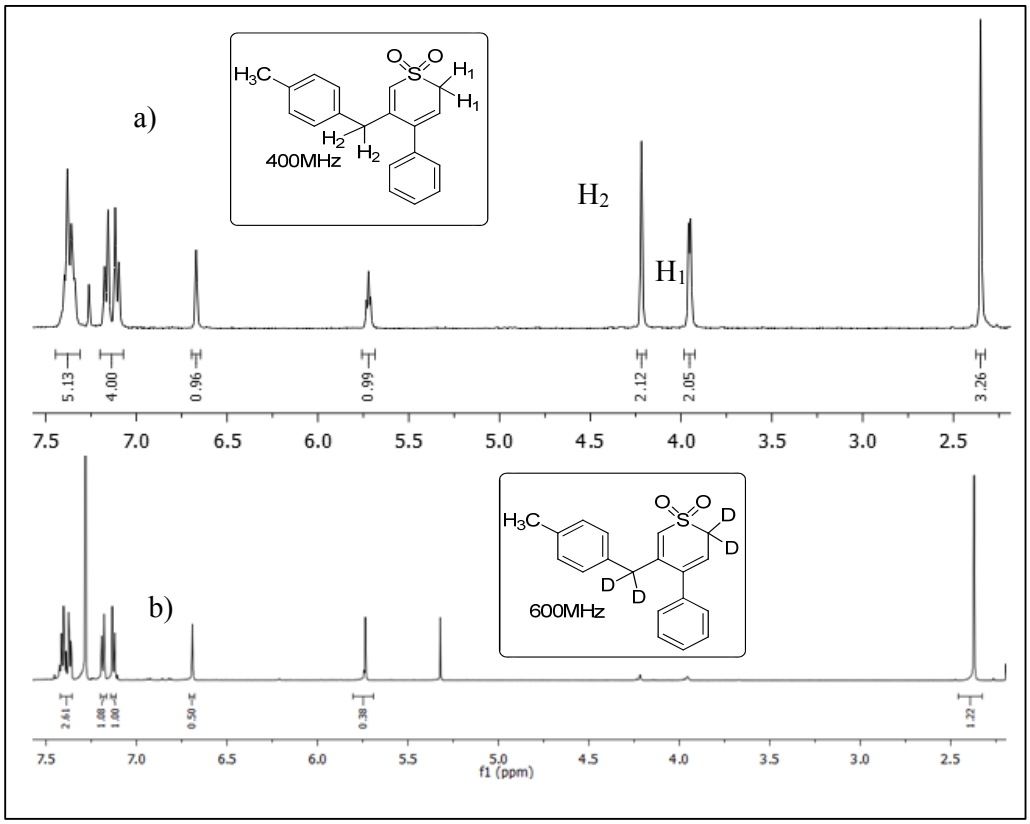

Figure 5.09: Representative ^{1}H-NMR spectrum of **5.099** a) reaction performed in NaH/DMSO followed by H_2O quenching b) reaction performed in NaH/DMSO followed by D_2O quenching

5.4 G. Spectral characterizations

The structure of all the compounds synthesized was elucidated by ^{1}H-NMR, ^{13}C-NMR, Dept-135, COSY and HRMS analysis.

In case of ^{1}H-NMR spectrum of compound **5.092 C**, recorded in 600 MHz, the three methyl protons of 4-methyl phenyl moiety appeared as sharp singlet at δ 2.37. The methylene protons H_3 adjacent to sulfone moiety appeared as doublet due to the coupling with vinyl protons H_4 at δ 3.96 with J = 4.2 Hz. The benzylic protons H_1 appeared as singlet at δ 4.23. Now coming to the vinylic protons H_4 appeared as triplet at δ = 5.73 with coupling constant J = 4.2 Hz. The other alkenyl proton H_2 appeared downfield as singlet at δ 6.65 due to the electron withdrawing effect of sulfone moiety. The aromatic protons H_7 appeared as doublet due to the coupling with H_8 protons at δ 7.12 with J = 7.8 Hz whereas H_8 protons appeared as doublet at δ 7.19

with J = 7.8 Hz. The other aromatic protons H_5 corresponding to 4-bromo phenyl ring appeared as doublet at δ 7.25 with J = 7.8 Hz and the maximum downfield shifted proton was H_6 that appeared as doublet at δ 7.55 with J = 7.8 Hz (**Figure 5.10**).

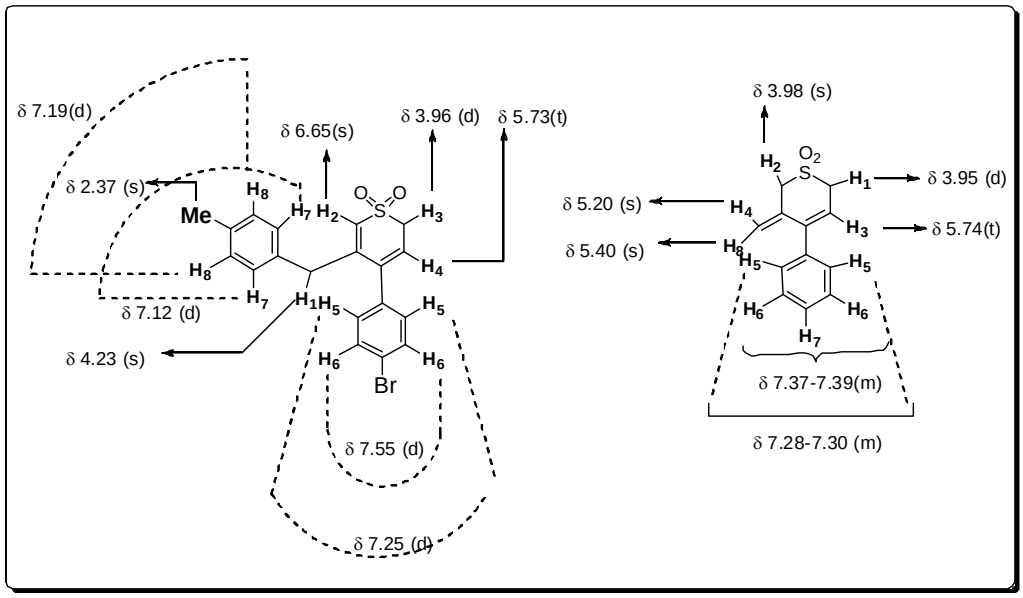

Figure 5.10: ^{1}H-NMR assignment of compound **5.092 C** and **5.095**

All the structures of the other analogues of this whole series were determined following the same clarification. The ^{13}C-NMR spectrum of **5.092 C** was also in conformity of the structure and showed the presence of methyl, methylene and benzylic carbons at 21.3, 52.0 and 52.1 ppm respectively which was further confirmed by DEPT-135 spectrum analysis. Mass spectral analysis of this compound showed a peak at 411.0034 (calcd 411.0030) corresponding to $[M+Na]^{+}$.The structure was further confirmed by the interactions (off-diagonal peaks) observed in COSY spectrum (**Figure 5.11 A**, **5.11 B**).

A)

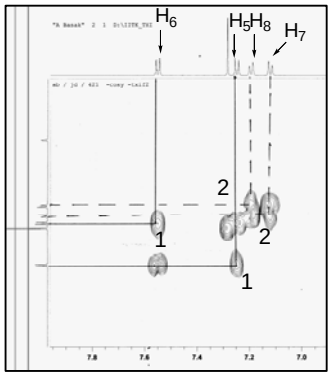

B)

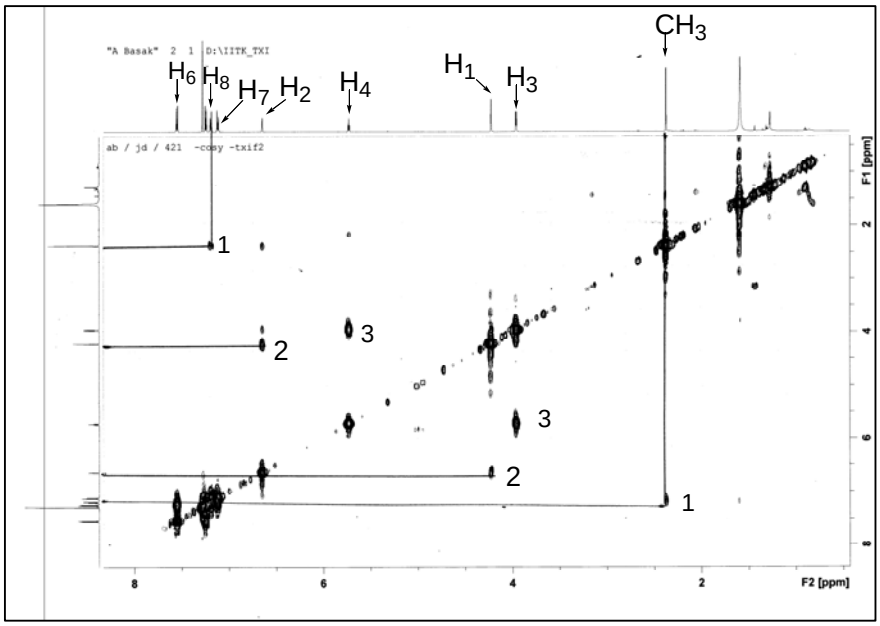

Figure 5.11: COSY spectrum of compound **5.092 C**. A) Only aromatic region of the spectrum B) Full spectrum. The numbers denote the contours arising from ^{1}H-^{1}H interaction through bond of the corresponding compound **5.092 C**.

In the ^{1}H-NMR spectrum of compound **5.095**, H_1 appeared as doublet due to coupling interaction with H_3 at δ 3.95 with J = 4.2 Hz whereas H_2 appeared as singlet at δ 3.98. The exomethylene proton H_4 appeared as singlet at δ 5.20 and H_8 appeared slight downfield as singlet at δ 5.40 due to deshielding effect of adjacent aryl ring π-electron cloud. The vinylic proton H_3 appeared at δ 5.74 as a triplet due to coupling with H_1 protons with J = 4.2 Hz. The aromatic protons H_5 appeared as multiplet in between δ 7.28-7.30 and H_6, H_7 also appeared as multiplet at δ 7.37-7.39. In ^{13}C-NMR the secondary methylene carbon appeared at δ 123.3 that was further confirmed by DEPT-135 NMR spectrum. Mass spectra showed a peak at 243.0452 (calcd 243.0456) corresponding to $[M+Na]^{+}$. Further confirmation of the structure was obtained from single crystal X-ray analysis of **5.095** (ORTEP diagram is shown in **Figure 5.12**).

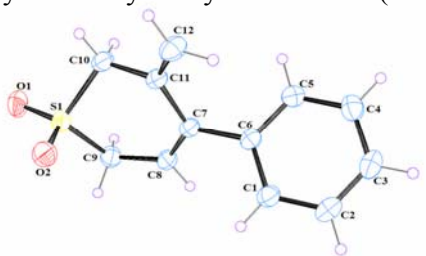

Figure 5.12: ORTEP diagram of compound **5.095** (CCDC number 1055927)

5.5 Conclusion

- We have successfully synthesized various alkenyl propargyl sulfones appended with different electron donating and withdrawing substituents and have been able to synthesize thiopyran dioxide derivatives *via* a 6π-electrocyclization process.
- The effect of solvent polarity on the outcome of the reaction was also investigated.
- The scope of the reaction was further extended to synthesize dihydro and tetrahydrothiopyran derivatives.
- The mechanism of 6π-electrocyclization was further investigated and confirmed.
- The synthesized thiopyran derivatives will be screened for any biological activity in future.

5.6 Experimental Details

5.6.1 General Experimental

General experimental procedures are same as described at page no. 59 in Chapter 2.

5.6.2 General procedure for synthesis of compounds and their spectral data

General Procedure for the synthesis of sulfones (5.091 A-F, 5.068)

The procedure is same as described at page no. 60 in Chapter 2.

(*E*)-1-bromo-4-(3-(3-phenylprop-2-ynylsulfonyl)-prop-1-enyl)-benzene (5.091 A)

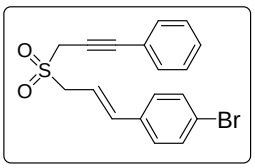

State: yellow solid; m.p. 94 - 95 °C; **yield**: 300 mg, 80%; IR (neat) ν_{max} 3045, 2967, 2245, 1635, 1445, 1312, 755, 550 cm^{-1}; ^{1}H NMR (600 MHz, Chloroform-*d*) δ 7.49 (d, *J* = 12 Hz, 3H), 7.43 - 7.40 (m, 1H), 7.38 - 7.35 (m, 2H), 7.30 (d *J* = 12 Hz, 2H), 7.28 (s, 1H), 6.78 (d, *J* = 18 Hz, 1H), 6.32 (dt, *J* = 18 Hz, 6 Hz, 1H), 4.12 (d, *J* = 6 Hz, 2H), 4.11 (s, 2H); ^{13}C NMR (150 MHz, Chloroform-*d*) δ 138.5, 134.4, 131.9, 129.3, 128.5,

128.3, 122.8, 121.4, 115.6, 88.15, 76.4, 55.7, 44.8; HRMS: Calcd. for $C_{18}H_{16}BrO_2S^+$ $[M+H]^+$ 375.0054 found 375.0060.

(*E*)-1-bromo-4-(3-(3-(4-methoxyphenyl)prop-2-ynylsulfonyl)-prop-1-enyl)-benzene (5.091 B)

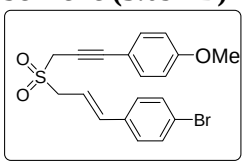

State: pale yellow solid; m.p. 145 - 146 °C; **yield**: 282 mg, 70%; IR (neat) ν_{max} 3087, 2975, 2950, 2835, 2219, 1610, 1313, 1159, 1130, 1050, 725, 575 cm^{-1}; ^1H NMR (600 MHz, Chloroform-*d*) δ 7.49 (d, *J* = 8.4 Hz, 2H), 7.41 (d, *J* = 9 Hz, 2H), 7.30 (d, *J* = 8.4 Hz, 2H), 6.88 (d, *J* = 9 Hz, 2H), 6.78 (d, *J* = 16.2 Hz, 1H), 6.32 (dt, *J* = 16.2 Hz, 6 Hz, 1H), 4.12 (d, *J* = 6 Hz, 2H), 4.09 (s, 2H), 3.85 (s, 3H); ^{13}C NMR (150 MHz, Chloroform-*d*) δ 160.4, 138.4, 134.4, 133.5, 131.9, 128.3, 122.8, 115.7, 114.2, 113.4, 88.2, 75.0, 55.6, 55.4, 44.9; HRMS: Calcd. for $C_{19}H_{18}BrO_3S^+$ $[M+H]^+$ 405.0160 found 405.0167.

(*E*)-1-bromo-4-(3-(3-*p*-tolylprop-2-ynylsulfonyl)-prop-1-enyl)-benzene (5.091 C)

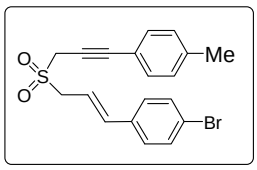

State: white solid; m.p. 180 - 181 °C; **yield**: 291 mg, 75%; IR (neat) ν_{max} 3077, 2974, 2850, 2220, 1659, 1440, 1323, 1126, 752, 560 cm^{-1}; ^1H NMR (600 MHz, Chloroform-*d*) δ 7.49 (d, *J* = 8.4 Hz, 2H), 7.38 (d, *J* = 7.8 Hz, 2H), 7.30 (d, *J* = 8.4 Hz, 2H), 7.18 (d, *J* = 7.8 Hz, 2H), 6.77 (d, *J* = 15.6 Hz, 1H), 6.32 (dt, *J* = 15.6 Hz, 6 Hz, 1H), 4.12 (d, *J* = 6 Hz, 2H), 4.09 (s, 2H), 2.40 (s, 3H); ^{13}C NMR (150 MHz, Chloroform-*d*) δ 139.7, 138.4, 134.4, 131.9, 131.8, 129.2, 128.3, 122.8, 118.3, 115.6, 88.4, 75.7, 55.6, 44.9, 21.6; HRMS: Calcd. for $C_{19}H_{18}BrO_2S^+$ $[M+H]^+$ 389.0211 found 389.0217.

(*E*)-1-methyl-4-(3-(3-phenylprop-2-ynylsulfonyl)-prop-1-enyl)-benzene (5.091 D)

State: off-white solid; m.p. 110 - 111 °C; **yield**: 239 mg, 77%; IR (neat) ν_{max} 3045, 2937, 2878, 2234, 1630, 1456, 1312, 1125, 750 cm^{-1}; ^1H NMR (600 MHz, Chloroform-*d*) δ 7.50 (d, *J* =8.4 Hz, 2H), 7.43 - 7.34 (m, 5H), 7.18 (d, *J* = 7.8 Hz, 2H), 6.82 (d, *J* = 15.6 Hz, 1H), 6.27 (dt, *J* = 15.6 Hz, 7.2 Hz, 1H), 4.12 (d, *J* = 7.8 Hz, 2H), 4.10 (s, 2H), 2.38 (s, 3H); ^{13}C NMR (150 MHz, Chloroform-*d*) δ 139.6, 139.0, 132.7, 132.0,

129.5, 129.3, 128.5, 126.8, 121.6, 113.7, 88.0, 76.5, 55.8, 44.4, 21.3; HRMS: Calcd. for $C_{19}H_{19}O_2S^+$ $[M+H]^+$ 311.1106 found 311.1108.

(*E*)-1-methoxy-4-(3-(3-*p*-tolylallylsulfonyl)-prop-1-ynyl)-benzene (5.091 E)

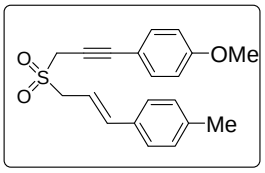

State: pale yellow solid; m.p. 115 - 116 °C; **yield**: 245 mg, 72%; IR (neat) ν_{max} 3078, 2925, 2235, 1656, 1456, 1320, 1125, 1055, 753 cm^{-1}; ^1H NMR (600 MHz, Chloroform-*d*) δ 7.44 (d, *J* =9 Hz, 2H), 7.32 (d, *J* = 7.8 Hz, 2H), 7.18 (d, *J* = 7.8 Hz, 2H), 6.89 (d, *J* = 8.4 Hz, 2H), 6.81 (d, *J* = 15.6 Hz, 1H), 6.26 (dt, *J* = 15.6 Hz, 7.8 Hz, 1H), 4.11 (d, *J* = 7.8 Hz, 2H), 4.08 (s, 2H), 3.85 (s, 3H), 2.38 (s, 3H); ^{13}C NMR (150 MHz, Chloroform-*d*) δ 160.3, 139.6, 138.9, 133.5, 132.8, 129.5, 126.8, 114.1, 113.7, 113.6, 88.0, 75.1, 55.7, 55.4, 44.5, 21.3; HRMS: Calcd. for $C_{20}H_{21}O_3S^+$ $[M+H]^+$ 341.1211 found 341.1213.

(*E*)-1-methyl-4-(3-(3-*p*-tolylallylsulfonyl)-prop-1-ynyl)-benzene (5.091 F)

State: off-white solid; m.p. 157 - 158 °C; **yield**: 217 mg, 67%; IR (neat) ν_{max} 3075, 2956, 2850, 2221, 1620, 1445, 1363, 1128, 753 cm^{-1}; ^1H NMR (600 MHz, Chloroform-*d*) δ 7.40 (d, *J* = 7.8 Hz, 2H), 7.34 (d, *J* = 7.2 Hz, 2H), 7.18 (d, *J* = 7.8 Hz, 4H), 6.82 (d, *J* = 16.2 Hz, 1H), 6.26 (dt, *J* = 16.2 Hz, 7.2 Hz, 1H), 4.12 (d, *J* = 7.2 Hz, 2H), 4.09 (s, 2H), 2.40 (s, 3H), 2.38 (s, 3H); ^{13}C NMR (150 MHz, Chloroform-*d*) δ 139.6, 139.5, 138.9, 132.7, 131.9, 129.5, 129.2, 126.8, 118.5, 113.7, 88.2, 75.8, 55.7, 44.5, 21.6, 21.3; HRMS: Calcd. for $C_{20}H_{21}O_2S^+$ $[M+H]^+$ 325.1262 found 325.1269.

(*E*)-(3-(3-phenylbut-2-enylsulfonyl)-prop-1-ynyl)-benzene (5.068)

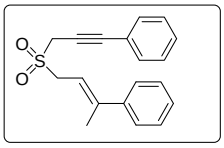

State: yellow liquid; **yield**: 186 mg, 60%; IR (neat) ν_{max} 3055, 2928, 2855, 2243, 1623, 1447, 1311, 755 cm^{-1}; ^1H NMR (600 MHz, Chloroform-*d*) δ 7.47 (dd, *J* = 9 Hz, 6 Hz, 4H), 7.40 - 7.28 (m, 6H), 5.95 (t, *J* = 6 Hz, 1H), 4.19 (d, *J* =6 Hz, 2H), 4.09 (s, 2H), 2.26 (s, 3H); ^{13}C NMR (150 MHz, Chloroform-*d*) δ 145.2, 141.9, 131.9, 129.2, 128.5, 128.2, 126.0, 121.5, 112.5, 87.6, 76.6, 52.2, 44.8, 16.8; HRMS: Calcd. for $C_{19}H_{19}O_2S^+$ $[M+H]^+$ 311.1106 found 311.1114.

General procedure for preparation of thiopyran 1,1-dioxides (5.092 A-F)

The respective sulfones **5.091 A-F**, **5.068** (0.3 mmol, 1.0 eq.) were dissolved in dry DMSO (10 mL) and cooled to ice-cold temperature. Sodium hydride (60% in oil) (9 mg, 0.36 mmol, 1.2 eq.) was then added and stirred for 5-10 min under nitrogen atmosphere. After completion of reaction (monitored by TLC) it was quenched with water (10 mL) and diluted with EtOAc (30 mL). The organic layer was separated, washed with brine solution (3 x 10 mL), dried over (Na_2SO_4) and concentrated under vacuum. The reaction mixture was purified by silica gel column chromatography using petroleum ether/EtOAc as eluent to give the final product.

5-Benzyl-4-(4-bromo-phenyl)-2*H*-thiopyran 1,1-dioxide (5.092 A)

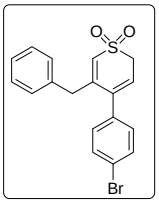

State: white solid; m.p. 195 - 196 °C; **yield**: 73 mg, 65%; IR (neat) ν_{max} 3065, 2943, 1655, 1448, 1305, 752, 556 cm^{-1}; ^1H NMR (600 MHz, Chloroform-*d*) δ 7.56 (d, *J* = 12 Hz, 2H), 7.39 (t, *J* = 6 Hz, 2H), 7.33 (t, *J* = 6 Hz, 1H), 7.25 (d, *J* = 6 Hz, 2H), 7.23 (d, *J* = 12 Hz, 2H), 6.7 (s, 1 Hz), 5.76 (t, *J* = 6 Hz, 1H), 4.22 (s, 2H), 3.97 (d, *J* = 6 Hz, 2H); ^{13}C NMR (150 MHz, Chloroform-*d*) δ 141.7, 138.6, 137.7, 134.9, 131.7, 130.9, 129.1, 128.9, 128.7, 128.3, 122.4, 119.2, 52.1, 30.9; HRMS: Calcd. for $C_{18}H_{15}BrNaO_2S^+$ $[M+Na]^+$ 396.9874 found 396.9875.

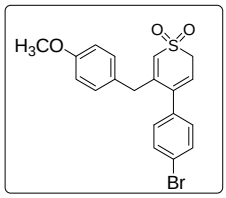

4-(4-Bromo-phenyl)-5-(4-methoxy-benzyl)-2H-thiopyran 1,1-dioxide (5.092 B)

State: off-white solid; m.p. 178 - 179 °C; **yield**: 84 mg, 70%; IR (neat) ν_{max} 3037, 2961, 2855, 1635, 1445, 1367, 1132, 1050, 855, 751, 560 cm^{-1}; ^1H NMR (600 MHz, Chloroform-*d*) δ 7.55 (d, *J* = 7.8 Hz, 2H), 7.24 (d, *J* = 8.4 Hz, 2H), 7.18 (d, *J* = 8.4 Hz, 2H), 6.92 (d, *J* = 8.4 Hz, 2H), 6.61 (s, 1H), 5.71 (t, *J* = 4.2 Hz, 1H), 4.23 (s, 2H), 3.96 (d, *J* = 3.6 Hz, 2H), 3.84 (s, 3H); ^{13}C NMR (150 MHz, Chloroform-*d*) δ 159.6, 141.9, 138.7, 137.4, 131.6, 130.9, 130.4, 127.6, 127.2, 122.3, 118.5, 114.2, 55.3, 52.2, 52.1; HRMS: Calcd. for $C_{19}H_{17}BrO_3SNa^+$ $[M+Na]^+$ 426.9974 found 426.9976.

4-(4-Bromo-phenyl)-5-(4-methyl-benzyl)-2H-thiopyran 1,1-dioxide (5.092 C)

State: pale brown solid; m.p. 172 - 173 °C; **yield**: 87 mg, 75%; IR (neat) ν_{max} 3026,

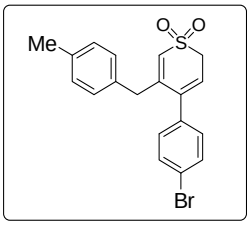

2914, 1632, 1439, 1330, 1110, 845, 754, 562 cm^{-1}; ^1H NMR (600 MHz, Chloroform-*d*) δ 7.56 (d, *J* = 7.8 Hz, 2H), 7.25 (d, *J* = 7.8 Hz, 2H), 7.19 (d, *J* = 7.8 Hz, 2H), 7.12 (d, *J* = 7.8 Hz, 2H), 6.65 (s, 1H), 5.73 (t, *J* = 4.2 Hz, 1H), 4.23 (s, 2H), 3.96 (d, *J* = 4.2 Hz, 2H), 2.37 (s, 3H); ^{13}C NMR (150 MHz, Chloroform-*d*) δ 141.8, 138.7, 138.4, 137.8, 131.9, 131.7, 130.9, 129.4, 128.9, 128.4, 122.4, 188.8, 52.2, 52.1, 21.3; HRMS: Calcd. for $C_{19}H_{17}BrO_2SNa^+$ $[M+Na]^+$ 411.0030 found 411.0034.

5-Benzyl-4-*p*-tolyl-2H-thiopyran 1,1-dioxide (5.092 D)

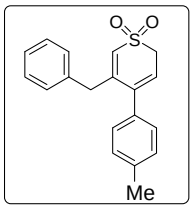

State: off-white solid; m.p. 147 - 148 °C; **yield**:70 mg, 76%; IR (neat) ν_{max} 3032, 2912, 1614, 1442, 1320, 1110, 840, 750 cm^{-1}; ^1H NMR (600 MHz, Chloroform-*d*) δ 7.38 (d, *J* = 7.8 Hz, 2H), 7.32 - 7.22 (m, 7H), 6.75 (s, 1H), 5.74 (t, *J* = 4.2 Hz, 1H), 4.22 (s, 2H), 3.97 (d, *J* = 4.2 Hz, 2H), 2.40 (s, 3H); ^{13}C NMR (150 MHz, Chloroform-*d*) δ 142.6, 138.1, 137.5, 136.8, 135.2, 129.4, 129.1, 128.9, 128.6, 128.1, 118.3, 52.3, 52.1, 21.3; HRMS: Calcd. for $C_{19}H_{18}O_2SNa^+$ $[M+Na]^+$ 333.0925 found 333.0925.

5-(4-Methoxy-benzyl)-4-*p*-tolyl-2H-thiopyran 1,1-dioxide (5.092 E)

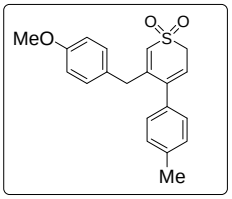

State: sticky white mass; **yield**: 70 mg, 69%; IR (neat) ν_{max} 3037, 2921, 1633, 1442, 1332, 1109, 847, 755 cm^{-1}; ^1H NMR (600 MHz, Chloroform-*d*) δ 7.26 (d, *J* = 7.8 Hz, 2H), 7.21 (d, *J* = 7.8 Hz, 2H), 7.18 (d, *J* = 8.4 Hz, 2H), 6.90 (d, *J* = 9.0 Hz, 2H), 6.69 (s, 1H), 5.70 (t, *J* = 4.8 Hz, 1H), 4.23 (s, 2H), 3.96 (d, *J* = 4.8 Hz, 2H), 3.84 (s, 3H), 2.40 (s, 3H); ^{13}C NMR (150 MHz, Chloroform-*d*) δ 159.5, 142.8, 138.0, 137.1, 136.9, 130.4, 129.1, 128.0, 127.6, 117.6, 114.1, 55.3, 52.2, 21.2; HRMS: Calcd. for $C_{20}H_{20}O_3SNa^+$ $[M+Na]^+$ 363.1031 found 363.1031.

5-(4-Methyl-benzyl)-4-*p*-tolyl-2H-thiopyran 1,1-dioxide (5.092 F)

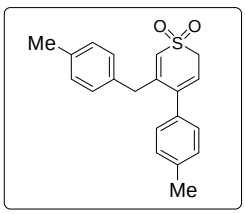

State: sticky white mass; **yield**:65 mg, 67%; IR (neat) ν_{max} 3037, 2922 1623, 1455, 1323, 1120, 847, 751 cm^{-1}; ^1H NMR (600 MHz, Chloroform-*d*) δ 7.26 (d, *J* = 7.8 Hz, 2H), 7.22 (d, *J* = 7.8 Hz, 2H), 7.18 (d, *J* = 7.8 Hz, 2H), 7.13 (d, *J* = 8.4 Hz,

2H), 6.72 (s, 1H), 5.72 (t, *J* = 4.2 Hz, 1H), 4.23 (s, 2H), 3.96 (d, *J* = 4.2 Hz, 2H), 2.41 (s, 3H), 2.37 (s, 3H); ^{13}C NMR (150 MHz, Chloroform-*d*) δ 142.7, 138.1, 138.0, 137.5, 136.9, 132.3, 129.3, 129.1, 128.9, 128.7, 117.9, 52.2, 21.3, 21.2; HRMS: Calcd. for $C_{20}H_{20}O_2SNa^+$ $[M+Na]^+$ 347.1076 found 347.1076.

For thiopyran 1,1-dioxides **5.096** and **5.099** see reference 97.

Hydrogenation of 5-(4-Methyl-benzyl)-4-phenyl-*2H*-thiopyran 1, 1-dioxide (5.099), isolation of compounds 5.100 and 5.101

The thiopyran 1,1-dioxide **5.099** (20 mg, 0.06 mmol) in dry methanol (5 mL) was hydrogenated over 10% Pd/C (8 mg) for 1 h at room temperature. After completion of the reaction, the mixture was filtered and the organic layer was evaporated to give a crude mixture from which partially hydrogenated sulfone **5.100** was isolated pure by fractional crystallization from dichloromethane-pet ether. The mother liquor comprised an inseparable mixture of cis and trans tetrahydropyran derivative **5.101**.

5-(4-Methyl-benzyl)-4-phenyl-3,4-dihydro-2*H*-thiopyran 1,1-dioxide (5.100)

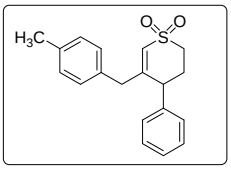

State: white solid; m.p. 145 - 146 °C; **yield**: 5 mg, 30%; IR (neat) ν_{max} 3039, 2934 1634, 1447, 1334, 1120, 752 cm^{-1}; ^{1}H NMR (600 MHz, Chloroform-*d*) δ 7.43 (t, *J* = 6 Hz, 2H), 7.35 (d, *J* = 12 Hz, 1H), 7.32 (d, *J* = 12 Hz, 2H), 7.22 (d, *J* = 6 Hz, 2H), 7.17 (d, *J* = 6 Hz, 2H), 6.41 (s, 1H), 4.08 (d, *J* = 12 Hz, 1H), 3.88 (d, *J* = 18 Hz, 1H), 3.70 (d, *J* = 18 Hz, 1H), 3.34 - 3.23 (m, 2H), 2.79 - 2.73 (m, 1H), 2.53 - 2.58 (m, 1H), 2.36 (s, 3H); ^{13}C NMR (150 MHz, Chloroform-*d*) δ 138.9, 137.5, 133.4, 132.4, 131.9, 129.2, 129.0, 128.8, 128.0, 127.4, 54.3, 53.4, 51.1, 48.1, 28.2, 21.2; HRMS: Calcd. for $C_{19}H_{20}O_2SNa^+$ $[M+Na]^+$ 335.1082 found 335.1089.

3-(4-Methyl-benzyl)-4-phenyl-tetrahydro-thiopyran 1,1-dioxide (*cis* and *trans*) (5.101)

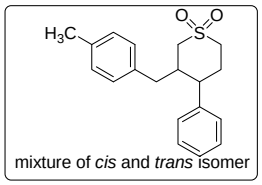

State: gummy mass; **yield** 5 mg, 30%; IR (neat) ν_{max} 3056, 2945 1665, 1458, 1320, 745 cm^{-1}; ^{1}H NMR (400 MHz, Chloroform-*d*) δ 7.43 - 7.41 (m, 3H), 7.34 - 7.24 (m, 6H), 7.12 - 7.05 (m, 3H), 6.94 (d, *J* = 8 Hz, 2H), 6.84 (d, *J* = 8 Hz,

1H), 3.30 - 3.01 (m, 9H), 2.79 - 2.58 (m, 4H), 2.53 - 2.48 (m, 1H), 2.44 - 2.28 (m, 8H), 2.24 - 2.17 (m, 1H), 2.10- 2.01 (m, 2H); ^{13}C NMR (100 MHz, Chloroform-*d*) δ 141.8, 136.3, 136.0, 129.6, 129.4, 129.1, 129.0, 127.8, 127.3, 55.3, 53.6, 52.3, 51.9, 48.7, 44.6, 43.9, 29.9, 25.0, 22.9, 21.2, 14.3 (some peaks may have overlapped); HRMS: Calcd. for $C_{19}H_{23}O_2S^+$ $[M+H]^+$ 315.1413 found 315.1407.

3-Methylene-4-phenyl-3,6-dihydro-2*H*-thiopyran 1,1-dioxide (5.095)

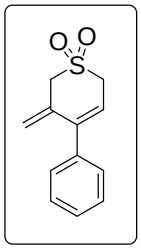

State: pale yellow solid; m.p. 135 - 136 °C; **yield**: 176 mg, 80%; IR (neat) ν_{max} 3210, 2945, 1615, 1420, 1310, 1125, 760 cm^{-1}; ^{1}H NMR (600 MHz, Chloroform-*d*) δ 7.39 - 7.37 (m, 3H), 7.30 - 7.28 (m, 2H), 5.74 (t, *J* = 4.2 Hz, 1H), 5.40 (s, 1H), 5.20 (s, 1H), 3.98 (s, 2H), 3.94 (d, *J* = 4.2 Hz, 2H); ^{13}C NMR (150 MHz, Chloroform-*d*) δ 141.4, 139.2, 135.9, 128.9, 128.3, 128.2, 123.3, 119.2, 57.0, 52.2; HRMS: Calcd. for $C_{12}H_{12}O_2SNa^+$ $[M+Na]^+$ 243.0450 found 243.0452.

5.6.3 ^{1}H and ^{13}C NMR spectra of selected compounds

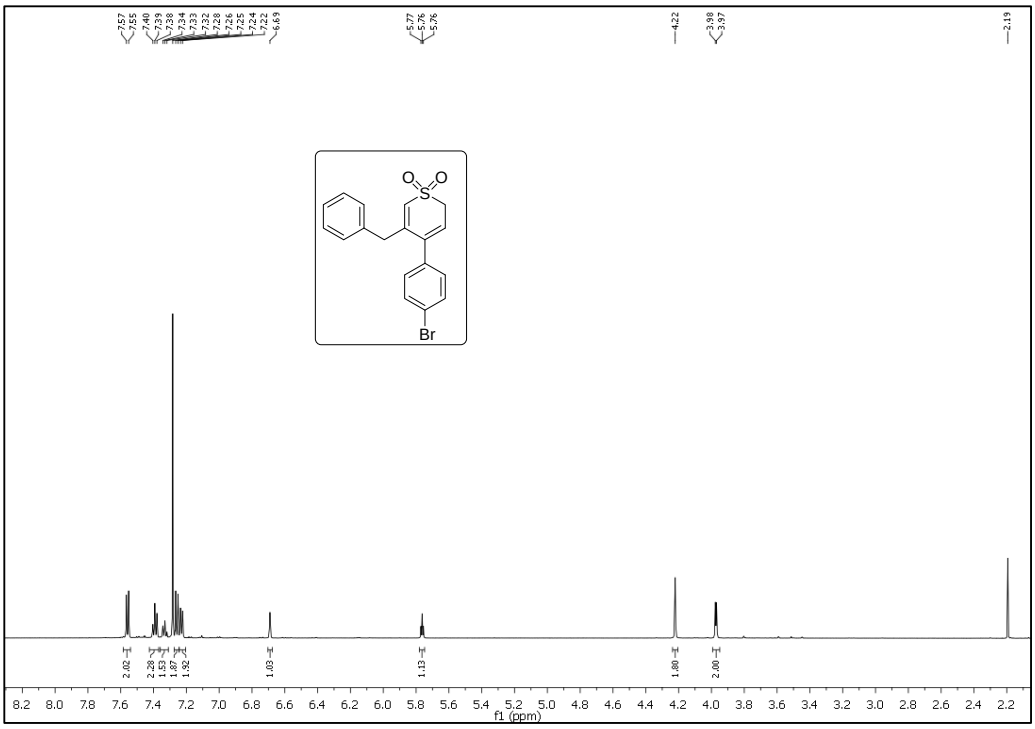

^{1}H NMR ($CDCl_3$, 600 MHz) spectrum of 5.092 A

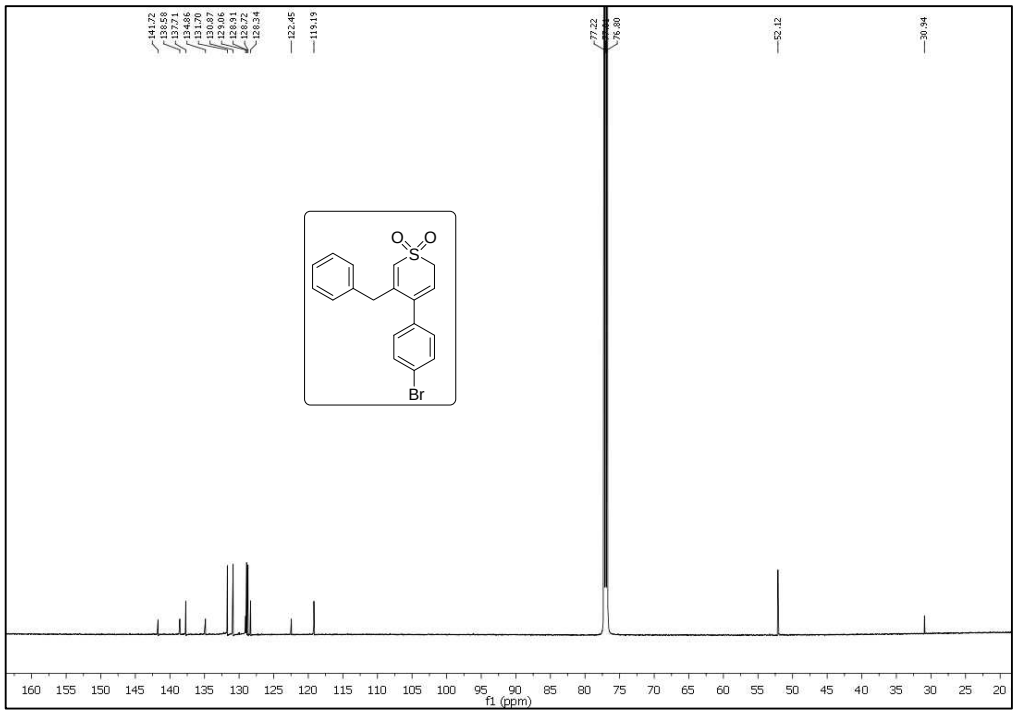

^{13}C NMR ($CDCl_3$, 150 MHz) spectrum of 5.092 A

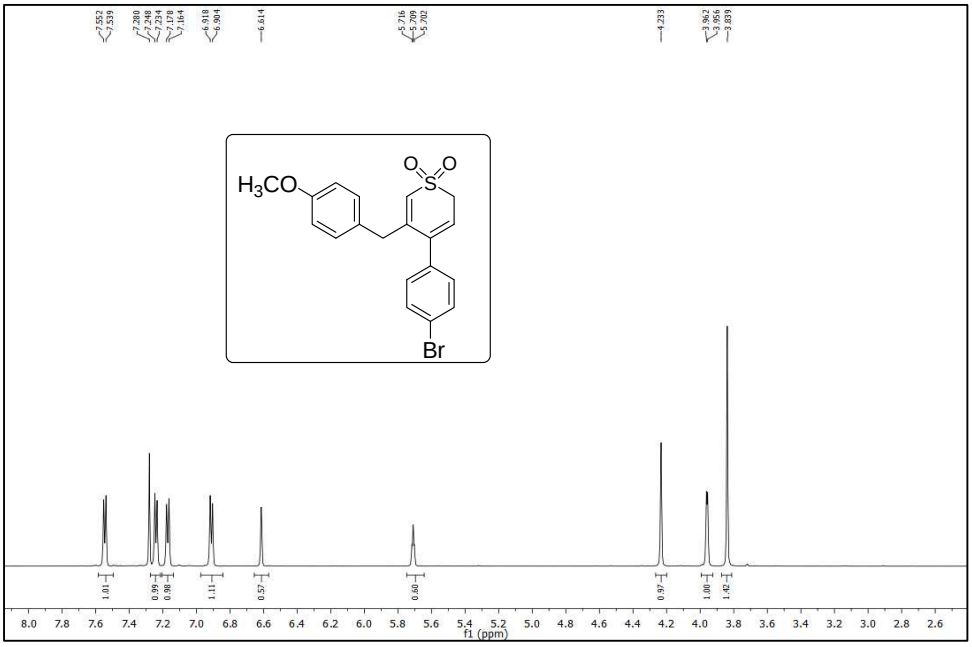

^{1}H NMR ($CDCl_3$, 600 MHz) spectrum of 5.092 B

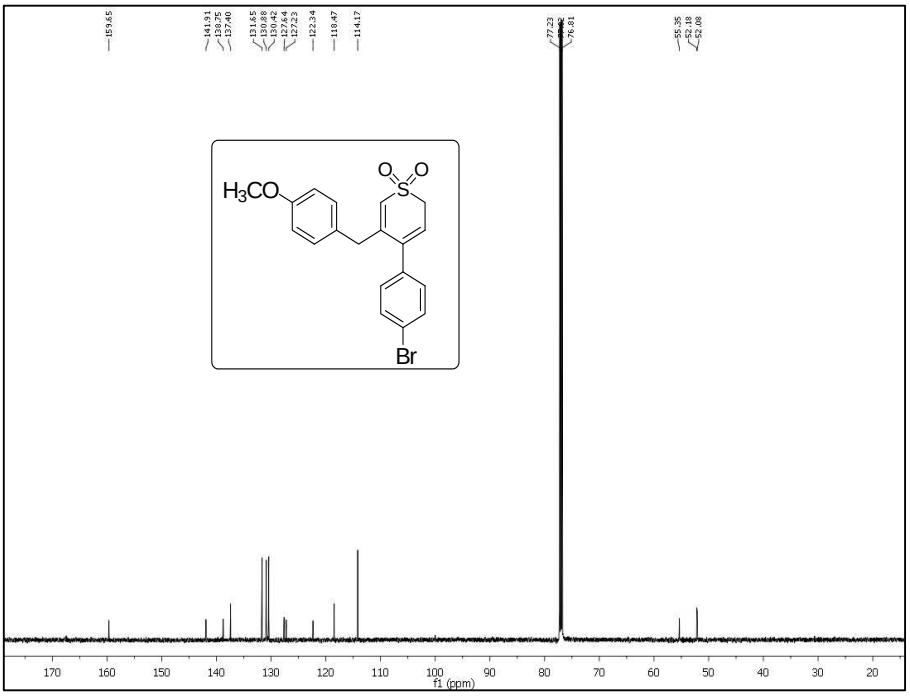

^{13}C NMR ($CDCl_3$, 150 MHz) spectrum of 5.092 B

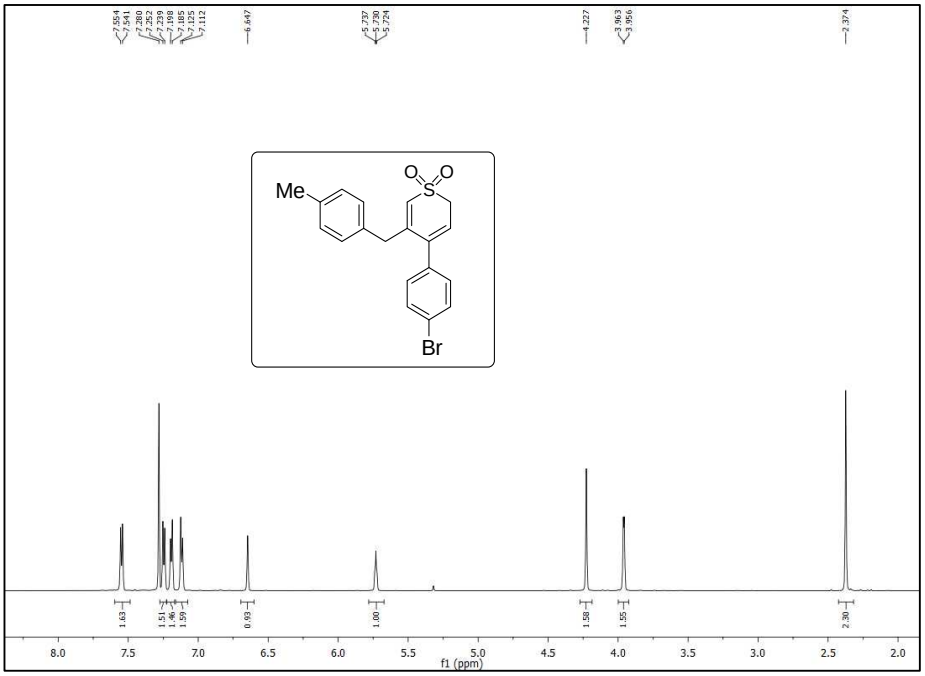

^{1}H NMR ($CDCl_3$, 600 MHz) spectrum of 5.092 C

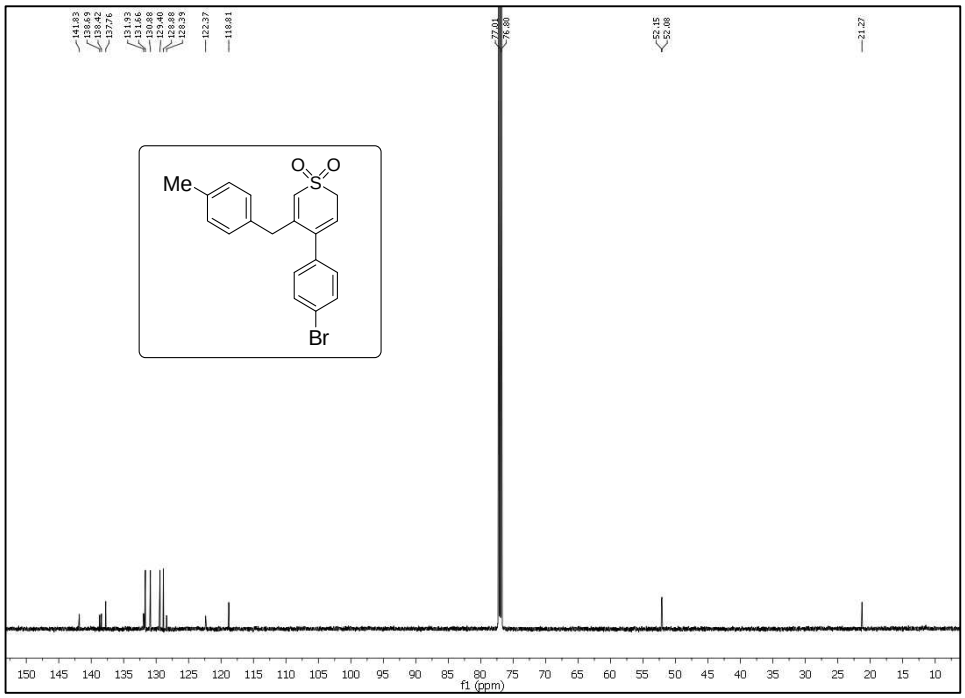

^{13}C NMR ($CDCl_3$, 150 MHz) spectrum of 5.092 C

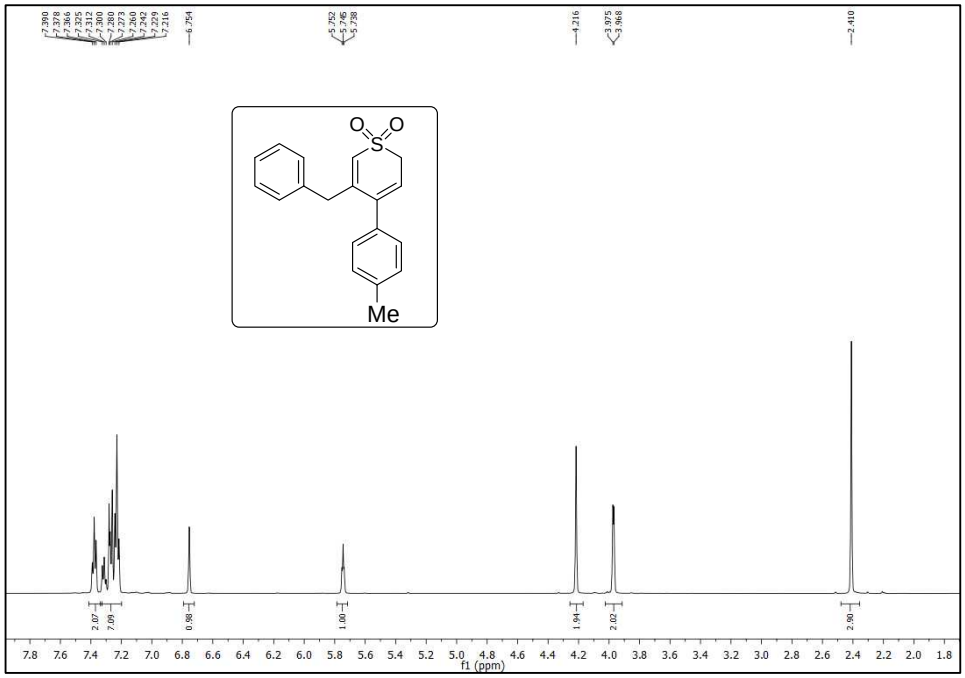

^{1}H NMR ($CDCl_3$, 600 MHz) spectrum of 5.092 D

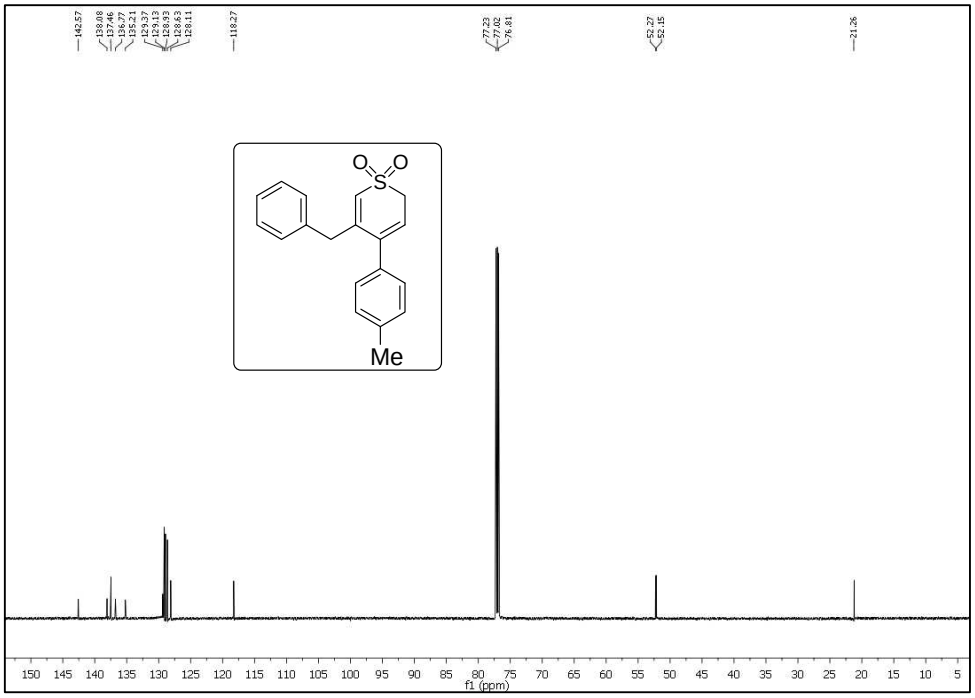

^{13}C NMR ($CDCl_3$, 150 MHz) spectrum of 5.092 D

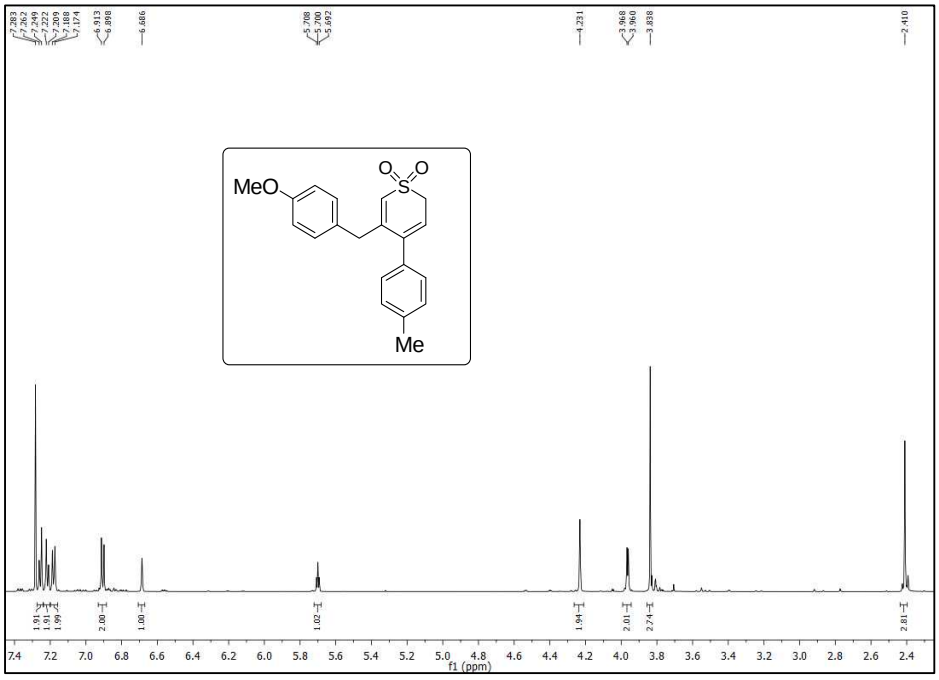

^{1}H NMR ($CDCl_3$, 600 MHz) spectrum of 5.092 E

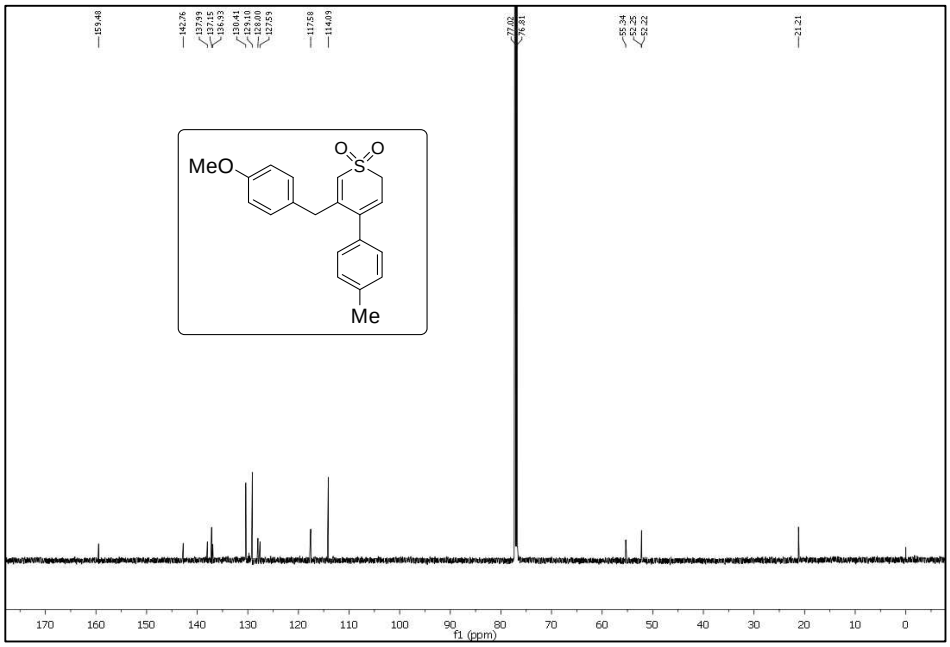

^{13}C NMR ($CDCl_3$, 150 MHz) spectrum of 5.092 E

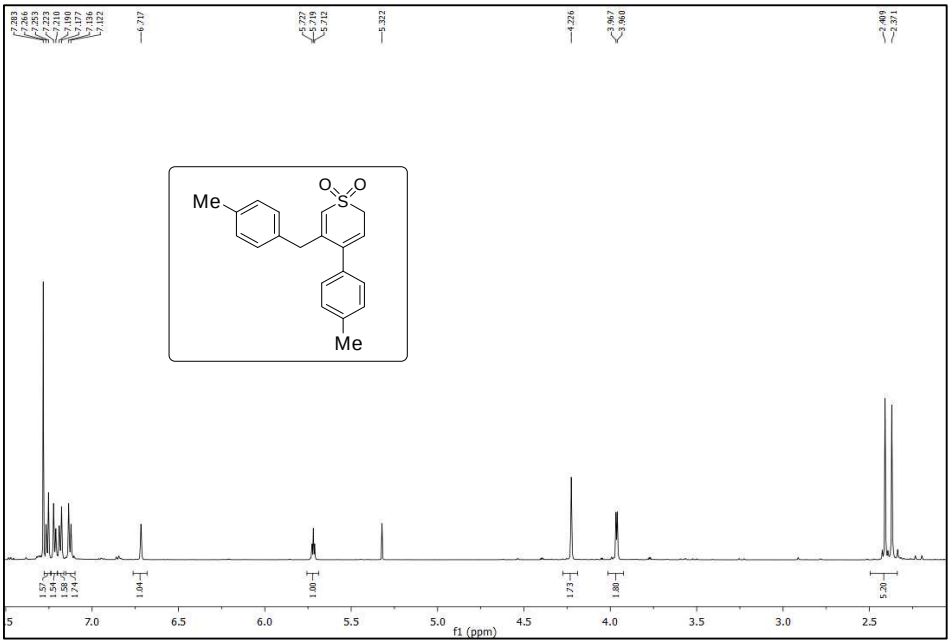

^{1}H NMR ($CDCl_3$, 600 MHz) spectrum of 5.092 F

^{13}C NMR ($CDCl_3$, 150 MHz) spectrum of 5.092 F

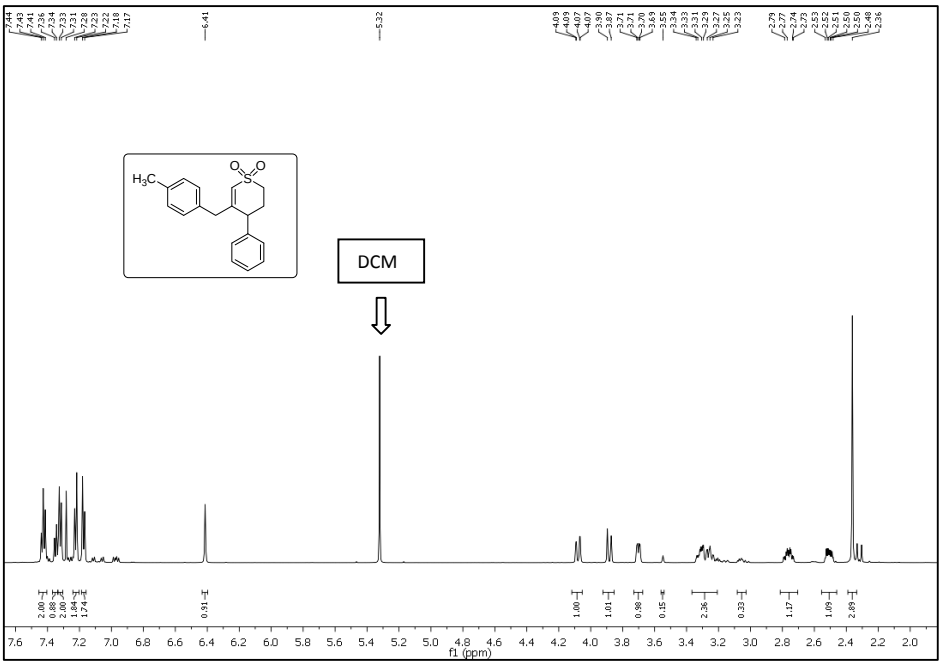

^{1}H NMR ($CDCl_3$, 600 MHz) spectrum of 5.100

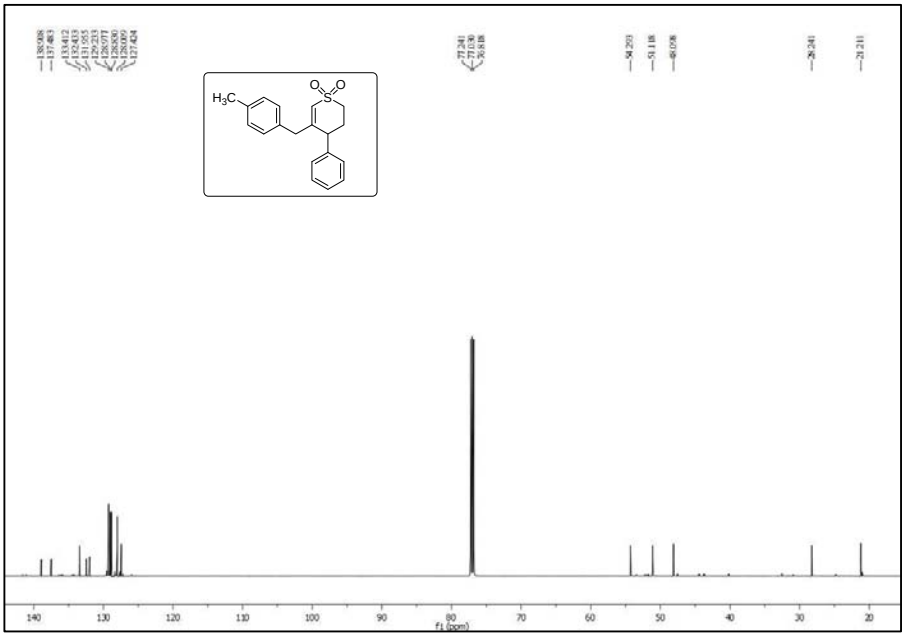

^{13}C NMR ($CDCl_3$, 150 MHz) spectrum of 5.100

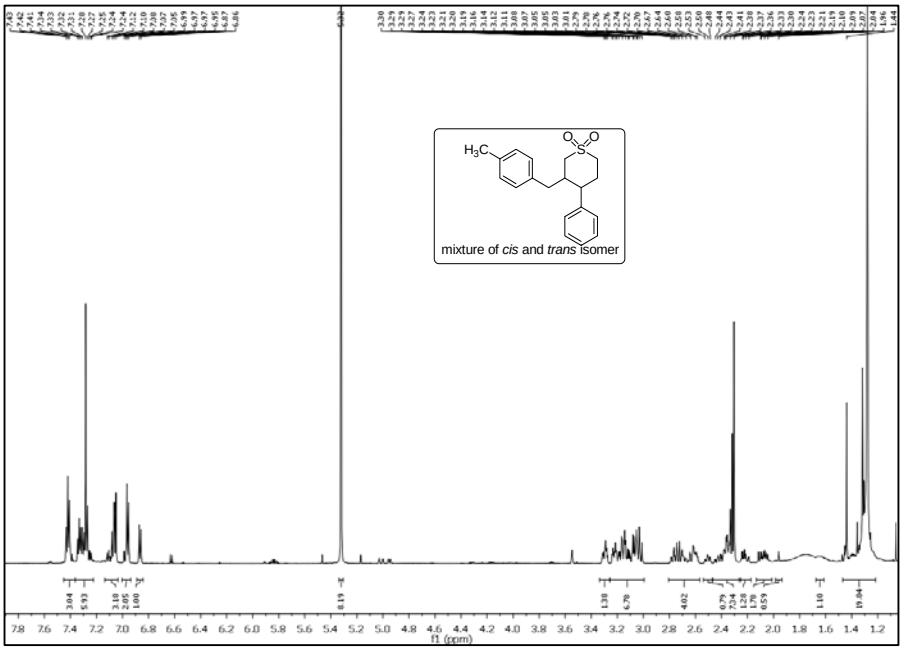

^{1}H NMR ($CDCl_3$, 400 MHz) spectrum of 5.101

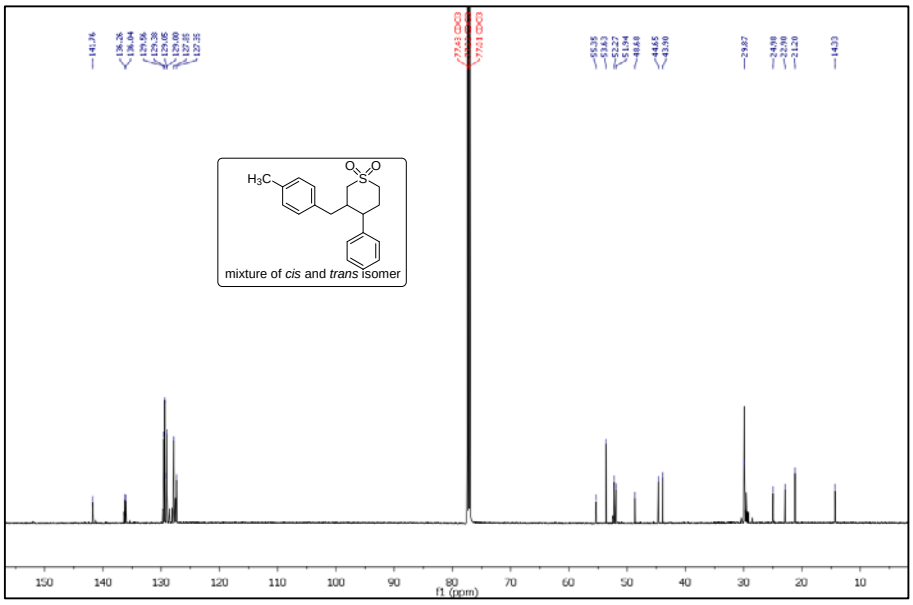

^{13}C NMR crude ($CDCl_3$, 100 MHz) spectrum of 5.101

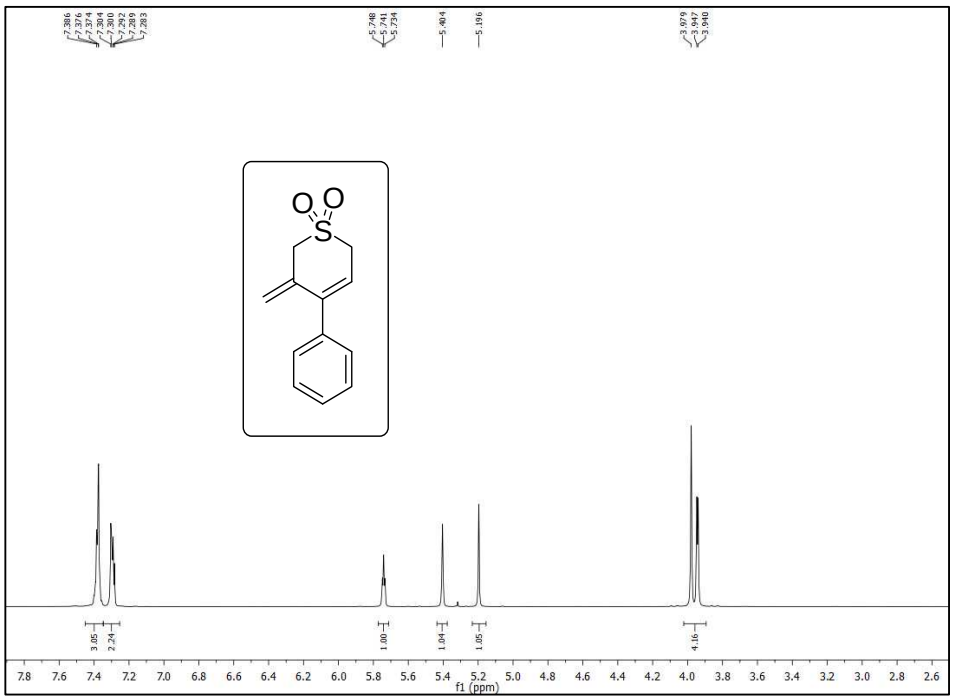

^{1}H NMR ($CDCl_3$, 600 MHz) spectrum of 5.095

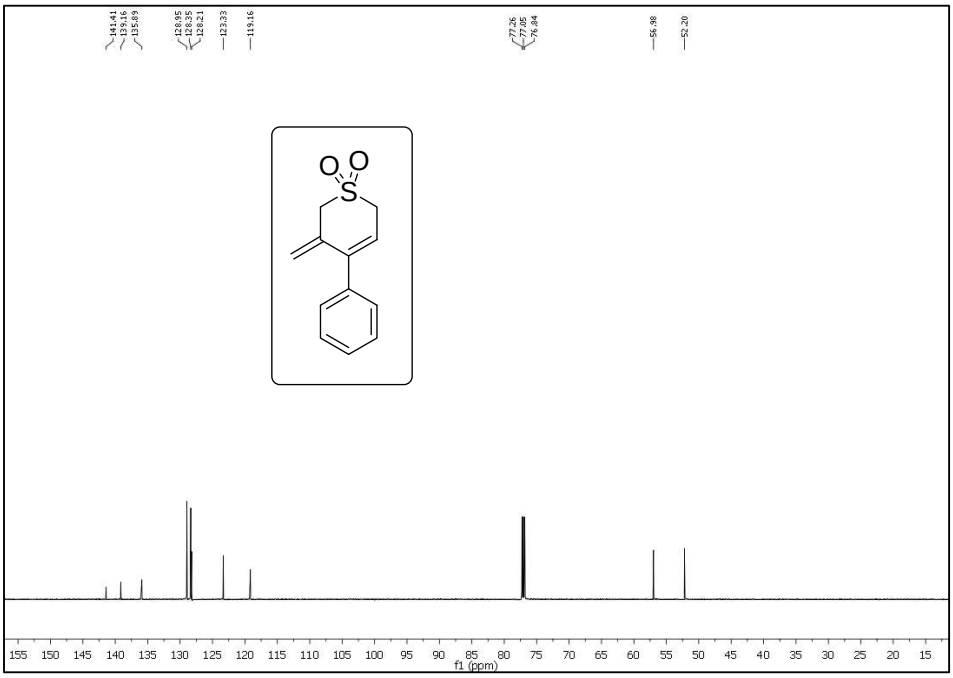

^{13}C NMR ($CDCl_3$, 150 MHz) spectrum of 5.095

Chapter 6

A One-Pot Garratt-Braverman and Scholl oxidation Reaction: Application in the Synthesis of Polyaromatic Compounds with Low Lying LUMO

6.1 Introduction

Polycyclic aromatic and hetero-aromatic compounds[108] (**Figure 6.01**) have attracted enormous interest for the construction of high performance optical and electronic organic devices due to their photo and electrochemical properties arising from their π-electrons.[109] In addition to the application in the construction of fullerenes and carbon nanotubes, these polyaromatic hydrocarbons have been extensively used in photovoltaic cells, liquid crystal displays, organic light emitting diodes (OLED) and organic field effect transistors (OFET).[110] Typical current carriers in organic semiconductors are holes and electrons in π-bond frameworks. Almost all organic solids are insulators. But when their constituent molecules have π-conjugated systems, electrons can move *via* π- electron cloud overlaps, especially by hopping, tunnelling and related mechanisms. Polycyclic aromatic hydrocarbons and phthalocyanine salt crystals are examples of this type of organic semiconductors.

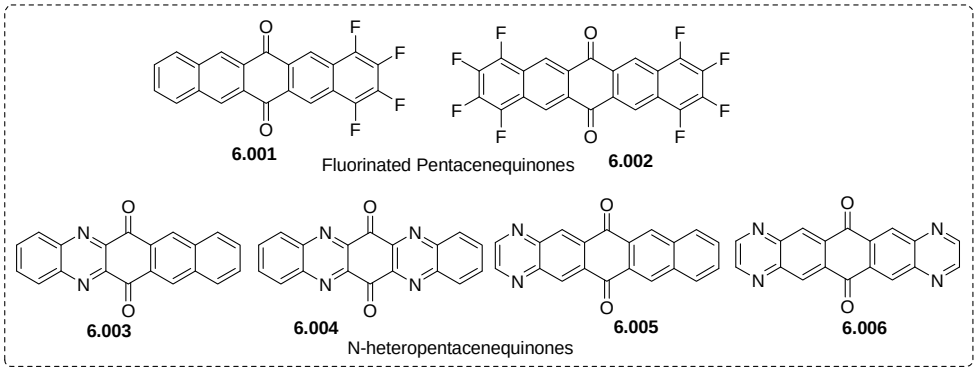

Figure 6.01: Example of some n-type semiconductor molecules from literature

Depending on the alignment of benzene rings, polyaromatic compounds can be classified into three different series (**Figure 6.02**). The first series comprises of [*n*] acenes[111] that are planar benzenoid hydrocarbons and have linearly fused benzene rings. These molecules have an increased reactivity owning lesser number of aromatic π-sextets (Clar sextet) with increasing HOMO energy level that also causes to decrease their stability as they readily undergo oxidative p-doping by aerial oxygen. The second series consists of [*n*] phenacenes[112] that are planar angular fused analogues of acenes making a zigzag shape of fused benzene rings. The third category of polyaromatic compounds corresponds to non-planar [*n*] helicenes[113] that have *ortho*-fused aromatic rings and adopt a helical structure to avoid overlapping between

terminal rings. The helicenes are considered to be most stable than their isomeric acenes and the stability can be explained by Clar's[114] model of aromaticity qualitatively in terms of number of aromatic π-sextets present in each substrate. In case of polyacenes, *i.e.* naphthalene, tetracene, pentacene or for any other larger homologues, there is only one π-electron sextet, thus making the acenes less stable and that one sextet is distributed over the whole assembly. The stability issue can also be explained by the fact of loss of benzenoid character of acenes using molecular orbital theory.

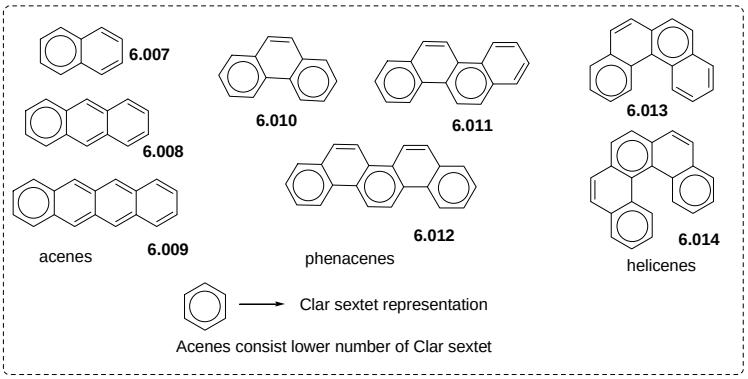

Figure 6.02: Clar's sextet concept and different classes of polyaromatic compounds

The electronic properties of polyaromatic compounds depend upon several factors such as HOMO-LUMO energy gap[114f], reversibility of electron transfer[115] and stability[116] towards aerial oxidation. The synthesis of polyaromatic compounds with lower number of Clar sextets (ratio of benzenoid to non-benzenoid rings must be small) are highly desirable as that leads to smaller band gap due to extended conjugation and the stability issue can be resolved with angular fusion of benzene rings[117] along with incorporation of substituents[118] and functional groups[119]. In this chapter we have discussed about synthesis of polyaromatic compounds in moderate to high yields which are classified as acene-helicene hybrids by using Garratt-Braverman cyclization and Scholl oxidation reaction by keeping in mind all the prerequisites discussed above.

6.2 Previous work

There are several methods reported till date for the synthesis of polyaromatic compounds. Some useful general techniques are mentioned here.

6.2 A. Flash vacuum pyrolysis

The synthesis of polyaromatic compounds started with flash vacuum pyrolysis (FVP) at higher temperature with a shorter reaction time. Such an example is FVP of 7,10-bis(1-chlorovinyl)fluoranthene **6.016** to synthesize corannulene **6.017** (**Scheme 6.01**).[120]

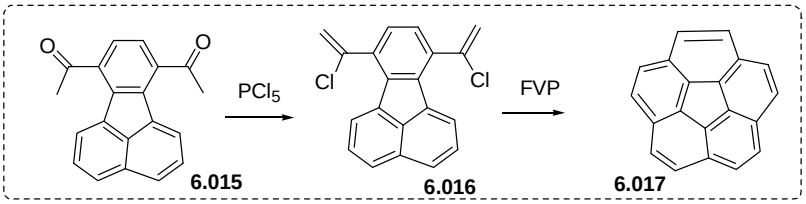

Scheme 6.01: Synthesis of corannulene by FVP method

6.2 B. Inter and Intramolecular Diels Alder reaction

In 2007 Fallis *et al*. reported a double intermolecular Diels-Alder reaction between a diene **6.018** and anthradiquinone **6.019** to a cycloadduct **6.020** that was further converted into pentacene **6.021** by using a deoxygenaton/aromatization reaction (**Scheme 6.02**).[121]

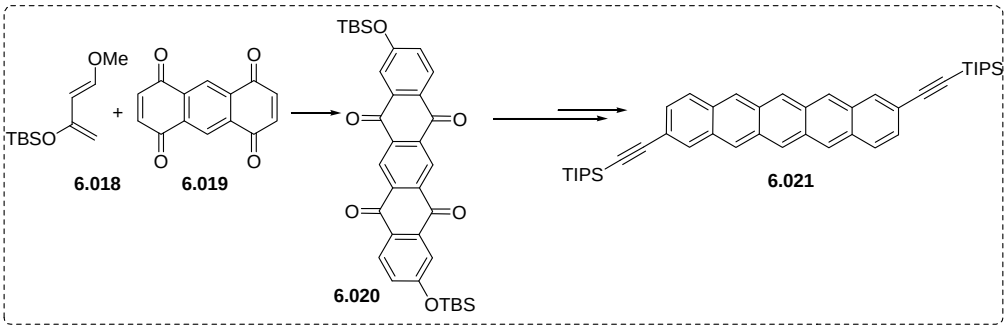

Scheme 6.02: Synthesis of pentacene by intermolecular Diels Alder reaction

Later Müllen *et al*. reported a sophisticated way of synthesizing polyaromatic compounds by using an intramolecular Diels-Alder reaction of phenylene-vinylene derivative **6.022** to cyclohexene derivative **6.023** followed by oxidation with DDQ and $CuCl_2/AuCl_3$ (**Scheme 6.03**).[122]

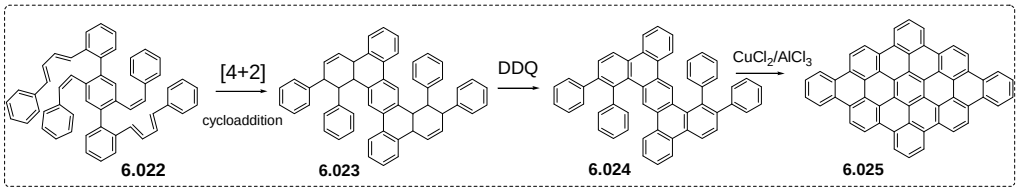

Scheme 6.03: Example of intramolecular Diels Alder reaction to synthesize PAHs

6.2 C. Ring closing olefin metathesis

King and Iuliano *et al*. reported[123] a mild condition of synthesizing polyaromatic compounds by using ring closing metathesis as a key step. A typical example is shown in **Scheme 6.04**.

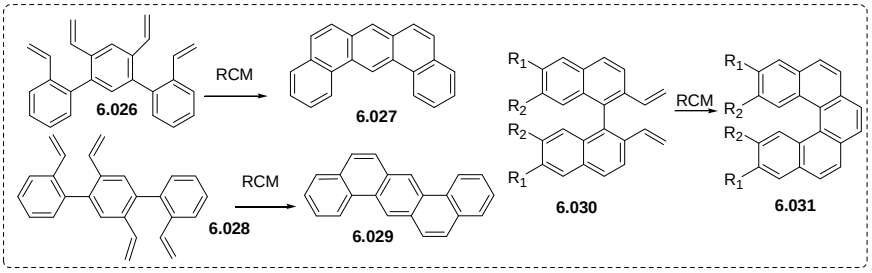

Scheme 6.04: Examples of RCM reaction to synthesize PAHs

6.2 D. Benzannulation and electrophilic cyclization

The typical synthesis of coronene **6.034** involved pyrolysis at higher temperature. Scott and his co-workers first reported[124] a convenient and efficient synthesis (**Scheme 6.05**) of coronene by using benzannulation of bis (1,1-ethynyl alkene) **6.033** in presence of 20 mol % $RuPPh_3(cymene)Cl_2$ catalyst starting from commercially available anthraquinone **6.032**. Later, Liu *et al*. optimized the reaction condition by using $TpRuPPh_3(CH_3CN)_2PF_6$ as catalyst that gave rise to the increase of yield upto 86%.

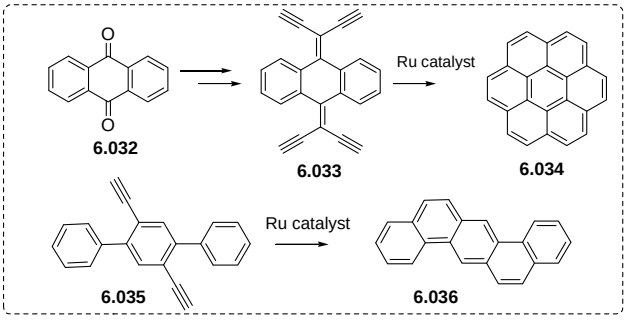

Scheme 6.05: Examples of metal catalyzed benzannulation reaction to synthesize PAHs

Swager and his co-workers developed a mild and efficient process of synthesizing polyaromatics by using electrophilic cyclization in presence of $I(pyridine)_2BF_4$ or trifluoroacetic acid (**Scheme 6.06**).[125]

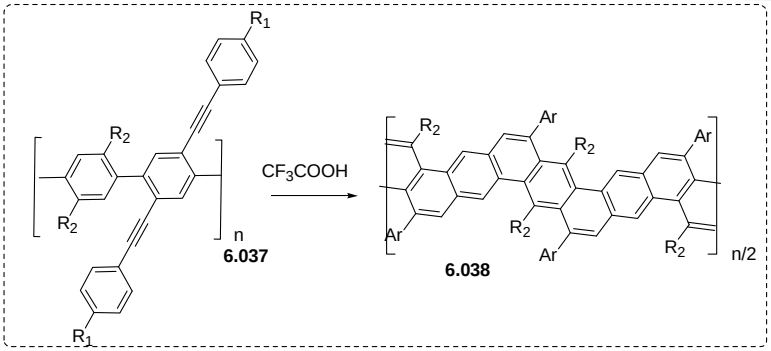

Scheme 6.06: Example of electrophilic cyclization reaction to synthesize PAHs

6.2 E. Intramolecular photocyclization of stilbene-type compounds

In 2005 Nuckolls and his co-workers reported[126] a photocyclization reaction for the synthesis of hexa-*cata*-hexabenzocoronene derivative **6.040** (**Scheme 6.07**).

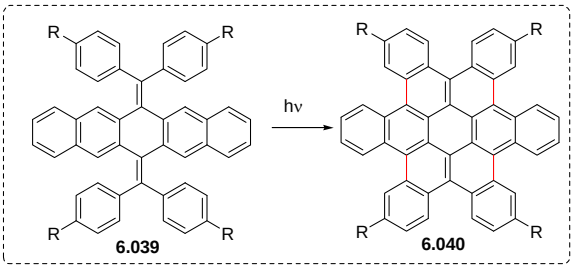

Scheme 6.07: Example of photocyclization reaction to synthesize PAHs

6.2 F. Oxidative cyclodehydrogenation

Regioselective cyclization followed by oxidative dehydrogenation in presence of Lewis acid catalyst has been employed to synthesize all-benzenoid polyaromatic compounds. The reaction is known as Scholl reaction[127] and considered to be the most powerful tool of synthesizing PAHs (**Scheme 6.08**).

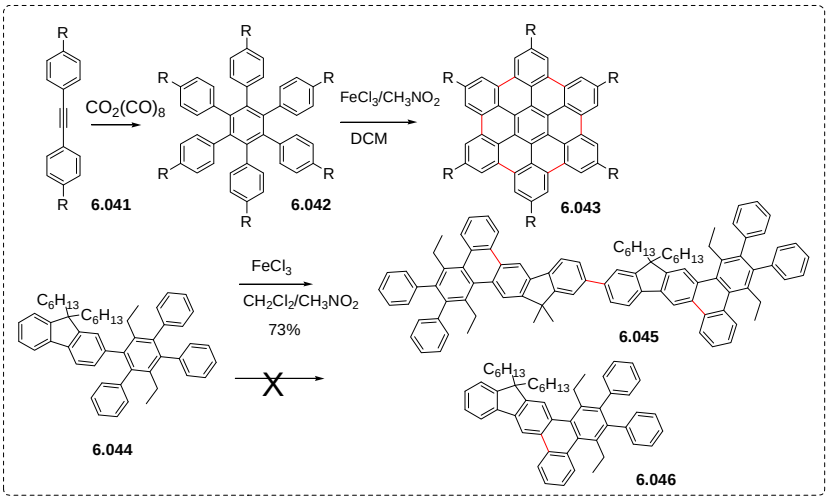

Scheme 6.08: Examples of oxidative cyclodehydrogenation reaction to synthesize PAHs

6.2 G. Combined Garratt-Braverman Cyclization and Scholl oxidation reaction to polyaromatics

It was figured out the synthetic relevance of GB cyclization to construct two new C-C bonds to synthesize benzene fused aromatic systems represented by **6.047 A´** starting from easily available bis-propargyl systems **6.047**. The pendant aromatic ring attached to C-4 is in a plane perpendicular to the molecular plane in the lowest energy conformation of the compound. However, a third C-C bond can be formed by oxidative coupling reaction (Scholl oxidation) with an inexpensive and mild oxidising agent $FeCl_3$ (anhydrous). The reaction involves either a radical cation or arenium cation intermediate[128] (**Scheme 6.10**). The dehydrogenative C-C coupling reaction also involves the formation of an equivalent amount of HCl that can be quenched by the base used during GB reaction. This one pot synthesis of polyaromatic compounds using GB Cyclization and Scholl oxidation gave rise to an efficient method of synthesizing polyaromatic compounds that are otherwise difficult to obtain. The polyaromatic compounds that were synthesized by one pot GB cyclization and Scholl oxidation reaction are shown in **Scheme 6.09**.

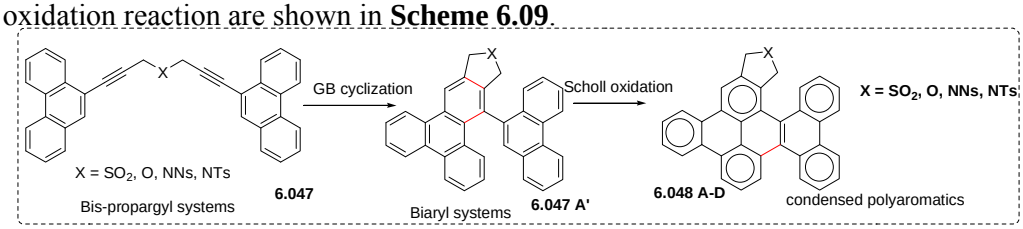

Scheme 6.09: Synthesis of polyaromatic compounds starting from bis-propargyl phenanthrene systems

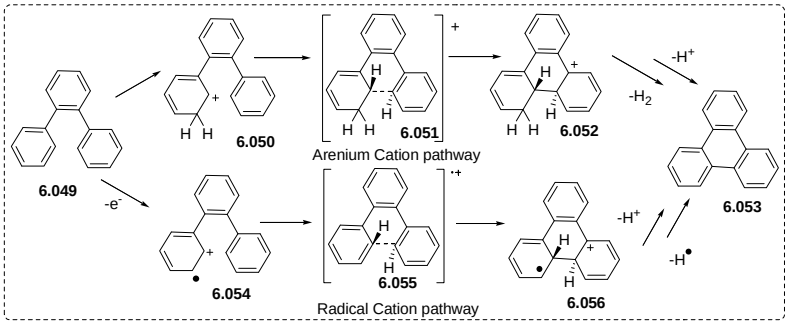

Scheme 6.10: Mechanism of Scholl reaction

The band gap of the polyaromatic compounds synthesized by Mitra *et al.*[129] was measured from λ_{edge} of their corresponding UV absorption spectra and the HOMO and LUMO energy levels were determined experimentally by cyclic voltammetry measurements and are given in **Table 6.01**.

Compound	Optical band gap (eV)	HOMO energy (eV)	LUMO energy (eV)
6.048 A	2.92	-5.70	-2.78
6.048 B	2.95	-5.85	-2.90
6.048 C	2.95	-5.80	-2.85
6.048 D	2.90	-6.05	-3.15
Pentacene	1.96	-4.96	-3.00
Tetracene	2.40	-5.40	-3.00

Table 6.01: Band gap and HOMO, LUMO energy levels

It was observed that the compounds were having band gap < 3 eV with low lying E_{HOMO} level as compared to that of pentacene[130] that gave rise to increased stability towards oxidative p-doping by air oxygen to the synthesized acenes. The X-ray structure[129] of polyaromatic sulfone **6.048 A** also showed the differences in various bond lengths and was in good agreement with its Clar structure (**Figure 6.03**).

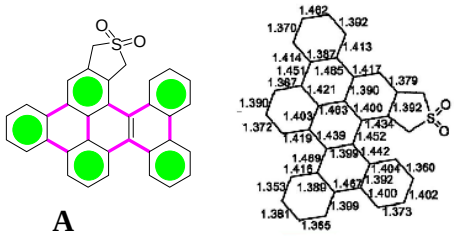

Figure 6.03: A) Clar structure of polyaromatic sulfone **6.048 A**, the longer bonds are shown in pink **B**) The bond lengths are given in angstrom unit from X-ray structure.

6.3 Objective

The polyaromatic compounds synthesized previously starting from bis-propargyl phenanthrenes had greater number of benzenoid rings (5) or Clar sextets than non-benzenoid rings (3). We wanted to select bis-propargyl naphthalene systems as the precursors for one pot GB cyclization and Scholl oxidation reaction into the aim to synthesize polyaromatic compounds having lower number of benzenoid rings with lower band gaps without compromising the stability. In this dissertation, we have limited our discussion to bis-propargyl sulfone precursors only as in that case we were successful to synthesize polyaromatics using intramolecular dehydrogenative C-C coupling Scholl oxidation reaction.

Taking all these aspects into consideration, the following objectives were framed:

- To synthesize various bis-propargyl sulfone precursors having a naphthalene moiety and to study their outcome of GB and Scholl oxidation reaction performed separately followed by in one pot procedure.

- To study the photo-physical properties of the synthesized compounds by UV-Vis spectroscopy and electrochemical properties by Cyclic Voltammetry.

6.4 Results and Discussion

6.4 A. Synthesis of bis-propargyl sulfone precursors

The synthesis of bis-propargyl precursors started with Sonogashira coupling of 2-bromo naphthalene **6.057** and 1-naphthyl triflate **6.062** in presence of propargyl alcohol and $PdCl_2(PPh_3)_2$. The detailed reaction procedure is shown in **Scheme 6.11**. The alcohols were then converted to the bromides **6.059** and **6.065** by following some functional group manipulations. The bromide was then treated with Na_2S under phase transfer condition to get the symmetrical sulfides. The unsymmetrical sulfides **6.064**, **6.066** were prepared by nucleophilic attack on corresponding bromides by the thiols generated *in situ* from hydrolysis of thioacetates in basic medium.[98,99] The sulfides were then oxidised to the sulfones **6.061 A-D** by treating them with 2 equivalent of m-CPBA in dry DCM.

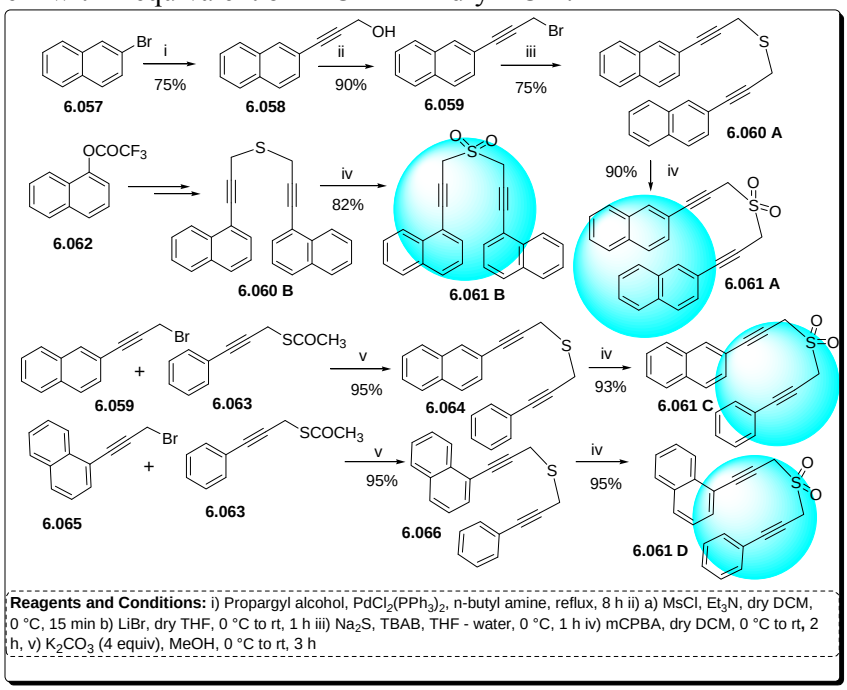

Scheme 6.11: Synthesis of bis-propargyl sulfone precursors

6.4 B. Synthesis of polyaromatics by GB Cyclization and Scholl oxidation reaction

After successfully synthesizing the bis-propargyl sulfones **6.061 A-D**, they were subjected to GB reaction condition. For this, the sulfones were dissolved in DCM and treated with catalytic amount of Et_3N at room temperature for 15 min. The reaction gave rise to benzene fused aromatic systems having similarity with the structural motif required for Scholl oxidation reaction. The GB cyclization products were isolated and individually subjected to the Scholl reaction condition by performing the reaction separately in presence of anhydrous $FeCl_3$ in dry DCM. In most of the situations including increasing the equivalency of $FeCl_3$ resulted in the formation of polymeric products. However, we could finally optimize the reaction condition and found that a total 25 equivalent of $FeCl_3$, added in two equal portions within a time interval as reported below (**Table 6.02**), ended up with the formation of polyaromatics in decent yields with formation of only intramolecular C-C bond. We then adopted the same reaction conditions to perform GB cyclization and Scholl reaction in a one pot procedure. For this, the bis-propargyl sulfones were dissolved in DCM and treated with catalytic amount of Et_3N for 15 min and 25 equiv of $FeCl_3$ was added into it in two equal portions by maintaining the time interval as mentioned in **Table 6.02**.

Bis-propargyl sulfones	Time of addition of 1st 12.5 eq of anh. $FeCl_3$	Time of addition of 2nd 12.5 eq of anh. $FeCl_3$	Reaction time
6.061 A	5 min	2 h	3 h
6.061 B	5 min	3 h	6 h
6.061 C	7 min	6 h	24 h
6.061 D	7 min	6 h	24 h

Table 6.02: One pot reaction condition

After completion of the reactions as indicated by TLC, (appearance of a new fluorescent spot), the polyaromatic compounds **6.068 A1-D** (**Scheme 6.12**) were isolated in pure form by column chromatography over silica gel using hexane-ethylacetate as eluent. The combined yields of the two steps performed separately were compared with the reactions performed in one-pot protocol and it was observed

that the yield of one-pot procedure was improved considerably as compared to reactions performed separately. This was similar to the observations made previously for the bis-propargyl phenanthrene systems[129]. The results are shown in **Table 6.03**. For substrates **6.061 A** and **6.061 B**, because of the presence of two non-equivalent oxidizable hydrogens (attached to *a* and *β* carbons), a mixture of products **6.068 A1**/**6.068 A2** and **6.068 B1**/**6.068 B2** were obtained.

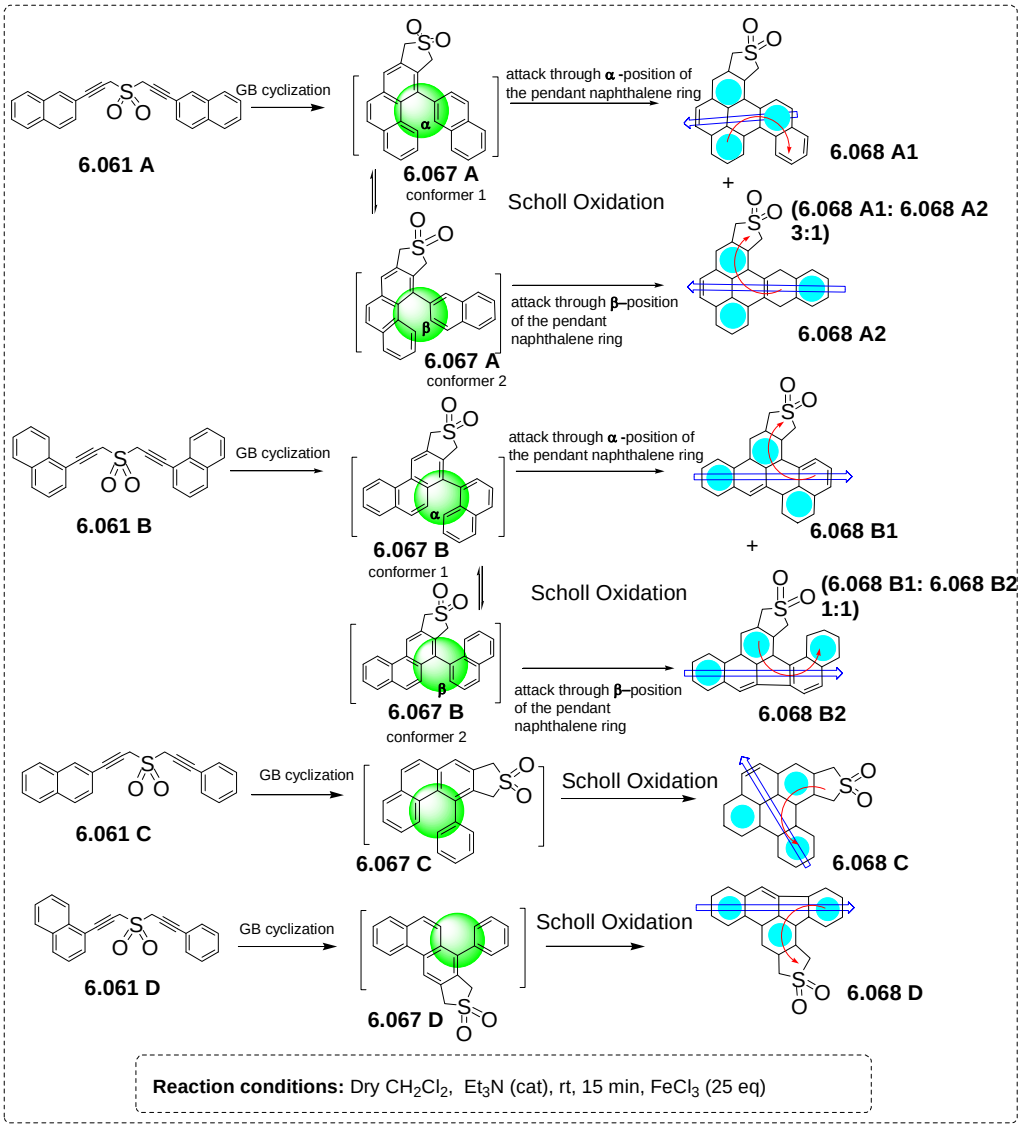

Scheme 6.12: Synthesis of PAHs by a one-pot GB cyclization and Scholl oxidation reaction (green circles denote structural motif for Scholl oxidation, red and blue arrows denote helical and acene motifs while blue circles show rings with Clar sextet)

Product	% yield for one pot reaction	Combined yield if separately done
6.068 A1	45	30
6.068 A2	15	10
6.068 B1	30	20
6.068 B2	30	20
6.068 C	70	55
6.068 D	70	55

Table 6.03: Comparison of % yield in one pot procedure and reactions performed separately

6.4 C. Spectral characterizations

The structure of the polyaromatic compounds was mainly confirmed by NMR spectroscopy recorded at 400 MHz. The cyclodehydrogenated products **6.068 A1-D** showed two protons less as compared to the GB products **6.067 A-D**. Finally HRMS study confirmed the formation of monomeric Scholl oxidized product rather than any polymers formed from intermolecular Scholl reaction. As already mentioned, for compound **6.061 A**, two products **6.068 A1, 6.068 A2** were formed in 3:1 ratio by attacking through α and β position of naphthalene rings and the product ratio depends on feasibility of electrophilic attack of naphthalene ring at α and β position. The presence of only one singlet in **6.068 A1** and three singlets in **6.068 A2** in ^{1}H NMR spectra distinguished the two products. In case of compound **6.061 B** only one product was expected. However, ^{13}C NMR spectrum of the product synthesized after cyclodehydrogenation showed extra signals in aromatic region than expected. We then injected the compound at HPLC and observed two peaks of equal intensity. Next we isolated the two compounds by HPLC with 100% CH_3CN (flow rate 1ml/min) at reverse phase column and confirmed the structure of two compounds **6.068 B1**, **6.068 B2** by ^{1}H-NMR spectroscopy. Among them one is the usual six-membered one **6.068 B1** (cyclization through C-8/α position) and the other is exceptional five-membered **6.068 B2** (cyclization through C-2/β position). The presence of two clear doublets without any other *meta* couplings indicated the structure **6.068 B2** (**Figure 6.04-6.07**).

All the PAHs have built-in helical motifs (showed by red arrows) and are expected to have some degree of non-planarity.

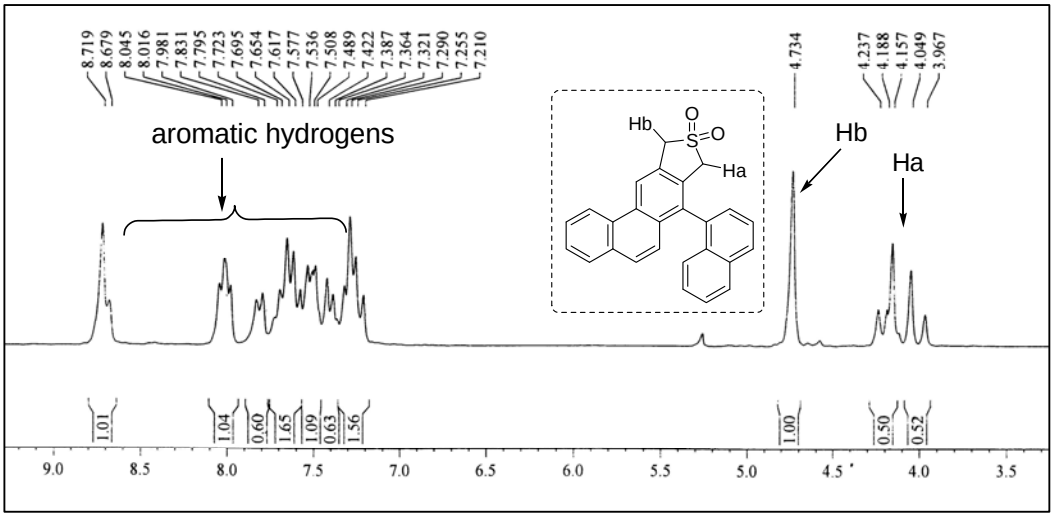

Figure 6.04: Expanded ^{1}H NMR (400 MHz) of compound **6.067 B** in $CDCl_3$

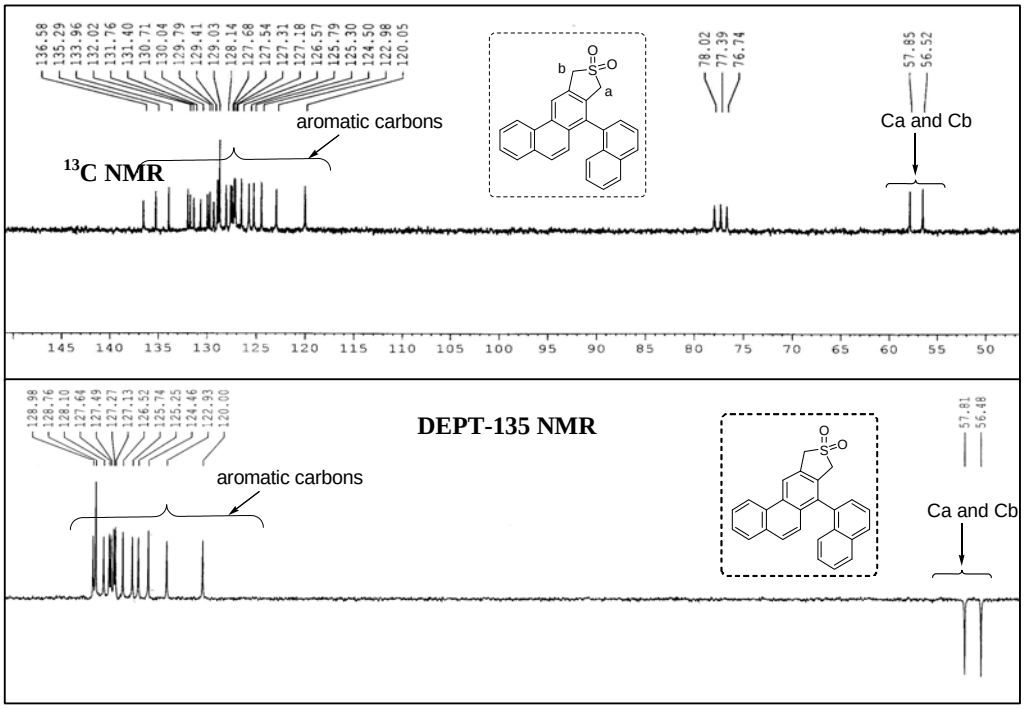

Figure 6.05: Expanded ^{13}C NMR (100 MHz) and DEPT-135 (100 MHz) NMR of **6.067 B** in $CDCl_3$ showing 13 aromatic methyne carbons with two signals overlapped at δ 128.8

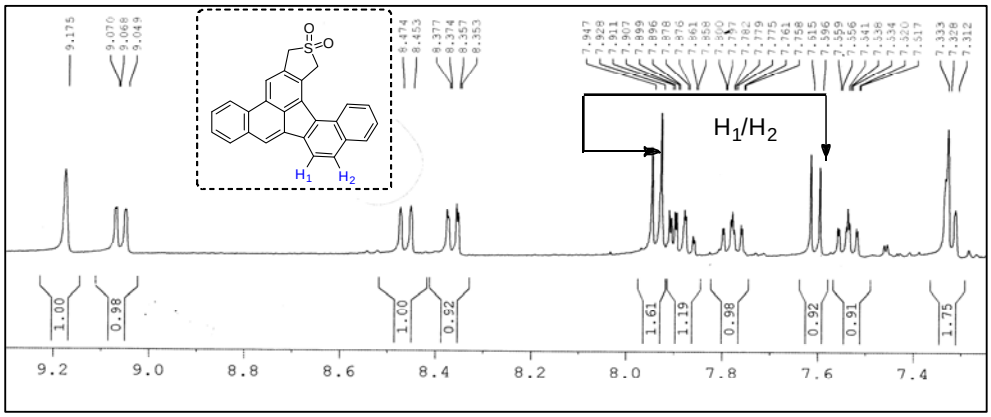

Figure 6.06: Expanded ^{1}H NMR (400 MHz) of compound **6.068 B2** in d_6-acetone

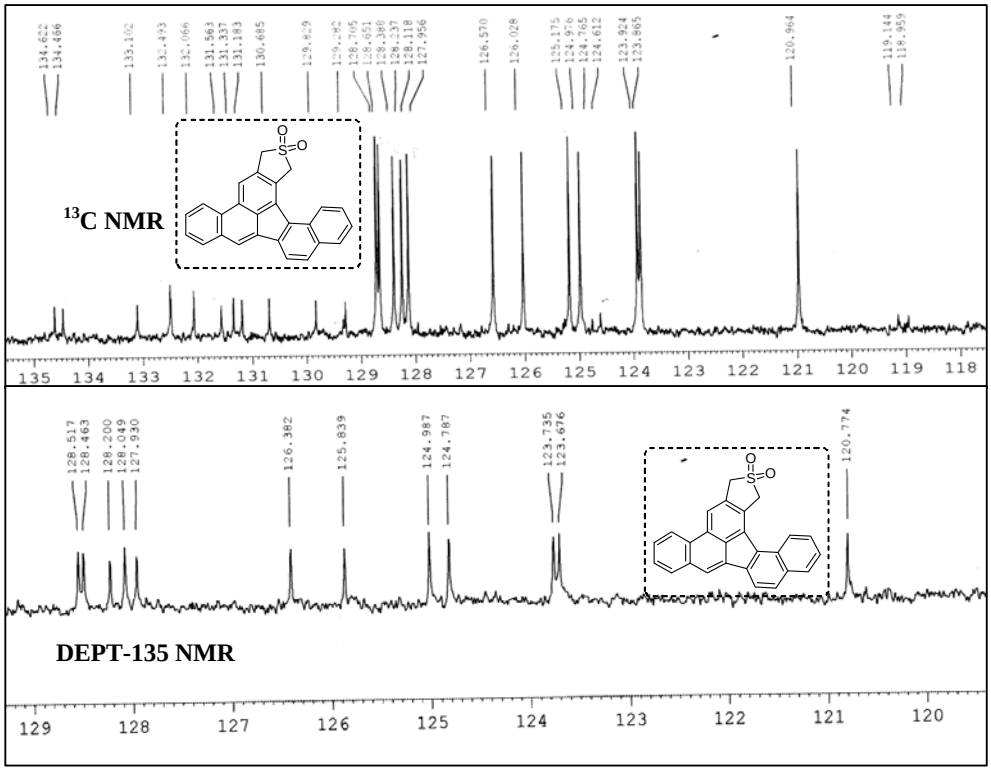

Figure 6.07: Expanded ^{13}C NMR and DEPT-135 NMR of **6.068 B2** in d_6-acetone showing the presence of 12 aromatic methyne carbons

6.4 D. Photophysical Properties

We then calculated the band gap of the synthesized polyaromatic compounds by recording the UV-Vis absorption spectra in CH_3CN (10^{-6} mol/L). An overlaid spectrum for compound **6.068 A1-B2** along with individual spectrum of **6.068 C-D** are shown in **Figure 6.08**. As the compounds are polyaromatic and have a rigid structure they showed fine spectra due to their higher energy difference in the vibrational energy levels. The peaks are attributed to the π-π* transition of the conjugated backbone. The optical band gap (E=hc/λ, By putting h=6.627×10^{-34}joule-sec, c=3×10^8m/s, λ=λ_{edge} (nm), 1eV=1.6×10^{-19} joules we have, E^0 (band gap) = 1240/λ_{edge} (nm) eV of compounds) was found to be in between 2.92-3.78 eV for the compounds (**Table 6.04**).

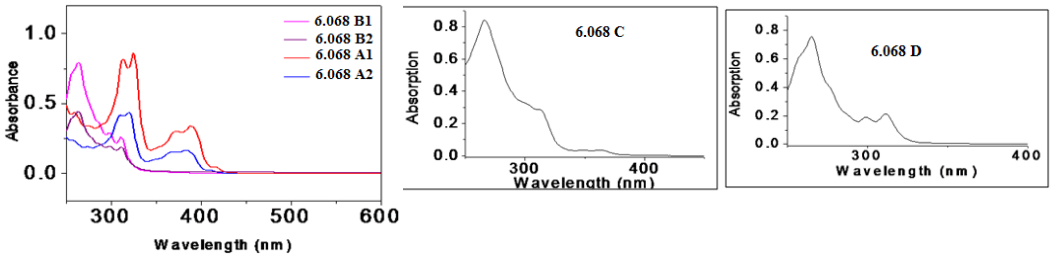

Figure 6.08: UV spectra of **6.068 A1-D**

6.4 E. Electrochemical properties

To understand the charge transport properties and assess the ionization potentials, electron affinity values as well as the electrochemical stability of the compounds synthesized the redox properties of compounds **6.068 A1-D** (measured at a concentration of 10^{-3} M) were investigated by cyclic voltammetry. The analyte was dissolved in CH_3CN containing tetrabutylammonium hexafluorophosphate (Bu_4NPF_6) as the supporting electrolyte and was analyzed at room temperature at a scan rate of 100 mV/s. A glassy carbon electrode and platinum wire were used as the working electrode and auxillary electrode respectively. A Ag/AgCl electrode was used as the quasi-reference electrode to calibrate against ferrocene/ferrocenium (0.06 V vs Ag/AgCl) at the beginning of the experiments. The cyclic voltammogram of **6.068 A1** is shown in **Figure 6.09** and the band gap and energy levels of the HOMO and LUMO are summarized in **Table 6.04**.

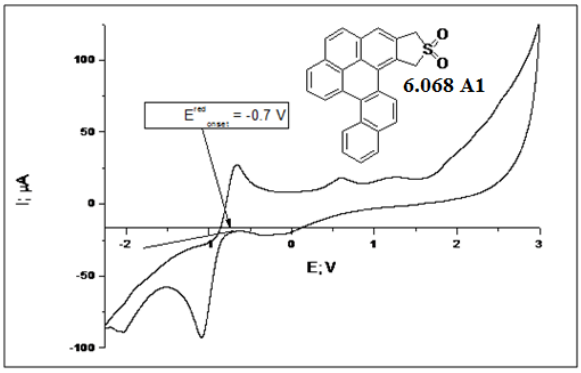

Figure 6.09: Representative cyclic voltammogram of **6.068 A1**

Compound	Optical band gap (eV)	HOMO energy (eV)	LUMO energy (eV)
6.068 A1	2.98	-7.08	-4.10
6.068 A2	2.92	-6.91	-3.99
6.068 B1	3.70	-7.86	-4.16
6.068 B2	3.70	-7.91	-4.21
6.068 C	3.26	-7.65	-4.39
6.068 D	3.78	-7.87	-4.09

Table 6.04: Band gap and HOMO, LUMO energy level

[EMPERICAL FORMULA: $E_{HOMO/LUMO} = - \{E_{onset\ (ox)/(red)} + 4.8 - E_{FOC}\}$ 4.8 is the reference energy level of FOC and E_{FOC} is the potential of FOC/FOC^+ vs Ag/AgCl (0.06 eV measured by cyclic voltammetry)][131].

The compound **6.068 A1** showed quasi reversible reduction peaks and irreversible oxidation peaks in the testing window (**Figure 6.09**). Assuming that the enegy level of FOC/FOC^+ reference is 4.8 eV below vacuum, the E_{LUMO} level (or electron affinity values) can readily be estimated and obtained in between 3.99-4.39 eV for compounds **6.068 A1-D**. Comparing with other well known n-type semiconductors[132] (fluorinated and N-heterocycled pentacenequinones) we can say that our designed molecules having low energy E_{LUMO} level due to the presence of electron withdrawing sulfone moeity. Although the band gap in some cases are higher than the previously synthesized polyaromatic compounds starting from bis-propargyl phenanthrene systems, the value of the E_{LUMO} level was lower for compound **6.068 A1-D**, thus indicating better semiconducting properties. As the band gap of polyaromatic compounds depends on several factors like, planarity of the structure, total number of aryl rings, substitution on aryl ring, the compounds synthesized from bis-propargyl naphthalene systems had larger band gap than the corresponding phenanthrene

systems. The E_{HOMO} level was also calculated to be in between 6.91-7.87 eV. The stability of organic semiconducting materials towards oxidative doping is related to their ionization potentials *i.e*. their HOMO energy levels from vacuum. Therefore lowering the HOMO level would improve the environmental stability by minimizing the level of p-doping by ambient oxygen. Compared to that of pentacene (-4.96 eV)[130] and other well-known current OFET materials the lower HOMO energy level of our compounds suggest that it should have better stability than traditional p-type semiconductor materials.

6.5 Conclusion

- We have successfully developed a synthetic route for one pot Garratt-Braverman and Scholl oxidation reaction to various polyaromatic compounds starting from bis-propargyl naphthalene systems.
- We have been able to synthesize polyaromatic compounds with low lying E_{LUMO} level without sacrificing the band gap and the stability of the compound.
- The fusion of acene and helicenes has increased the stability of the PAHs as indicated by the decreased HOMO energy level.

6.6 Experimental Details

6.6.1 General Experimental

General experimental procedures are same as described at page no. 59 in Chapter 2.

6.6.2 General procedure for synthesis of compounds and their spectral data

General procedure for the synthesis of sulfides (6.060 A-B, 6.064, 6.066)

For symmetrical sulfides **6.060 A-B**, the bromide (1.0 eq) was taken into THF-water (5:1), TBAB (0.1 eq) and Na_2S (0.5 eq) were added to it at 0 °C. The reaction was complete at room-temperature within 1 h. The reaction mixture was then extracted with ethyl-acetate, washed with water and brine, dried over anhydrous sodium sulfate, concentrated in vacuum and subjected to column chromatography (Si-gel, petroleum ether-ethyl acetate mixture as eluent).

For unsymmetrical sulfides **6.064**, **6.066**, the thioacetate **6.063** (1.0 eq) were dissolved in 10 ml of MeOH and cooled to -20 °C under nitrogen atmosphere. Then K_2CO_3 (1.0 eq) was added to generate the thiol *in situ*. After 15 minutes, the corresponding bromides were added and the temperature of the reaction mixture was gradually increased from -20 °C to +20 °C through 3 h. Then the whole mixture was evaporated and the residue was poured into water and the organic compound was extracted by ethyl-acetate. The organic layer was then dried over sodium sulfate and concentrated and the crude sulfides were purified by column chromatography (Si-gel, petroleum ether-ethyl acetate mixture as eluent).

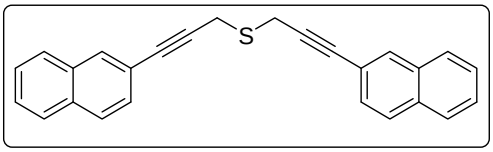

Bis-(2-naphthylpropargyl) sulfide (6.060 A)

State: yellow liquid; **yield**: 75%; ^{1}H NMR (400 MHz, Chloroform-*d*) δ 8.06 (s, 2H); 7.89 - 7.81 (m, 6H), 7.61 - 7.52 (m, 6H), 3.91 (s, 2H), 3.90 (s, 2H); ^{13}C NMR (100 MHz, Chloroform-*d*) δ 133.0, 132.9, 131.8, 128.6, 128.0, 127.8, 126.7, 126.6, 120.4, 85.2, 84.0, 20.6 (1C signal was merged).

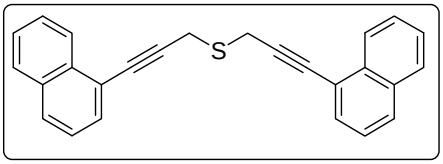

Bis-(1-naphthylpropargyl) sulfide (6.060 B)

State: yellow liquid; **yield**: 75%; ^{1}H NMR (200 MHz, Chloroform-*d*) δ 8.57 (d, *J* = 7.8 Hz, 2H), 7.94 - 7.82 (bm, 6H), 7.69 - 7.59 (bm, 4H), 7.55 - 7.44 (bm, 2H), 4.07 (s, 4H); ^{13}C NMR (50 MHz, Chloroform-*d*) δ 133.7, 133.4, 130.9, 129.0, 128.5, 127.1, 126.6, 126.3, 125.4, 120.8, 89.8, 82.1, 20.8.

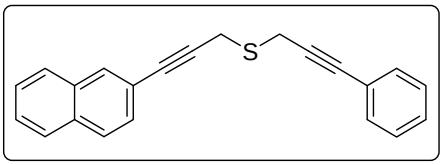

2-[3-(3-Phenyl-prop-2-ynylsulfanyl)-prop-1-ynyl]-naphthalene (6.064)

State: yellow liquid; **yield** 95%; ^{1}H NMR (200 MHz, Chloroform-*d*) δ 8.01 (s, 1H), 7.83 - 7.79 (m, 4H), 7.55 - 7.35 (m, 7H), 3.83 (s, 2H), 3.81 (s, 2H); ^{13}C NMR (50 MHz, Chloroform-*d*) δ 133.2, 133.0, 132.0, 131.9, 128.8, 128.5, 128.1, 127.9, 126.8, 126.7, 123.2, 122.9, 122.6, 120.5, 85.2, 84.9, 84.0, 83.7, 20.6 (1C signal was merged).

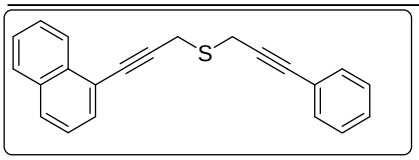

1-[3-(3-Phenyl-prop-2-ynylsulfanyl)-prop-1-ynyl]-naphthalene (6.066)

State: yellow liquid; **yield:** 95%; ^{1}H NMR (200 MHz, Chloroform-*d*) δ 8.42 - 8.39 (m, 1H), 7.88 - 7.35 (m, 11H); 3.94 (s, 2H), 3.84 (s, 2H); ^{13}C NMR (50 MHz, Chloroform-*d*) δ 133.7, 133.4, 132.0, 130.8, 128.9, 128.5, 127.0, 126.6, 126.4, 125.4, 123.2, 120.8, 89.7, 84.8, 83.9, 81.9, 20.6, 20.5 (2C signals were merged).

General procedure for the synthesis of sulfones (6.061 A-D)

To an ice-cold solution of sulfide (1.0 eq.) in 15 ml of dry DCM, mCPBA (2.0 eq.) was added and allowed the reaction to stir under nitrogen atmosphere. After 20 minutes the ice was taken off to convert the sulfoxide (intermediate of the reaction) into sulfone fully and the reaction mixture was kept 2 h at room temperature. The reaction was quenched by diluting the reaction mixture with water and DCM and washed with saturated solutions of $NaHCO_3$, Na_2SO_3 and Na_2CO_3 successively to make the organic layer free of m-CPBA and *m*-chloro benzoic acid. DCM layers were dried over anhydrous Na_2SO_4 and the solutions were concentrated under reduced pressure and subjected to column chromatography (Si-gel, pet ether-ethyl acetate mixture as eluent).

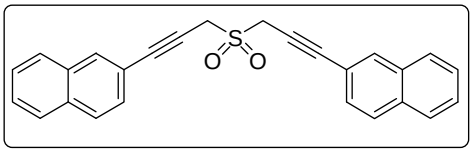

2,2'-(3,3'-sulfonylbis(prop-1-yne-3,1-diyl))dinaphthalene (6.061 A)

State: yellow solid; **yield**: 90%; ^{1}H NMR (200 MHz, Chloroform-*d*) δ 8.07 (2H, s), 7.88 - 7.78 (6H, m), 7.60 - 7.52 (6H, m), 4.45 (4H, s); ^{13}C NMR (50 MHz, Chloroform-*d*) δ 135.6, 133.0, 128.8, 128.4, 128.0, 127.8, 127.4, 127.0, 124.8, 117.8, 88.8, 45.1 (1C signal was merged).

1,1'-(3,3'-sulfonylbis(prop-1-yne-3,1-diyl))dinaphthalene (6.061 B)

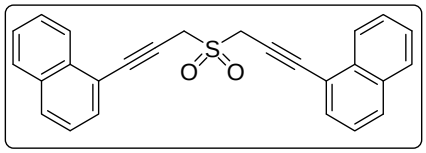

State: yellow solid; yield: 82%; ^{1}H NMR (200 MHz, Chloroform-*d*) δ 8.41 (d, *J* = 7.4 Hz, 2H), 7.90 - 7.75 (bm, 6H), 7.56 - 7.40 (bm, 6H), 4.57 (s, 4H); ^{13}C NMR (100 MHz, Chloroform-*d*) δ

133.5, 133.2, 131.4, 130.0, 128.5, 127.4, 126.8, 125.9, 125.2, 119.1, 86.6, 80.9, 45.0.

2-(3-(3-phenylprop-2-ynylsulfonyl)prop-1-ynyl)naphthalene (6.061 C)

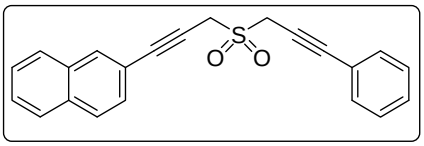

State: yellow solid; **yield**: 93%; ^{1}H NMR (200 MHz, Chloroform-*d*) δ 8.03 (s, 1H), 7.84 - 7.79 (m, 3H), 7.53 - 7.51 (m, 3H), 7.40 - 7.32 (m, 3H), 4.42 - 4.37 (m, 4H); ^{13}C NMR (50 MHz, Chloroform-*d*) δ 133.3, 132.9, 132.6, 132.2, 129.4, 128.6, 128.3, 128.3, 128.0, 127.9, 127.4, 126.9, 121.6, 118.8, 88.5, 88.2, 76.3, 76.1, 44.8, 44.8,

1-(3-(3-phenylprop-2-ynylsulfonyl)prop-1-ynyl)naphthalene (6.061 D)

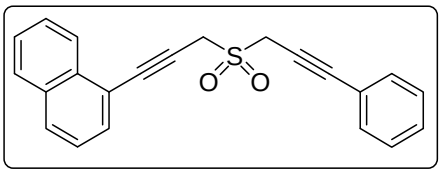

State: yellow solid; yield: 95%;^{1}H NMR (200 MHz, Chloroform-*d*) δ 8.40 - 8.30 (m, 1H), 7.90 - 7.80 (m, 2H), 7.74 - 7.73 (m, 1H), 7.57 - 7.30 (m, 8H), 4.50 (s, 2H), 4.40 (s, 2H); ^{13}C NMR (50 MHz, Chloroform-*d*) δ 133.7, 133.3, 132.2, 131.5, 130.0, 129.5, 128.6, 127.5, 126.8, 126.0, 125.3, 121.6, 119.2, 88.4, 86.6, 80.9, 76.2, 45.0, 44.9 (1C signal was merged).

Synthesis of acenes (6.068 A1-D)

The sulfones **6.061 A-D** (1 eq) were treated with catalytic amount of triethylamine in dry DCM at room temperature to furnish the GB products. After the completion of GB, as monitored by TLC, 25 eq. of anh. $FeCl_3$ in two equal portions was added to the reaction mixture. The reaction mixture was then directly subjected to column chromatography (Si-gel, Petroleum ether-ethylacetate mixture as eluent) and the products were isolated.

11-Naphthalen-2-yl-8,10-dihydro-9-thia-cyclopenta[b]phenanthrene 9,9-dioxide (6.067 A)

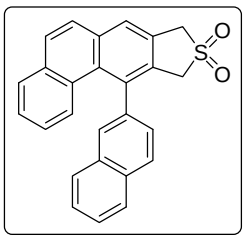

State: yellow solid; **yield**: 95%; ^{1}H NMR (200 MHz, Chloroform-*d*) δ 8.00 - 7.91 (m, 2H), 7.80 - 7.69 (m, 6H), 7.57 - 7.52 (m, 3H), 7.39 - 7.19 (m, 2H), 6.93 (t, *J* = 7.8 Hz, 1H), 4.58 (s, 2H), 4.19, 4.02 (ABq, *J* = 16.5 Hz, 2H); ^{13}C NMR (100

MHz, Chloroform-*d*) δ 139.6, 138.1, 134.1, 133.8, 133.7, 132.9, 131.2, 130.3, 130.1, 129.1, 128. 9, 128.9, 128.3, 128.2, 127.8, 127.3, 127.0, 126.9, 126.7, 126.6, 126.0, 125.9, 57.7, 57.6 (2C signals were merged); MS: m/z = 417.08 $[M+Na]^+$, 395.12 $[M+H]^+$.

7-Naphthalen-1-yl-8,10-dihydro-9-thia-cyclopenta[b]phenanthrene 9,9-dioxide (6.067 B)

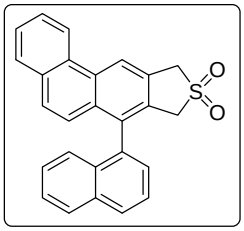

State: yellowish white solid; **yield** 96%; ^{1}H NMR (400 MHz, Chloroform-*d*) δ 8.72 - 8.68 (2H, m), 8.04 - 7.98 (t, *J* = 6.4 Hz, 2H), 7.83 - 7.79 (d, *J* = 7.2 Hz, 1H), 7.72 - 7.62 (m, 3H), 7.58 - 7.49 (m, 2H), 7.42 - 7.36 (m, 1H), 7.32 - 7.21(m, 3H), 4.73 (s, 2H), 4.20, 4.01 (ABq, *J* = 16.2 Hz, 2H); ^{13}C NMR (100 MHz, Chloroform-*d*) δ 136.6, 135.3, 134.0, 132.0, 131.8, 131.4, 130.7, 130.0, 129.8, 129.4, 129.0, 128.1, 127.7, 127.5, 127.3, 127.2, 126.6, 125.8, 125.3, 124.5, 123.0, 120.0, 57.8, 56.5 (2C signals were merged); MS: m/z = 417.09 $[M+Na]^+$, 395.11 $[M+H]^+$.

11-Phenyl-8,10-dihydro-9-thia-cyclopenta[b]phenanthrene 9,9-dioxide (6.067 C)

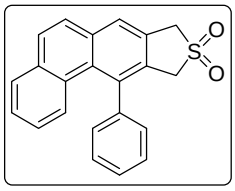

State: yellowish white solid; **yield** 96%; ^{1}H NMR (400 MHz, Acetone-d_6) δ 8.08 (s, 1H), 7.92 (d, *J* = 7.6 Hz, 1H), 7.88 (s, 2H), 7.65 - 7.57 (m, 4H), 7.47 (t, *J* = 7.2 Hz, 1H), 7.38 - 7.35 (m, 2H), 7.09 (t, *J* = 7.2 Hz, 1H), 4.71 (s, 2H), 4.16 (s, 2H); ^{13}C NMR (100 MHz, Chloroform-*d*) δ 142.2, 138.4, 133.9, 133.8, 130.9, 130.3, 129.0, 128.9, 128.6, 128.5, 127.8, 127.0, 126.8, 126.0, 125.9, 57.8, 57.7; MS: m/z = 367.07 $[M+Na]^+$, 345.08 $[M+H]^+$.

7-Phenyl-8,10-dihydro-9-thia-cyclopenta[b]phenanthrene 9,9-dioxide (6.067 D)

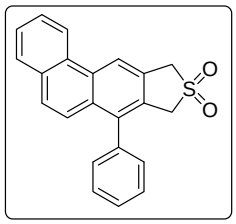

State: yellowish white solid; **yield** 96%; ^{1}H NMR (400 MHz, Acetone-d_6): δ 9.08 (s, 1H), 8.88 (d, J = 8.0 Hz, 1H), 7.97 (d, J = 8.0 Hz, 1H), 7.80 - 7.41 (m, 7H), 4.77 (s, 2H), 4.27 (s, 2H); MS: m/z = 367.08 $[M+Na]^+$, 345.09 $[M+H]^+$.

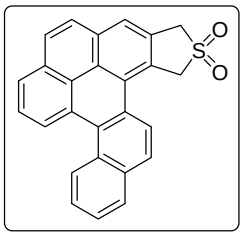

6.068 A1 State: white solid; m.p. 239 - 240 °C; **yield** 90%; ^{1}H NMR (400 MHz, Acetone-d_6) δ 8.92 - 8.89 (m, 2H), 8.45 - 8.40 (m, 4H), 8.34 (s, 1H), 8.20 (d, J = 9.6 Hz, 1H), 8.10 (d, J = 8.8 Hz, 1H), 7.87 (t, J = 7.4 Hz, 2H), 7.81 (t, J = 7.8 Hz, 1H), 5.32 (s, 2H), 4.88 (s, 2H); ^{13}C NMR (100 MHz, Chloroform-d) δ 130.7, 130.6, 130.5, 130.4, 129.9, 129.3, 128.7, 128.1, 127.9, 127.6, 127.5, 127.3, 127.0, 126.8, 126.0, 125.8, 125.7, 125.2, 124.9, 124.7, 124.1, 123.8, 123.5, 121.9, 60.4, 55.6; MS: m/z = 415.03 $[M+Na]^+$, 393.10, $[M+H]^+$; HRMS: Calcd. for $C_{26}H_{17}O_2S^+$ $[M+H^+]$ 393.0949 found 393.0953.

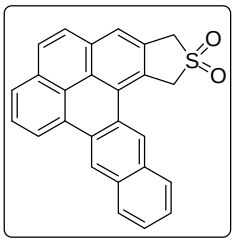

6.068 A2 State: yellow solid; m.p. 241 - 242 °C; **yield**: 95%; ^{1}H NMR (400 MHz, Chloroform-d) δ 8.91 - 8.87 (m, 2H), 8.56 - 8.49 (m, 2H), 8.16 - 8.06 (m, 5H), 7.84 - 7.74 (m, 3H); 5.13 (s, 2H), 4.77 (s, 2H); ^{13}C NMR (100 MHz, Chloroform-d) δ 131.6, 131.4, 131.1, 130.8, 130.7, 129.5, 129.0, 128.9, 128.4, 128.2, 128.1, 128.0, 127.6, 127.5, 127.5, 127.4, 127.3, 127.1, 125.8, 125.6, 125.5, 124.9, 124.8, 124.1, 59.6, 56.0; MS: m/z = 415.05 $[M+Na^+]$, 393.09, $[M+H^+]$; HRMS: Calcd. for $C_{26}H_{17}O_2S^+$ $[M+H^+]$ 393.0949 found 393.0951.

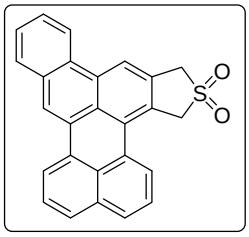

6.068 B1 State: yellowish solid; m.p. >250 °C; **yield**: 30%; ^{1}H NMR (400 MHz, Acetone-d_6) δ 9.16 (s, 1H), 9.06 (bd, J = 8 Hz, 1H), 8.37 - 8.35 (m, 1H), 8.18 (bd, J = 8.4 Hz, 1H), 8.13 (bd, J = 8 Hz, 1H), 7.94 - 7.87 (m, 2H), 7.80 - 7.76 (m, 1H), 7.62 - 7.59 (m, 2H), 7.45 - 7.41 (m, 1H), 7.31 (s, 1H), 7.25 (d, J = 8.8 Hz, 1H), 4.86 (s, 2H), 4.25, 3.96 (ABq, J = 16 Hz, 2H); ^{13}C NMR (100 MHz, Acetone-d_6) δ 135.6, 134.7, 134.2, 132.3, 132.0, 131.8, 131.4, 131.3, 130.7, 129.8, 129.3, 129.0, 128.6, 128.6, 128.1, 127.3, 126.7, 126.0, 125.1, 124.6, 124.0, 123.9, 120.6, 57.2, 55.9 (1C signal was merged); MS: m/z = 415.08 $[M+Na^+]$, 393.23, $[M+H^+]$; HRMS: Calcd. for $C_{26}H_{17}O_2S^+$ $[M+H^+]$ 393.0949 found 393.0943.

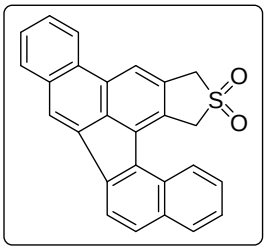

6.068 B2 State: yellow solid; m.p. >250 °C; **yield**: 95%; ^{1}H NMR (400 MHz, Acetone-d_6) δ 9.17 (s, 1H), 9.07 - 9.05 (m, 1H), 8.46 (bd, J = 8.4 Hz, 1H), 8.38 - 8.35 (m, 1H), 7.94 (d, J = 7.6 Hz, 1H), 7.91 - 7.86 (m, 1H), 7.80 - 7.76 (m, 1H), 7.60 (d, J = 7.6 Hz, 1H), 7.56 - 7.52 (m, 1H), 7.33 - 7.10 (m, 2H), 4.85 (s, 2H), 4.30, 4.00 (ABq, J = 16.4 Hz, 2H); ^{13}C NMR (100 MHz, Acetone-d_6) δ 134.6, 134.5, 133.1, 132.5, 132.1, 131.6, 131.3, 131.2, 130.7, 129.8, 129.3, 128.7, 128.6, 128.4, 128.2, 128.1, 126.6, 126.0, 125.2, 125.0, 123.9, 123.9, 121.0, 57.2, 55.9 (1C signal was merged); MS: m/z = 415.05 $[M+Na]^+$, 393.15, $[M+H]^+$; HRMS: Calcd. for $C_{26}H_{17}O_2S^+$ $[M+H]^+$ 393.0949 found 393.0941.

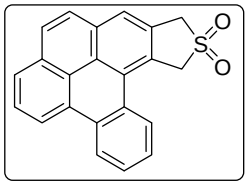

6.068 C State: yellow solid; m.p. 239 - 240 °C; **yield**: 95%; ^{1}H NMR (400 MHz, Chloroform-d) δ 8.47 (s, 1H), 7.94 (s, 1H), 7.75 (d, J = 7.6 Hz, 1H), 7.74 - 7.44 (m, 5H), 7.28 (s, 1H), 7.09 (t, J = 8.4 Hz, 1H), 4.70 (s, 2H), 4.19 (s, 2H); ^{13}C NMR (100 MHz, Chloroform-d) δ 142.0, 138.7, 133.3, 132.2, 130.7, 130.4, 130.1, 129.3, 129.1, 128.9, 128.7, 128.5, 128.3, 128.1, 127.9, 127.5, 126.2, 122.9, 58.0, 57.9; MS: m/z = 365.11 $[M+Na]^+$, 343.07 $[M+H]^+$; HRMS: Calcd. for $C_{22}H_{15}O_2S^+$ $[M+H]^+$ 343.0793 found 343.0798.

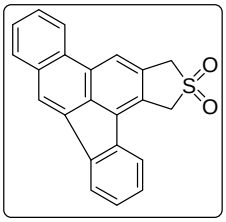

6.068 D State: yellow solid; m.p. 240 - 241 °C; **yield**: 95%, ^{1}H NMR (400 MHz, Chloroform-d) δ 8.71 (s, 1H), 8.67 - 8.64 (m, 1H), 8.44 - 8.41 (m, 1H), 7.77 - 7.75 (m, 2H), 7.46 - 7.45 (m, 3H), 7.22 - 7.20 (m, 2H), 4.69 9s, 2H), 4.15 (s, 2H); ^{13}C NMR (100 MHz, Chloroform-d) δ 138.0, 137.1, 132.1, 130.7, 130.4, 129.8, 129.6, 129.5, 129.4, 129.2, 128.8, 128.6, 128.2, 128.1, 127.9, 125.5, 123.9, 123.0, 119.7, 57.8, 56.8; MS: m/z = 365.10 $[M+Na]^+$, 343.08 $[M+H]^+$; HRMS: Calcd. for $C_{22}H_{15}O_2S^+$ $[M+H]^+$ 343.0793 found 343.0788.

6.6.3 ^{1}H and ^{13}C NMR spectra of selected compounds

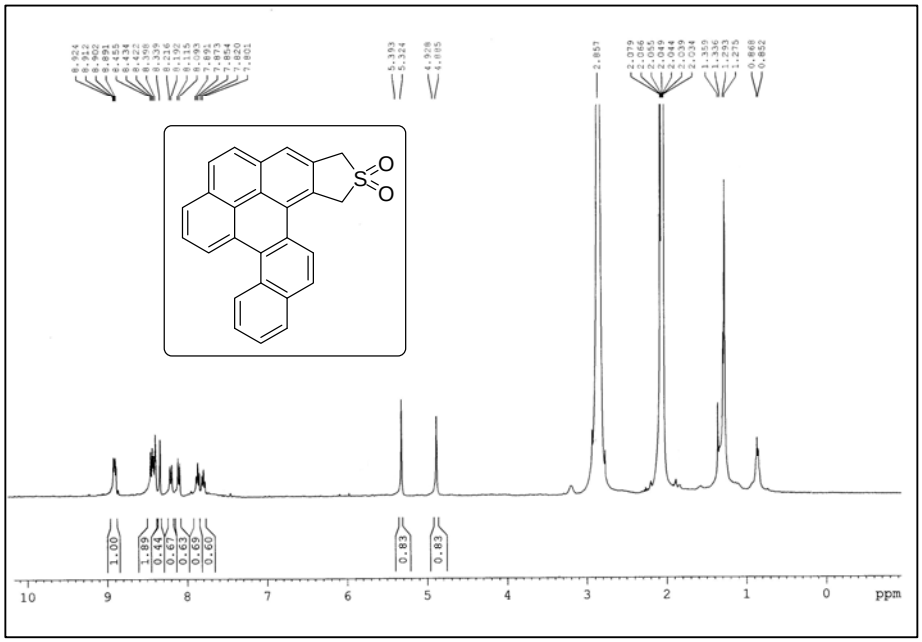

^{1}H NMR (400 MHz, d_6-Acetone) spectrum of 6.068 A1

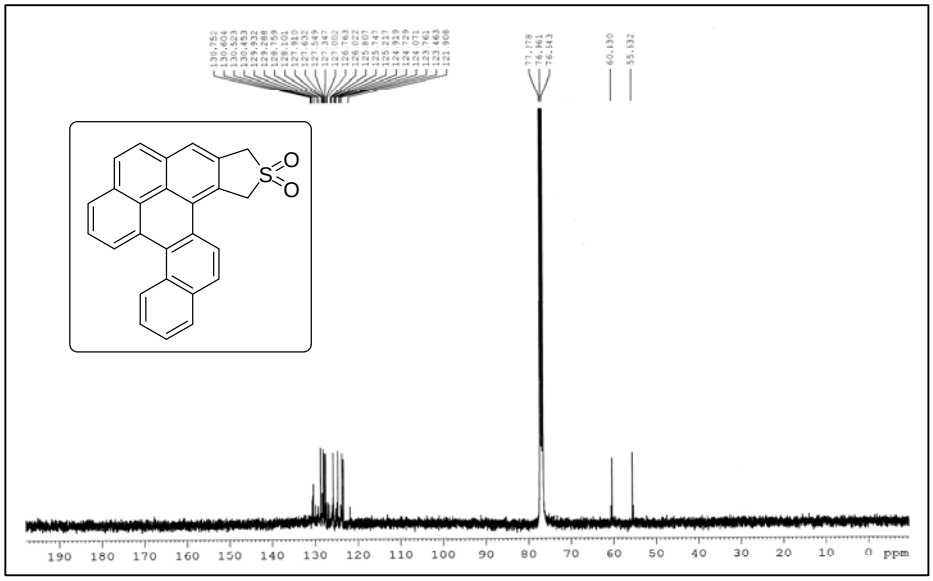

^{13}C NMR (100 MHz) spectrum of 6.068 A1

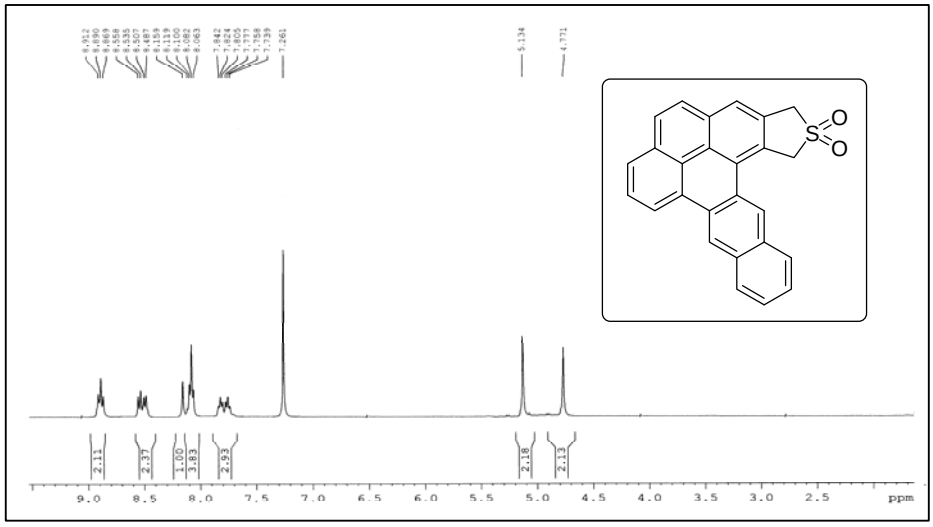

^{1}H NMR (400 MHz) spectrum of 6.068 A2

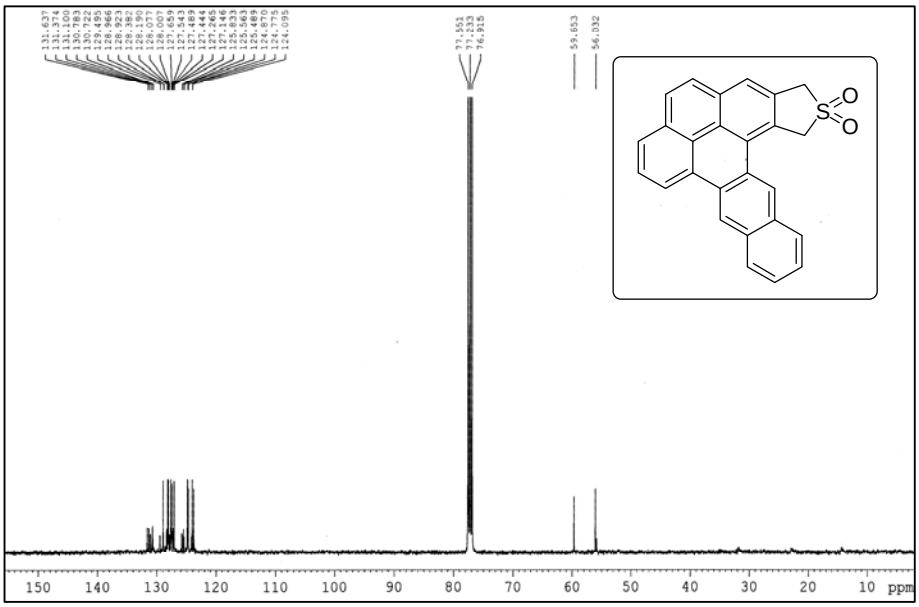

^{13}C NMR (100 MHz) spectrum of 6.068 A2

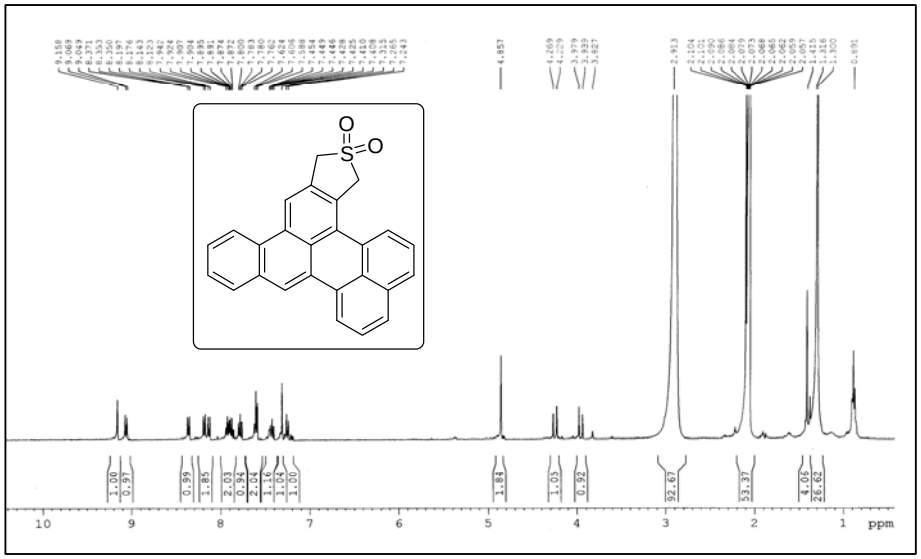

^{1}H NMR (400 MHz, d_6-Acetone) spectrum of 6.068 B1

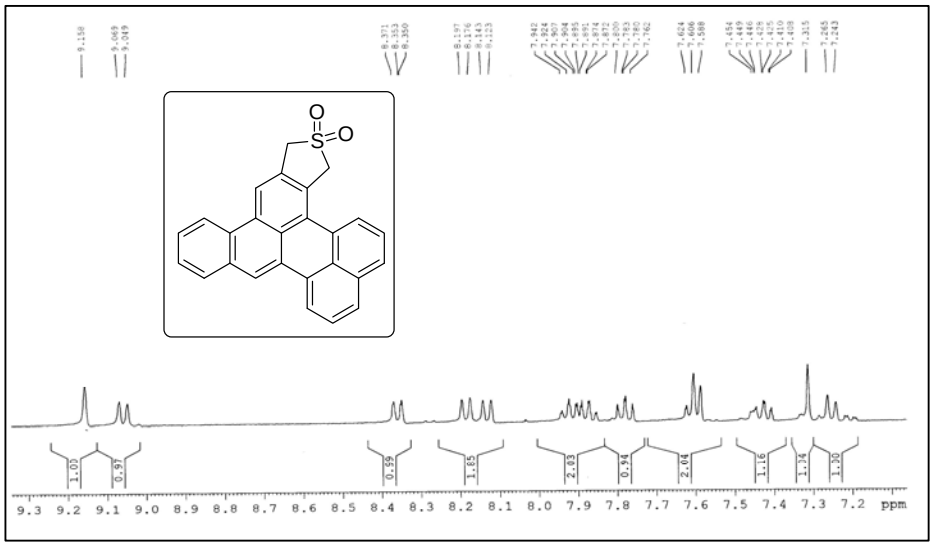

Expanded ^{1}H NMR (400 MHz, d_6-Acetone) spectrum of 6.068 B1

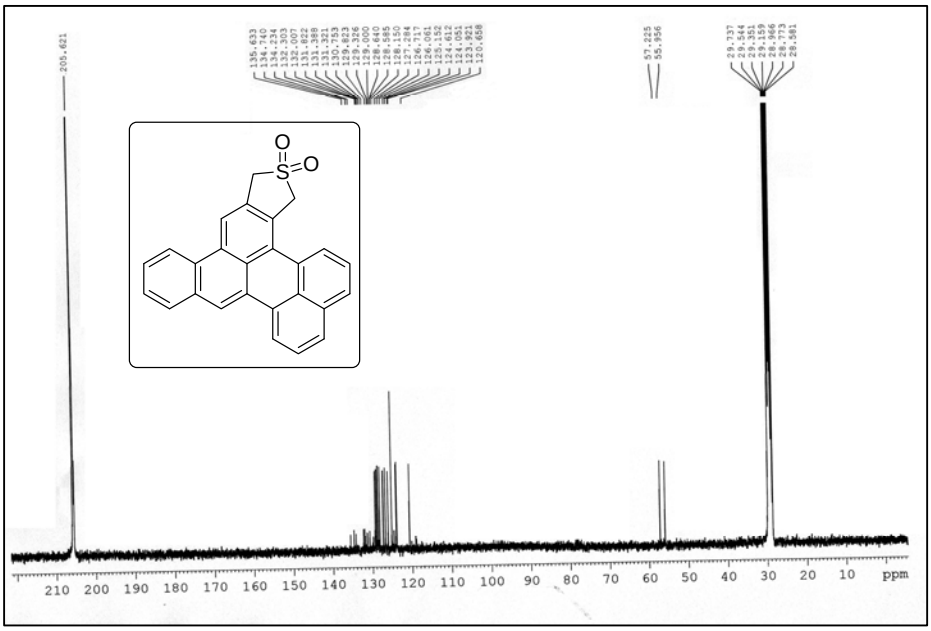

^{13}C NMR (100 MHz, d_6-Acetone) spectrum of 6.068 B1

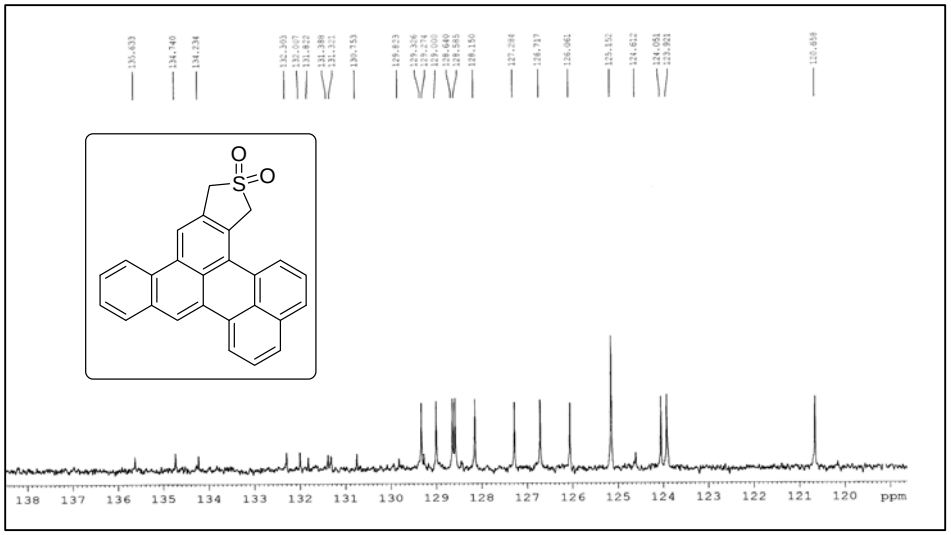

Expanded ^{13}C NMR (100 MHz, d_6-Acetone) spectrum of 6.068 B1

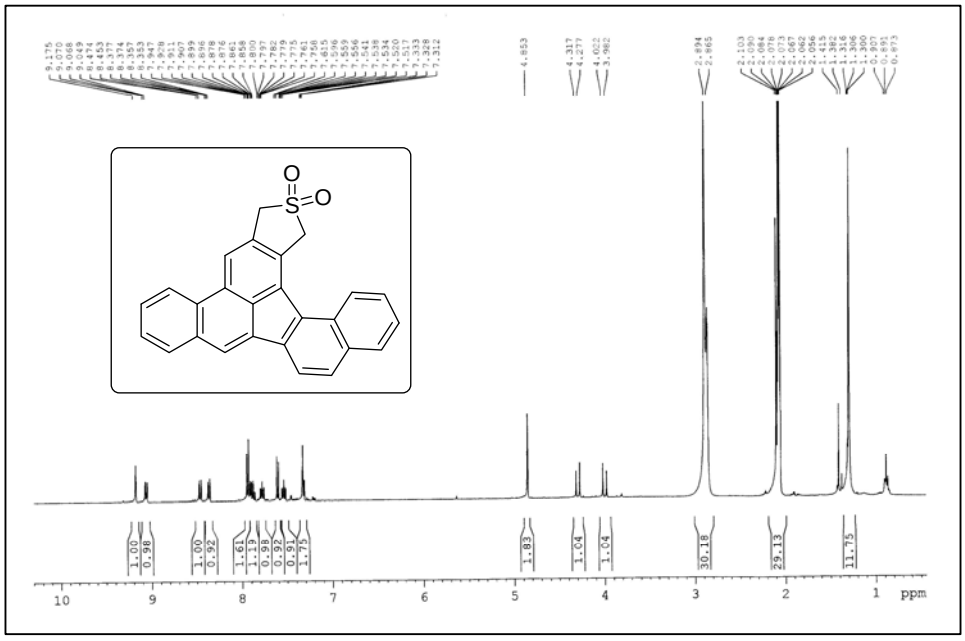

^{1}H NMR (400 MHz, d_6-Acetone) spectrum of 6.068 B2

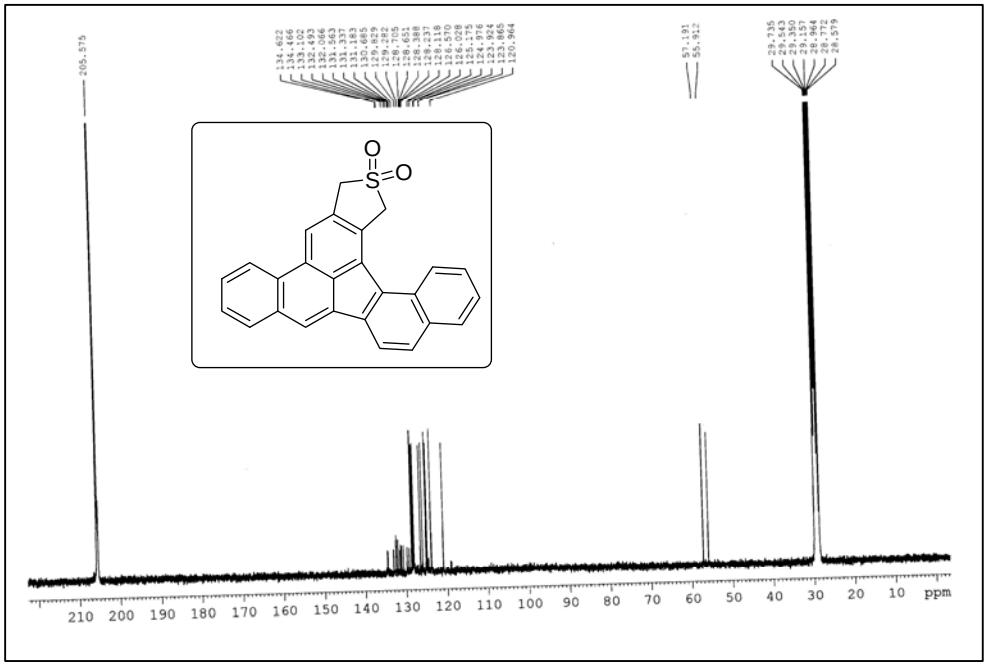

^{13}C NMR (100 MHz, d_6-Acetone)) spectrum of 6.068 B2

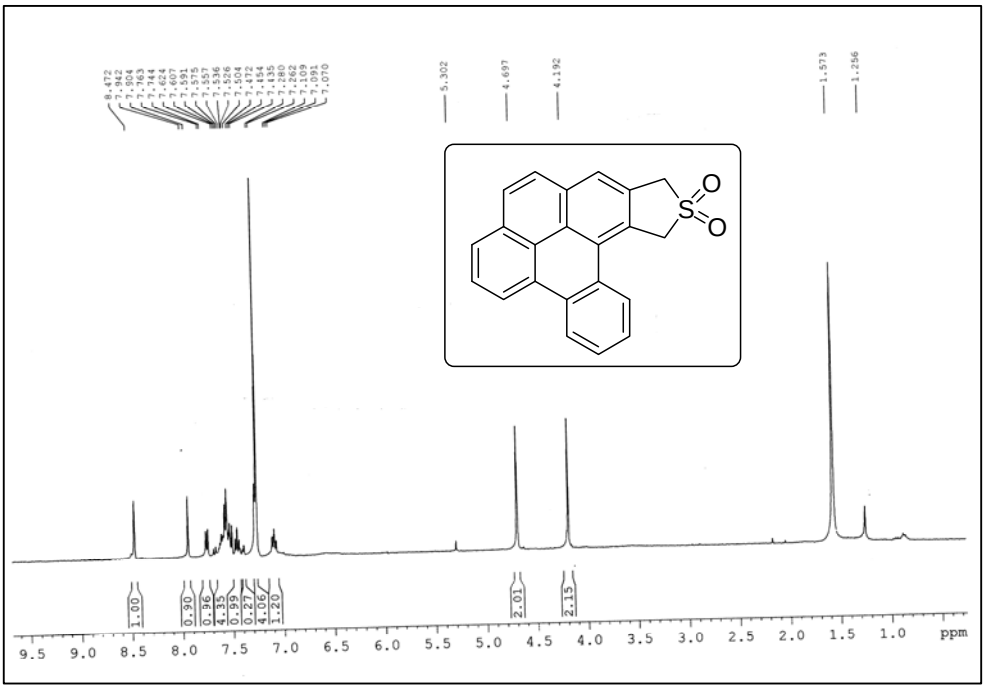

^{1}H NMR (400 MHz) spectrum of 6.068 C

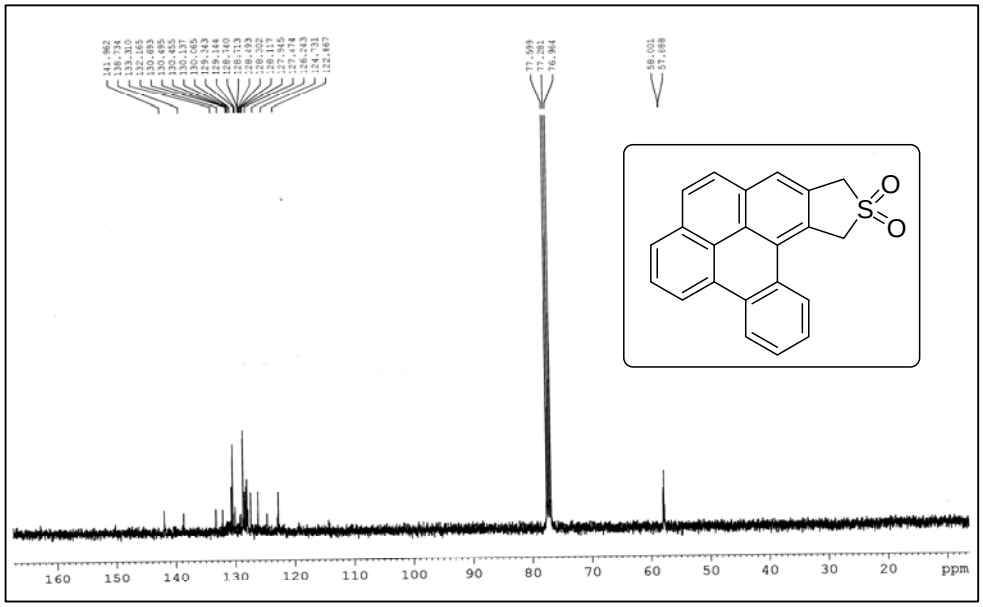

^{13}C NMR (100 MHz) spectrum of 6.068 C

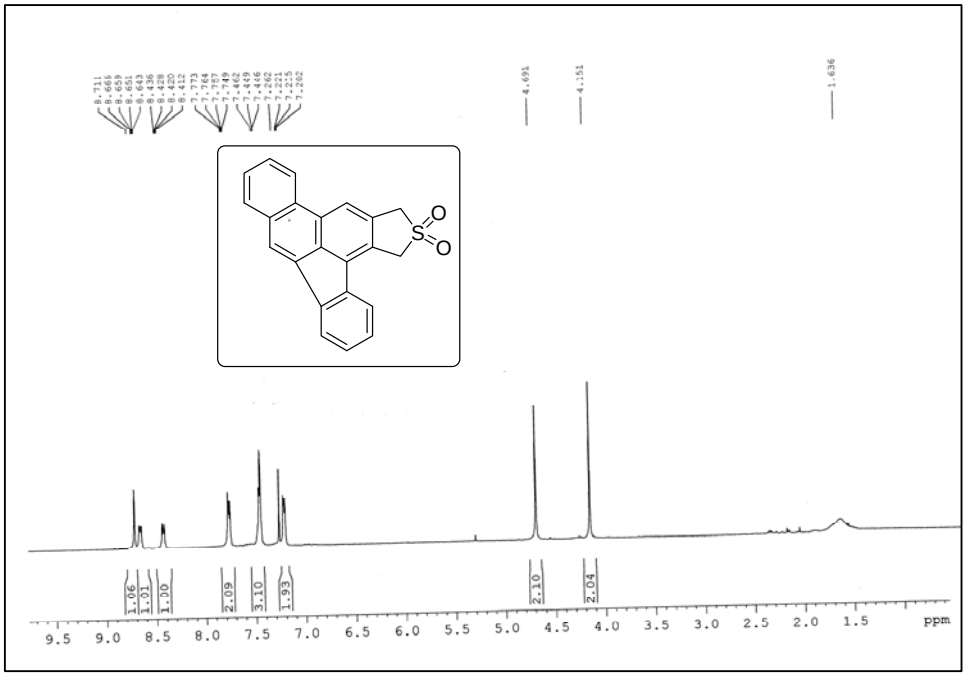

^{1}H NMR (400 MHz) spectrum of 6.068 D

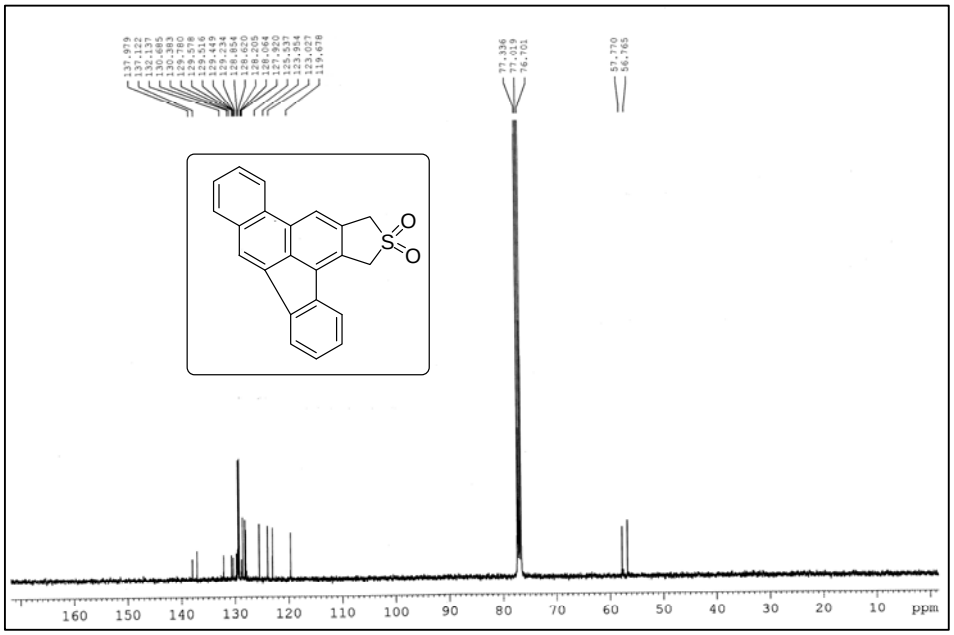

^{13}C NMR (100 MHz) spectrum of 6.068 D

Chapter 7

Summary and Conclusion

7.1 Summary and Conclusion

In this section of the dissertation, major findings of the present investigations have been summarized as follows.

1. The mechanism of Garratt-Braverman cyclization of bis-propargyl sulfones and ethers has been revisited in order to settle the dichotomy involving the diradical and anionic Diels Alder pathways. A thorough study involving the fate of deuterium labeled substrates, trapping of mono or bis-allenes by external nucleophile, use of several experimental techniques like ^{2}H NMR, LA-LDI MS, EPR measurement, supported the intramolecular anionic Diels Alder reaction (IMDAR) mechanism for bis-propargyl ethers involving the mono-allene and a diradical pathway for cyclization of bis-propargyl sulfones involving the bis-allene.

2. Enediyne based protein capture compounds have been synthesized and we have shown that they can selectively bind to HCA II from a mixture of protein. The capture experiments demonstrated the photo cross-linking ability of enediyne possibly occurred *via* the addition of nucleophilic amino acid to the partial zwitterionic form of the diradical generated through photo Bergman cyclization.

3. We have successfully developed strategies to shift the preference of reactivity of various bis-propargyl ethers from Garratt-Braverman cyclization route to 1,5-H shift process. This has led to the synthesis of 3,4-disubstituted furans, which serve as important synthons and appear in various biologically active compounds. As furans are susceptible towards electrophilic attack at 2/5 position, it was a challenge to synthesize 3,4-substituted furans. Bis-propargyl ethers appended with 2-tetrahydropyranyloxy methyl or ethoxy methyl group was observed to follow the alternate 1, 5-H shift process upon base treatment. The initially formed *E*-isomer was shown to isomerize to *Z*-isomer that appeared to be more stable. The factors affecting the interplay of reactivity as well as *E* to *Z* isomerization were evaluated and explained.

4. Bis-propargyl ethers, sulfones and sulfonamides are known to undergo Garratt-Braverman cyclization under basic condition. Similar is the situation for propargyl-alkenyl ethers and sulfonamides. Unlike these ethers and sulfonamides, propargyl-alkenyl sulfones underwent a 6π-electrocyclization process instead of Garratt-Braverman cyclization to thiopyran dioxide derivatives. The method gave rise to a convenient procedure for the synthesis of six-membered cyclic sulfones with a variety of substituents important in medicinal and materials chemistry.

5. A one-pot Garratt-Braverman cyclization and Scholl oxidation route to construct 3 new C-C bonds to synthesize polyaromatic compounds having comparable numbers of benzenoid and non- benzenoid rings was developed. The compounds synthesized have low lying E_{LUMO} level with better oxidative stability as validated by their HOMO energy levels.

7.2 Contribution and future scope

We have been successful in executing a strategy to interchange the preference of GB cyclization to1, 5-H shift for bis-propargyl ethers. The experimental results fit nicely with the theoretical calculations. The method gave rise to a convenient synthetic pathway to 3, 4-disubstituted furans. One of the intriguing aspects of this project was the *E* to *Z* isomerization of the vinyl ethers that need further studies. The reactivity and mechanism of reaction of propargyl alkenyl sulfones under basic condition to give substituted thiopyran dioxides has also been disclosed. The synthesized thiopyran dioxides can be screened for possible biological activities in future. The synthetic importance of GB cyclization has been further elaborated by the synthesis of polyaromatic compounds that has significant applications in materials science. The mechanism of GB cyclization for bis-propargyl sulfones and ethers has also been investigated and proved to be system dependent. In protein capture research, an importance of the present work is the demonstration of the ability of enediyne moiety to act as a photo cross-linker of the protein HCA II.

In future it will be interesting to find out the mechanism of GB cyclization of bis-propargyl amines. The scope of enediyne in protein capture research may be explored further against different proteins of interest by attaching suitable selectivity functionalities. In addition, it will be interesting to investigate the capture study of enediynes in cell cytoplasmic extract. The newly developed route for preparing 3,4-disubstituted furans *via* intramolecular 1,5-H shift pathway can be of great significance to the synthetic chemists and can be pursued in the quest of some priorly reported 3,4-disubstituted furan scaffold based bio-active molecules.

References

1. (a) Mohamed, R. K.; Peterson, P. W.; Alabugin, I. V. Concerted reactions that produce diradicals and zwitterions: Electronic, steric, conformational, and kinetic control of cycloaromatization processes. *Chem. Rev*. **2013**, *113*, 7089-7129; (b) Peterson, P. W.; Mohamed, R. K.; Alabugin I. V. How to lose a bond in two ways - The diradical/zwitterion dichotomy in cycloaromatization reactions. *Eur. J. Org. Chem.* **2013**, *2013*, 2505-2527.

2. (a) Jones, R. G.; Bergman, R. G. P-Benzyne, Generation as an intermediate in a thermal isomerization reaction and trapping evidence for the 1,4-benzenediyl structure. *J. Am. Chem. Soc*. **1972**, *9*, 660-661; (b) Bergman, R. G. Reactive 1,4-dehydroaromatics. *Acc. Chem. Res*. **1973**, *6*, 25-31; (c) Lockhart, T. P.; Bergman, R. G. Kinetic evidence for the formation of discrete 1,4-dehydrobenzene intermediates. Trapping by inter- and intramolecular hydrogen atom transfer and observation of high-temperature CIDNP. *J. Am. Chem. Soc*. **1981**, *103*, 4082-4090; (d) Mayer, J.; Sondheimer, F. 1,5,9-Tridehydro[14]annulene and Bicyclo[9.3.0]tetradeca-1,5,7,11,13-pentaene-3,9-diyne, an acetylenic homolog of azulene containing fused five- and eleven-membered rings. *J. Am. Chem. Soc*. **1966**, *88*, 602-603; (e) Wong, H. N. C.; Sondheimer, F. 5,12-dihydro-6,11-didehydronaphthacene, A derivative of 1,4-didehydronaphthalene. *Tetrahedron Lett.* **1980**, *21*, 217-220; (f) Darby, N.; Kim, C. U.; Salaün, J. A.; Shelton, K. W.; Takada, S.; Masamune, S. Concerning the 1,5-didehydro[10]annulene system. *J. Chem. Soc*. **1971**, *23*, 1516-1517.

3. (a) Mandal, S.; Bag, S. S.; Basak, A. Chelation-controlled Bergman cyclization: Synthesis and reactivity of enediynyl ligands. *Chem. Re*V. **2003**, *103*, 4077-4094; (b) Kar, M.; Basak, A. Design, synthesis, and biological activity of unnatural enediynes and related analogues equipped with pH-dependent or phototriggering devices. *Chem. Rev*. **2007**, *107*, 2861-2890; (c) *DNA and RNA Clea*V*ers and Chemotherapy of Cancer and Viral Diseases*; Meunier, B., Ed.; Kluwer Publishers: Dordrecht, The Netherlands, **1996**; p 1; (d) Xi, Z.; Goldberg, I. H. *Comprehensi*V*e Natural Product Chemistry*; Barton, D. H. R., Nakanishi, K., Eds.; Pergamon: Oxford, U.K., **1999**; *7*, 553.

4. (a) Garratt, P. J.; Neoh, S. B. Strained heterocycles. Properties of five-membered heterocycles fused to four-, six-, and eight-membered rings prepared by base-catalyzed rearrangement of 4-Heterohepta-l,6-diynes *J. Org. Chem*. **1979**, *44*, 2667-2674; (b) Cheng, Y. S. P.; Garratt, P. J.; Neoh, S. B.; Rumjanek, V. H. Synthesis and thermal rearrangement of 4-heterohepta-1,2,5,6-tetraenes. *Isr. J. Chem*. **1985**, *26*, 101-107; (c) Braverman, S.; Duar, Y.; Segev, D. Cycloaromatizartion and cyclodimerization of bridged diallenes. *Tetrahedron Lett*. **1976,** 3181-3184.

5. (a) Maxam, A. M.; Gilbert, W. Sequencing end-labeled DNA with base-specific chemical cleavages. *Methods Enzymol*. **1980**, *65*, 499-560; (b) Nicolaou, K. C.; Wendeborn, S.; Maligres, P.; Isshiki, K.; Zein, N.; Ellestad, G. Selectivity and mechanism of action of novel DNA-cleaving Sulfones.*Angew. Chem. Int. Ed. Engl.* **1991**, *30*, 418-420.

6. Calkins, T. L.; Grissom, J. W. Kinetic and Mechanistic studies of the tandem enediyne-radical cyclization. *J. Org. Chem*. **1993**, *58*, 5422-5427.

7. Calkins, T. L.; M^{c}Millen, H. A.; Jiang, Y.; Grissom, J. W.; Determination of the activation parameters for the Bergman cyclization of aromatic enediynes. *J. Org. Chem.* **1994**, *59*, 5833-5835.

8. Ramkumar, D.; Kalpana, M.; Varghese, B.; Sankararaman, S. Cyclization of enediyne radical cations through chemical, photochemical, and electrochemical oxidation: The role of state symmetry. *J. Org. Chem.* **1996**, *61,* 2247-2250.

9. David, W. M.; Kerwin, S. M. Synthesis and thermal rearrangement of *C*,*N*-dialkynyl Imines: A potential Aza-Bergman Route to 2,5-didehydropyridine. *J. Am. Chem. Soc.* **1997**, *119,* 1464-1465.

10. Hoffner, J.; Schottelius, M. J.; Feichtinger, D.; Chen, P. Chemistry of the 2,5-didehydropyridine biradical: Computational, kinetic, and trapping studies toward drug design. *J. Am. Chem. Soc.* **1998,** *120,* 376-385.

11. Evenzahav, A.; Turro, N. J. Photochemical rearrangement of enediynes: Is a "Photo-Bergman" cyclization a possibility? *J. Am. Chem. Soc.* **1998,** *120,* 1835-1841.

12. Koseki, S. Benzannelation effect on enediyne cycloaromatization: An ab initio molecular orbital study. *J. Phys. Chem. A*. **1999**, *103,* 7672-7675.

13. Jones, G. B.; Warner, P. M. On the mechanism of quinone formation from the Bergman Cyclization: some theoretical insights. *J. Org. Chem.* **2001**, *66,* 8669-8672.

14. Kovalenko, S. V.; Alabugin, I. V. C1-C5 Photochemical cyclization of enediynes. *J. Am. Chem. Soc*. **2002**, *124*, 9052-9053.

15. Friese, S. J.; Tichenor, M.; O'Connor, J. M. Ruthenium-mediated cycloaromatization of acyclic enediynes and dienynes at ambient temperature. *J. Am. Chem. Soc*. **2002**, *124*, 3506-3507.

16. Manoharan, M.; Kovalenko, S. V.; Alabugin, I. V. Tuning rate of the Bergman cyclization of benzannelated enediynes with ortho substituents. *Org. Lett.* **2002**, *4*, 1119-1122.

17. Feng, L.; Kerwin, S. M. Isolation of a cyclopropane-containing product from the rearrangement of a 3-aza-3-ene-1,5-diyne under acid catalysis. *Tetrahedron Lett.* **2003**, 44, 3463–3466.

18. Mifsud, N.; Mellon, V.; Perera, K. P. U.; Smith Jr., D. W.; Echegoyen, L. In situ EPR spectroscopy of aromatic diyne cyclopolymerization. *J. Org. Chem.* **2004**, *69*, 6124-6127.

19. Usuki, T.; Mita, T.; Das. P.; Yoshimura, F.; Inoue, M.; Kubota, S. T.; Hirama, M.; Akiyama, K.; Lear, M. J. Spin trapping of ^{13}C-Labeled p-benzynes generated by Masamune–Bergman cyclization of bicyclic nine-membered enediynes. *Angew. Chem. Int. Ed*. **2004**, *43*, 5249-5253.

20. Lewis, K. D.; Matzger, A. J. Bergman cyclization of sterically hindered substrates and observation of phenyl-shifted products. *J. Am. Chem. Soc.* **2005**, *127*, 9968-9969.

21. Nakanishi, K.; Usuki, T.; Ellestad, G. A. Spin-trapping of the p-benzyne intermediates from ten-membered enediyne Calicheamicin γ_1^1. *Org. Lett*. **2006**, *8*, 5461-5463.

22. Rodgers, B. L.; O'Connor, J. M.; Perrin, C. L. Nucleophilic addition to a *p*-Benzyne derived from an enediyne: A new mechanism for halide incorporation into biomolecules. *J. Am. Chem. Soc.* **2007**, *129*, 4795-4799.

23. Laroche, C.; Li, J.; Kerwin, S. M. Cytotoxic 1,2-dialkynylimidazole-based aza-enediynes: aza-Bergman rearrangement rates do not predict cytotoxicity. *J. Med. Chem*. **2011**, *54*, 5059–5069.

24. Baroudi, A.; Mauldin, J.; Alabugin, I. V. Conformationally gated fragmentations and rearrangements promoted by interception of the Bergman cyclization through intramolecular H-abstraction: A possible mechanism of auto-resistance to natural enediyne antibiotics? *J. Am. Chem. Soc*. **2010**, *132*, 967–979.

25. Grdičak, M.; Matanović, I.; Zimmermann, B.; Jerić, I. Bergman cyclization of acyclic amino acid derived enediynes leads to the formation of 2,3-dihydrobenzo[f]isoindoles. *J. Org. Chem*. **2010**, *75*, 6219–6228.

26. Poloukhtine, A.; Rassadin, V.; Kuzmin, A.; Popik, V. V. Nucleophilic cycloaromatization of ynamide-terminated enediynes. *J. Org. Chem*. **2010**, *75*, 5953-5962.

27. Roy, S.; Anoop, A.; Biradha, K.; Basak, A. Synthesis of angularly fused aromatic compounds from alkenyl enediynes by a tandem radical cyclization process. *Angew. Chem. Int. Ed*. **2011**, *50*, 8316-8319.

28. Ylijoki, K. E. O.; Lavy, S.; Fretzen, A.; Kündig, E. P. A synthetic and mechanistic investigation of the chromium tricarbonyl-mediated Masamune−Bergman cyclization. Direct observation of a ground-state triplet p-benzyne biradical. *Organometallics* **2012**, *31*, 5396−5404.

29. Greer, E. M.; Quezada, C. S.; Cosgriff, C. V. Butylated hydroxytoluene enediyne: access to diradical and electrophilic quinone methide intermediates. *J. Phys. Org. Chem*. **2015**, *28*, 365–369.

30. (a) Iwai, I.; Ide, J. Studies on acetylenic compounds. The novel cyclization reaction of diacetylenic compounds to naphthalene derivatives involving prototropic rearrangement. *Chem. Pharm. Bull. Jpn.* **1964**, *12*, 1094-1100; (b) Iwai. I. in *Mechanisms of Molecular Migrations*, Vol. 2, B. S. Thyagarajan, Ed., Interscience, New York, N.Y., **1969**.

31. Braverman, S.; Segev, D. A novel cyclization of diallenic sulfones. *J. Am. Chem. Soc*. **1974**, *96*, 1245-1247.

32. Garratt, P. J.; Neoh, S. B. Base Catalyzed Rearrangement of Bispropargyl Sulfides, Ethers, and Amines. The synthesis of novel heterocyclic systems. *J. Am. Chem. Soc.* **1975**, *97*, 3255-3257.

33. Cheng, Y. S. P.; Dominguez, E.; Garratt, P. J.; Neoh, S.B. Reaction of bispropadienyl sulphides. The 3,4-dimethylenethiophene diradical. *Tetrahedron Lett.* **1978**, *19*, 691-694.

34. Braverman, S.; Duar, Y. Thermal Rearrangements of allenes. Synthesis and mechanism of cycloaromatization of π and heteroatom bridged diallenes. *J. Am. Chem. Soc*. **1990**, *112*, 5830-5837.

35. Zafrani, Y.; Gottlieb, H. E.; Braverman, S. Tandem rearrangement, cyclization and aromatization of sulfur bridged propargylic systems. *Tetrahedron Lett.* **2000**, *41*, 2675-2678.

36. Zafrani, Y.; Cherkinsky, M.; Gottlieb, H. E.; Braverman, S. A new approach to the synthesis of 2-vinylthiophenes and selenophenes; competition between free radical and anionic cycloaromatization of bridged di and tetrapropargylic sulfides and selenides. *Tetrahedron* **2003**, *59*, 2641-2649.

37. Kumar, E. V. K. S.; Cherkinsky, M.; Sprecher, M.; Goldberg, I.; Braverman, S. Electron depleted bis(methylene)cyclobutenes: sulfinyl and sulfonyl substitution. *Tetrahedron* **2005**, *61*, 3547-3557.

38. Kudoh, T.; Mori, T.; Shirahama, M.; Yamada, M.; Ishikawa, T.; Saito, S.; Kobayashi, H. Intramolecular Anionic Diels-Alder Reactions of 1-Aryl-4-oxahepta-1,6-diyne Systems in DMSO. *J. Am. Chem. Soc*. **2007**, *129*, 4939-4947.

39. Maji, M.; Mallick, D.; Mandal, S.; Anoop, A.; Bag, S. S.; Basak, A.; Jemmis, E. D. Selectivity in Garratt-Braverman cyclization: An experimental and computational Study. *Org. Lett*. **2011**, *13,* 888-891.

40. (a) Feldman, K. S.; Selfridge, B. R. Exploration of Braverman reaction chemistry. Synthesis of tricyclic dihydrothiophene dioxide derivatives from bis-propargyl sulfones. *Heterocycles* **2010**, *81*, 117-143; (b) Mondal, S.; Maji, M.; Basak, A. A Garratt-Braverman route to aryl naphthalene lignans. *Tetrahedron Lett*. **2010**, *52,* 1183-1186; (c) Mondal, S.; Mitra, T.; Mukherjee, R.; Addy, P. S.; Basak, A. Garratt-Braverman cyclization, a powerful tool for C-C bond formation. *Synlett* **2012**, *23*, 2582-2602; (d) Addy, P. S.; Dutta, S.; Biradha, K.; Basak, A. A facile Garratt-Braverman cyclization route to intercalative DNA-binding bisquinones.*Tetrahedron Lett*. **2012**, *53*, 19-22; (e) Mitra, T.; Das, J.; Maji, M.; Das, R.; Das, U. K.; Chattaraj, P. K.; Basak, A. A one pot Garratt-Braverman cyclization and Scholl oxidation route to acene-helicene hybrids. *RSC Adv*. **2013**, *3*, 19844-19848; (f) Mitra, T.; Jana, S., Pandey, S.; Bhattacharya, P.; Khamrai, U. K.; Anoop, A.; Basak, A. Asymmetric Garratt–Braverman cyclization: A route to axially chiral aryl naphthalene–amino acid hybrids. *J. Org. Chem.* **2014**, *79*, 5608-5616.

41. Khatib, A-M.; Mohottalage, D.; Basak, S.; Kolajova, M.; Bag, S. S.; Basak, A. *PloS one* **2009**, *4*, e7700.

42. (a) Galm, U.; Hager, M. H.; Lanen, S. G. V.; Ju, J.; Thorson, J. S.; Shen, B. Antitumor Antibiotics: Bleomycin, Enediynes, and Mitomycin. *Chem. Rev.* **2005**, *105*, 739-758; (b) Myers, A. G.; Kuo, E. Y.; Finney, N. S.; Thermal generation of α,3-dehydrotoluene from

(z)-1,2,4-heptatrien-6-yne. *J. Am. Chem. Soc.* **1989**, *111*, 8057-8059; (c) Myers, A. G.; Dragovich, P. S. Design and dynamics of a chemically triggered reaction cascade leading to biradical formation at subambient temperature. *J. Am. Chem. Soc.* **1989**, *111*, 9130-9132; (d) Schmittel, M.; Strittmatter, M.; Kiau, S. Switching from the Myers reaction to a new thermal cyclization mode in enyne-allenes. *Tetrahedron Lett.* **1995**, *36*, 4975-4978; (e) Schmittel, M.; Strittmatter, M.; Vollman, K.; Kiau, S. Intramolecular Formal Diels-Alder Reaction in Eneyne Allenes. A New Synthetic Route to Benzofluorenes and Indeno[1,2-g]quinolines *Tetrahedron Lett.* **1996**, *37*, 999-1002; (f) Hopf, H.; Musso, H. Preparation of Benzene by Pyrolysis of cis- and trans- 1,3-Hexadien-5-yne. *Angew. Chem. Int. Ed.* **1969**, *8*, 680; (g)Vavilala, C.; Byrne, N.; Kraml, C. M.; Ho, D. M.; Pascal, R. A. J. Thermal C^1-C^5 Diradical Cyclization of Enediynes. *J. Am. Chem. Soc.* **2008**, *130*, 13549-13551.

43. Zafrani, Y.; Gottlieb, H, E.; Sprecher, M.; Braverman. S. Sequential intermediates in the base-catalyzed conversion of bis(π-conjugated propargyl) sulfones to 1,3-dihydrobenzo- and naphtho[*c*]thiophene-2,2-dioxides. *J. Org. Chem.* **2005**, *70*, 10166-10168.

44. (a) Bowes, C. M.; Montecalvo, D. F.; Sondheimer, F**.** O-Dipropadienylbenzene and 2,3-dipropadienylnaphthalene. The oxidation of diallenes to cyclic peroxides with triplet oxygen. *Tetrahedron Lett.* **1973**, *14*, 3181-3184; (b) Bell, T. W.; Bowes, C. M.; Sondheimer, F. Structure and conformational isomerism of the major dimer of 2,3-naphthoquinodimethane. *Tetrahedron Lett.* **1980**, *21*, 3299-3302.

45. Keskin, S.; Balci, M. Intramolecular Heterocyclization of *O*-Propargylated Aromatic Hydroxyaldehydes as an Expedient Route to Substituted Chromenopyridines under Metal-Free Conditions. *Org. Lett.* **2015**, *17*, 964−967.

46. Viehe, H. G.; Janousek, Z.; Merenyi, R.; Stella, L. The captodative effect. *Acc. Chem. Res.* **1985**, *18*, 148−154.

47. Das, J.; Mukherjee, R.; Basak. A. Selectivity in Garratt−Braverman Cyclization of Aryl-/Heteroaryl-Substituted Unsymmetrical Bis-Propargyl Systems: Formal Synthesis of 7′-Desmethylkealiiquinone. *J. Org. Chem.* **2014**, *79*, 3789-3798.

48. Sainsbury, M. *Heterocyclic Chemistry*; RSC Publishing: Cambridge, **2001**; p 93.

49. (a) Mulzer, J.; Bilow, J.; Wille G. The Anionic [1,3]-H-Shift Applied in Synthesis: A Novel Access to (+)-Citreoviral. *J. Prakt. Chem.* **2000**, *342*, 773-778; (b) Mulzer, J.; Wille, G.; Bilow, J.; Arigoni, D.; Martinoni, B.; Roten, K. A mechanistically unusual base induced [1,3]-H-shift in homoallylic ethers. *Tetrahedron Lett.* **1997**, *38*, 5469-5472.

50. (a) Cabrera-Pardo, J. R.; Chai, D. I.; Liu, S.; Mrksich M.; Kozmin, S. A. Label-assisted mass spectrometry for the acceleration of reaction discovery and optimization. *Nat. Chem.* **2013**, *5*, 423-427; (b) Addy, P. S.; Basu Roy, S.; Mandal, S. M.; Basak, A. Polyaromatic label-assisted laser desorption ionization mass spectrometry (LA-LDI MS): a new analytical technique for selective detection of zinc ion. *RSC Adv.* **2014**, *4*, 23314-23318;

(c) Addy, P. S.; Bhattacharya, A.; Mandal, S. M.; Basak, A. Label-assisted laser desorption/ionization mass spectrometry (LA-LDI-MS): an emerging technique for rapid detection of ubiquitous *cis*-1,2-diol functionality. *RSC Adv*. **2014**, *4*, 46555-46560; (d) Mondal, A.; Das, A. K.; Basak, A. Label-assisted laser desorption/ionization mass spectrometry (LA-LDI-MS): use of pyrene aldehyde for detection of biogenic amines, amino acids and peptides. *RSC Adv.* **2015**, *5*, 106912-106917.

51. (a) Shultz, D. A.; Boal, A. K.; Lee, H.; Farmer, G. T. Structure−Property Relationships in Trimethylenemethane-Type Biradicals. 2. Synthesis and EPR Spectral Characterization of Dinitroxide Biradicals. *J. Org. Chem.* **1999**, *64*, 4386-4396; (b) Burton, G. W.; Doba, T.; Gabe, E. J.; Hughes, L.; Lee, F. L.; Prasad, L.; Ingold, K. U. Autoxidation of biological molecules. 4. Maximizing the antioxidant activity of phenols. *J. Am. Chem. Soc.* **1985**, *107*, 7053-7065; (c) Adam, W.; Barneveld, C. van.; Bottle, S. E.; Engert, H.; Hanson, G. R.; Harrer, H. M.; Heim, C.; Nau, W. M.; Wang, D. EPR Characterization of the Quintet State for a Hydrocarbon Tetraradical with Two Localized 1,3-Cyclopentanediyl Biradicals Linked by *meta*-Phenylene as a Ferromagnetic Coupler. *J. Am. Chem. Soc.* **1996**, *118,* 3974-3975; (d) Komaguchi, K.; Iida, T.; Goh,Y.; Ohshita, J.; Kunai, A.; Shiotani, M. An ESR study of dynamic biradicals of two TEMPOs bridged with –($SiMe_2$)*n*– (*n*=1–4) in liquid solution. *Chem. Phys. Lett.* **2004**, *387*, 327-331; (e) Closs, G. L.; Forbes, M. D. E.; Piotrowiak, P. Spin and reaction dynamics in flexible polymethylene biradicals as studied by EPR, NMR, optical spectroscopy, and magnetic field effects. Measurements and mechanisms of scalar electron spin-spin coupling. *J. Am. Chem. Soc.* **1992**, *114*, 3285-3294.

52. (a) Grinberg, O. Y.; Williams, B. B.; Ruuge, A. E.; Grinberg, S. A.; Wilcox, D. E.; Swartz, H. M.; Freed, J. H. Oxygen Effects on the EPR Signals from Wood Charcoals: Experimental Results and the Development of a Model. *J. Phys. Chem. B* **2007**, *111,* 13316-13324; (b) Chirkov, A. K.; Koryakov, V. I.; Nekrasov, V. N.; Matevosyan, R. O. Effect of oxygen on the EPR spectra of solutions of the stable DPPH radical. *Zhurnal Strukmrnoi Khimii,* **1969**, *10*, 454-458.

53. (a) Talsi, E.P.; Semikolenova, N.V.; Panchenko, V.N.; Sobolev, A.P.; Babushkin, D.E.; Shubin, A.A.; Zakharov, V.A. The metallocenermethylaluminoxane catalysts formation: EPR spin probe study of Lewis acidic sites of methylaluminoxane. *J. Mol. Cat. A: Chemical* **1999**, *139*, 131-137; (b) Gafurov, M.; Lyubenova, S.; Denysenkov, V.; Ouari, O.; Karoui, H.; Moigne, F. L.; Tordo, P.; Prisner, T. EPR Characterization of a Rigid Bis-TEMPO–Bis-Ketal for Dynamic Nuclear Polarization. *Appl. Magn. Reson*. **2010**, *37*, 505; (c) Ottaviani, M. F.; Garcia-Garibay, M.; Turro N. J. TEMPO radicals as EPR probes to monitor the adsorption of different species into X zeolite. *Colloids Surfaces A: Physicochem. Eng. Aspects* **1993**, *72*, 321-332.

54. (a) Wróbel, A. Decrease in 2,2,6,6-tetramethyl-piperidine-1-oxyl (TEMPO) EPR signal in peroxynitrite-treatederythrocyte membranes. *Cell. Mol. Biol. Lett.* **2001**, *6*, 941-953; (b) Drago, R. S. In *Physical Methods in Chemistry* (Saunders golden sunburst series), Saunders College publishing, **1977**, p 504.

55. (a) Geurink, P. P.; Prely, M. M.; van der Marel, G. A.; Bischoff, R.; Overkleeft, H. S. Photoaffinity labeling in activity-based protein profiling. *Top. Curr. Chem*. **2012**, 324, 85-113; (b) Willems, L. I.; van der Linden, W. A.; Li, N.; Li, K. Y.; Liu, N.; Hoogendoorn, S.; van der Marel, G. A.; Florea, B. I.; Overkleeft, H. S. Bioorthogonal chemistry: Applications in activity based protein profiling. *Acc. Chem. Res*. **2011**, *44*, 718-729 and references therein; (c) Heal, W. P.; Dang, T. H. T.; Tate, E. W. Activity based probes: Discovering new biology and new drug targets. *Chem. Soc. Rev*. **2011**, *40*, 246-257.

56. (a) Anderson, N. L.; Anderson, N. G. Proteome and proteomics: New Technologies, New concepts and New words. *Electrophoresis* **1998**, *19*, 1853-1861; (b) Fonovic, M.; Bogyo, M. Activity based probes as a tool for functional proteomic analysis of proteases. *Proteomics* **2008**, *5*, 721-730; (c) Saghatelian, A.; Jessani, N.; Joseph, A.; Humphrey, M.; Cravatt, B. F. Activity based probes for the proteomic profiling of metalloproteases. *Proc. Natl. Acad. Sci. USA*. **2004**, *101*, 10000-10005; (d) Aebersold, R.; Mann, M. Mass spectrometry based proteomics. *Nature* **2003**, *422*, 198-207.

57**.** Dutta, A. K.; Tran, T.; Napadensky, B.; Teella, A.; Brookhart, G.; Roop, P. A.; Zhang, A. W.; Tustian, A. D. Zydney, A. L.; Shinkazh, O. Purification of monoclonal antibodies from clarified cell culture fluid using Protein A capture continuous countercurrent tangential chromatography. *J. Biotechnol*. **2015**, *213*, 54-64.

58. (a) Li, X.; Cao, J-H.; Ying, L.; Rondard, P.; Zhang, Y.; Yi, P.; Liu, J-F.; Nan, F-J. Activity based probe for specific photoaffinity labeling gamma-aminobutyric acid B (GABAB) receptors on living cells: Design, synthesis and biological evaluation. *J. Med. Chem*. **2008**, *51*, 3057-3060 and references therein; (b) Hosoya, T.; Inoue, A.; Hiramatsu, T.; Aoyama, H.; Ikemoto, T. Suzuki, M. Facile synthesis of diazido-functionalized biaryl compounds as radioisotope-free photoaffinity probes by Suzuki-Miyaura coupling. *Bioorg. Med. Chem*. **2009**, *17*, 2490-2496.

59. Fischer, J. J.; Graebner, O. Y.; Dalhoff, C.; Michaelis, S.; Schrey, A. K.; Ungewiss, J.; Andrich, K.; Jeske, D.; Kroll. F.; Glinski, M.; Sefkow, M.; Dreger, M.; Koester, H. Comprehensive Identification of Staurosporine-Binding Kinases in the Hepatocyte Cell Line HepG2 using Capture Compound Mass Spectrometry (CCMS). *J. Proteome Res.* **2010**, *9*, 806–817.

60. (a) Lapinsky, D. J. Tandem photoaffinity labeling bioorthogonal conjugation in medicinal chemistry. *Bioorg. Med. Chem.* **2012**, 6237-6347; (b) Sumranjit, J.; Sang, J. C. Recent advances in target characterization and identification by photoaffinity probes. *Molecules* **2013**, *18*, 10425-10451.

61. (a) Buchmueller, K. L.; Hill, B. T.; Platz, M. S.; Week, K. M. RNA-tethered phenyl azide photocrosslinking via a short-lived indiscriminant electrophile. *J. Am. Chem. Soc.* **2003**, *125*, 10850-10861.

62. (a) Kuroda, T.; Suenaga, K.; Sakakura, A.; Handa, T.; Okamoto, K.; Kigoshi, H. Study of the interaction between actin and antitumor substance Aplyronine A with a novel

fluorescent photoaffinity probe. *Bioconjugate Chem*. **2006**, *17*, 524-529; (b) Dubinsky, L.; Krom, B. P.; Meijler, M. M. Diazirine based photoaffinity labeling. *Bioorg. Med. Chem.* **2012**, *20*, 554-570; (c) Chattopadhaya, S.; Chan, E. W.; Yao, S. Q. An affinity based probe for the proteomic profiling of aspartic proteases. *Tetrahedron Lett.* **2005**, *46*, 4053-4056.

63. Addy, P. S.; Saha, B., Singh, N. D. P.; Das, A. K.; Bush, J. T.; Lejeune, C.; Schofield, C. J.; Basak, A. 1,3,5-Trisubstituted benzenes as fluorescent photoaffinity probes for human carbonic anhydrase II capture. *Chem. Commun.* **2013**, *49*, 1930-1932.

64. (a) Böttcher, T.; Sieber, S. A. *β*-Lactams and *β*-lactones as activity-based probes in chemical biology. *Med. Chem. Commun.* **2012**, *3*, 408-417; (b) Chigrinova, M.; Mackenzie, D. A.; Sherratt, A. R.; Cheung, L. L.; Pezacki, J. P. Kinugasa reactions in water: from green chemistry to bioorthogonal labelling. *Molecules* **2015**, *20*, 6959-6969.

65. (a) Alterio, V.; Fiore, A. D.; D' Ambrosio, K.; Supuran, C. T.; Simone, G. D. Multiple binding modes of inhibitors to Carbonic Anhydrases: How to design specific drug targeting 15 different isoforms? *Chem. Rev***.** **2012**, *112*, 4421-4468; (b) Iyer, R.; Barrese, III, A. A.; Parakh, S.; Parker, C. N.; Tripp, B. C. Inhibition profiling of Human Carbonic Anhydrase II by high-throughput screening of structurally diverse, biologically active compounds. *J. Biomol*. *Screen* **2006**, *11*, 782-791.

66. (a) Ram, S.; Celik, G.; Khloya, P.; Vullo, D.; Supuran, C. T. Benzenesulfonamide bearing 1,2,4-triazole scaffolds as potent inhibitors of tumor associated carbonic anhydrase isoforms hCA IX and hCA XII. *Bioorg. Med. Chem*. **2014**, *22*, 1873-1882; (b) Leitans, J.; Kazaks, A.; Balode, A.; Ivanova, J.; Zalubovskis, R.; Supuran, C. T.; Tars, K. Efficient Expression and Crystallization System of Cancer-Associated Carbonic Anhydrase Isoform IX. *J. Med. Chem*. **2015**, *58*, 9004-9009.

67. Li, X.; Cao, J.-H.; Ying, L.; Rondard, P.; Zhang, Y.; Yi, P.; Liu, J. F.; Nan F. J Activity-Based Probe for Specific Photoaffinity Labeling *γ*-Aminobutyric Acid B ($GABA_B$) Receptors on Living Cells: Design, Synthesis, and Biological Evaluation. *J. Med. Chem*. **2008**, *51*, 3057-3060 and references therein.

68. (a) Scozzafava, A.; Casini, A.; Supuran, C. T. Carbonic anhydrase inhibitors. *Medicinal Research Reviews*, **2003**, *23*, 146-189; (b) A. Maresca, C. Temperini, H. Vu, N. B. Pham, S. A. Poulsen, A. Scozzafava, R. J. Quinn, C. T. Supuran, Non-Zinc Mediated Inhibition of Carbonic Anhydrases: Coumarins Are a New Class of Suicide Inhibitors. *J Am Chem Soc.* **2009**, *131*, 3057-3062.

69. (a) Choy, N.; Blanco, B.; Wen, J.; Krishnan, A.; Russell, K. C. Photochemical and Thermal Bergman Cyclization of a Pyrimidine Enediynol and Enediynone. *Org. Lett*. **2000**, *2*, 3761-3764; (b) Karpov, G. V.; Popik, V. V. Triggering of the Bergman Cyclization by Photochemical Ring Contraction. Facile Cycloaromatization of Benzannulated Cyclodeca-3,7-diene-1,5-diynes. *J. Am. Chem. Soc*. **2007**, *129*, 3792-3793; (c) Poloukhtine, A.; Popik, V. V. Two-Photon Photochemical Generation of Reactive Enediyne. *J. Org. Chem*. **2006**, *71*, 7417-7421; (d) Pandithavidana, D. R.; Poloukhtine, A.; Popik, V. V. Photochemical

Generation and Reversible Cycloaromatization of a Nine-Membered Ring Cyclic Enediyne. *J. Am. Chem. Soc.* **2009**, *131*, 351-356; (e) Mohamed, R. K.; Peterson, P. W.; Alabugin, I. V. Concerted Reactions That Produce Diradicals and Zwitterions: Electronic, Steric, Conformational, and Kinetic Control of Cycloaromatization Processes. *Chem. Rev*. **2013**, *113*, 7089-7129.

70. (a) Wright, J. M.; Plourde, II, G. W.; Purohit, A. D.; Wyatt, J. K.; Hynd, G.; Fouad, F.; Jones, G. B. Synthesis and Photochemical Activity of Designed Enediynes. *J. Am. Chem. Soc.* **2000**, *122*, 9872-9873; (b) Kovalenko, S. V.; Alabugin, I. V. Lysine–enediyne conjugates as photochemically triggered DNA double-strand cleavage agents. *Chem. Commun*. **2005**, 1444-1446; (c) Hynd, G.; Wright, J. M.; Purohit, A.; Plourde, II, G. W.; Huber, R. S.; Mathews, J. E.; Li, A.; Kilgore, M. W.; Bubley, G. J.; Yancisin, M.; Brown, M. A.; Jones, G. B. Target-Directed Enediynes: Designed Estramycins. *J. Org. Chem*. **2001**, *66*, 3688-3695.

71. Breiner, B.; Kaya, K.; Roy, S.; Yang, W. Y.; Alabugin, I. V. Hybrids of amino acids and acetylenic DNA-photocleavers: optimising efficiency and selectivity for cancer phototherapy. *Org. Biomol. Chem*. **2012**, *10*, 3974-3987.

72**.** Hatial, I.; Addy, P. S.; Ghosh, A. K.; Basak, A. Synthesis of highly efficient pH-sensitive DNA cleaving aminomethyl N-substituted cyclic enediyne and its L-lysine conjugate. *Tetrahedron Lett.* **2013**, *54*, 854-857.

73. Banci, L.; Merz, K. M. Binding of Azide to Human Carbonic Anhydrase II: The Role Electrostatic Complementarity Plays in Selecting the Preferred Resonance Structure of Azide. *J. Phys. Chem*. **1996**, *100*, 17414-17420.

74. The protein HCA II itself has fluorescent properties due to the presence of amino acids like tryptophan, tyrosine and phenyl alanine but with low quantum yield. (Teale F. W. J.; Weber, G. Ultraviolet fluorescence of the aromatic amino acids. *Biochem. J.* **1957**, *65*, 476-482. Thus, low intensity fluorescent bands for the protein appear at relatively higher concentrations. The concentrations of HCA II used in lane 6 in **Fig. 3.10 M** and lane 6 in **Fig. 3.10 N** were 40 μM, higher than that used in lane 3 in **Fig. 3.10 P** (20 μm). Thus we observed faint fluorescence signals in lane 6 in **Fig. 3.10 M** and lane 6 in **Fig. 3.10 N** which was not visible in lane 3 in **Fig. 3.10 P**.

75. Kumar, C. V.; Buranaprapuk, A.; Opiteck, G. J.; Moyer, M. B.; Jockusch, S.; Turro, N. J. Photochemical protease: site-specific photocleavage of hen egg lysozyme and bovine serum albumin. *Proc. Natl. Acad. Sci.USA*, **1998**, *95*, 10361-10366.

76. **(**a) http://web.expasy.org/peptide_mass/; (b) Huynh, M. L.; Russell, P.; Walsh, B. Tryptic digestion of in-gel proteins for mass spectrometry analysis. *Methods Mol Biol*. **2009**, *519*, 507-513.

77. It is known that photochemically excited enediynes (and even alkynes) can react with nitrogen atoms of nucleobases. This type of reactivity may have similar origin to the reactions of proteins reported in this paper by Alabugin *et al*. They have predicted the formation of a DNA–protein crosslinking through lysine–DNA adducts occurring through initial oxidation of lysine and reaction of an N-centered radical with DNA. (see ref. 71). A possible lysine cross-linking is shown below:

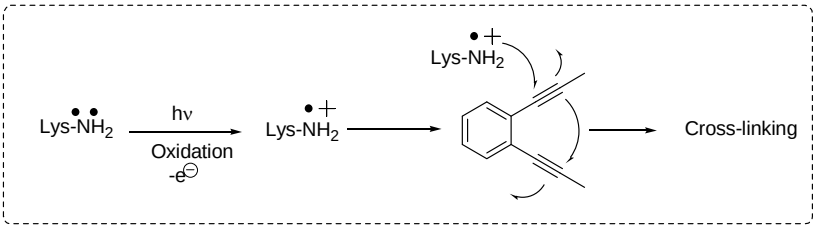

78. (a) Zafrani, Y.; Braverman, S.; Gottlieb, H. E. Dynamic NMR study of the rotation around "biphenyl-type" bonds in polycyclic sulfoxides. *J. Org. Chem.* **2002**, *67*, 3277-3283; (b) Pechenick, T.; Gottlieb, H. E.; Sprecher, M.; Braverman, S. New Structures from Multiple Rearrangements of Propargylic Dialkoxy Disulfides. *J. Am. Chem. Soc.* **2003**, *125*, 14290-14291; (c) Pechenick, T.; Gottlieb, H. E.; Sprecher, M.; Braverman, S. Reactivity Pattern of Bis(propargyloxy) Disulfides: Tandem Rearrangements and Cyclizations. *Synthesis* **2011**, 1741-1750.

79. (a) Braverman, S.; Zafrani, Y.; Gottlieb, H. E. Base catalyzed rearrangement of π-conjugated sulfur and selenium bridged propargylic systems. *Tetrahedron* **2001**, *57*, 9177-9185; (b) Samanta, D.; Rana, A.; Schmittel, M. Nonstatistical dynamics in the thermal Garratt–Braverman/[1,5]-H shift of one ene–diallene: An experimental and computational study. *J. Org. Chem*. **2014**, *79*, 8435-8439;

80. (a) Thiel, D.; Doknic, D.; Deska, J. Enzymatic aerobic ring rearrangement of optically active furylcarbinols. *Nat*. *Commun*. **2014**, *5*, 5278; (b) Shinohara, H.; Atobe, S.; Masuno, H.; Ogawa, A.; Sonoda, M. $IrCl_3$ or $FeCl_3$ catalyzed convenient synthesis of 3-hydroxyphthalates. *Tetrahedron Lett.* **2011**, *52*, 6238-6241; (c) Gubina, T. I.; Kharchenko, V. G. *Chem.* Furan and its derivatives in the synthesis of other heterocycles. *Heterocycl. Compd.* **1995**, *31*, 900-916.

81. Ansell, M. F.; Caton, M. P. L.; North, P. C. The synthesis of 3,4-disubstituted furan prostanoids. *Tetrahedron Lett.* **1981,** *22,* 1727-1728.

82. Jana, S.; Anoop, A. Does the Mechanism of the Garratt–Braverman Cyclization Differ with Substrates? A Computational Study on Bispropargyl Sulfones, Sulfides, Ethers, Amines, and Methanes. *J. Org. Chem.* **2016**, *81*, 7411-7418.

83. (a) Yang, Y.; Wong, H. N. C. 3,4-Bis(tributylstannyl)furan: a versatile building block for the regiospecific synthesis of 3,4-disubstituted furans. *J. Chem. Soc. Chem. Commun.* **1992**, 656-658; (b) Yang, Y.; Wong, H. N. C. Regiospecific Synthesis of 3,4-Disubstituted Furans and 3-Substituted Furans Using 3,4-Bis(tri-n-butylstannyl)furan and 3-(Tri-n-butylstannyl)furan as BuiIding Blocks. *Tetrahedron.* **1994**, *50,* 9583-9608.

84. Garcia, E. S.; Mardyukov, A.; Studentkowski, M.; Montero, L. A.; Sander, W. Furan−Formic Acid Dimers: An ab Initio and Matrix Isolation Study. *J. Phys. Chem. A* **2006**, *110*, 13775-13785.

85. Muhamadejev, R.; Vigante, B.; Cekavicus, B.; Plotniece, A.; Duburs, G.; Liepinsh, E.; Petrova, M. Intramolecular C-H···O Hydrogen Bonding in 1,4-Dihydropyridine Derivatives. *Molecules* **2011**, *16*, 8041-8052.

86. (a) Gaoni, Y. Fragmentation of 6,6-dichloro-3-thiabycyclo[3,1,O]hexane-3,3-dioxides in acids. 2H-thiopyran-1,1dioxides and 4H-thiopyran-4-ones. *Tetrahedron Lett.* **1976**, *17*, 2167-2170; (b) Mouradzadegun, A.; Pirelahi, H. Synthesis and photoisomerization Of 4,4-Diphenyl-2,6-Di(p-Methoxyphenyl)-4H-Thiopyran-1,1-Dioxide, An approach to the regioselectivity in photorearrangement of 2,4,4,6-tetraaryl-4H-Thiopyran-1,1-Dioxides. *Phosphorus, Sulfur and Silicon* **2000**, *165*, 149-154; (c) Skattebol, L.; Boulette, B.; Solomon, S. Thiopyran 1,1-dioxide derivatives from addition of amines to propargyl sulfone *J. Org. Chem*. **1968**, *33*, 548-552; (d) Wong, S. S. Y.; Brant, M. G.; Barr, C.; Oliver, A. G.; Wulff, J. E. Dipolar addition to cyclic vinyl sulfones leading to dual conformation tricycles. *Beilstein J. Org. Chem.* **2013**, *9*, 1419-1425.

87. (a) Choy, N.; Choi, H.; Jung, W. H.; Kim, C.R.; Yoon, H.; Lee, T. G.; Kim, S. C.; Koh, J. S. Synthesis of irreversible HIV-1 protease inhibitors containing sulfonamide and sulfone as amide bond isosteres. *Bioorg.& Med. Chem. Lett.* **1997**, *7*, 2635-2638; (b) Yarmolchuk, V. S.; Mukan, I. L.; Grygorenko, O. O.; Tolmachev, A. A.; Shishkina, S. V.; Shishkin, O. V.; Komarov, I. V. An Entry into Hexahydro-2*H*-thieno[2,3-*c*]pyrrole 1,1-Dioxide Derivatives. *J. Org. Chem*. **2011**, *76*, 7010-7016; (c) Xue, F.; Seto, T. C. A Comparison of Cyclohexanone and Tetrahydro-4*H*-thiopyran-4-one 1,1-Dioxide as Pharmacophores for the Design of Peptide-Based Inhibitors of the Serine Protease Plasmin. *J. Org. Chem*. **2005**, *70*, 8309-8321; (d) Baumgarth, M.; Beier, N.; Gericke, R. Bicyclic Acylguanidine Na^+/H^+ Antiporter Inhibitors. *J. Med. Chem.* **1998**, *41*, 3736-3747; (e) Koch, F. M.; Peters, R. Lewis Acid/Base Catalyzed [2+2]-Cycloaddition of Sulfenes and Aldehydes: A Versatile Entry to Chiral Sulfonyl and Sulfinyl Derivatives. *Chem. Eur. J.* **2011**, *17*, 3679-3692; (f) Zajac, M.; Peters, R. Catalytic Asymmetric Synthesis of *β*-Sultams as Precursors for Taurine Derivatives. *Chem. Eur. J.* **2009**, *15*, 8204-8222; (g) Brant, M. G.; Wulff, J. E.

A Rigid Bicyclic Platform for the Generation of Conformationally Locked Neuraminidase Inhibitors. *Org. Lett*. **2012**, *14*, 5876-5879; (h) http://www.enamine.net/index.php?option=com_content&task=view&id=131.

88. Shukla, J. P.; Singh, R. K.; Sawant, S. R.; Varadarajan, N. Liquid-liquid extraction of palladium(II) from nitric acid by bis(2-ethylhexyl) sulphoxide. *Anal. Chim. Acta* **1993**, *276*, 181.

89. (a) Wielpütz, T.; Strey, R.; Klemmer, H. F. M. A Journey toward Sulfolane Microemulsions Suggested as Inert, Nonaqueous Reaction Media. *Langmuir* **2015**, *31*, 11227-11235; (b) Balducci, L.; Bianchi, D.; Bortolo, R.; Aloisio, R.; Ricci, M.; Tassinari, R.; Ungarelli, R. Direct Oxidation of Benzene to Phenol with Hydrogen Peroxide over a Modified Titanium Silicalite. *Angew. Chem. Int. Ed*. **2003**, *42*, 4937-4940; (c) Krishna, P. R.; Manjuvani, A.; Kannan, V.; Sharma, G. V. M. Sulpholane-A new solvent for Baylis-Hillman reaction. *Tetrahedron Lett.* **2004**, *45*, 1183-1185.

90. (a) Tso, H.; Hung, S. C.; Chou, T. 4-Bromo-2-sulfolenes. Butadienyl cation equivalents. *J. Org. Chem*. **1987**, *52*, 3394-3399; (b) Tso, H.; Lee, S.; Chou, T. A cyclization approach to functionalized seven-membered carbocycles. *J. Org. Chem*. **1987**, *52*, 5082-5085.

91. Ren, X.; Lake, C. H.; Churchill, M. R.; Turos, E. Regiochemical and stereochemical studies on halocyclization reactions of unsaturated sulfides. *J. Org. Chem*. **1995**, *60*, 6468-6483.

92. Quin, L. D.; Leimert, J.; Middlemas, E. D.; Miller, R. W.; Mcphail, A. T. 3,8-Thionanedione 1,1-dioxide. Synthesis and solid-state conformation. *J. Org. Chem*. **1979**, *44*, 3496-3500.

93. Afrasiabi, R.; Farsani, M. R.; Yadollahi, B. Highly selective and efficient oxidation of sulphides with hydrogen peroxide catalyzed by a chromium substituted Keggin type polyoxometalate. *Tetrahedron Lett.* **2014**, *55*, 3923-3925.

94. Chakravarthy, R. D.; Ramkumar, V.; Chand, D. K. A molybdenum based metallomicellar catalyst for controlled and selective sulfoxidation reactions in aqueous medium. *Green Chem.* **2014**, *16*, 2190-2196.

95. Fukuda, N.; Ikemoto, T. Imide-Catalyzed Oxidation System: Sulfides to Sulfoxides and Sulfones. *J. Org. Chem*. **2010**, 75, 4629-4631.

96. Lim, K. M.; Hayashi, T. Rhodium-Catalyzed Asymmetric Arylation of Allyl Sulfones under the Conditions of Isomerization into Alkenyl Sulfones. *J. Am. Chem. Soc*. **2015**, *137*, 3201-3204.

97. Hatial, I. PhD. Dissertation, Indian Institute of Technology Kharagpur, **2015**, p 89.

98. (a) Aoyama, T.; Takido, T.; Kodomari, M. A Convenient Synthesis of Thioacetates and Thiobenzoates Using Silica-Gel Supported Potassium Thioacetate. *Synth. Commun*. **2003**, *33*, 3817-3824; (b) Cao, P. X. Stereoselective synthesis of substituted all-*trans* 1,3,5,7-octatetraenes by a modified Ramberg–Bäcklund reaction. *Tetrahedron* **2002**, *58*, 1301-1307.

99. (a) Cao, X.; Yang, Y.; Wang, X. A direct route to conjugated enediynes from dipropargylic sulfones by a modified one-flask Ramberg–Bäcklund reaction. *J. Chem. Soc. Perkin Trans*. *1* **2002**, *22*, 2485-2489; (b) Kato, K.; Ono, M.; Akita, H. New total synthesis of (±)-, (−)- and (+)-chuangxinmycins. *Tetrahedron* **2001**, *57*, 10055-10062.

100. Bordwell, F. G. Equilibrium acidities in dimethyl sulfoxide solution. *Acc. Chem. Res.* **1988**, *21*, 456-463.

101. Raboisson, P. J-M. B.; Vandyck, K.; Nyanguile, O.; McGowan, D. C.; Vendeville, S. M. H.; Amssoms, K. I. E.; Boutton, C. W. M.; Lory, P. M. J.; Hu, L.; Van den Broeck W. M. M.; WO 2008099020 A1, **2008**.

102. Rossi, S.; Pagani, G. 3-phenyl-2H-thiopyran, 1,1-dioxide and 2H-thiocromen, 1,1-dioxide. Synthesis and acidic properties. *Tetrahedron Lett.* **1966**, *7*, 2129-2134.

103. Exothermicity has been assumed in view of the fact that in this 6π-electrocyclization one C–C π bond is replaced by a C–C σ bond, along with the formation of a stable six-membered ring. Moreover, the reaction occurs at a low temperature (0 °C). DFT-based calculations on an oxa-6π-electrocyclization predicted exothermicity, see: Kienzler, M. A. Ph. D. dissertation, **2010**, p. 4 http://escholarship.org/uc/item/6158904v.

104. Simkin, B. Y.; Makarov, S. P.; Minkin, V. I. Photo- and thermochromic spirans. 13. Calculation of the pathways of the thermal electrocyclic reactions of chromenes and their structural analogs by the MINDO/3 method. *Chem. Heterocycl. Compd* (N. Y., NY, U. S.) **1982**, *18*, 779.

105. Corey, E. J.; Koenig, H.; Lowry, T. H. Stereochemistry of α-sulfonyl carbanions. *Tetrahedron Lett*. **1962**, *3*, 515-520.

106. Kumar, R.; Nair, D.; Namboothiri, I. Reactions of vinyl sulfone with α-diazo-β-ketosulfone and Bestmann–Ohira reagent for the regioselective synthesis of highly functionalized pyrazoles. *Tetrahedron* **2014**, *70*, 1794-1799.

107. Baldwin, J. E. Rules for ring closure. *J. Chem. Soc., Chem Commun* **1976**, 734-736.

108. (a) Barnes, J. C.; Juríček, M.; Strutt, N. L.; Frasconi, M.; Sampath, S.; Giesener, M. A.; Mcgrier, P. L.; Bruns, C. J.; Stern, C. L.; Sarjeant, A. A.; Stoddart, J. F. ExBox: A Polycyclic Aromatic Hydrocarbon Scavenger. *J. Am. Chem. Soc.* **2013**, *135*, 183-192; (b) Byers, P. M.; Rashid, J. I.; Mohamed, R. K.; Alabugin, I. V. Polyaromatic Ribbon/Benzofuran Fusion via Consecutive Endo Cyclizations of Enediynes. *Org. Lett.* 2012, *14*, 6032-6035.

109. (a) Clar, E. *Polycyclic Hydrocarbons*, Academic Press, New York, **1964**; (b) Harvey, R. G. *Polycyclic Aromatic Hydrocarbons*, Wiley-VCH, New York, **1997**; (c) Hopf, H. *Classics in Hydrocarbon Chemistry*, Wiley VCH, Weinheim, Germany, **2000**; (d) Diederich, F.; Rubin, Y. Synthetic Approaches toward Molecular and Polymeric Carbon Allotropes. *Angew. Chem. Int. Ed.* **1992**, *31*, 1101-1123; (e) Boese, R.; Matzger, A. J.; Mohler, D. L.; Vollhardt, K. P. C. C_3-Symmetric Hexakis(trimethylsilyl)[7]phenylene["Tris(biphenylenocyclobutadieno)cyclohexatriene"], a Polycyclic Benzenoid Hydrocarbon with Slightly Curved Topology. *Angew. Chem. Int. Ed.* **1995**, *34*, 1478-1481; (f) Tong, L.; Lau, H.; Ho, D. M.; Pascal Jr, R. A. Polyphenylbiphenyls and Polyphenylfluorenes. *J. Am. Chem. Soc*. **1998**, *120*, 6000-6006; (g) Percec, V.; Glodde, M.; Bera, T. K.; Miura, Y.; Shiyanovskaya, I.; Singer, K. D.; Balagurusamy, V. S. K.; Heiney, P. A.; Schnell, I.; Rapp, A.; Spiess, H. W.; Hudson, S. D.; Duan, H. Self-organization of supramolecular helical dendrimers into complex electronic materials. *Nature* **2002**, *419*, 862; (h) Ajami, D.; Oeckler, O.; Simon A.; Herges, R. Synthesis of a Möbius aromatic hydrocarbon. *Nature* **2003**, *426*, 819-821; (i) Sakurai, H.; Daiko T.; Hirao, T. A Synthesis of Sumanene, a Fullerene Fragment. *Science* **2003**, *301*, 1878.

110. (a) Allard, S.; Forster, M.; Souharce, B.; Thiem H.; Scherf, U. Organic Semiconductors for Solution-Processable Field-Effect Transistors (OFETs). *Angew. Chem. Int. Ed*. **2008**, *47*, 4070-4098; (b) Pisula, W.; Mishra, A.K.; Li, J.; Baumgarten M.; Müllen, K. Carbazole-based Conjugated Polymers as Donor Material for Photovoltaic Devices. *Org. Photovoltaics* **2008**, 93-128; (c) Thompson B. C.; Frechet, J. M. J. Polymer–Fullerene Composite Solar Cells. *Angew. Chem. Int. Ed*. **2008**, *47*, 58-77; (d) Arias, A. C.; MacKenzie, J. D.; McCulloch, I.; Rivnay, J.; Salleo, A. Materials and Applications for Large Area Electronics: Solution-Based Approaches. *Chem. Rev*. **2010**, *110*, 3-24.

111. (a) Houk, K. N.; Lee, P. S.; Nendel, M. Polyacene and Cyclacene Geometries and Electronic Structures: Bond Equalization, Vanishing Band Gaps, and Triplet Ground States Contrast with Polyacetylene. *J. Org. Chem.* **2001**, *66*, 5517-5521; (b) Garcia–Bach, M. A.; Peñaranda, A.; Klein, D. J. Valence-bond treatment of distortions in polyacene polymers. *Phys. Rev. B* **1992**, *45*, 10891; (c) Raghu, C.; Pati, A.; Ramasesha, S. Structural and electronic instabilities in polyacenes: Density-matrix renormalization group study of a long-range interacting model. *Phys. Rev. B* **2002**, *65,* 155204.

112. (a) Komura, N.; Goto, H.; He, X.; Mitamura, H.; Eguchi, R.; Kaji, Y.; Okamoto, H.; Sugawara, Y.; Gohda, S.; Sato, K.; Kubozono, Y. Characteristics of [6]phenacene thin film field-effect transistor. *Appl. Phys. Lett*. **2012**, *101*, 083301; (b) Ionkin, A. S.; Marshall, W. J.; Fish, B. M.; Bryman, L. M.; Wang, Y. A tetra-substituted chrysene: orientation of multiple electrophilic substitution and use of a tetra-substituted chrysene as a blue emitter for OLEDs. *Chem. Commun.* **2008***,* 2319-2321.

113. (a) Shen, Y.; Chen, C. F. Helicenes: Synthesis and Applications. *Chem. Rev*. **2012**, *112*, 1463-1535; (b) Martin, R. H. The Helicenes. *Angew. Chem. Int. Ed*. **1974**, *13*, 649-660.

114. (a) Müller, M.; Kübel, C.; Müllen, K. Giant polycyclic aromatic hydrocarbons. *Chem. Eur. J*. **1998**, *4*, 2099-2109; (b) Clar, E. *The Aromatic Sextet*, Wiley, New York, **1972**; (b) Clar, E. *Polycyclic Hydrocarbons Vol. 1–2*, Academic, London, **1964**; (c) Wu, T. C.; Chen, C. H.; Hibi, D.; Shimizu, A.; Tobe Y.; Wu, Y. T. Synthesis, Structure, and Photophysical Properties of Dibenzo[*de*,*mn*]naphthacenes . *Angew. Chem. Int. Ed.* **2010**, *49*, 7059-7062; (d) Zhang, X.; Jiang, X.; Zhang, K.; Mao, L.; Luo, J.; Chi, C.; Chan, H. S. O.; Wu, J. Synthesis, Self-Assembly, and Charge Transporting Property of Contorted Tetrabenzocoronenes. *J. Org. Chem*. **2010**, *75*, 8069-8077; (e) Criado, A.; Peňa, D.; Cobas, A.; Guiti, E. Domino Diels–Alder Cycloadditions of Arynes: New Approach to Elusive Perylene Derivatives. *Chem. Eur. J*. **2010**, *16*, 9736-9740; (f) Shirakawa, H.; Lewis, E. J.; McDiarmid, A. G.; Chiang C. K.; Heeger, A. J. Synthesis of electrically conducting organic polymers: halogen derivatives of polyacetylene, $(CH)_x$. *J. Chem. Soc. Chem. Commun*. **1977**, 578-580.

115. Koezuka, H.; Tsumura, A.; Ando, T. Field-effect transistor with polythiophene thin film. *Synth. Met*. **1987**, *18*, 699-704.

116. Aihara, J. Reduced HOMO−LUMO Gap as an Index of Kinetic Stability for Polycyclic Aromatic Hydrocarbons. *J. Phys. Chem. A*, **1999**, *103*, 7487-7495.

117. 80. Lyons, L. E. Energy gaps in organic semiconductors derived from electrochemical data. *Aust. J. Chem*. **1980**, *33*, 1717-1725.

118. (a) Moorthy, J. N.; Natarajan, P.; Venkatakrishnan, P.; Huang, D.; Chow, T. J. Steric Inhibition of π-Stacking: 1,3,6,8-Tetraarylpyrenes as Efficient Blue Emitters in Organic

Light Emitting Diodes (OLEDs). *Org. Lett*. **2007**, *9*, 5215-5218; (b) Debije, M. G.; Piris, J.; Haas, M. P.; Warman, J. M.; Tomović, Ž.; Simpson, C. D.; Watson, M. D.; Müllen, K. The Optical and Charge Transport Properties of Discotic Materials with Large Aromatic Hydrocarbon Cores. *J. Am. Chem. Soc*. **2004**, *126*, 4641-4645.

119. Anthony, J. E. Functionalized Acenes and Heteroacenes for Organic Electronics. *Chem. Rev*. **2006**, *106*, 5028-5048.

120. (a) Scott, L. T.; Boorum, M. M.; McMahon, B. J.; Hagen, S.; Mack, J.; Blank, J.; Wegner, H.; Meijere, A. De A rational chemical synthesis of C60. *Science* **2002**, *295*, 1500-1503; (b) Boorum, M. M.; Vasil'ev, Y. V.; Drewello, T.; Scott, L. T. Groundwork for a rational synthesis of C60: cyclodehydrogenation of a C60H30 polyarene. *Science* **2001**, *294*, 828-831; (c) Tsefrikas, V. M.; Scott, L. T. Geodesic Polyarenes by Flash Vacuum Pyrolysis. *Chem. Rev.* **2006**, *106*, 4868-4884.

121. Benard, C. P.; Geng, Z.; Heuft, M. A.; VanCrey, K.; Fallis. A. G. Double Diels−Alder Strategies to Soluble 2,9- and 2,9,6,13-Tetraethynylpentacenes, Photolytic [4 + 4] Cycloadditions, and Pentacene Crystal Packing. *J. Org. Chem.* **2007**, *72*, 7229-7236.

122. (a) Müller, M.; Petersen, J.; Strohmaier, R.; Günther, C.; Karl, N.; Müllen. K. Polybenzoid C_{54} Hydrocarbons: Synthesis and Structural Characterization in Vapor-Deposited Ordered Monolayers. *Angew. Chem., Int. Ed.* **1996**, *35*, 886-888; (b) Müller, M.; Kübel, C.; Müllen. K. Giant polycyclic aromatic hydrocarbons. *Chem. Eur. J.* **1998**, *4*, 2099-2109.

123. (a) Bonifacio, M. C.; Robertson, C. R.; Jung, J. Y.; King, B. T. Polycyclic Aromatic Hydrocarbons by Ring-Closing Metathesis. *J. Org. Chem.***2005**, *70*, 8522-8526; (b) Iuliano, A.; Piccioli, P.; Fabbri, D. Ring-Closing Olefin Metathesis of 2,2'-Divinylbiphenyls: A Novel and General Approach to Phenanthrenes. *Org. Lett.* **2004**, *6*, 3711-3714.

124. Donovan, P.M.; Scott, L. T. Elaboration of Diaryl Ketones into Naphthalenes Fused on Two or Four Sides: A Naphthoannulation Procedure. *J. Am. Chem. Soc.* **2004**, *126*, 3108-3112.

125. Goldfinger, M. B.; Swager, T. M. Fused Polycyclic Aromatics via Electrophile-Induced Cyclization Reactions: Application to the Synthesis of Graphite Ribbons. *J. Am. Chem. Soc.* **1994**, *116*, 7895-7896.

126. Xiao, S. X.; Myers, M.; Miao, Q.; Sanaur, S.; Pang, K. L.; Steigerwald, M. L.; Nuckolls, C. Molecular Wires from Contorted Aromatic Compounds. *Angew. Chem., Int. Ed.* **2005**, *44*, 7390-7394.

127. (a) Rempala, P.; Kroulik, J.; King, B. T. A Slippery Slope: Mechanistic Analysis of the Intramolecular Scholl Reaction of Hexaphenylbenzene. *J. Am. Chem. Soc*. **2004**, *126*, 15002-15003; (b) Stefano, M. D.; Negri, F.; Carbone, P.; Müllen, K. Oxidative cyclodehydrogenation reaction for the design of extended 2D and 3D carbon nanostructures: A theoretical study. *Chem. Phys.* **2005**, *314*, 85-99; (c) Balaban, A. T.; Nenitzescu, C. D. *Dehydrogenation Condensation of Aromatics (Scholl and Related Reactions) in Friedel–Crafts and Related Reactions*, ed. Olah, G. Wiley, New York, **1964**, *2*, 979; (d) Pradhan, A.; Dechambenoit, P.; Bock H.; Durola, F. Twisted Polycyclic Arenes by Intramolecular Scholl Reactions of C3-Symmetric Precursors. *J. Org. Chem.* **2013**, *78*, 2266-2274; (e) Pradhan, A.; Dechambenoit, P.; Bock, H.; Durola, F. Highly Twisted Arenes by Scholl Cyclizations with Unexpected Regioselectivity. *Angew. Chem. Int. Ed*. **2011**, *50*, 12582-12585.

128. Rempala, P.; Kroulik, J.; King, B. T.; Investigation of the Mechanism of the Intramolecular Scholl Reaction of Contiguous Phenylbenzenes. *J. Org. Chem.* **2006**, *71*, 5067-5081.

129. Mitra, T. PhD. Dissertation, Indian Institute of Technology Khargpur, **2014**, p 180.

130. Dissanayeke, D.; Hatton, R.; Lutz, T.; Curry, R.; Silva, S. Charge transfer between acenes and PbS nanocrystals. *Nanotechnology*, **2009**, *20*, 195205.

131. Huang, X. Q.; Yang, Z. G.; Hoshino, D.; Kitanaka, S.; Zhao, G. Y.; Nishioka, Y.; Duan, Z. F. A Novel Thiophene-Fused Polycyclic Aromatic with a Tetracene Core: Synthesis, Characterization, Optical and Electrochemical Properties. *Molecules* **2011**, *16*, 4467-4481.

132. Liang, Z.; Tang, Q.; Liu, J.; Li, J.; Yan, F.; Miao, Q. N-Type Organic Semiconductors Based on π-Deficient Pentacenequinones: Synthesis, Electronic Structures, Molecular Packing, and Thin Film Transistors. *Chem. Mater*. **2010**, *22*, 6438-6443.

Appendix

Appendix I

X-Ray Crystallographic Data

X-Ray Crystallographic Data for Compound 5.095 (CCDC No. 1055927)

Empirical formula	C12 H12 O2 S
Formula Weight	220.28
Crystal color	Pale yellow
Crystal size	0.21 mm × 0.30 mm × 0.06 mm
Temperature	293 (2) K
Wavelength	0.71073 Å
Crystal system	Triclinic
Space group	p-1
Unit cell dimension	a = 6.2162 (18) Å; α = 94.645 (8) b = 8.325 (2) Å; β = 99.555 (8) c = 10.661 (3) Å; γ = 96.670 (8)
Volume	537.6 (3) $Å^3$
Z	2
Calculated density	1.361 gm/cm^3
Absorption coefficient	0.276 mm^{-1}
F(000)	232
Theta range for data collection	1.95 to 24.93 degree
R_1	0.0380
wR_2	0.1079

Appendix II

Publications

RSC Advances

RSC Publishing

COMMUNICATION

View Article Online
View Journal | View Issue

A one-pot Garratt–Braverman cyclization and Scholl oxidation route to acene–helicene hybrids†

Cite this: *RSC Adv.*, 2013, **3**, 19844

Received 31st May 2013
Accepted 15th August 2013

DOI: 10.1039/c3ra42696c

www.rsc.org/advances

Tapobrata Mitra, Joyee Das, Manasi Maji, Ranjita Das, Uttam Kumar Das, Pratim K. Chattaraj* and Amit Basak*

We report a one-pot Garratt–Braverman cyclization and Scholl oxidation route to polyaromatic compounds, some having a band gap below 3 eV, starting from bis-propargyl sulfones, ethers and protected amines. The method has the advantage of constructing 3 C–C bonds in one-pot in good yields.

Polycyclic aromatic compounds (PAC)[1] although regarded as widespread pollutants and carcinogens;[2] are often endowed with unique electronic and optical properties.[3] An important class of PACs are the acenes and helicenes that differ in the connectivity of benzene rings. However, this minor difference imparts very distinctive properties to these classes of molecules. Acenes comprise linearly fused benzene rings and are planar while helicenes are *ortho*-fused benzene rings that adopt a helical conformation to avoid the overlapping of the terminal rings. Helicenes are more stable and persistent than acenes; to date, the largest acene synthesized is heptacene ([7]acene),[4] while the longest helicene known is [14]helicene.[5] Although the electronic properties of PACs depend on several factors, the HOMO–LUMO energy gap (band gap),[6] the reversibility of electron transfer[7] and stability[8] are major criteria to be considered. PACs with fewer aromatic π-sextets (Clar sextets)[9] are desirable as that facilitates creation of small energy gaps. Acenes like pentacene and tetracene derivatives belonging to such low Clar-sextet containing systems are now regularly employed as the semiconducting layers in field effect transistors.[10] However, concerns regarding their environmental (mostly oxidative) stability and solubility still exist. Incorporation of substituents,[11] angularly fused benzene rings[12] and functional groups[13] can improve these properties. In this paper, we report a novel synthetic approach combining Garratt–Braverman cyclization (GB)[14] and Scholl oxidation[15] in a single pot that led to PACs which can be regarded as acene–helicene hybrids, which are otherwise difficult to obtain, in moderate to high yields. Additionally, some of these hybrids have band gap <3 eV along with low lying HOMO to impart better oxidative stability.

We realized that synthesis of condensed aromatics by Scholl oxidation requires two adjacent aryl systems as represented by A. The latter can be accessed *via* GB cyclization of appropriate bispropargyl systems which is usually carried out with a base whereas anhydrous $FeCl_3$ is the reagent of choice for Scholl oxidation. Although the latter may involve an arenium cation or a radical cation intermediate,[16] the reaction is accompanied by the formation of an equivalent amount of HCl that can be partially quenched by the base used for GB cyclization. Thus the idea of a one-pot GB cyclization and Scholl reaction leading to the formation of 3 C–C bonds was conceived (Scheme 1).

The precursor bispropargyl systems for the one-pot reaction were prepared from readily available starting materials (1-naphthyl triflate, 2-bromonaphthalene and 9-bromophenanthrene) in overall yield of 70–80% (Scheme 2). The sequence of steps is only described for phenanthrene based sulfone, ether and sulfonamide. (For details of synthesis of other precursors see ESI.†) Sonogashira coupling[17] of 9-bromophenathrene with propargyl alcohol followed by functional group manipulation gave the corresponding bromide **4**. The latter upon treatment with sodium sulfide in THF–water under phase transfer conditions produced the sulfide **5** which was converted to the

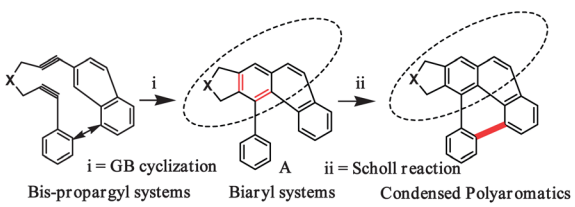

Scheme 1 Synthetic strategy towards condensed polyaromatics.

Department of Chemistry, Indian Institute of Technology, Kharagpur 721302, India. E-mail: absk@chem.iitkgp.ernet.in; Fax: +91 3222 282552; Tel: +91 3222 283300

† Electronic supplementary information (ESI) available: Experimental procedure, compound characterization, copies of NMR, CV and computational details. CCDC 930529 and 938978. For ESI and crystallographic data in CIF or other electronic format see DOI: 10.1039/c3ra42696c

JOC The Journal of Organic Chemistry

Article

pubs.acs.org/joc

Selectivity in Garratt−Braverman Cyclization of Aryl-/Heteroaryl-Substituted Unsymmetrical Bis-Propargyl Systems: Formal Synthesis of 7′-Desmethylkealiiquinone

Joyee Das, Raja Mukherjee,* and Amit Basak*

Department of Chemistry, Indian Institute of Technology, Kharagpur 721 302, India

Supporting Information

ABSTRACT: Unsymmetrical bis-propargyl ethers and sulfonamides containing various combinations of aryl/heteroaryl substituents at the acetylene termini were synthesized, and their reactivity under basic conditions was studied. Moderate to high (chemo)selectivity was observed, which followed a trend opposite to that reported earlier for the corresponding sufones. The major products obtained in most cases (except with indole) were formed via participation of the heteroaryl ring or the less electron rich aryl ring. The selectivity observed in imidazole-based systems was exploited to complete a formal total synthesis of 7′-desmethylkealiiquinone, an analogue of the marine alkaloid kealiiquinone.

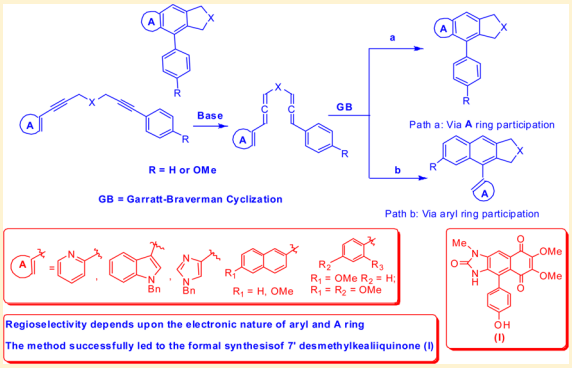

INTRODUCTION

Garratt−Braverman (GB) cyclization[1a−k] is the rearrangement of aryl-substituted bis-allenic sulfone/sulfides, ethers, and amines/sulfonamides leading to aromatic systems. The reaction involves formation of two C−C bonds, believed to pass through a biradical intermediate, and belongs to the class of cycloaromatization reactions.[11] The reactive bis-allenic system is made in situ from the corresponding bis-propargyl counterparts via a base-mediated isomerization. The GB reaction of unsymmetrical bis-propargyl sulfones, ethers, and sulfonamides can follow two pathways, involving either of the two aryl rings at the termini. It was earlier shown[2] by our group that the GB reaction of such sulfones can be made chemoselective by suitable perturbation of the electronic character of the terminal aryl groups (Scheme 1). The reaction follows a pathway in which the aryl group with greater electron-donating ability preferentially participates in the rearrangement. The rationale behind such selectivity was the greater nucleophilic character of the benzylic radical attached to the aryl ring having electron-donating properties. This interpretation was also supported by theoretical calculations. Unlike sulfones, there has been no systematic study of selectivity of GB cyclization involving bis-propargyl ethers or sulfonamides. Moreover, the effect of replacing one of the aryl groups with a heterocyclic ring such as pyridine, indole, or imidazole or an electronically different aryl ring such as naphthyl or methoxyphenyl also has not been evaluated (Scheme 2). Such a study, especially for heteroaryl systems, is relevant, as natural products of the kealiinine family[3] are imidazolyl fused benzenoid systems with a pendant aryl ring (Figure 1). This skeleton, at least in principle, may be obtainable via the GB reaction of a suitably heteroaryl substituted bis-propargyl system, provided proper selectivity is achieved during GB cyclization. It may be mentioned here that the selectivity issue addressed in the present cases is close to chemoselectivity rather than regioselectivity. The two different aryl rings or the aryl and heteroaryl rings on the two arms of the bis-propargyl system may be considered as representing two different functionalities, and thus chemoselectivity is involved in the two possible GB pathways and is used henceforth.[4]

RESULTS AND DISCUSSION

With this in mind, we proceeded with the synthesis of target bis-propargyl ethers and sulfonamides; key synthetic steps involved Sonogashira coupling[5] and O- or N-propargylation.[6] As an example, ether **1a** was prepared via a NaH-mediated O-alkylation of the alcohol **4a** with the propargyl bromide **7**. The alcohol **4a** was prepared by a Sonogashira reaction between *N*-benzyl-3-iodoindole (**6a**) and propargyl alcohol, while the bromide **7** was obtained via a similar reaction of iodobenzene with propargyl alcohol followed by bromination via mesylation and displacement with LiBr. O-alkylation of **4a** with the bromide **7** was achieved using NaH in THF at 0 °C (Scheme 3).

In order to follow the outcome of the Garratt−Braverman rearrangement, these bis-propargyl ethers/sulfonamides were treated with base (KO^{t}Bu/DBN/DBU depending upon the substrate) in toluene at reflux. The ratio of the products, as determined from the ^{1}H NMR spectrum of the crude reaction mixture by comparing the ratio of integrations for characteristic

Received: December 11, 2013
Published: April 3, 2014

   dx.doi.org/10.1021/jo402749d | J. Org. Chem. 2014, 79, 3789−3798

EurJOC European Journal of Organic Chemistry

FULL PAPER

DOI: 10.1002/ejoc.201500633

Base-Induced Cyclization of Propargyl Alkenylsulfones: A High-Yielding Synthesis of 4,5-Disubstituted 2*H*-Thiopyran 1,1-Dioxides

Ishita Hatial,[a][‡] Joyee Das,[a][‡] Ananta K. Ghosh,[b] and Amit Basak*[a]

Keywords: Sulfur heterocycles / Cyclization / Electrocyclic reactions / Alkynes / Allylic compounds

A convenient synthesis of 4,5-disubstituted 2*H*-thiopyran 1,1-dioxides is reported through a base induced process starting from eneyne sulfones. Except for strongly electron-withdrawing groups, the reaction tolerated a wide variety of substituents in the two aryl rings. This finding represents a major departure from the behaviour of the corresponding ethers. The reaction most probably proceeds through a 6π-electrocyclization from an in-situ-generated 1,3,5-trienyl sulfinate.

Introduction

The reactivity of bispropargyl sulfones, ethers, and sulfonamides has been well studied, especially in recent years.[1] The reaction leads to the formation of two C–C bonds in high yield under mild conditions, and is popularly known as the Garratt–Braverman (GB) cyclization.[2] The synthetic utility of the reaction has recently been reported in a series of papers.[3] Although doubts remain about the exact mechanism of the reaction, a diradical mechanism involving a bis-allene intermediate (Scheme 1), as proposed initially by Garratt and Braverman and later supported by computations and selectivity profiles,[4] is the generally accepted one. In 2007, while studying the rearrangement of ethers, Kudoh et al.[5] proposed an anionic intramolecular Diels–Alder mechanism involving a monoallenyl anion (Scheme 2); this mechanism has the support of deuterium-labelling experiments as well as computations based on the HUMO–LUMO gap. The same authors also used the intramolecular Diels–Alder reaction mechanism to explain the selectivity of the cyclization of propargyl alkenyl ethers, which, upon treatment with a suitable base, generate products following a similar pathway (Scheme 3). Because of the

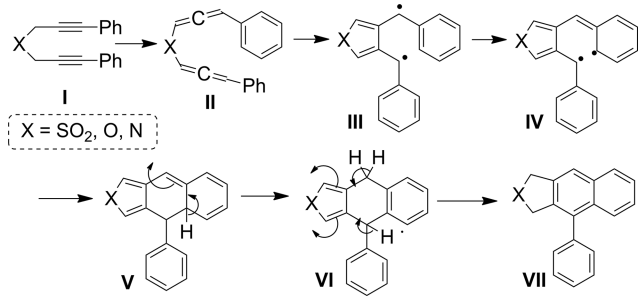

Scheme 1. Mechanism proposed by Garratt and Braverman.

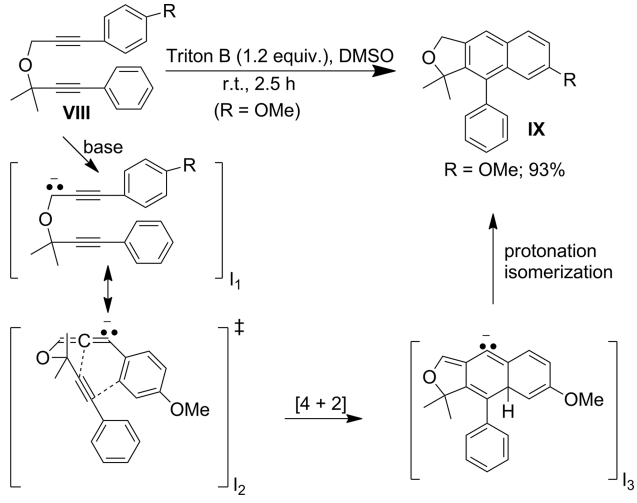

Scheme 2. Mechanism proposed by Kudoh et al.

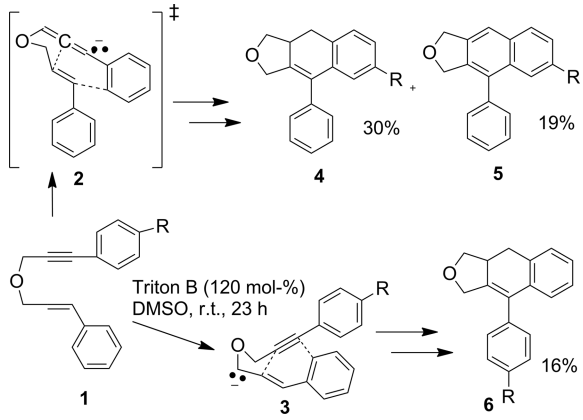

Scheme 3. Reaction with eneyne–ether system, as reported by Kudoh et al.[5]

[a] Department of Chemistry, Indian Institute of Technology, Kharagpur 721302, India
E-mail: absk@chem.iitkgp.ernet.in
http://www.chemistry.iitkgp.ac.in/~absk/
http://www.iitkgp.ac.in/
[b] Department of Biotechnology, Indian Institute of Technology, Kharagpur 721302, India
[‡] Equal contribution
Supporting information for this article is available on the WWW under http://dx.doi.org/10.1002/ejoc.201500633.

JOC The Journal of Organic Chemistry

Article

pubs.acs.org/joc

Shifting the Reactivity of Bis-propargyl Ethers from Garratt–Braverman Cyclization Mode to 1,5-H Shift Pathway To Yield 3,4-Disubstituted Furans: A Combined Experimental and Computational Study

Joyee Das,[†] Eshani Das,[‡] Saibal Jana, Partha Sarathi Addy, Anakuthil Anoop,* and Amit Basak*

Department of Chemistry, Indian Institute of Technology Kharagpur, Kharagpur 721 302, India

Supporting Information

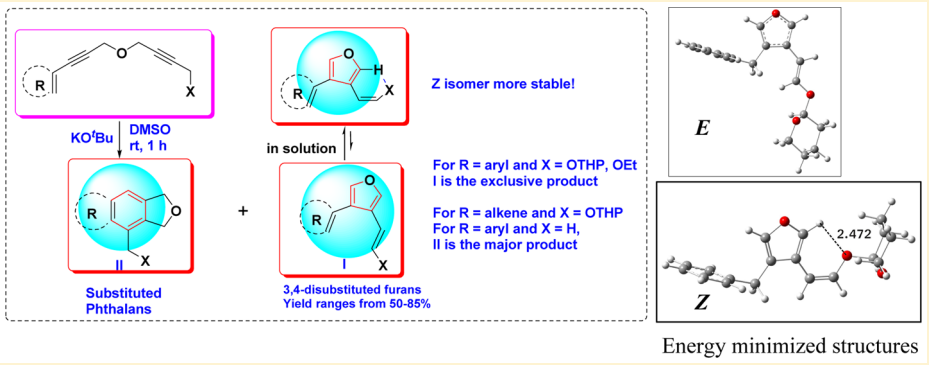

ABSTRACT: Aryl or vinyl substituted bis-propargyl ethers upon base treatment generally form phthalans via the Garratt–Braverman (GB) cyclization pathway. In a major departure from this usual route, several aryl/vinyl bis-propargyl ethers with one of the acetylenic arms ending up with 2-tetrahydropyranyloxy methyl or ethoxy methyl have been shown to follow the alternative intramolecular 1,5-H shift pathway upon base treatment. The reaction has led to the formation of synthetically as well as biologically important 3,4-disubstituted furan derivatives in good yields. The initially formed *E* isomer in solution ($CDCl_3$) slowly isomerizes to the *Z* isomer, indicating greater stability of the latter. The factors affecting the interplay between the 1,5-H shift and GB rearrangement have also been evaluated, and the results are supported by DFT-based computational study.

INTRODUCTION

The study of reactivity of bis-propargyl sulfones, ethers, and sulfonamides has drawn interest in recent years.[1] The reaction involves the formation of two C–C bonds in high yields under mild conditions, leading to the formation of an aromatic ring and is popularly known as Garratt–Braverman (GB) cyclization.[2] The synthetic utility of the reaction has recently been elaborated in a series of publications.[3] The involvement of a diradical intermediate from an *in situ* generated bis-allene intermediate (Scheme 1), as proposed initially by Garratt and Braverman[4] and later supported by computations and selectivity profiles,[5] is the generally accepted mechanism, although other possibilities like an anionic intramolecular Diels–Alder reaction has also been proposed.[6] One interesting aspect of the reactivity of appropriately substituted bis-propargyl systems is the possibility of a 1,5-H shift to internally quench the diradical intermediate (Scheme 2). Normally, this reaction occurs when there is no involvement of a double bond (from an alkene or an existing aromatic ring). For systems where this participation is possible, the GB cyclization pathway becomes dominant as that creates a stabilized aromatic ring. It is thus a challenge to shift the reaction toward the 1,5-H shift pathway, which creates a lesser stabilized furan system. We have undertaken a project to study the parameters that might help in tilting the preference from GB to 1,5-H shift pathway. The present study has been restricted to bis-propargyl ether systems only as, in these cases, we have achieved a fair amount of

Scheme 1. GB Cyclization of Aryl Substituted Bis-propargyl Systems

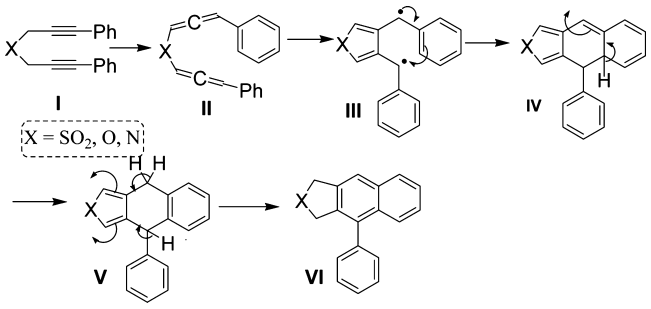

Received: September 25, 2015
Published: December 16, 2015

DOI: 10.1021/acs.joc.5b02246
J. Org. Chem. 2016, 81, 450–457

JOC The Journal of Organic Chemistry

Article

pubs.acs.org/joc

Mechanistic Studies on Garratt–Braverman Cyclization: The Diradical–Cycloaddition Puzzle

Joyee Das,[†] Subhendu Sekhar Bag,*[,‡] and Amit Basak*[,†]

[†]Department of Chemistry, Indian Institute of Technology Kharagpur, Kharagpur 721302, India

[‡]Department of Chemistry, Indian Institute of Technology Guwahati, Guwahati 781039, India

Supporting Information

ABSTRACT: In this work, we present the results of extensive multiprong studies involving the fate of deuterium-labeled substrates, EPR, trapping experiments, and LA-LDI mass spectrometry to sort out the controversies relating to the mechanism of Garratt–Braverman cyclization in two systems, namely bis-propargyl sulfones and ethers. The results are in conformity with a diradical mechamism for the sulfone, while for the ether, the anionic [4 + 2] appears to be the preferred pathway. This shows that the mechanistic pathway toward GB cyclization is dependent upon the nature of heteroatom (O or S in sulfone) bridging the propargyl arms.

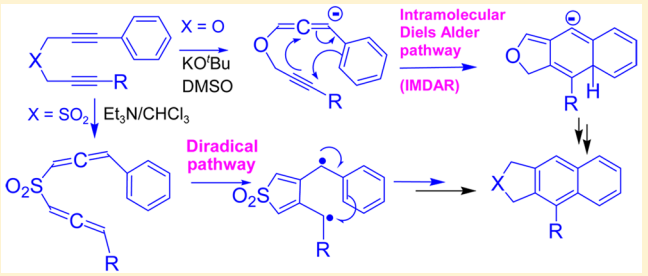

INTRODUCTION

Cycloaromatization reactions[1] have become an important research area because of their interesting mechanistic possibilities[2] which control the reactivity of molecules undergoing such reactions and the extent of their interactions with biomolecules.[3] Several cycloaromatization reactions are known starting from the famous Bergman cyclization reported first in 1971.[4,5] A few years after Bergman's paper, Garratt and Braverman[6,7] independently reported the reactivity of the bis-propargyl systems (sulfide, sulfone, ether, amine) under base-mediated conditions. The final outcome of the reaction, now popularly known as the Garratt–Braverman (GB) cyclization, was dependent upon the nature of the substituent in the propargyl arm as well as the reaction conditions. For example, in the case of an unsubstituted thioether, a dimeric product was obtained in virtually quantitative yield via the bis-allene (path A).[8a] The reaction was carried out in two stages: an initial treatment with KO^{t}Bu at −65 °C to get the bis-allene followed by warming the latter in $CHCl_3$ to 50 °C. For di-*tert*-butyl propargyl thioether, the product was mainly the cyclobutane-fused thiophene.[8a] Later on, Garratt et al. reported the isolation of similar products in low yields from all of the systems (thioether, ether, and amine) using KOH/MeOH.[8b] For alkyl-substituted substrates, 3,4-disubstitued 5-membered heterocycles were formed (path B).[9] On the other hand, aryl- or vinyl-substituted starting materials provide a new aromatic system via the participation of the aryl or vinyl double bond, ultimately leading to the formation of a naphthalene- or benzene-fused heterocyclic system (path C).[10] All of these possibilities are shown in Scheme 1

The generally accepted mechanism for the process as depicted in pathways **A**–**C** of Scheme 1 involves the formation of a diradical from a bis-alleneic intermediate[8] (Scheme 2A). Support for this mechanism came from various experiments like successful trapping of the diradical with $^3O_2$ to form the *endo* peroxide[11] (in case of sulfide), the nonperturbation of the rate upon varying solvent polarity,[12] as well as the isolation of **XIII** as an intermediate (Scheme 2A). In recent years, through a combination of experiment and computations on the selectivity of aryl-substituted bis-propargyl sulfones, the diradical mechanism was shown to be the preferred pathway.[13] Moreover, the complete GB selectivity of substrates capable of undergoing multiple reactions could be successfully explained on the basis of the diradical mechanism.[14]

Some ambiguities still remain regarding the diradical mechanism for the GB process, especially for reactions going through path C in view of the fact that the bis-allene, the progenitor of the diradical, is generated only after double isomerization and also has multiple mechanistic options. In some of the earlier experiments with sulfones by Braverman,[7a] the bis-allene was directly generated, and hence, not much ambiguity existed for those cases. However, in the classical GB reaction, where bis-propargyl systems are the starting materials, bis-allene formation is an important issue which should be a sequential event. If the mono- to the bis-allene formation is slow,[15] by the time it undergoes isomerization, it may give rise to the same products via an alternate route. For example, one can draw a [4 + 2] cycloaddition (intramolecular Diels–Alder reaction (IMDAR) mechanism) to arrive at the products from aryl-substituted systems. Such a mechanism was originally proposed by Iwai and Ide[10a] and later on reinforced by Kudoh et al.[16] for rearrangement of bispropargyl ethers in the presence of strong bases like NaH or Triton B in DMSO involving a

Received: March 7, 2016
Published: April 26, 2016

DOI: 10.1021/acs.joc.6b00490
J. Org. Chem. 2016, 81, 4623–4632

Organic & Biomolecular Chemistry

PAPER

View Article Online
View Journal | View Issue

Cite this: *Org. Biomol. Chem.*, 2017, **15**, 1122

Enediyne-based protein capture agents: demonstration of an enediyne moiety acting as a photoaffinity label†

Joyee Das,[a] Sayantani Roy,*[b] Swapnil Halnor,[a] Amit Kumar Das*[b] and Amit Basak*[a,b]

Received 21st September 2016,
Accepted 18th October 2016

DOI: 10.1039/c6ob02075e

rsc.li/obc

Two enediyne based protein-capture compounds **1** and **2** were synthesized. Both these molecules have an aryl sulfonamide for reversible binding with Human Carbonic Anhydrase II (HCA II) and a pyrene moiety for the visualization of a capture event. While compound **1** has an aryl azide as a photo cross-linking agent, compound **2** lacks the azide moiety. Capture experiments with HCA II however show that both **1** and **2** can photo cross-link with the protein as indicated in gel electrophoresis as well as MALDI analysis after tryptic digestion of HCA II. This observation demonstrates the ability of the enediyne moiety to act as a photo-affinity label possibly *via* the addition of nucleophilic amino acids to the partially zwitterionic singlet form of the diradical generated by photo Bergman cyclization.

Introduction

Small molecules as molecular probes for selective protein capture have become an area of recent research interest, especially in the field of proteomics.[1] The technique has potential for profiling protein–small molecule interactions which is important for understanding cellular processes and also in drug design. These small molecule probes are known as capture compounds (or photoaffinity probes). Their design involves decorating a template with three functionalities comprising (i) a selectivity function, such as an enzyme inhibitor, (ii) a photo-cross linking group (capture function) and (iii) a sorting group (to enable separation of the captured protein from biological mixtures). Biotin or an alkyne[2] is generally used for such selective sorting. Instead of a sorting functionality, one can attach a visualization hand in the form of a fluorophore, if the objective is to show the presence of a target protein.[3] Various 'tripodal' molecules have been employed for protein capture by small molecules, for example amino acids, peptides and trisubstituted aromatics including 1,2,4-trisubstituted benzene derivatives.[4] There are also a few examples of the use of 1,3,5-trisubstituted benzenes for this purpose.[5] Recently, Basak *et al.*[6] have reported the use of 5-amino dimethylisophthalate template-based compounds for the capture and subsequent visualization of Human Carbonic Anhydrase II (HCA II). Increase in the level of some isoforms of HCA II is indicative of diseases related to hypoxia and cancer (CA IX).[7] In continuation of our earlier work we decided to design a 1,2,4-trisubstituted aromatic enediyne based template to which the required functionalities were attached that included an aryl azide for photo cross-linking, a sulfonamide[8] for reversible binding to HCA and a pyrene moiety for the purpose of visualization. In the course of the capture experiment, we were surprised to note that both compounds **1** and **2** could crosslink with the protein even if the aryl azide moiety was removed from **2**. This aspect points to the cross-linking ability of enediynes under photoirradiation and thus supports the partial zwitterionic or singlet character of the diradical intermediate in the photo Bergman cyclization process.[9] The design, docking, synthesis and the capture experiments are described in detail in this paper.

Results and discussion

The initial basis of our design was to find out whether an enediyne moiety can be used as a template for protein capture; in the present case the target protein was HCA II. It was hoped that the enediyne framework would allow the photo cross-linking moiety, namely the azide to be in close proximity with the protein surface after the sulfonamide was anchored to the active site of HCA. Irradiation should yield nitrene which is expected to form cross-links with the protein (path A). Another interesting point worthy of consideration was the possibility of radical mediated protein cleavage[10] once the diradical was

[a]*Department of Chemistry, Indian Institute of Technology Kharagpur, Kharagpur-721302, India. E-mail: absk@chem.iitkgp.ernet.in*
[b]*School of Bioscience, Indian Institute of Technology Kharagpur, Kharagpur-721302, India*

†Electronic supplementary information (ESI) available: Experimental procedure, compound characterization, copies of NMR, and HRMS of selected compounds. See DOI: 10.1039/c6ob02075e

Sensors and Actuators B 251 (2017) 985–992

Contents lists available at ScienceDirect

Sensors and Actuators B: Chemical

journal homepage: www.elsevier.com/locate/snb

Nanomolar level detection of explosive and pollutant TNP by fluorescent aryl naphthalene sulfones: DFT study, in vitro detection and portable prototype fabrication

Pritam Ghosh[a,1], Joyee Das[b,1], Amit Basak[b,*], Subhra Kanti Mukhopadhyay[c], Priyabrata Banerjee[a,d,**]

[a] Surface Engineering & Tribology Group, CSIR-Central Mechanical Engineering Research Institute, Mahatma Gandhi Avenue, Durgapur-713209, Burdwan, West Bengal, India
[b] Organic Chemistry Division, Indian Institute of Technology Kharagpur, Kharagpur, West Bengal, 721302, India
[c] Department of Microbiology, The University of Burdwan, Burdwan 713104, India
[d] Academy of Scientific and Innovative Research at CSIR-Central Mechanical Engineering Research Institute (CMERI) Campus, CSIR-Central Mechanical Engineering Research Institute, Mahatma Gandhi Avenue, Durgapur 713209, West Bengal, India

ARTICLE INFO

Article history:
Received 24 November 2016
Received in revised form 19 May 2017
Accepted 23 May 2017
Available online 25 May 2017

Keywords:
Explosive and pollutant
Fluorescence
Aryl napthyl sulfones
AIE-ACQ-RET-ICT
in vitro detection-paper & solution kit
Real sample analysis

ABSTRACT

Luminescent Aryl Naphthalene Sulfones have been prepared via Garratt-Braverman cyclization of γ-substituted bis-propargyl sulfones for explosive and pollutant 2,4,6-Tri nitrophenol (TNP) recognition in aqueous medium by fluorescence quenching. The quenching can be explained through AIE-ACQ-RET-ICT based mechanisms. *In vitro* detection of TNP has been performed inside pollen cells. In real time stepping, paper strip and pocket solution kit has been fabricated for on spot detection of TNP. Moreover as an analytical application TNP has been detected from several surface water specimens collected throughout West Bengal, India. The limit of detection has been found as low as 10 nM together with quenching constant as $6.8 \times 10^5\ M^{-1}$, which is even superior to the recently published sensor materials.

1. Introduction

Detection of explosives remain in the forefront of research considering the prevailing world scenario. Amongst the various explosives, 2,4,6-trinitro phenol (TNP) and 2,4,6-trinitro toluene (TNT) are commonly used in IEDs (Improvised Explosive Devices) for several military applications, mining sector and simultaneously misused by terrorists. As a result rapid detection of explosives is significant from both constructive and destructive outrage. The dark side is that terrorism causes thousands of innocent deaths and therefore spot detection of illegal carriage of TNP prior to any sorts of misuse has become an important target of research. Although the explosion power of TNP is even lethal than TNT, till date, major attention has been paid for TNT detection [1–6]. Apart from its use as explosive, TNP has also been used in several synthetic industries from where incautious release to environment may happen. In mammalian's digestive cycle it is transformed into mutant picramic acid [4]. As a consequence, detection of TNP-like explosives and pollutant nitro aromatics (epNACs) are essential considering their detrimental impacts on environment and homeland security thus bringing the challenges for its *in vitro* detection and prototype fabrication for onsite recognition.

Till date onsite detection is mostly dependent on canine's efficacy or other expensive and less portable instrumental techniques. On the other hand, fluorescence based method is known as a cheap, easy and safe way out for guest analyte detection and as a signalling tool this methodology have been well accepted in chemistry [7]. In this present study Luminescent Aryl Naphthalene Sulfones (LANS) have been designed and synthesized for detection of epNACs like TNP. The outcome reveals that LANS could be a good addition to the family of explosive sensors for it's unique features like high sensitivity and high emissive property leading to quick response time.

* Corresponding author.
** Corresponding author at: Surface Engineering & Tribology Group, CSIR-Central Mechanical Engineering Research Institute, Mahatma Gandhi Avenue, Durgapur-713209, Burdwan, West Bengal, India.
E-mail addresses: absk@chem.iitkgp.ernet.in (A. Basak), pr_banerjee@cmeri.res.in, priyabrata_banerjee@yahoo.co.in (P. Banerjee).
[1] Authors have contributed equally.

http://dx.doi.org/10.1016/j.snb.2017.05.126
0925-4005/